Uncertainty in acid deposition modelling and critical load assessments

R&D Technical Report P4-083(5)/1

J Abbott[1], G Hayman[1], K Vincent[1], S Metcalfe[2], T Dore[3], R Skeffington[4], P Whitehead[4], D Whyatt[5], N Passant[1], M Woodfield[1]

1. **AEA Technology plc**
2. **University of Edinburgh**
3. **Centre for Ecology and Hydrology, Bush**
4. **Water Resource Associates**
5. **University of Lancaster**

Publishing Organisation
Environment Agency, Rio House, Waterside Drive, Aztec West, Almondsbury, BRISTOL, BS32 4UD.

Tel: 01454 624400 Fax: 01454 624409
Website: www.environment-agency.gov.uk

 June 2003

ISBN 1 84432 113 4

Dissemination Status
Internal: Released to Regions
External: Released to Public Domain

Statement of Use

The research results provide a valuable baseline for critical load assessments of value to IPPC and Habitats Directive assessments. However they are of broader significance in developing a full risk based approach to air quality assessment of processes under Agency regulation. Further work on testing the uncertainty bounds using measurement data has also been completed as supplementary work. The results of this aspect of air quality assessment will be included within a framework for all air quality assessments following further development.

Keywords
Critical loads, uncertainty, acidification, eutrophication, dynamic models, Monte-Carlo analysis.

Research Contractor
This document was produced under R&D Project P4-083(5) by AEA Technology plc, Culham Science Centre,:Abingdon, Oxfordshire. OX13 3ED.

Tel: 01235 463184

Environment Agency's Project Manager
The Environment Agency's Project Manager for Project P4-083(5) was:
Dr Bernard Fisher, National Centre for Risk Analysis and Options Appraisal.

Further copies of this report are available from:
Environment Agency R&D Dissemination Centre, c/o WRc, Frankland Road, Swindon, Wilts SN5 8YF

tel: 01793-865000 fax: 01793-514562 e-mail: publications@wrcplc.co.uk

EXECUTIVE SUMMARY

The critical loads approach has been developed as an aid to the regulation of acidifying gas emissions, both within the UK and internationally. The critical load is broadly defined as the amount of pollutant deposition a part of the environment can tolerate without harm. Trajectory models such as HARM, TRACK and FRAME have been developed to assess acid deposition to sensitive areas. They use a spatially dis-aggregated emissions inventory and predict deposition at grid squares throughout the United Kingdom.

The use of trajectory models and critical loads is now recognised as the accepted assessment method and is likely to be used to meet the Environment Agency's obligation under the Habitats Directive. Hence, the Environment Agency would like to have an understanding of the uncertainties associated with these models and methods. They need to know how robust the models are so that they know to what extent they can rely on them. For example:

1. Are they merely the best cost/time effective guess based on the available evidence but useful for general policy development?
2. Are they sufficiently robust to form the basis of methods to assess the contribution of specific emissions to deposition, or critical load exceedence?
3. Are they sufficiently robust that they could be relied upon in court as proof of harm to the environment in the event of a breach of an authorisation?

The Environment Agency commissioned this project to get a better understanding of the uncertainties in using trajectory models and the critical loads approach. The aim of the project was to assess the influence of uncertainty in three main areas:

1. Emission estimates;
2. The parameterisation of long range trajectory models;
3. The description of critical loads functions.

Consideration of uncertainty also improves understanding of the characteristics of environmental models and avoids treating them as "black boxes". The report has been prepared as the result of collaboration. AEA Technology provided the overall project management, assessed and quantified the uncertainties in model inputs including the uncertainties in emissions, contributed to acid deposition studies and carried out data analysis. CEH Edinburgh carried out acid deposition studies using the FRAME model. Edinburgh and Lancaster Universities collaborated on the acid deposition studies, using the HARM model, and contributed to the assessment of model input uncertainties. Water Research Associates carried out the literature review of uncertainties in critical load estimates and the Liphook case study.

The acid deposition models HARM, FRAME and TRACK are all trajectory models employing broadly similar chemical reaction schemes. They have many common features and might be expected to demonstrate similar behaviour. The model equations can to some extent be solved analytically. Analytical solutions have been developed as part of this project and have been used to help identify the critical input parameters, make sensitivity analyses more amenable, and to develop methods of data analysis.

The main input parameters included within the models are:

1. Chemical reaction rate constants:
2. Dry deposition velocities;
3. Wet scavenging coefficients (including enhancement in high rainfall areas);
4. Background concentrations of chemical species;
5. Wind speed;
6. Frequency of winds from each wind direction sector;
7. Boundary layer height;
8. Emissions;
9. Speciation of emitted sulphur dioxide and oxides of nitrogen.

Plausible ranges of these input parameters have been identified based on literature surveys, current practice and expert judgement. The uncertainty in some of the input parameters, such as the rate of reaction of simple gaseous species, is quite small; the uncertainty in other parameters such as the rate of reaction of gases with particulate matter may be quite large, approaching an order of magnitude.

A systematic sensitivity analysis of the uncertainty in the national emissions leads to some estimates, notably for sulphur and nitrogen oxides, which are substantially lower than those which would have been estimated by expert judgement. It is not within this study to explore alternative methodologies, but it is recognised that Monte Carlo analysis is not able to treat uncertainties in processes which are unknown. In addition uncertainties in individual processes are treated as independent variables.

A summary of the sensitivity analyses performed on the models now follows. The uncertainty in sulphur deposition was investigated by Monte Carlo analysis of the analytical model with the values of input parameters selected from their plausible ranges using a single source. The 95^{th} percentile of the predicted deposition rates was approximately a factor of 2 times the average value and the 5^{th} percentile was approximately half the average value. A first order error analysis of the uncertainty in sulphur deposition, in which each of the input variables was changed one variable at a time explained 95% of the overall variance throughout the range of prediction. The major contributor to the overall variance of predicted values was the uncertainty in the dry deposition velocity for sulphur dioxide in the vicinity of the receptor. Other significant contributors to the variance were the uncertainties in the rate of emission, boundary layer height, wind speed, frequency of the wind direction in the relevant sector and the wet deposition coefficient for sulphur dioxide. At 800 km from the source, the largest contributors to the variance in the predicted total sulphur deposition rate at receptors are the uncertainties in the dry deposition velocity for sulphur dioxide both upwind and local to the receptor.

The analytical model was used to compare the performance of Monte Carlo simulation with that of more limited sampling based on a Latin Square with only 13 model runs. The Latin Square sampling strategy provided a reasonable estimate of the distribution derived from the Monte Carlo analysis in the cumulative probability range between 0.1 and 0.9. In both cases, the sulphur deposition distribution function could be approximated by a log-normal.

Monte Carlo analysis of the analytical model for nitrogen deposition was also carried out. The 95th percentile of the predicted rates of deposition was approximately twice the mean value and the 5th percentile was approximately one third of the mean value. Approximately 10-30% of the variance is not explained by first order analysis and is associated with more complex interactions between parameters. The largest contributors to the variance in the predicted rates of deposition were the background concentration of the hydroxyl radical, the wet deposition of the aerosols, the frequency of the wind direction, the wind speed, the rate constant for the formation of nitrogen pentoxide, the rate of emission, and the rate constant for the formation of nitric acid.

Monte Carlo simulations of sulphur, oxidised nitrogen and reduced nitrogen deposition using the TRACK model, using a 1990 emissions inventory for the UK and three hundred model runs, showed that:

1. The 95th percentile of predicted rates of sulphur deposition at a range of sites throughout the UK (the Secondary Network sites) was typically 1.3 times the mean value predicted at each site: the mean was typically around 1.45 times the 5th percentile.
2. The 95th percentile of predicted rates of oxidised nitrogen deposition was typically around 1.9 times the average: the average was typically around 2 times the 5th percentile.
3. The 95th percentile of predicted rates of reduced nitrogen deposition was typically around 1.5 times the average: the average is typically around 1.7 times the 5th percentile.
4. The probability distributions of the predicted rates of sulphur, oxidised and reduced nitrogen deposition were approximately log-normal.

A first order error analysis of the TRACK model in which the input parameters were varied one variable at a time was also carried out. From this the 5th percentile and 95th percentile rates of sulphur deposition could be estimated. These were approximately 30% greater than those provided by the Monte Carlo analysis. The range of uncertainty in nitrogen deposition rates were similar to those provided by the Monte Carlo analysis. The estimated 5th percentile rate of reduced nitrogen deposition was similar to that provided by the Monte Carlo analysis. The 95th percentile rate of deposition was typically 50% greater than that provided by the Monte Carlo analysis.

The uncertainty in the estimates made by TRACK of the incremental impact of an additional 150 kt per annum source of oxides of nitrogen was also investigated using Monte Carlo analysis. The 95th percentile of the additional oxidised nitrogen deposition was approximately twice the average value: the 5th percentile was approximately half the average value. Comparison of the predictions of the TRACK model with those for the analytical model showed acceptable agreement, suggesting that the results of uncertainty analysis for the analytical model are more generally applicable.

The non-linear incremental impact of additional sources was investigated using the TRACK model. Far from the source, the incremental contribution from a 75 kt source of oxides of nitrogen was half that for a 150 kt source i.e. the predictions varied linearly with emission. Closer to the source, the predicted impact showed evidence of sublinearity: the deposition of oxidised nitrogen associated with a 150 kt source was only 1.8 times that for a 75 kt source.

The uncertainty in predictions of nitrogen deposition made by the HARM model was investigated using a sampling strategy based on a Latin Square. This was based on just 12 model runs. The estimated 92nd percentile rates of oxidised and reduced nitrogen were typically around 1.5 times the mean values: averages were typically around 1.5 times the 5th percentiles. The probability distributions of predicted rates of deposition approximated to log-normal.

First order error analysis of the uncertainty in HARM model predictions of oxidised and reduced nitrogen was also carried out. This provided estimates of oxidised nitrogen deposition similar to those provided by the Latin Square sampling analysis. Estimates of average and 5th percentile rates of reduced nitrogen deposition were similar to those determined by Latin Square sampling: the 95th percentile value was typically 30% greater than that provided by the Latin Square sampling.

A review of the literature on the uncertainty in critical loads has been carried out. The review concluded that further work was required to quantify the uncertainty in critical loads estimates. A case study for Liphook, a forested area in the south of England, was therefore carried out in order to investigate the uncertainty in the critical load estimate at a well-documented site. The case study involved Monte Carlo simulation, selecting input values from a plausible range of parameters describing this well-documented site. The coefficients of variation of the variables describing the critical load function $CL_{min}N$, $CL_{max}S$ and $CL_{max}N$ were 22%, 30% and 14 % respectively. The probability distribution of the critical load variables could be approximated by a normal distribution.

The uncertainty in the prediction of the exceedence of the critical load at the Liphook site was investigated. Estimates of critical loads sampled from the Liphook Monte Carlo simulation were randomly matched with estimates of the rate of acid deposition sampled from the TRACK Monte Carlo simulation. The simulation indicated that there was a high probability (>99.9%) that the critical load was exceeded at the site based on 1990 emissions. Reducing the rates of deposition to around 40% of that for 1990 emissions would reduce the probability of exceedence to around 50%. It would be necessary to reduce acid deposition to approximately 20 % of that predicted from 1990 emissions in order to have a high degree of confidence (95%) that the critical load was not exceeded at this site. This example suggests that the critical load and deposition model methodology can provide an effective tool for emissions reduction policies at the regional scale, but the uncertainties in the assessment of exceedences should be taken into account

The incremental contribution to sulphur and nitrogen deposition from a large point source was considered in relation to the uncertainty in the exceedence at the Liphook site. For the example considered, the incremental contribution to nitrogen deposition from a 150kt per annum emission of NOx 50km away would increase the risk of exceedence of the critical load by around 1%. The incremental contribution to sulphur deposition would appear to be greater with a typical increase in the risk of exceedence of the critical load of approximately 5-10% because of the addition of a major stationary source. These examples suggest that the impact of large point sources should be expressed in terms of risk of increasing exceedence. The assessment of sources of nitrogen oxides should consider the aggregate impact of a number of sources on the risk of exceedence.

The assessment of uncertainty carried out in this study does not take account of measured rates of deposition. In practice, the predicted rates of deposition may be compared with observed, or independently estimated rates of deposition at Secondary Network sites throughout the United Kingdom. An integrated assessment approach would allow the performance of the model at these sites to be taken into account when estimating the likelihood of exceedence of the critical load at other sites. A simple probabilistic method for incorporating measured deposition rates in the assessment of uncertainty is suggested.

The following conclusions and recommendations are made:

1. The uncertainty in the prediction of rates of deposition resulting from the uncertainty in input parameters may be assessed by Monte Carlo analysis.
2. Latin Square sampling or first order analysis should provide useful estimates of the uncertainty where Monte Carlo analysis is not practical because of the large number of model runs required. The probability distribution of rate of deposition can usually be approximated by a log-normal distribution.
3. The uncertainty in acid deposition models currently used for assessment purposes in the UK may be broadly described as within a "factor of two".
4. Analytical deposition models may be used to test Monte Carlo techniques. Their real value may arise in their flexibility to optimise input parameters when comparing predictions against observations, using for example Bayesian Monte-Carlo methods
5. The uncertainty in prediction of critical loads resulting from uncertainties in input parameters may also be assessed by Monte Carlo analysis.
6. The uncertainty in predicting exceedence of critical loads (deposition minus critical load) may be obtained by sampling from the probability distributions of the predicted critical loads and rates of acid deposition.
7. Further investigations should be carried out to integrate measurements of rates of deposition into the analysis of uncertainty to counter criticism that only "known" sources of uncertainty have been taken into account.

CONTENTS

List of Figures

List of Tables

APPENDICES

1 INTRODUCTION

The Environment Agency is responsible for the protection and management of the environment in England and Wales by regulating pollutant releases to land, air and water. More specifically the Environment Agency has a duty under the EC Habitats Directive (Council Directive 92/43/EEC on the conservation of natural habitats and of wild fauna and flora) to review the possible effects of emissions from regulated processes on ecologically sensitive areas. The Directive provides for the creation of a network of ecologically sensitive sites throughout Europe, to be known as Natura 2000 sites. This network includes SACs (Special Areas of Conservation) for the protection of natural habitats of wild fauna and flora other than birds, and SPAs (Special Protected Areas) which support wild birds and their habitats. It is the Environment Agency's responsibility to review all existing and prospective emissions to assess how a regulated process might affect a Natura 2000 site in England and Wales by 2010. The Agency is involved in reviewing existing permissions that could affect existing SPAs and SACs.

The emission of oxides of nitrogen and sulphur from combustion sources in England and Wales leads to the deposition of oxidised and reduced nitrogen and sulphur over wide areas. This deposition may lead to the increased acidification of soils and water, particularly in upland areas. Nitrogen deposition may also contribute to the eutrophication of susceptible water bodies.

The critical loads approach has been developed as an aid to the regulation of acidifying gas emissions, both within the UK and internationally. The critical load is broadly defined as the amount of pollutant deposition a part of the environment can tolerate without harm. In the UK straight line trajectory models such as HARM, TRACK and FRAME have been developed to assess acid deposition to sensitive areas. They use a spatially disaggregated emissions inventory and predict deposition at grid squares throughout the United Kingdom. The use of straight line trajectory models and critical loads is now considered to be the standard assessment approach in the UK and is likely to be used to meet the Environment Agency's obligation under the Habitats Directive. Hence the Environment Agency would like to have an understanding of the uncertainties associated with these models and assessment methods. The Agency needs to know to what extent it can rely on the methods. For example the questions raised include:

1. Are the models merely the best cost/time effective guess based on the available evidence, and useful for general policy development?
2. Are they sufficiently accurate to form the basis of methods to assess the contribution of specific emissions to deposition, or to critical load exceedences?
3. Are they sufficiently robust that they could be relied upon in court as evidence of harm to the environment in the event of a breach of an authorisation.

This project addresses the issues associated with the uncertainties in the use of trajectory models and the critical loads approach. The aim of the project is to assess the influence on uncertainty in three main areas:

1. Emission estimates;

2. The parameterisation of long range transport models;
3. The description of critical loads functions.

There are several sources of uncertainty in models. These include the uncertainty associated with:

1. the input parameters;
2. the model structure and its spatial and temporal resolution;
3. the random nature of some natural processes specifically atmospheric processes.

There appears to be a tendency to neglect uncertainty as our description of environmental interactions becomes more detailed and complex. This study tries to redress the balance. Uncertainty is associated with measurements, but the primary approach to estimating uncertainty is to compare modelled predictions with field measurements. The TRACK, HARM and FRAME model predictions have been compared with measurements in other studies [e.g. Metcalfe, Whyatt and Derwent, 1995; Lee, Kingdon, Jenkin and Garland, 2000; Singles, Sutton and Weston, 1998]. There is generally not sufficient measurement data to allow a comprehensive assessment of uncertainty to be made, but quite good agreement between modelled predictions and measurements has been achieved by judicious selection of input parameters.

The deposition models all have many input parameters, some of which are ill-defined or very uncertain. Consequently, the uncertainty arising from the uncertainty in the input parameters may be a large component of overall uncertainty. This report addresses the uncertainty associated with only the model input parameters. Uncertainty associated with processes erroneously treated or neglected in the models have not been investigated in this study.

A Monte Carlo approach is taken to assess the uncertainty arising from the uncertainty in model inputs. Predicted rates of acid deposition are not compared with measured values: the empirical assessment of uncertainty is outside the scope of this project. A probabilistic method of assessment of overall uncertainty that takes account of measured rates of deposition is suggested as the subject of further work.

AEA Technology Environment have provided the overall management of the project, the assessment of the uncertainty in the emissions estimates and TRACK model output. The University of Edinburgh and the Centre for Ecology and Hydrology at Bush provided HARM and FRAME model output respectively. Water Research Associates provided the uncertainty analysis and critical review of critical loads.

1.1 Structure of Report

Sections 2 to 4 of the report are concerned with the uncertainty in the prediction of deposition rates. Section 2 provides a brief description of the main features of the models HARM, TRACK and FRAME. Section 2 also introduces simple analytical models described in Appendices 2 and 3 for the prediction of acid deposition; the analytical models provided the basis for understanding the general behaviour of the acid deposition models and helped in the development of the methods used in the investigation

Section 3 identifies the parameters used in the input to the acid deposition models and the plausible ranges in these input parameters. Detailed consideration is given to the uncertainty in a key input to the models - the emissions inventory.

Section 4 contains the results of the assessment of the uncertainty in the acid deposition model outputs attributable to the uncertainty in the model inputs. Various techniques have been used to assess the uncertainty including Monte Carlo simulation, First Order Error analysis using Taylor's formula and randomised trials using Latin Square sampling. The performance of the assessment methods is compared.

Section 5 of the report is concerned with the uncertainty in the assessment of critical loads. It draws upon a literature review of the uncertainty in critical loads prepared as part of this project and Monte Carlo simulations of critical load assessment for soils in a woodland area at Liphook, Surrey.

Section 6 of the report provides an assessment of the overall uncertainty in the prediction of critical load exceedences. It draws upon the probability distributions for the deposition and the critical load at a receptor. Monte Carlo simulation is used to develop the probability distribution of deposition in excess of the critical load.

Section 7 contains conclusions and recommendations.

2 ACID DEPOSITION MODEL DESCRIPTIONS

2.1 Introduction

Process models of the atmosphere have been widely used to evaluate the impact of emissions on the environment. These models aim to describe the many different and complex chemical and physical processes occurring in the real atmosphere. Process models are therefore used

1. to assess the understanding of the processes involved;
2. to interpret observations made of the atmosphere;
3. to quantify the relative importance of different processes, and
4. to assess how the atmospheric system will respond to different emission scenarios.

Lack of knowledge and computational limitations force many simplifications. The accuracy and precision of the numerical results obtained and hence, the conclusions that can be drawn, depend on many factors:

1. the representation of the atmospheric processes in the model;
2. the assumptions and simplifications introduced;
3. the quality of the input data.

The models investigated in this study are described in outline below. More detailed descriptions are available in the references cited. Justification for the assumptions and simplifications inherent in the numerical models is also provided in the references.

The models considered are all straight line trajectory models and so have many features in common. The models differ in their incorporated chemical models, their treatment of deposition and of vertical dispersion and the assumed wind fields. The models are not simulations of actual transport and approximate removal and transformation processes. The main parameters are in some sense composite, idealised representations of actual processes. One cannot measure the parameter values explicitly.

Straight-line trajectory models are most widely applied in the United Kingdom. Other models formulations, such as the EMEP Lagrangian and Eulerian Acid Deposition Models LADM and MADE50 are also used, but are not considered here. These models are examples of cases in which the meteorological description is much more detailed. The changes in the chemical composition of air masses is followed explicitly, rather than by considering representative averages. One cannot conclude from this study whether more complex models would give better predictions.

2.2 HARM - version 11.5

HARM employs a simple trajectory model approach to predict the concentrations and rates of deposition of gases and aerosols containing sulphur and nitrogen over north-west Europe. It is described in more detail by Metcalfe, Whyatt and Derwent(1995). The time development of the trace constituents in a parcel of air advected by a wind field has been represented by the following differential equation:

$$\frac{d[c_i]}{dt} = \frac{E_i}{h} + P_i - L_i[c_i] - \frac{V_i}{h}[c_i] - S_i[c_i]$$

where
$[c_i]$ is the concentration of species i;
t is time;
E_i is the instantaneous emission rate of species i per unit area per unit time;
h is the box height, set at the top of the boundary layer;
P_i is the instantaneous production rate of the species i from the coupled chemistry of the acid gases;
L_i is the instantaneous loss coefficient of the species i from the coupled chemistry of the acid gases;
V_i is the dry deposition velocity for species i;
S_i is the wet scavenging coefficient for species i.

The model allows for spatial variations in the emission rates of sulphur dioxide, nitric oxide, ammonia and hydrogen chloride and in the wet scavenging coefficients and dry deposition velocities. The spatial variation in dry deposition velocity of sulphur dioxide, nitrogen dioxide and ammonia with land use type is represented in the model. Enhanced oxidation of sulphur and wet scavenging of aerosols in areas of high rainfall is taken into account within the model.

The differential equation describes the application of mass conservation to the species in a well-mixed parcel of air within the atmospheric boundary layer, where the assumption of instantaneous mixing ensures that both vertical and horizontal concentration gradients can be ignored. Furthermore, the assumption is made that the integrity of the air parcel is preserved throughout the travel time (96 hours). Thus wind shears are neglected and a stable well-defined advection field is assumed.

The model calculates long-term average concentrations and rates of deposition at each receptor point by averaging over the results obtained for trajectories arriving at that point from each wind direction sector, suitably weighted by the frequency of winds in that sector. The user can select the number of trajectories with typically 72 to 360 used in model studies. The same wind rose is used for all receptor points in the United Kingdom.

The coupled chemistry scheme included within the model is described in Appendix 1. The model ignores diurnal variation in the rates of chemical reactions.

2.2 TRACK- version 1.8

The TRACK model is described in some detail elsewhere (Lee, Kingdon, Jenkin and Garland, 2000). TRACK has single level and multi-level options. The single layer option is similar to that used in the HARM model and has been used in this investigation**.** The main differences between the HARM model and the single layer TRACK model are associated with the coupled chemistry reaction schemes. The coupled chemistry scheme included within the TRACK model is described in Appendix

1. The model can take into account the diurnal variation in the rates of chemical reaction.

The TRACK multi-layer option describes the vertical diffusion of species by the K-theory diffusion equation, based upon Monin-Obukhov similarity theory:

$$\frac{\partial c}{\partial t} = \frac{\partial}{\partial z}\left(K_z \frac{\partial c}{\partial z} \right)$$

where K_z is the eddy diffusivity at height z above the ground.

The eddy diffusivity depends on the atmospheric stability. For neutrally stable atmospheric conditions K_z is calculated from:

$$K_z = \kappa u_* z\left(1 - \frac{z}{h} \right)$$

where κ is the von Karman constant (0.41) and u_* is the friction velocity.

The friction velocity is calculated from:

$$u_* = \frac{\kappa u_{10}}{\ln(10 / z_0)}$$

where u_{10} is the mean wind speed measured 10 m above the ground and z_0 is the mean roughness length.

The TRACK model has the facility to model the effects of an additional point source on predicted concentrations and rates of deposition. The approach taken for the additional point source is slightly different from that used for the other "area" sources. The model first calculates the concentration and rates of deposition at receptors in the absence of the additional point source and then performs the calculations with the additional source present: the incremental contribution from the additional point source is the difference between predicted values with and without it. The model allows for the spread of the plume from the point source: it calculates the width of the wind direction sector at the receptor and applies this dispersion all at once at the source when inputting the emission, as a rate of change of concentration. This is considered to be a reasonable approximation if the emitted species do not react rapidly.

2.3 FRAME - version 4.2

The FRAME model is similar to the multi-layer TRACK model. It is described in some detail elsewhere (Singles, Sutton and Weston, 1998). The main differences between the FRAME and multi-layer TRACK model are associated with (1) the chemical reaction scheme, (2) the vertical variation in eddy diffusivity and (3) the inclusion of diurnal and seasonal variation in the boundary layer height. The chemical reaction scheme is described in Appendix 1. The vertical diffusivity is defined as a function of height, atmospheric stability and time of day. It increases linearly with height up to a specified height and then remains at the same value up to the top of the mixing layer. Figure 2.1

shows the diurnal variation in the boundary layer height assumed to be representative for the whole of Great Britain (Singles, 1996).

The main application of FRAME is the prediction of the deposition of reduced nitrogen. The vertical structure of the model and its treatment of vertical dispersion is considered to be of particular importance in this application, because the main sources of ammonia are at ground level and dry deposition of ammonia is a major part of the total deposition of reduced nitrogen. The vertical structure of the models is less important for the prediction of the deposition of sulphur and oxidised nitrogen, because a large part of the sulphur dioxide and oxides of nitrogen are released from tall stacks and dry deposition of nitric oxide is not significant. The time required for these pollutants to disperse uniformly throughout the boundary layer is small compared to the time required for deposition.

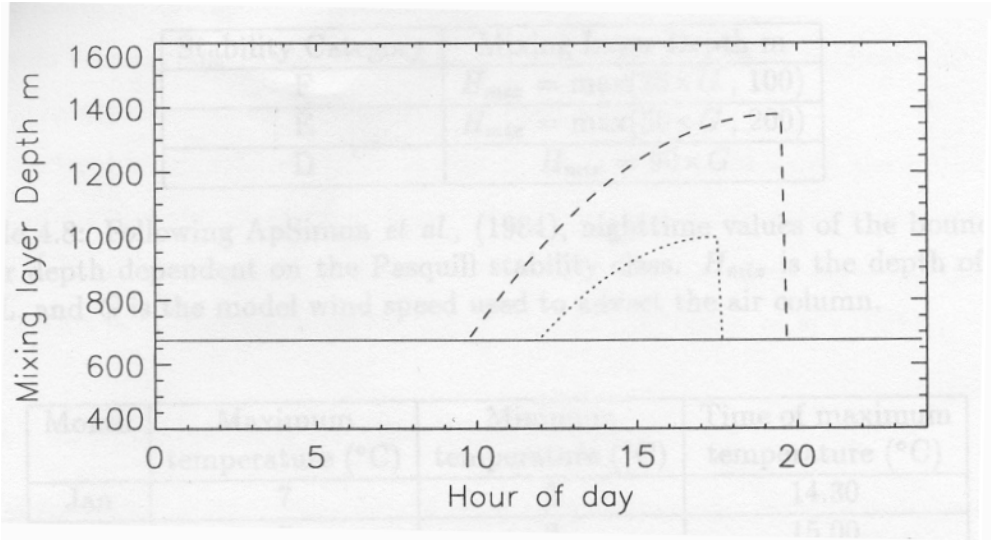

Figure 2.1 Diurnal variation in the boundary layer depth with a cloud cover of 6 oktas. Winter (full line): Spring (dotted line): Summer (dashed line).

2.4 Analytical models

The differential equations describing the processes involved in the deposition of sulphur and nitrogen are to some extent amenable to analytical solution following simplification. Analytical solutions do not have the flexibility of the numerical models and do not include a number of important features. Nevertheless, they are expected to demonstrate similar behaviour to the numerical models and their ease and speed of evaluation has facilitated the identification of the most sensitive model input parameters and the development of methods of analysis of model uncertainty. Analytical models used in this study are described in Appendix 2 and Appendix 3. Appendix 2 provides an analytical solution for the incremental impact of a point source emission of sulphur dioxide. Appendix 3 provides analytical solutions for the incremental impact of point source emissions of oxides of nitrogen for the cases where (1) no ammonia is present in the atmosphere and (2) excess ammonia is present.

3 ACID DEPOSITION MODEL INPUT PARAMETER UNCERTAINTIES

3.1 Introduction

In order to conduct a sensitivity analysis one must consider the range of uncertainty in the main model parameters. The main input parameters included within the models are:

1. Chemical reaction rate constants:
2. Dry deposition velocities;
3. Wet scavenging coefficients (including enhancement in high rainfall areas);
4. Background concentrations of chemical species;
5. Wind speed;
6. Frequency of winds from each wind direction sector;
7. Boundary layer height;
8. Emissions;
9. Speciation of emitted sulphur dioxide and oxides of nitrogen.

The ranges of plausible values for the input parameters are assessed in this section and provide the basis for the baseline model in the uncertainty analysis.

3.2 Reaction rate constants

The expressions used to represent the rates of reaction of the species modelled in the three models are summarised in Appendix 1. The expressions are compared with similar expressions obtained from recent literature. The expressions have been evaluated for typical parameters (temperature 283 K, zenith angle 30^0): the calculated reaction rates are summarised in Table 3.1. Reaction rate expressions for some reactions in recent literature have included uncertainty estimates. Table 3.1 includes an assessment of the range of values. The ranges are expressed in terms of the maximum and minimum values: these may have been estimated as (1) the mean plus and minus two standard deviations, (2) the upper and lower bounds of measured values, or (3) best estimates depending on the quality of the data. The aim of Table 3.1 is to provide working ranges for further analysis.

The reactions schemes included within each of the models are incomplete. Many other possible reactions are possible between the modelled chemical species and other substances in the atmosphere. In some cases, the model reaction schemes represent a complex chain of reactions by a single reaction. The reaction schemes included in the models have been selected on the basis of theoretical considerations and practicality. As a subset of the full chemistry they are therefore only representative of main reactive processes and should not be taken to be an exact simulation of atmospheric reactions. The investigation of uncertainties has considered the reaction schemes included within the models and has not considered the effects of alternative reaction schemes on the predicted rates of deposition.

Table 3.1 Summary of reaction rates

	Reaction rates, cm^3 $molecule^{-1}$ s^{-1}, unless otherwise stated.							
	HARM	TRACK	FRAME	Latest[1] mean	Latest[1] minimum	Latest[1] maximum	Minimum	Maximum
$NO + O_3 \rightarrow NO_2 + O_2$	$1.42 .10^{-14}$	$1.42 . 10^{-14}$	$1.25 . 10^{-14}$	$1.42 . 10^{-14}$	$1.14. 10^{-14}$	$1.71.10^{-14}$	$1.14. 10^{-14}$	$1.71. 10^{-14}$
$NO_2 + h\nu \rightarrow NO + O$ Units s^{-1}	$9.14 . 10^{-3}$	$6.68 . 10^{-3}$	$6.37 . 10^{-3}$	$8.15 . 10^{-3}$	$4.08 . 10^{-3}$	$1.63 . 10^{-2}$	$4.08 . 10^{-3}$	$1.63 . 10^{-2}$
$O + O_2 + M \rightarrow O_3 + M$	$6.40 . 10^{-34}$	Assumed instantaneous	Assumed instantaneous	$6.86 . 10^{-34}$	$6.06 . 10^{-34}$	$7.55 . 10^{-34}$	$6.06 . 10^{-34}$	Assumed instantaneous
$OH + NO_2 (+ M) \rightarrow HNO_3 (+ M)$	$1.50 . 10^{-11}$	$1.46 . 10^{-11}$	$1.10 . 10^{-11}$	$1.59 . 10^{-11}$	$1.01 . 10^{-11}$	$2.50 . 10^{-11}$	$1.01 . 10^{-11}$	$2.50 . 10^{-11}$
$NO_2 + O_3 \rightarrow NO_3 + O_2$	$2.09 . 10^{-17}$	$2.09 . 10^{-17}$	$2.09 . 10^{-17}$	$2.09 . 10^{-17}$	$1.46 . 10^{-17}$	$2.71 . 10^{-17}$	$1.46 . 10^{-17}$	$2.71 . 10^{-17}$
$NO_3 + h\nu \rightarrow NO_2 + O$ Units s^{-1}	$8.34 . 10^{-2}$	Assumed instantaneous	Assumed instantaneous	$1.21 . 10^{-1}$	$6.03 . 10^{-2}$	$2.41 . 10^{-1}$	$6.03 . 10^{-2}$	$2.41 . 10^{-1}$
$NH_3 + HCl \rightarrow NH_4Cl$	$1.00 . 10^{-14}$	$1.00 . 10^{-14}$					$5.00 . 10^{-15}$	$2.00 . 10^{-14}$
$HNO_3 \rightarrow$ marine aerosol Units s^{-1}	$3.00 . 10^{-5}$	$2.30 . 10^{-4}$	$1.00 . 10^{-5}$				$1.00 . 10^{-5}$	$2.30 . 10^{-4}$
$HNO_3 \rightarrow$ rural aerosol Units s^{-1}	$3.00 . 10^{-5}$	$9.10 . 10^{-4}$	$1.00 . 10^{-5}$				$1.00 . 10^{-5}$	$9.10 . 10^{-4}$
$NO_3^- \rightarrow HNO_3$ Units s^{-1}			$5.00 . 10^{-6}$					$5.00 . 10^{-6}$
$NO_3 + NO_2 \rightarrow N_2O_5$	$6.72 . 10^{-15}$	Assumed instantaneous	Assumed instantaneous	$2.44 . 10^{-13}$	$8.02 . 10^{-15}$	$5.86 . 10^{-13}$	$6.72 . 10^{-15}$	$5.86 . 10^{-13}$
$N_2O_5 \rightarrow$ marine aerosol, Units s^{-1}	$3.00 . 10^{-5}$	$1.10 . 10^{-4}$	Assumed instantaneous				$3.00 . 10^{-5}$	Assumed instantaneous
$N_2O_5 \rightarrow$ rural aerosol, Units s^{-1}	$3.00 . 10^{-5}$	$2.20 . 10^{-4}$	Assumed instantaneous				$3.00 . 10^{-5}$	Assumed instantaneous
$NH_3 + HNO_3 \rightarrow NH_4NO_3$	$1.00 . 10^{-14}$	$1.00 . 10^{-14}$	Assumed instantaneous				$5.00 . 10^{-15}$	$2.00 . 10^{-14}$
$SO_2 + OH \rightarrow SO_4$		$1.06 . 10^{-12}$		$4.74 . 10^{-13}$	$1.66 . 10^{-13}$	$7.50 . 10^{-13}$		$1.06 . 10^{-12}$
$SO_2 \rightarrow SO_4$, Units s^{-1}	$2.80 . 10^{-6}$	$2.00 . 10^{-6}$	$2.80 . 10^{-6}$				$1.40 . 10^{-6}$	$4.20 . 10^{-6}$
$SO_4 + 2NH_3 \rightarrow (NH_4)_2SO_4$		3.3×10^{-15}						
$OH + NO (+ M) \rightarrow HONO (+ M)$		$1.05 . 10^{-11}$		$7.59 . 10^{-12}$	$5.36 . 10^{-12}$	$9.85 . 10^{-12}$	$5.36 . 10^{-12}$	$1.05 . 10^{-11}$
$HONO + h\nu \rightarrow OH + NO$, Units s^{-1}		$1.40 . 10^{-3}$		$1.83 . 10^{-3}$	$9.13 . 10^{-4}$	$3.65 . 10^{-3}$	$9.13 . 10^{-4}$	$3.65 . 10^{-3}$
$HONO \rightarrow$ marine nitrite aerosol, Units s^{-1}		$9.00 . 10^{-5}$					$4.50 . 10^{-5}$	$1.80 . 10^{-4}$
$HONO \rightarrow$ rural nitrite aerosol, Units s^{-1}		$3.20 . 10^{-4}$					$1.60 . 10^{-4}$	$6.40 . 10^{-4}$
$NO_2 \rightarrow HONO$, Units s^{-1}		$7.00 . 10^{-7}$					$3.50 . 10^{-7}$	$1.40 . 10^{-6}$
$NO_2 + CH_3COO_2 (+ M) \rightarrow PAN (+ M)$		$1.11 . 10^{-11}$	$3.20 . 10^{-12}$	$8.17 . 10^{-13}$	$1.26 . 10^{-12}$	$7.91 . 10^{-13}$	$7.91 . 10^{-13}$	$1.11 . 10^{-11}$

[1]The "latest" values were obtained from a review of the chemical kinetic literature. Further details of the reference sources can be found in Appendix 1. Blank cells indicate that the reaction is not included explicitly in the model, or no value was found in the literature survey.

3.3 Dry deposition velocities

Table 3.2 summarises typical values and ranges obtained from the literature for the dry deposition velocities of the reactive gas species modelled in HARM, TRACK and FRAME. The dry deposition of aerosol particulates depends on particle size, wind speed and the nature of the underlying surface. The NRPB working group on atmospheric dispersion (Jones, 1983) suggested that the deposition velocity for particles used in modelling studies would be in the range 0.1-1 mm s^{-1} for particles of around 1 μm. This work has recently been updated. Underwood (2001) suggests a best estimate of 0.661 mm s^{-1} for 1 μm particles, for deposition to meadow grass and low crops under typical meteorological conditions: he gives a conservative estimate of 3.35 mm s^{-1}. His values for urban grass, roofs and paved areas are similar.

Table 3.3 shows the values of the dry deposition velocities used in the HARM, TRACK and FRAME models.

The models do not distinguish between the rates of dry deposition of sulphuric acid and of ammonium sulphate. Sulphuric acid is treated effectively as particulate aerosol. However the rate of homogeneous nucleation of sulphuric acid is rather slow in atmospheres deficient in ammonia. The critical concentration of sulphuric acid required for nucleation may be around 1 ppb in the absence of ammonia (Finlayson-Pitts and Pitts, 2000) so that under some conditions the sulphuric acid is present as a reactive gas with enhanced rates of dry deposition.

Table 3.2 Dry deposition velocities

SPECIES	ACID GRASSLAND	CALCAREOUS GRASSLAND	HEATHLAND	CONIFEROUS WOODLAND	DECIDUOUS WOODLAND
SO_2	12±3mms^{-1} [1]		8±4 mms^{-1} [1]	2±1mms^{-1} [2] 7.2±6.5mms^{-1} [3]	10.1mms^{-1} (Day) [4] 6-7.2mms^{-1} (Seasonal)[4] 5-11mms^{-1} [5] 3-13mms^{-1} [6] 6.9-19.2mms^{-1} [26]
NO_2	1.1-2.4mms^{-1} [7]		1mms^{-1} [8]	1.5±1.3mms^{-1} [9] 1.4±1.1mms^{-1} [9] 1-2mms^{-1} [10]	
HNO_3	17-35mms^{-1} [11] 25±9mms^{-1} [27]			76mms^{-1} [12] [10-135mms^{-1} [13,14]] 6-34mms^{-1} [15]	20-100mms^{-1} [16] 22-60mms^{-1} [17]
NH_3	15-20mms^{-1} [18] (pH=3.9)	1-11mms^{-1} [18]	19mms^{-1} [19] 8.3mms^{-1} [20] 11.7mms^{-1} [21]	20-30mms^{-1} [22] 66mms^{-1} [18] 32mms^{-1} [23,24] 14-200mms^{-1} [25]	

References:

1. Erisman *et al*. (1993), Atmos. Environ. 27, 1153-1161
2. Galbally (1979), Nature 280, 49-50
3. Lorenz and Murphy (1985), Atmos. Environ. 19, 797-802
4. Finkelstein *et al*. (2000), J. Geophys. Res. 105, 15365-15377
5. Meyers and Baldocchi (1988), Tellus 40B, 270-284
6. Baldocchi (1988), Atmos. Environ. 22, 869-884
7. Hesterberg *et al*. (1996), Environ. Pollut. 91, 21-34
8. Coe and Gallagher (1992), Q. J. Roy. Met. Soc. 118, 767-786
9. Rondón *et al*. (1993), J. Geophys. Res. 98, 5159-5172
10. Johansson (1987), Tellus 39B, 426-438
11. Müller *et al*. (1993), Tellus 45B, 346-367
12. Sievering *et al*. (2001), Atmos. Environ. 35, 3851-3859
13. Anderson and Hovmand (1995), Water Air Soil Pollut. 85, 2211-2216
14. Goulding (1998), New Phyt. 139, 49-58
15. Hanson and Garten (1992), New Phtol. 122, 329-337
16. Hanson and Lindberg (1991), Atmos. Environ. 25A, 1615-1634
17. Meyers *et al*. (1989), B.-Layer Meteorol. 49, 395-410
18. Sutton *et al*. (1993), Q.J.Roy. Met. Soc. 119, 1023-1045
19. Duyzer (1994), J. Geophys. Res. 99, 18757-18763
20. Hansen (1999), Water Air Soil Pollut. 113, 357-370
21. Flechard and Fowler (1998), Q.J.Roy. Met. Soc. 124, 759-791
22. Duyzer *et al*. (1994), Atmos. Environ. 28, 1241-1253
23. Duyzer *et al*. (1992), Environ. Pollut. 75, 3-13
24. Wyers *et al*. (1992), Environ. Pollut. 75, 25-28
25. Andersen *et al*. (1993), Atmos. Environ. 27A, 189-202
26. Matt *et al*. (1987), Water Air Soil Pollut. 36, 331-347
27. Huebert and Robert (1985) J. Geophys. Res. 90, 2085-209

Table 3.2 Dry deposition velocities used in the HARM, TRACK and FRAME models

	Dry deposition velocity, mm s^{-1}		
	HARM (UK land area)	**TRACK (default values)***	**FRAME**
Sulphur dioxide	Land use dependent 0.4-50.5	3.5 Daytime 0 Night	8
Nitric oxide	0	Not applicable	0
Oxides of nitrogen	Not applicable	2	Not applicable
Nitrogen dioxide	0.7-1.6	2	1
Nitric acid	40	40	40
Ammonia	0.1-31.4	10	Land use and time variable
Hydrogen chloride	20	20	Not applicable
Nitrous acid	Not applicable	10	Not applicable
Peroxy acetyl nitrate	Not applicable	1	2
Nitrate and nitrite aerosols	1	1	1
Sulphate aerosols	1	0.5	1
Ammonium aerosols	1	0.5	1
Chloride aerosol		1	Not applicable
All aerosols	1		
		*Model has optional land use dependency	

3.4 Wet deposition scavenging coefficients

The rate of wet deposition of particulate aerosol depends on the particle terminal velocity and the rate of precipitation. For a particle with terminal velocity of 1mm s^{-1}, the theoretical scavenging coefficient or washout coefficient is approximately1 $\times 10^{-4}$ s^{-1} at a rainfall rate of 1mm h^{-1}. This value increases to approximately 4×10^{-4} s^{-1} for a particle with a terminal velocity of 50 mm s^{-1}. The washout coefficient increases non-linearly with rainfall rate, increasing approximately in proportion to the rainfall rate raised to the 2/3 power (Pasquill and Smith, 1983).

For gaseous species, the washout coefficient depends on the solubility of the gas in the raindrops and the rate of rainfall.

Table 3.4 shows values of the wet scavenging coefficient for a rainfall rate of 1 mm h^{-1} suggested by the NRPB working group on atmospheric dispersion (Jones, 1983). This work has recently been updated (Underwood, 2001). He suggests a best estimate of 3×10^{-5} s^{-1} for 1 μm particles for a rainfall rate of 1mm h^{-1}: he gives a conservative estimate of 4×10^{-4} s^{-1}. He also gives a best estimate value of 6×10^{-5} s^{-1} for reactive gases and considers this to provide a conservative upper limit on wet deposition. The rate is limited by the gas phase resistance between the air and the rain droplets.

Table 3.4 Suggested values for the wet scavenging coefficient for 1 mm h^{-1} rainfall rate

Type of material	Wet removal coefficient, s^{-1}
Noble gas	0
Reactive gas	3×10^{-5} to 3×10^{-4}
Particles ~1 μm	3×10^{-5} to 3×10^{-4}
Particles ~10 μm	3×10^{-5} to 3×10^{-4}

The models HARM, TRACK and FRAME do not distinguish between periods when it is raining and periods when it is not raining. Wet deposition is represented by a "constant drizzle" approximation. To a first approximation, constant drizzle wet scavenging coefficients may be estimated pro rata on the basis of total rainfall (annual precipitation in mm/8760). The constant drizzle scavenging coefficients would then be approximately 10% of those shown in Table 3.4. A more sophisticated modelling approach was taken during the development of HARM. An air parcel containing an initial concentration of each wet-scavenged pollutant was subjected to alternating wet and dry periods. Dry deposition was assumed to occur at a constant rate fixed by the dry deposition velocity. Wet scavenging was assumed to occur only during wet periods, with a first order removal coefficient proportional to rain rate. Distributions about the central values of rainfall rate (1 mm h^{-1}), dry and wet period lengths (40 and 8 hours respectively) were assumed and each parameter was sampled in a Monte Carlo analysis. Constant drizzle coefficients were obtained by fitting a simple first order loss coefficient to the time dependent average wet scavenging rates. Table 3.5 shows the constant drizzle coefficients derived. Table 3.5 also shows the values used in TRACK and FRAME. The TRACK values are often the same as those used in HARM, reflecting the common parentage of the models. The values used in FRAME are markedly larger.

Table 3.5 Wet scavenging coefficients used in HARM, TRACK and FRAME

	HARM (based on 1990 rainfall)	TRACK	FRAME (based on annual rainfall of 1000 mm)
Nitrate aerosol	1.3×10^{-5}	1.3×10^{-5}	4×10^{-5}
Sulphate aerosol	1.3×10^{-5}	1.3×10^{-5}	4×10^{-5}
Ammonia	9×10^{-6}	9×10^{-6}	5.7×10^{-5}
Nitric acid	9×10^{-6}	9×10^{-6}	5.7×10^{-5}
Sulphur dioxide	1×10^{-6}	1×10^{-6}	1.1×10^{-5}
Nitrite aerosol	Not applicable	1.3×10^{-5}	Not applicable
Hydrochloric acid	1.89×10^{-5}	1.9×10^{-5}	Not applicable
Ammonium aerosol	1.3×10^{-5}	1.3×10^{-5}	4×10^{-5}
Chloride aerosol	1.0×10^{-5}	1.3×10^{-5}	Not applicable

Enhanced wet scavenging of gases and particulates occurs in upland areas as the result of "seeder-feeder enhancement" in which seeder rain falling from high altitudes sweeps out particles in the feeder cloud surrounding a hill cap. The models represent this mechanism by means of a seeder-feeder enhancement factor. HARM increases the wet scavenging coefficient of all species, except sulphur dioxide, ammonia and hydrogen chloride in unit steps for each 500 mm additional rainfall. TRACK increases the wet

scavenging coefficient of aerosols by a factor of 1 to 3 when the annual rainfall exceeds typically 800 mm. It also has a more sophisticated direction dependent enhancement option. The rate of sulphur dioxide oxidation is also increased in upland areas in HARM and TRACK. HARM increases the reaction rate in unit steps for each 250mm additional rainfall. TRACK increases the rate of oxidation by a factor of typically 1.3.

3.5 Background concentrations

The models include an assumption about the initial concentration of ozone. HARM assumes that there is an initial concentration of 30 ppb at the start of the trajectory and that the ozone is depleted by the reactions that take place. TRACK assumes an initial concentration of 34 ppb and that ozone depleted by reaction is regenerated with the concentration being maintained in dynamic equilibrium controlled by an effective dry deposition velocity of 6 mm s^{-1}. FRAME assumes a constant ozone concentration of 30 ppb across the model domain.

TRACK also includes reactions involving hydroxyl, nitrate and acetyl peroxy radicals. The concentration fields are taken from the output of a global 3-D model of the troposphere, STOCHEM. The model can also use invariant radical fields. Default values are:

OH	1.6×10^6 molecules cm^3 (day only);
CH_3COO_2	1.6×10^6 molecules cm^3 (day only);
NO_3	2.5×10^7 molecules cm^3 (night only).

3.6 Wind speed

All three models assume a constant geostrophic wind speed that is independent of location. HARM and TRACK assume that the wind speed is independent of wind direction. FRAME uses a direction-dependent wind speed. The wind speeds used are:

HARM	10.4 m s^{-1}
TRACK	7.5 m s^{-1}
FRAME	5.62-8.61 m s^{-1} (direction dependent)

All three models refer to Jones (1981) as the source of the wind speed data used in the derivation of the average wind speed. Table 3.6 shows the source data presented by Singles (1996, p103).

The arithmetic mean of this data is 10.4 m s^{-1} as used in HARM. Singles (1996) carried out model runs using the FRAME model for each wind speed/direction class and then calculated an optimised single value wind speed, for each wind direction, that best reproduced the combined model predictions for ammonia deposition and concentrations. The optimised wind speed was direction dependent and was in the range 5.62-8.61 m s^{-1}. In earlier work related to the development of the HARM model Derwent, Dollard and Metcalfe (1988) used the mid-point of the modal wind speed range (7.5 m s^{-1}).

Table 3.6 Representative wind rose used to derive average wind speed

Wind sector	Wind speed band, m s^{-1}					
	0-5 (2.5)	5-10(7.5)	10-15 (12.5)	>15 (20)	Arithmetic Mean	Harmonic mean
0-45	2.556	3.567	2.7	2.073	9.9	6.0
45-90	2.895	2.387	1.437	1.16	8.4	4.8
90-135	2.73	2.818	0.8571	0.23	6.5	4.3
135-180	2.98	2.88	1.094	1.64	8.8	4.9
180-225	2.61	3.602	1.85	3.51	11.0	6.3
225-270	2.61	6.785	4.26	5.655	11.6	7.5
270-315	3.089	4.773	4	5.972	11.9	7.2
315-360	2.99	5.937	4.242	4.09	10.8	6.8
Total					10.4	6.2

The form of the model equations is such that the modelled concentrations are inversely proportional to wind speed. This would suggest that the appropriate average is the harmonic mean. The Warren Spring Laboratory statistical dispersion model LPAM made use of direction dependent harmonic mean wind speeds. Table 3.6 shows the arithmetic and harmonic means for each wind direction. The harmonic mean value is rather less than the arithmetic mean.

Table 3.6 shows marked differences in wind speed with direction. The error in wind speed associated with using a wind speed that is independent of wind direction for a particular source receptor pair is approximately +/- 25%.

The models use a limited number of wind roses to represent the whole of the United Kingdom. Table 3.7 summarises geostrophic wind data obtained at a number of sites in the UK.

Table 3.7 Geostrophic wind data at a number of UK sites

Site OS grid reference	Wind speeds, m s^{-1}			
	Direction dependent arithmetic means	Arithmetic mean	Direction dependent harmonic means	Harmonic mean
3404 4119	7.5-11.4	9.9	5.6-8.4	7.2
5260 1350	7.9-12.6	9.6	5.9-8.9	6.9
1645 0386	6.6-13.9	10.6	5.2-10.1	7.7
6500 3178	7.1-11.5	9.6	5.5-7.9	7.0
4445 11353	8.4-12.6	10.7	6.0-9.4	7.7
1346 5194	7.1-12.2	10.2	5.2-9.1	7.5
3445 7234	7.2-10.2	9.0	5.3-8.1	6.3
1474 9315	6.4-12.0	10.1	5.2-9.4	7.2
All sites		10.0		7.2

Table 3.7 shows that the variation in average wind speeds across the UK is approximately +/- 5 to10%. The variation is small compared to the directional variation in average wind speeds and the uncertainty over the most appropriate definition for the average wind speed.

3.7 Wind direction

All three models use a single wind rose to represent the frequency of wind direction over the whole of the United Kingdom. Table 3.8 shows the frequency of geostrophic winds in the wind sectors 15-45 degrees and 195-225 degrees. The use of a single wind rose is likely to result in uncertainty in the frequency that the wind is in the relevant sector between a source–receptor pair of +/- 10 to 50%.

Table 3.8 Frequency of wind in two wind sectors at sites throughout the UK

Site OS grid reference	Frequency of wind in sector, %	
	15-45^{o}	195-225^{o}
3404 4119	4.11	15.33
5260 1350	7.21	15.24
1645 0386	3.33	12.2
6500 3178	4.53	14.14
4445 11353	4.14	12.93
1346 5194	3.97	12.71
3445 7234	5.48	14.5
1474 9315	4.12	14.8

3.8 Boundary layer height

HARM and TRACK assume a constant boundary layer height of 800 m throughout the model domain. FRAME on the other hand allows for seasonal and diurnal variations in the boundary layer height (Fig .2.1), but applies the same profile over the whole of the UK.

TRACK and HARM use the boundary layer height to provide an upper bound to the model domain. The value of 800 m has been selected as representative of typical neutral stability conditions occurring for much of the time in the UK (Clarke, 1979). Clarke presents nomograms that may be used to assess the height of the boundary layer. Examination of these nomograms suggests that earlier subjective estimates of the uncertainty in the boundary layer height (Derwent and Curtis, 1988) of +/-20% are reasonable.

3.9 Emissions

3.9.1 Background

The National Atmospheric Emissions Inventory (NAEI) contains estimates of emissions to air of 39 pollutants (including seven pollutant groups) covering greenhouse gases, air quality strategy pollutants, acidifying gases, tropospheric ozone precursors, and

hazardous air pollutants. The NAEI is updated each year, with results reported in an annual report (most recently in Goodwin *et al*, 2001).

Each annual report includes expert judgements of uncertainty in the national emission total for each pollutant. These are intended as 'ball-park' estimates of the overall uncertainty in each inventory and are made by the NAEI team member responsible for compilation of that inventory.

With limited exceptions, these 'ball-park' estimates have not changed in recent years, giving the impression that the NAEI has not improved in that period despite the considerable research into emission factors carried out. In reality, the inventory is more complete, detailed and accurate now than in the past; it is more useful and national emission totals are more likely to be accurate. The problem lies in the presentation of uncertainty, since the current expression of uncertainty is simplistic and lacks rigour in its use of quasi-statistical terminology, and so it is not capable of reflecting improvement.

As part of the programme of work to maintain the NAEI, a more detailed assessment has been made of the uncertainty in the NAEI using software better able to manipulate and display statistical information. This detailed approach provides a more quantitative measure of uncertainty.

3.9.2 Methods

Quantitative estimates of the uncertainties in the NAEI have been calculated using a direct simulation approach. This procedure corresponds to the IPCC Tier 2 approach discussed in the Good Practice Guidance (IPCC, 2000), as well as the Tier 2 method proposed in the draft 'Good Practice Guidance for CLRTAP Emission Inventories', produced for inclusion in the EMEP/CORINAIR Guidebook on Emission Inventories. The approach, as applied to the UK greenhouse gas inventory, has also been described in detail by Charles *et al* (1998).

A brief summary of the method is given below.

1. An uncertainty distribution is allocated to each emission factor and each activity rate. The distributions used were drawn from a limited set of either uniform, normal, triangular, beta, or log-normal distributions. The parameters of the distributions for each emission factor or activity rate were set either by analysing the available data on emission factors and activity data, or by expert judgement.
2. A calculation was set up to estimate the emission of each pollutant by sampling individual data values from each of the emission factor and activity rate distributions on the basis of probability density and evaluating the resulting emission. Using the software tool @RISK™, this process could be repeated many times in order to build up an output distribution of emission estimates, both for individual sources but also for total UK emissions of each pollutant.
3. The mean value for each emission estimate and the national total was recorded, as well as the standard deviation and the 95% confidence limits i.e. the emission values at the 2.5% cumulative probability and the 97.5% cumulative probability.
4. The process was carried out first using data for 1999, taken from the 1999 version of the NAEI (published in Goodwin *et al*, 2001). The analysis was then extended to data for the year 2000, taken from the 2000 version of the NAEI (report in preparation) for those pollutants where changes had been made to the methodology

used to estimate emissions. For this repeat of the analysis it was necessary to re-evaluate the probability distributions used for emission factors and activity rates and make modifications to the assumptions where appropriate.

5. A key source analysis was undertaken, following the IPCC Tier 2 method (IPCC, 2000). The key source analysis identifies the major contributors to inventory uncertainty.

The method was applied to the known sources of emissions that have been included in the NAEI: other sources of emission may also contribute to the overall uncertainty in the emissions estimates, but the contribution has not been quantified.

3.9.3 Results

Results of the analysis are shown in Table 3.9. There are some significant differences in the detailed numbers compared with the expert judgements made for the 1999 NAEI report (*ibid*), as shown in Table 3.10. In general the expert judgements gives higher estimates of the uncertainty in the emission inventories.

Key sources of uncertainty in the estimation of emissions identified using the IPCC Tier 2 method are listed in Table 3.11.

Table 3.9 Results of uncertainty analysis for gaseous pollutants (national emissions in ktonnes) from known sources

Pollutant	Year	Mean	2.5%	97.5%	Std Dev	Range as % of mean
Hydrogen chloride	1999	98.1	80.4	116	9.0	+/- 18%
Ammonia	1999	348	284	417	34	+ 20% / - 18%
Ammonia	2000	320	262	383	31	+ 19% / - 18%
Oxides of nitrogen	1999	1605	1497	1718	57	+/- 7%
Oxides of nitrogen	2000	1525	1421	1634	54	+/- 7%
Sulphur dioxide	1999	1187	1149	1225	19	+/- 3%
Sulphur dioxide	2000	1156	1117	1197	21	+ 4% / - 3%

Table 3.10 Comparison of uncertainty in known sources according to expert judgement and by detailed Monte Carlo analysis

Pollutant	Expert judgement	Uncertainty analysis
Sulphur dioxide	+/- 10-15%	+/- 3%
Oxides of nitrogen	+/- 30%	+/- 7%
Volatile organic compounds	+/- 30%	+ 11% / - 9%
Ammonia	> +/- 30%	+ 20% / - 18%

Table 3.11 Key sources of uncertainty in emissions estimates

Source	NH_3	HCl	NOx	SO_2
Chemicals manufacture				
Cold start emissions from catalyst cars			X	
Cold start emissions from non-catalyst cars				
Domestic use of coal as a fuel				
Domestic use of natural gas as a fuel			X	
Domestic use of wood as a fuel				
Process emissions from cement production			X	
Process emissions from crude oil refineries				
Tailpipe emissions from articulated HGVs on motorways			X	
Tailpipe emissions from articulated HGVs on rural roads			X	
Tailpipe emissions from buses			X	
Tailpipe emissions from catalyst cars on motorways			X	
Tailpipe emissions from catalyst cars on rural roads			X	
Tailpipe emissions from catalyst cars on urban roads			X	
Tailpipe emissions from non-catalyst cars on motorways			X	
Tailpipe emissions from non-catalyst cars on rural roads			X	
Tailpipe emissions from non-catalyst cars on urban roads			X	
Tailpipe emissions from rigid HGVs on rural roads			X	
Tailpipe emissions from rigid HGVs on urban roads				
Use of coal by power stations		X	X	X
Use of coke in sinter production				
Use of gas oil by coastal shipping			X	
Use of gas oil in agricultural vehicles and machinery			X	
Use of gas oil in industrial off-road vehicles and machinery			X	
Use of landfill gas by power stations			X	
Use of natural gas by the general industry sector			X	
Use of petrol in garden vehicles and machinery				
Use of petrol in industrial off-road vehicles and machinery				
Use of process gases as fuels on offshore oil & gas installations			X	
Emissions from soils	X			
Non-dairy cattle wastes	X			
Wastes of other poultry	X			
Pig wastes	X			
Sheep wastes	X			

3.10 Speciation of emissions

The emissions of sulphur from large sources such as power stations are mostly in the form of sulphur dioxide. However, a small part is released as sulphur trioxide, sulphates or as sulphuric acid. The US EPA report AP42 indicates that approximately 0.7 % of the sulphur in the fuel in bituminous coal combustion is released as sulphur trioxide and a similar quantity is released as particulate sulphate. For fuel oil combustion, AP42 estimates that 1 to 5% is released as sulphur trioxide and a further 1 to 3% is released as particulate sulphate. TRACK allows for a certain proportion of sulphur dioxide released as sulphur trioxide and gaseous and particulate sulphates.

For most fossil fuel combustion systems the major part of the oxides of nitrogen released is in the form of nitric oxide. AP42 indicates that the proportion of nitrogen dioxide is usually less than 5%. TRACK and FRAME allow for a certain proportion of the release to be as nitrogen dioxide.

This systematic sensitivity analysis of the uncertainty in the national emissions leads to some estimates, notably for sulphur and nitrogen oxides, which are substantially lower than those which would have been estimated by expert judgement (see Table 3.10). It is not within this study to explore alternative methodologies, but it is recognised that Monte Carlo analysis is not able to treat uncertainties in processes which are unknown. In addition uncertainties in individual processes are treated as independent variables.

4 DEPOSITION MODEL UNCERTAINTIES

4.1 Introduction

The uncertainty in the predicted deposition resulting from the uncertainty in the input parameters has been assessed for each of the models in turn. Initial studies were made using the analytical models described in Appendices 2 and 3. The initial studies were carried out to help identify the most important parameters affecting model outputs and to assist in the development of data handling methods. Further investigation was then carried out using the numerical models TRACK, HARM and FRAME.

The general approach taken in the investigation was to use the models to predict rates of deposition for various combinations of input parameter values selected from the plausible range of values identified in Section 3. Three alternative sampling strategies were employed:

1. Monte Carlo simulation in which the values of all the input parameters were selected at random from their plausible ranges;
2. First order error analysis in which the input parameters were changed one at a time from the baseline value;
3. Sampling based on a Latin Square.

The alternative sampling strategies have been compared.

The sampling strategies employed assume that the input parameters may be sampled independently of each other. Consideration was given to whether the input parameters might be strongly correlated. Some parameters (the dry deposition velocities and washout coefficients of the various aerosol species) were considered likely to be strongly correlated and were not sampled independently. The remaining parameters may be correlated slightly, but the effects have not been taken into account.

There are many ways of expressing the uncertainty in model results. The approach taken here has been to determine the arithmetic mean, and the 5^{th} and 95^{th} percentile values, to represent the working value and upper and lower bounds for the predicted rates of deposition. The data has also been presented in terms of cumulative probability distributions: the cumulative probability distribution is compared with that for an idealised log-normal distribution. (The log-normal distribution was selected empirically-see Section 4.2.3, for example).

Acid deposition models may be used to predict both the total rates of deposition from all sources and the incremental rate of deposition from a particular source, for example an individual power station. The uncertainty in both these types of prediction has been addressed. The general approach taken was to carry out model runs for the baseline case first (i.e. in the absence of the particular source) and then to repeat the model runs with the additional source for identical sets of input parameters. The effects of linearity of the acid deposition models with respect to the rate of emission of pollutants were investigated by carrying out two sets of model runs with different rates of emission from the additional source.

4.2 Sulphate deposition analytical model

4.2.1 Monte Carlo analysis

The equations representing the analytical solution of the model equations presented in Appendix 2 have been evaluated for input values in ranges identified from the assessment described in Section 3. The input ranges are shown in Table 4.1. Values of each parameter were taken at random from the range. A uniform distribution was assumed within the range: this assumption implies that there is no information about the shape of the distribution and is expected to lead to a conservative estimate of the consequent uncertainty in the model output. One thousand evaluations were carried out.

Table 4.1 Ranges of input parameters used in Monte Carlo analysis of sulphate deposition analytical model

Parameter	Units	Baseline	Range
Emission rate into 20 km wide parcel of air	molecules/s	$6.023 \cdot 10^{23}$	+/-20%
Boundary layer height	m	800.0	+/-20%
Wind speed	m/s	7.5	+/-25%
Wind direction frequency		0.15	+/-20%
Fraction emitted as sulphur trioxide or sulphates		0.03	+/-70%
Homogeneous rate of oxidation of sulphur dioxide, k_{s1}	cm^3 $molecule^{-1}$ s^{-1}	$4.74\ 10^{-13}$	+/-100%
[OH]	molecules cm^{-3}	$8\ 10^5$	+/-100%
Aqueous phase oxidation of sulphur dioxide, k_{s2}	s^{-1}	$2.\ 10^{-6}$	+/-50%
Dry deposition sulphur dioxide	m s^{-1}	0.008	+/-80%
Dry deposition total sulphate	m s^{-1}	0.0005	0%,+100%
Wet scavenging coefficient sulphur dioxide	s^{-1}	$1.\ 10^{-6}$	0%, +600%
Wet scavenging coefficient total sulphate	s^{-1}	$1.3.\ 10^{-5}$	0%, +400%

Figure 4.1 shows the mean, 5th percentile and 95th percentile total sulphate concentrations predicted by the model as a function of distance downwind of the source. The model predicts that the maximum sulphate concentration will be present at approximately 200 km downwind of the source. The 95th percentile concentration at around the location of maximum impact is approximately a factor of 2 times the average value: the 5th percentile is approximately half the average value.

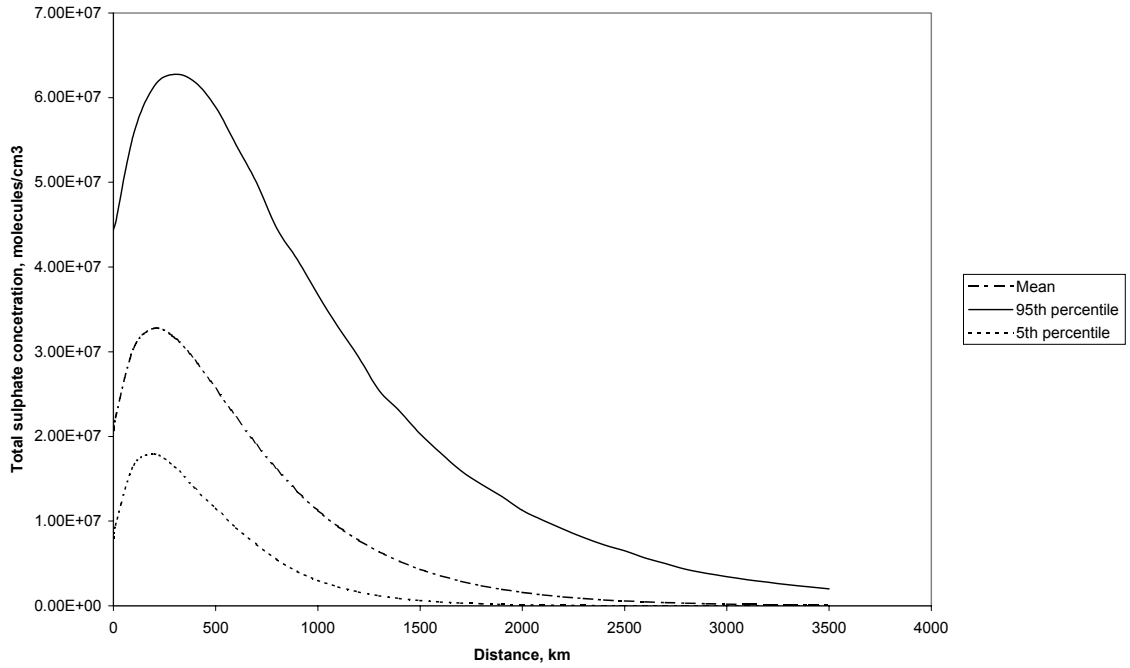

Figure 4.1 Mean, 5th and 95th percentiles of predicted total sulphate concentrations using the analytical model

Figure 4.2 shows the mean, 5th percentile and 95th percentile total sulphur deposition rates predicted by the model as a function of distance downwind of the source. The model predicts that the maximum sulphur deposition rate will be close to the source. The 95th percentile deposition rate is approximately a factor of 2 times the average value: the 5th percentile is approximately half the average value.

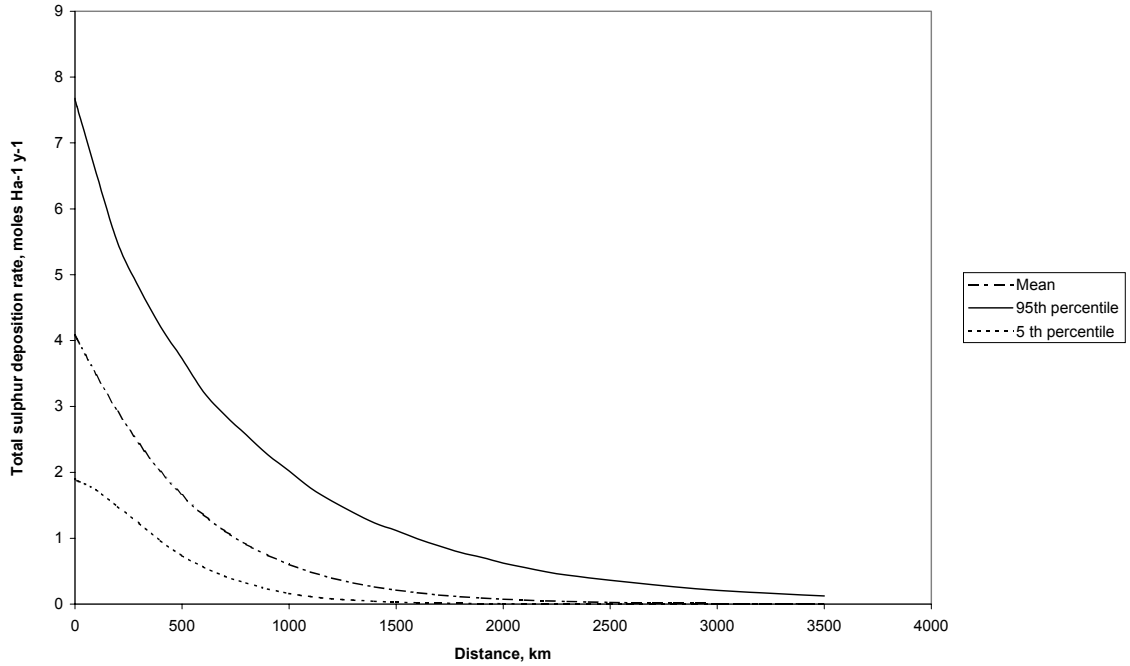

Figure 4.2 Mean, 5th and 95th percentiles of predicted total sulphur deposition at receptors using the analytical model

Figure 4.3 shows the predicted mean, 5th percentile and 95th percentile distance integrated total sulphur deposition as a function of distance down wind of the source. The integrated deposition is shown to increase rapidly up to a distance of approximately 500 km. At greater distances the total deposition approaches the total quantity of material released i.e. nearly all the material released is deposited. Close to the source, the 95th percentile total deposition is approximately twice the mean value: the 5th percentile is approximately half the mean value. At greater distances, the range of predicted values simply reflects the assumed uncertainty in the rate of emission.

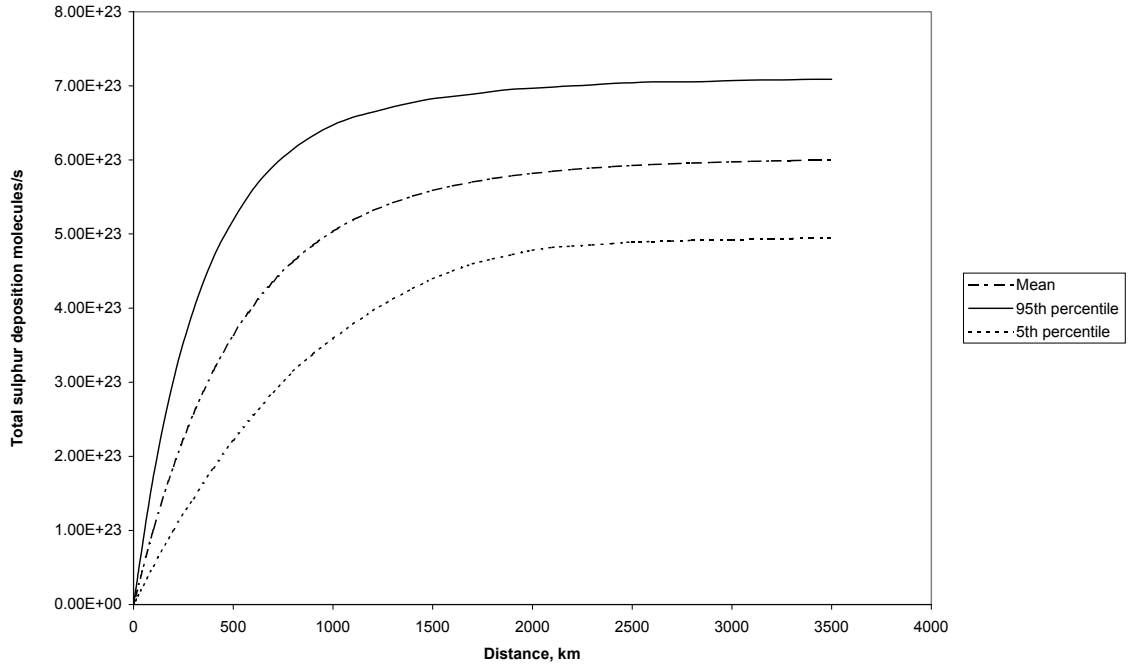

Figure 4.3 Mean, 5th and 95th percentiles of predicted distance integrated total sulphur deposition using the analytical model

4.2.2 Contribution to variance

The contribution, C(p), of the variance, V(p) of each of the parameters, p, to the overall variance, V(ϕ), can be estimated on the basis of a Taylor Series expansion, and this constitutes a first order error analysis:

$$C(p) = \left(\frac{\partial \phi}{\partial p}\right)^2 \frac{V(p)}{V(\phi)}$$

where ϕ is the natural logarithm of the species concentration, or rate of deposition. The slope $\partial\phi/\partial p$ was determined by linear regression of the model results.

Figure 4.4 shows the cumulative contributions to the variance in the logarithm of the total sulphate concentration from each of the model parameters.

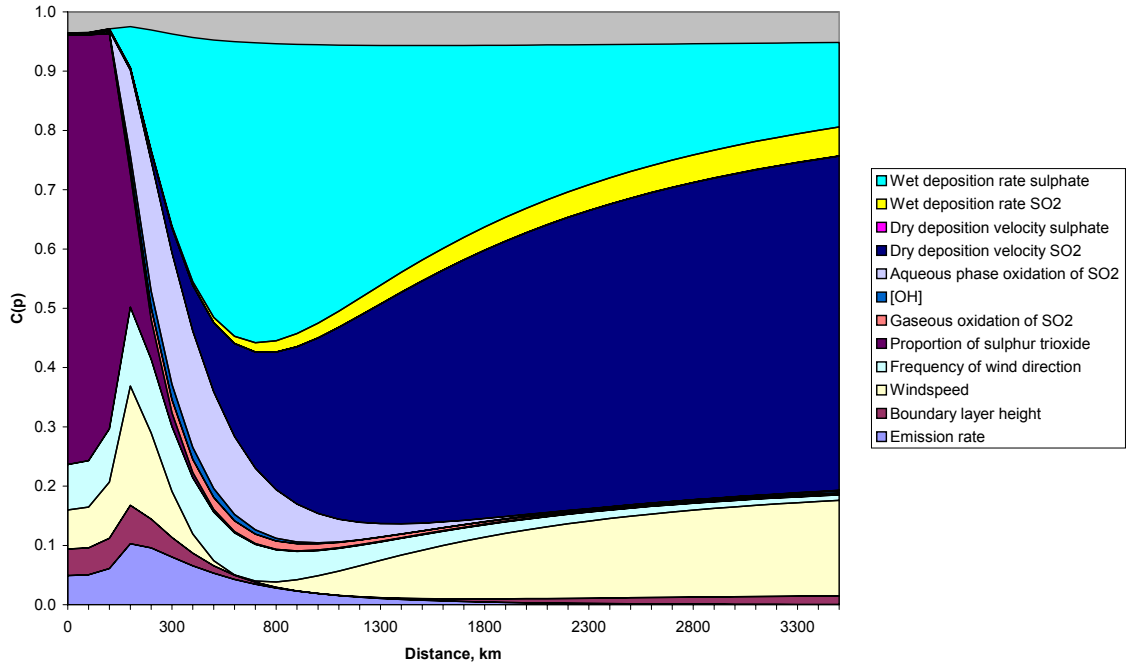

Figure 4.4 Cumulative contributions to variance in predicted total sulphate concentration using the analytical model as a function of distance

Close to the source, the first order error analysis explains nearly all of the overall variance. The major contributors to the overall variance of predicted values were the uncertainties in the rate of emission, boundary layer height, wind speed, frequency of the wind direction in the relevant sector and the proportion of the emission released as sulphate, or sulphur trioxide.

The proportion of the overall variance in the predicted sulphate concentrations explained by the first order analysis decreases with distance from the source. Nevertheless the proportion explained remains close to unity. At 800 km from the source, the largest contributors to the variance in the predicted total sulphate concentration are the uncertainties in the wet deposition coefficient for sulphate aerosol, the dry deposition velocity for sulphur dioxide, the wet deposition coefficient for sulphur and the rate of homogeneous (gas phase) oxidation of sulphur dioxide to sulphate.

Figure 4.5 shows the cumulative contributions to the variance in the predicted total sulphur deposition rate at receptors from each of the model parameters.

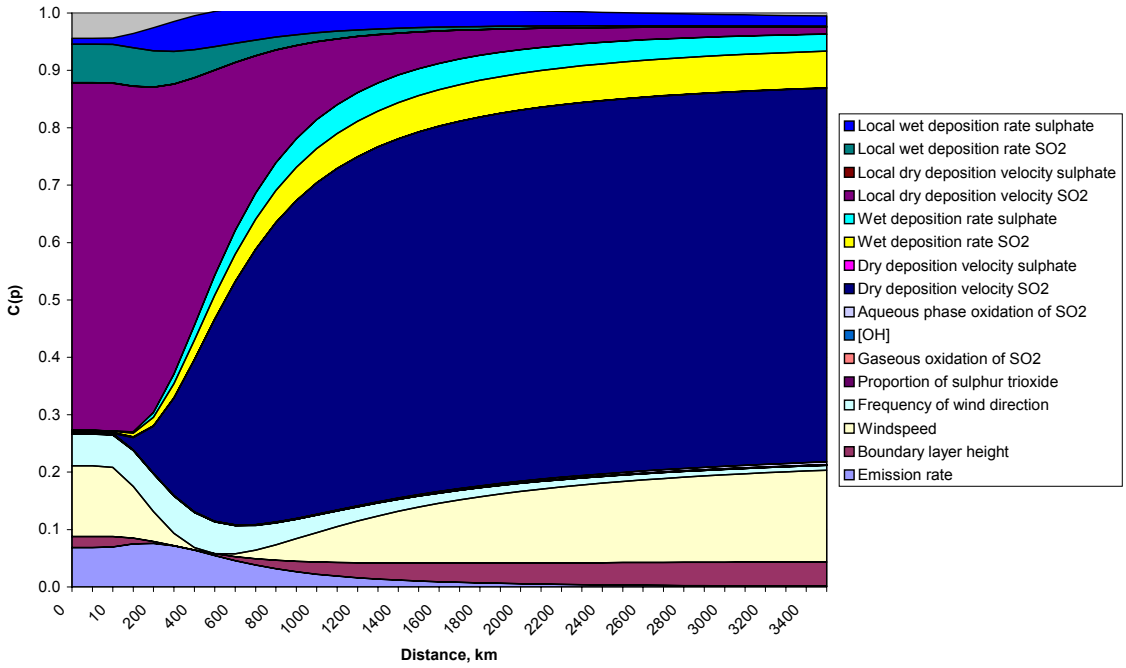

Figure 4.5 Cumulative contribution to variance in predicted total sulphur deposition at receptor using the analytical model as a function of distance

The first order analysis explains most of the overall variance throughout the range of prediction. The major contributor to the overall variance of predicted values was the uncertainty in the dry deposition velocity for sulphur dioxide in the vicinity of the receptor. Other significant contributors to the variance were the uncertainties in the rate of emission, boundary layer height, wind speed, frequency of the wind direction in the relevant sector and the wet deposition coefficient for sulphur dioxide.

At 800 km from the source, the largest contributors to the variance in the predicted total sulphur deposition rate at receptors are the uncertainties in the dry deposition velocity for sulphur dioxide, both upwind and local to the receptor.

Figure 4.6 shows the cumulative contributions to the variance in the predicted distance integrated total sulphur deposition rate from each of the model parameters. It shows that the first order analysis explains 95% or more of the variance in the predicted "distance integrated" total sulphur deposition throughout the range of calculation. Close to the source, the major contributor to the variance was the uncertainty in the dry deposition velocity for sulphur dioxide. Other contributors were the uncertainties in the rate of emission, the boundary layer height, wind speed and wet deposition coefficient for sulphur dioxide. At greater distances the uncertainty in the emission rate makes an increasingly large contribution to the variance.

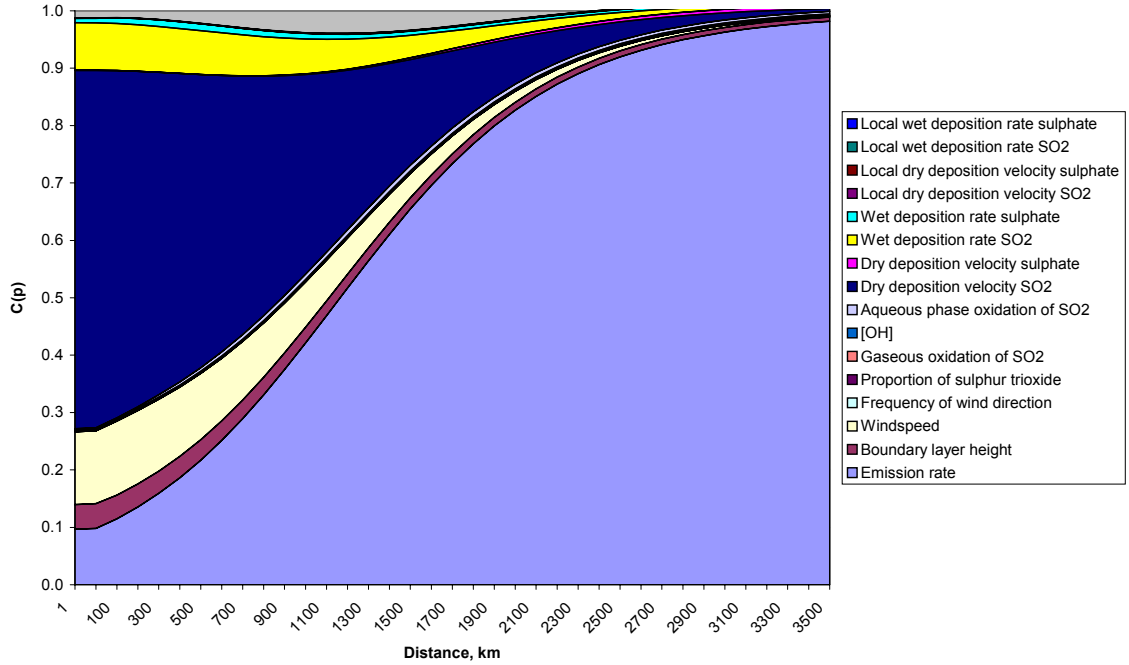

Figure 4.6 Cumulative contribution to variance in predicted "distance integrated" total sulphur deposition using the analytical model as a function of distance

4.2.3 Latin Square sampling

The input parameters were selected for a small number of runs using a method based on Latin Squares. A Latin Square of order n is an n by n array of n symbols, in which every symbol occurs exactly once in each row and column. Different Latin Squares of order greater than 3 are extremely numerous. The possible range of each of n parameters (n=13 in this case) was divided into n bands. For the first model run, each parameter was chosen from a specific band selected at random, such that no band was assigned to more than one variable. Parameter values were chosen randomly from within the range covered by the specified band. The process was repeated for n-1 subsequent model runs ensuring that no variable was chosen from any band more than once. The aim of Latin Square sampling is to reproduce Monte Carlo simulation, but in a more efficient manner which requires many fewer model runs.

Figure 4.7 shows the mean, maximum and minimum total sulphate concentrations predicted using the Latin Square sampling technique. Figure 4.7 also shows the mean and corresponding 93rd %ile (n/(n+1)) and 7th %ile (1/(n+1)) values predicted using the Monte Carlo analysis with 1000 runs. Comparison of the predicted values shows that the Latin Square sampling technique provides a good estimate of the mean: it also provides a reasonable estimate of the range of predicted values.

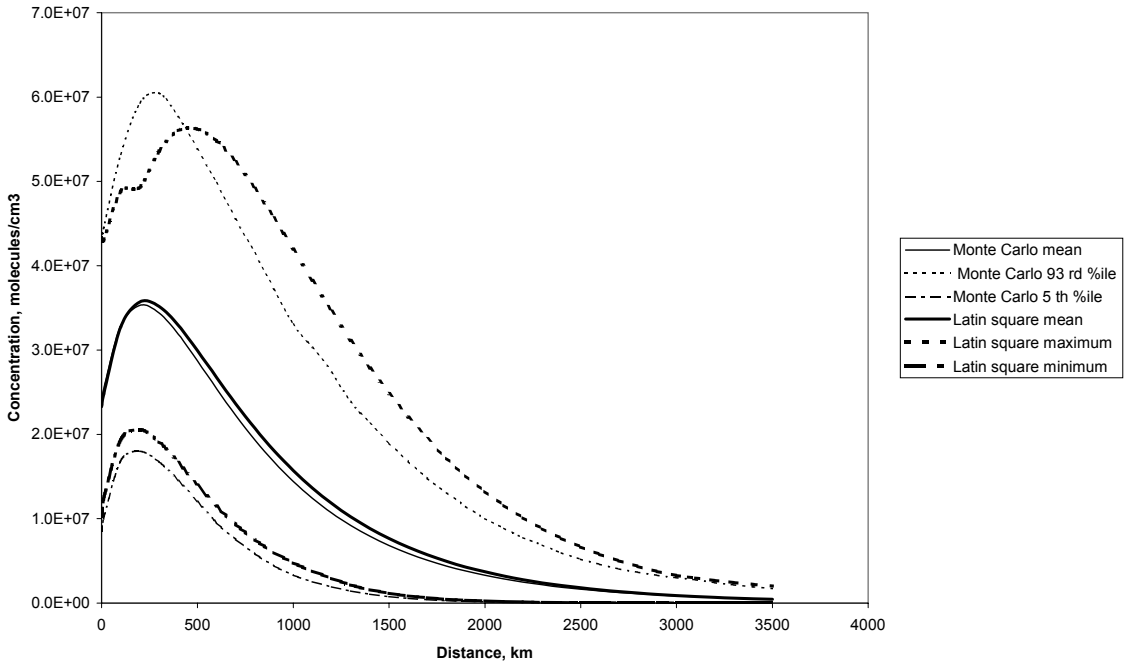

Figure 4.7 Comparison of Latin Square sampling estimates of the range of total sulphate concentrations with Monte Carlo analysis using the analytical model

Figure 4.8 shows the cumulative probability distribution of predicted total sulphate concentrations at a distance of 200 km downwind from the source for the distributions derived from the Monte Carlo and Latin Square sampling strategies. It also shows the log-normal distribution. Examination of Figure 4.8 indicates that the results of the Monte Carlo analysis closely approximate to the log-normal distribution. The distribution derived using the Latin Square sampling strategy provides a reasonable estimate of the distribution in the predicted concentrations in the cumulative probability range between 0.1 and 0.9, but provides little information at the extremes of the distribution.

It was concluded that Latin Square sampling is an effective surrogate for full Monte Carlo analysis apart from extremes of the probability distribution.

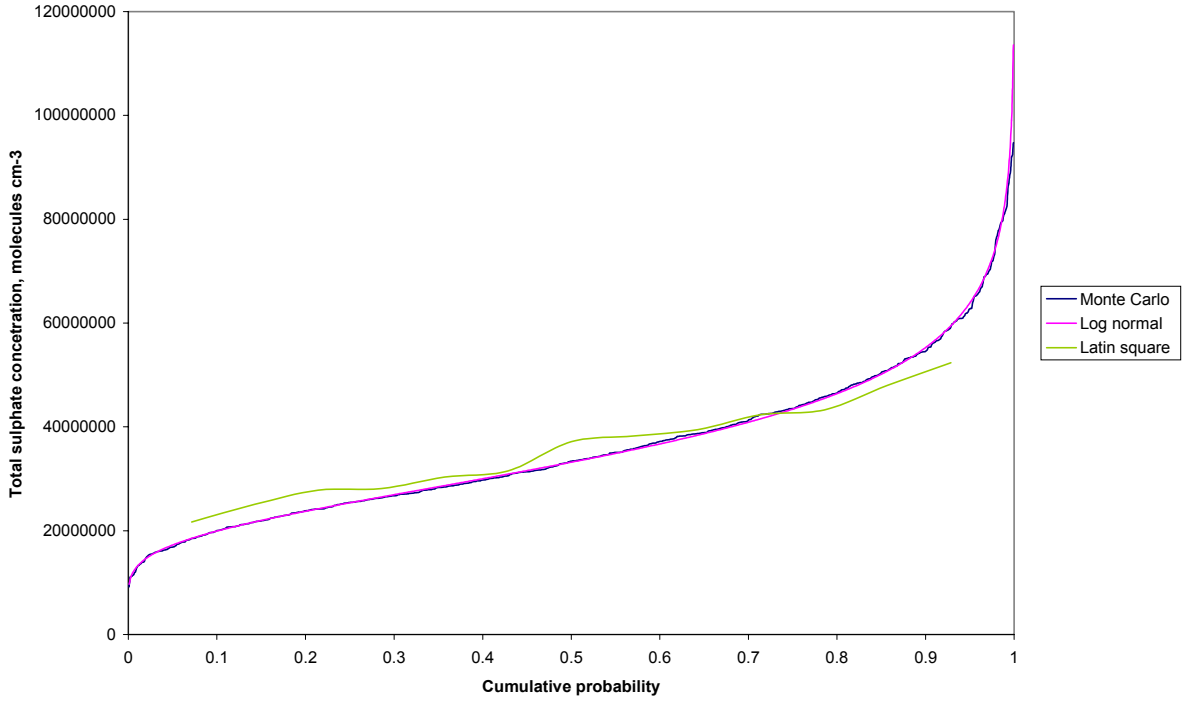

Figure 4.8 Cumulative probability distributions of total sulphate concentration 20 km downwind of the source based on Latin Square and Monte Carlo sampling of input parameters using the analytical model

4.3 Oxidised nitrogen deposition analytical model

4.3.1 Monte Carlo analysis

The equations representing the analytical solution of the model equations have been evaluated for input values in ranges identified in the assessment described in Section 3.2. The input ranges are shown in Table 4.2. Values of each parameter were taken at random from the range assuming a uniform distribution. One thousand evaluations were carried out. Figure 4.9 shows the results for the no ammonia case: Figure 4.10 shows the results for the excess ammonia case.

Figure 4.9 for the no ammonia case shows that the maximum deposition is predicted at distances of around 250 km downwind of the source. The 95th percentile rate of deposition is approximately twice the mean value. The 5th percentile is approximately one third of the mean value. The mean value is approximately twice the baseline value, reflecting the asymmetry in the input ranges around the baseline value for many of the input parameters.

Figure 4.10 for the excess ammonia case is similar to Figure 4.9. The 95th percentile and mean deposition predicted in each case is very similar. However, the deposition predicted for the baseline case is rather different with peak deposition predicted rather further from the source for the excess ammonia case.

Figure 4.11 shows the cumulative distribution of predicted deposition rates a distance of 200 km from the source. Figure 4.11 also shows, for comparison, the log-normal

distribution. It appears from inspection of Figure 4.11 that the log-normal distribution provides a good representation of the distribution of predicted rates of deposition.

Table 4.2 Ranges of input parameters used in Monte Carlo analysis of nitrogen deposition analytical model

Parameter	Units	Baseline	Range
Reaction rate, k_1, $NO+O_3 \rightarrow NO_2$	cm^3 $molecule^{-1}$ s^{-1}	$1.42 \cdot 10^{-14}$	+/-20%
Baseline ozone concentration	ppb	30	+/-13%
Proportion NO_x emitted as NO		0.95	+/-5%
Reaction rate, J_1, $NO_2 \rightarrow NO+O_3$	s^{-1}	$9.14 \cdot 10^{-3}$	-55%,+78%
Baseline NO concentration	molecules cm^{-3}	$2.5 \cdot 10^{10}$	-50%,+100%
Emission rate into 10 km wide parcel of air	molecules s^{-1}	$6.023 \cdot 10^{23}$	+/-20%
Hydroxyl radical concentration	molecules cm^{-3}	10^6	-50%,+100%
Reaction rate, k_4, $OH+M+NO_2 \rightarrow HNO_3+M$	cm^3 $molecule^{-1}$ s^{-1}	$1.5 \cdot 10^{-11}$	-33%,+67%
Reaction rate, k_5, $NO_2+O_3 \rightarrow NO_3+O_2$	cm^3 $molecule^{-1}$ s^{-1}	$2.09 \cdot 10^{-17}$	+/-30%
Reaction rate, k_{10}, $NO_2+NO_3 \rightarrow N_2O_5$	cm^3 $molecule^{-1}$ s^{-1}	$6.72 \cdot 10^{-15}$	Factors 1-100
Dry deposition, NO_2	m s^{-1}	0.0015	+/-70%
Boundary layer height	m	800	+/-20%
Baseline NO_3 concentration	molecules cm^{-3}	$2.5 \cdot 10^7$	-50%,+100%
Baseline NO_2 concentration	molecules cm^{-3}	$2.5 \cdot 10^{11}$	+/-50%
Reaction rate, J_2, $NO_3 \rightarrow NO_2+O$	s^{-1}	$8.34 \cdot 10^{-2}$	-28%,+188%
Reaction rate, k_{11}, $N_2O_5 \rightarrow$ aerosol	s^{-1}	$3 \cdot 10^{-5}$	Factor 1-10
Dry deposition, O_3	m s^{-1}	0.006	+/-50%
Wind speed	m s^{-1}	7.5	+/-25%
Dry deposition, HNO_3	m s^{-1}	0.04	-50%,+100%
Wet deposition, HNO_3	s^{-1}	$9 \cdot 10^{-6}$	-70%,+1000%
Dry deposition, aerosol	m s^{-1}	0.001	-50%,+100%
Wet deposition, aerosol	s^{-1}	$1.3 \cdot 10^{-5}$	-70%,+1000%
Reaction rate, $HNO_3 \rightarrow$ aerosol, k_9	s^{-1}	$3 \cdot 10^{-5}$	-70%,+1000%
Wind direction frequency		0.15	+/-25%

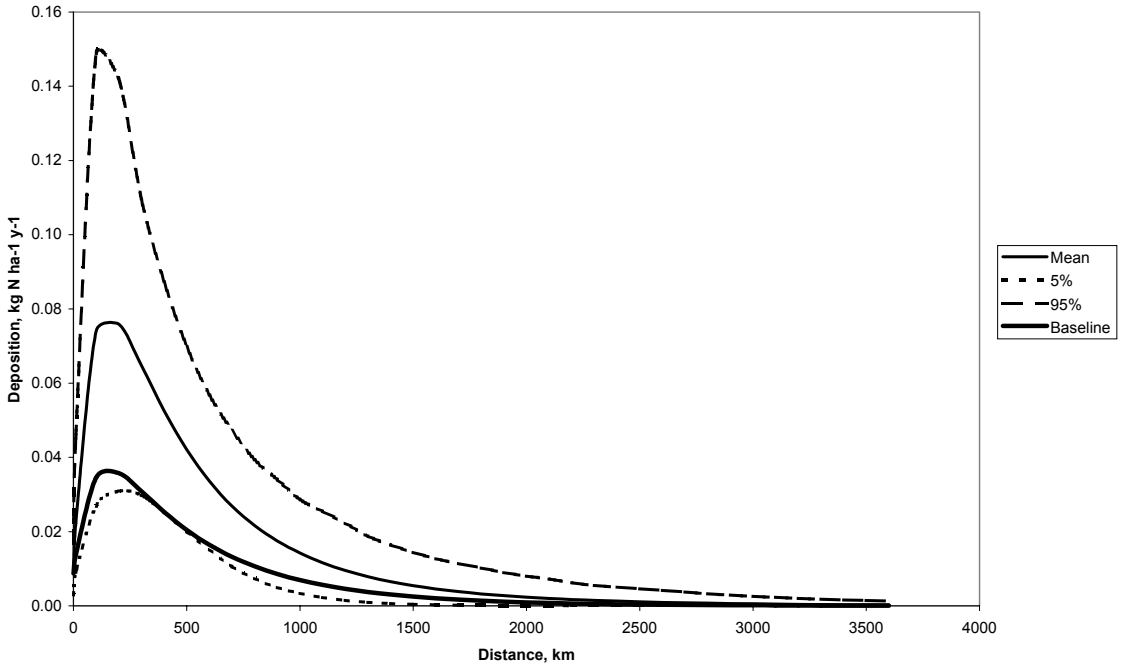

Figure 4.9 Deposition of oxidised nitrogen for a 1 mole s^{-1} release, W=10 km, no ammonia using the analytical model

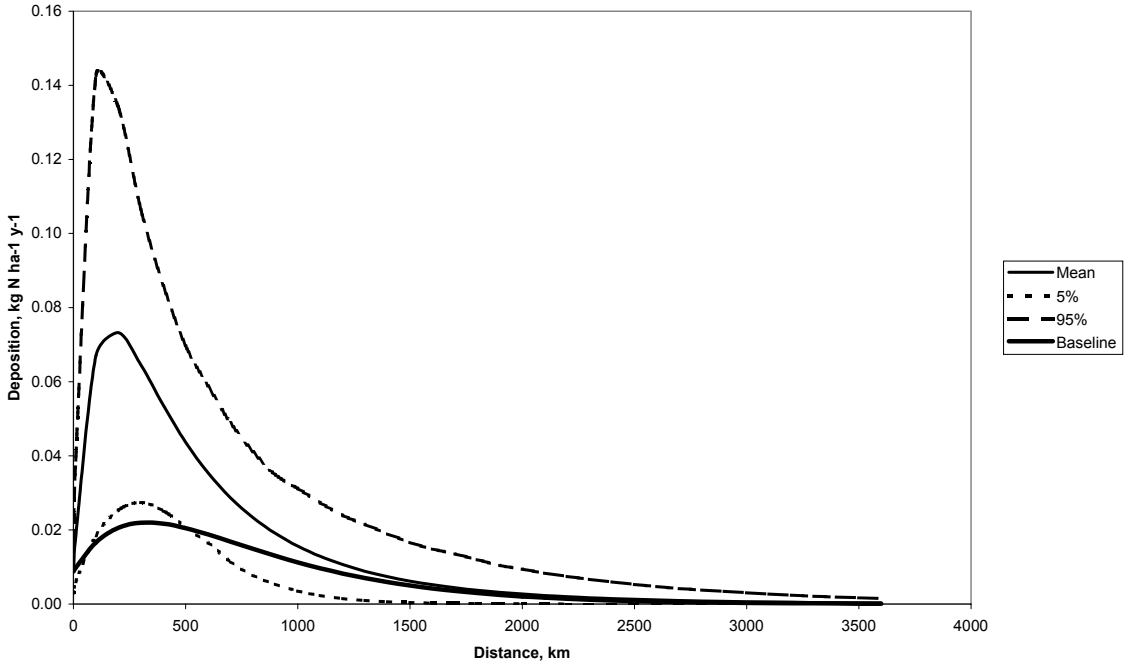

Figure 4.10 Deposition of oxidised nitrogen for a 1 mole s^{-1} release, W=10 km, excess ammonia, using the analytical model

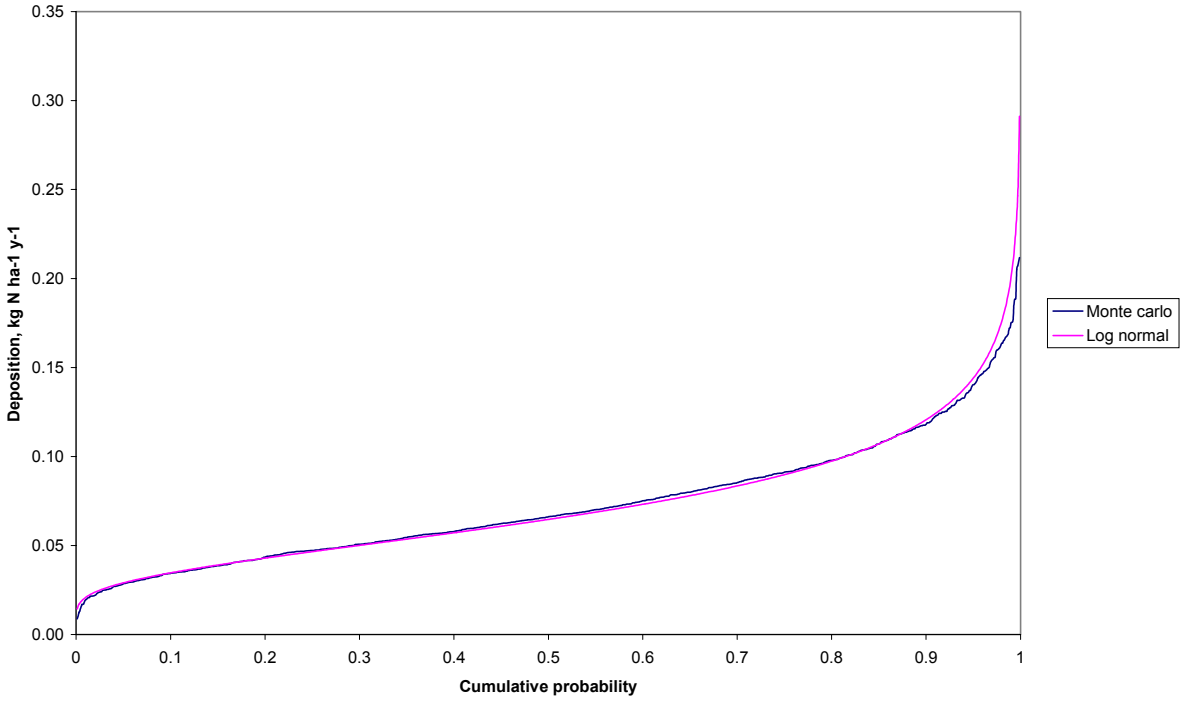

Figure 4.11 Cumulative probability distribution of predicted nitrogen deposition rates, 200 km downwind of the source using the analytical model

4.3.2 Contribution to variance

Figure 4.12 shows the first order contribution to the variance in the predicted deposition associated with the variance in each of the input parameters for the no ammonia case. At the location of maximum deposition approximately 200-300 km downwind from the source, the largest contributions to the variance are the background concentration of the hydroxyl radical, the wet deposition of the aerosols, the frequency of the wind direction, the wind speed, the rate constant for the formation of nitrogen pentoxide, the rate of emission, and the rate constant for the formation of nitric acid. Approximately 10-30% of the variance is not explained by the first order variance model and is associated with more complex interactions between parameters.

Figure 4.13 shows the first order contribution to the variance in the predicted deposition associated with the variance in each of the input parameters for the excess ammonia case. At the location of maximum deposition approximately 200-300 km downwind from the source, the largest contributions to the variance are the associated with the same set of input parameters.

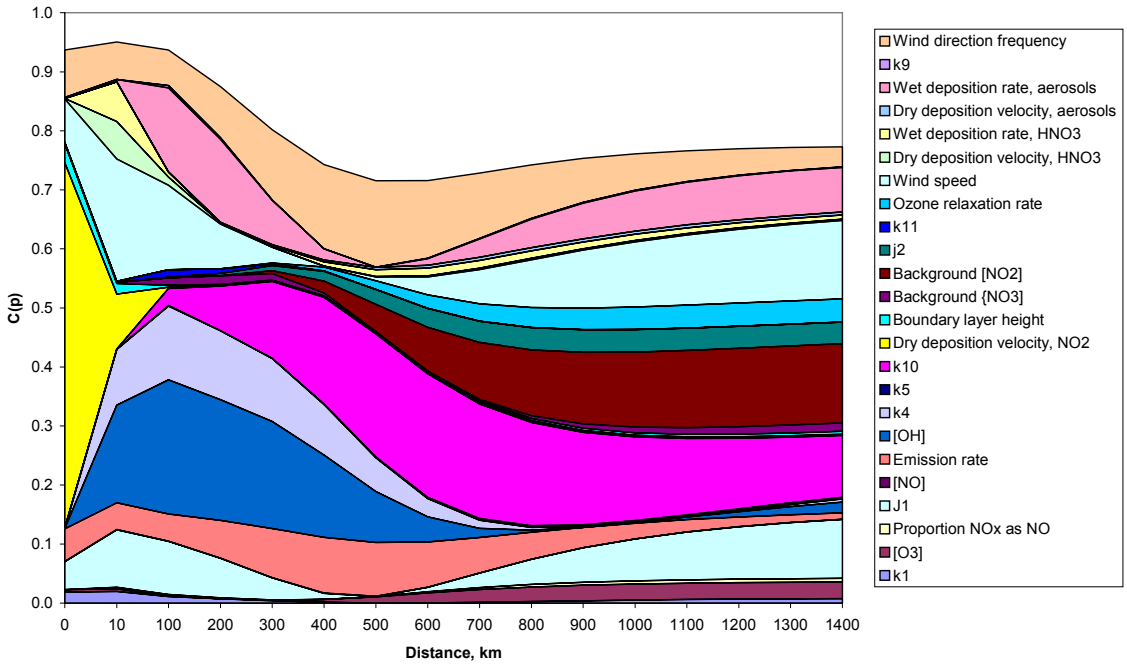

Figure 4.12 Contribution to variance in predicted oxidized nitrogen deposition, no ammonia case, using the analytical model

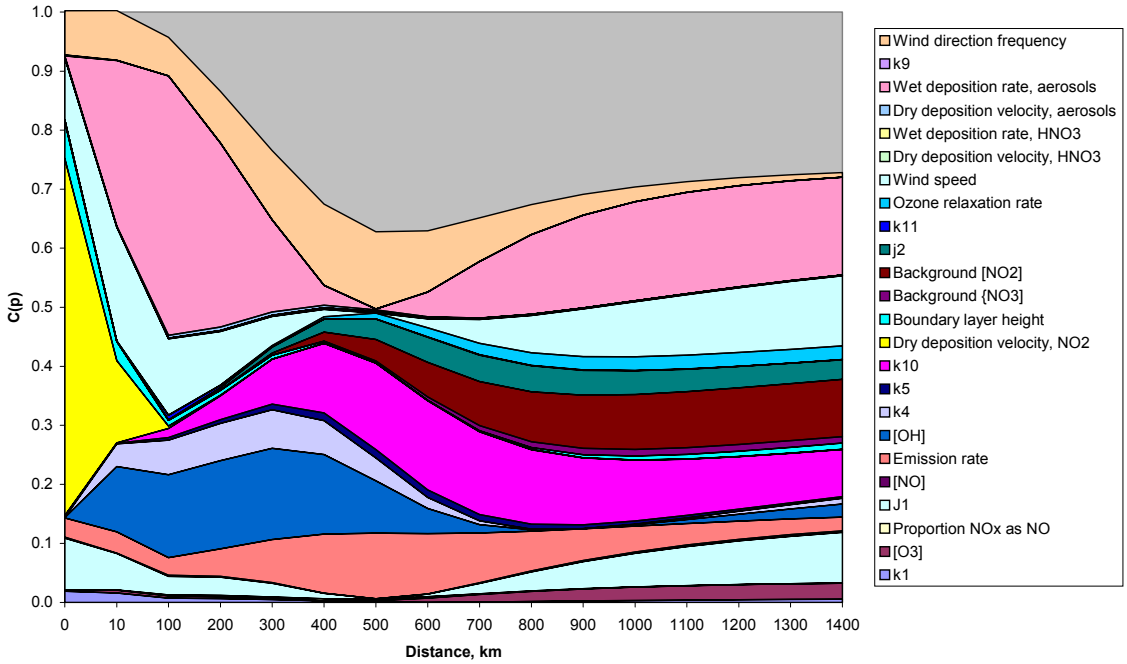

Figure 4.13 Contribution to variance in predicted oxidized nitrogen deposition, excess ammonia case, using the analytical model

4.4 TRACK - Baseline predictions

4.4.1 Monte Carlo simulation

The TRACK model was used to predict sulphur deposition and oxidised and reduced nitrogen deposition for the baseline scenario for input parameters in ranges identified in the assessment described in Section 3. The baseline scenario was based on the 1990 emissions inventory for the UK and for the EMEP grid. The input ranges are shown in Table 4.3. Values of each parameter were taken at random from the range assuming a uniform distribution. Three hundred model runs were carried out.

Figure 4.14 shows the predicted mean and 5th and 95th percentile rates of sulphur deposition at grid cells containing Acid Deposition Network sites throughout the United Kingdom. The sites include a mixture of sites close to and far from the main sources and in upland and lowland areas. The 95th percentile value is typically around 1.3 times the average: the average is typically around 1.45 times the 5th percentile. The uncertainty as a proportion of the mean predicted rate of deposition is affected by distance from the main sources of emission. The 5th to 95th percentile range decreases from around 80% of the mean at those sites near to the major sources (e.g. Bottesford, Jenny Hurn) to around 40% of the mean at more remote sites (e.g. Goonhilly, Polloch, Strathvaich Dam).

Figure 4.15 shows the predicted mean and 5th and 95th percentile rates of oxidised nitrogen deposition at grid cells containing Acid Deposition Network sites throughout the United Kingdom. The 95th percentile value is typically around 1.9 times the average: the average is typically around 2 times the 5th percentile. The uncertainty as a proportion of the mean predicted rate of deposition is affected by distance from the main sources of emission. The 5th to 95th percentile range tends to increase from around 100% of the mean at those sites near to the major sources (e.g. Bottesford, Jenny Hurn) to around 250% of the mean at more remote sites (e.g. Goonhilly, Polloch).

Figure 4.16 shows the predicted mean and 5th and 95th percentile rates of reduced nitrogen deposition at grid cells containing Acid Deposition Network sites throughout the United Kingdom. The 95th percentile value is typically around 1.5 times the average: the average is typically around 1.7 times the 5th percentile. The relationship between the uncertainty as a proportion of the mean predicted rate of deposition and distance from the major emission sources is not clear for reduced nitrogen deposition.

Figure 4.17 shows the predicted mean and 5th and 95th percentile rates of total oxidised and reduced nitrogen deposition at grid cells containing Acid Deposition Network sites throughout the United Kingdom. The 95th percentile value is typically around 1.5 times the average: the average is typically around 1.5 times the 5th percentile.

Figure 4.18 shows the predicted mean and 5th and 95th percentile rates of total oxidised nitrogen, reduced nitrogen and sulphur deposition at grid cells containing Acid Deposition Network sites throughout the United Kingdom. The 95th percentile value is typically around 1.3 times the average: the average is typically around 1.4 times the 5th percentile. [Note 1 equivalent (eq) = 16g sulphur or 14 g nitrogen].

Table 4.3 Input ranges of parameters used in Monte Carlo simulation and first order error analysis for the TRACK model

Parameter	Units	Baseline	Range, % of baseline		Increment, % of baseline
			Lower limit	Upper limit	
Dry deposition velocity, NO2		Land use dependent	40	160	33
Dry deposition velocity, HNO_3		Land use dependent	50	200	50
Dry deposition velocity, aerosols		Land use dependent	50	200	-50
Dry deposition velocity, ammonia		Land use dependent	50	200	100
Dry deposition velocity, sulphur dioxide		Land use dependent	50	200	100
Ozone relaxation rate	$m\ s^{-1}$	$50.\ 10^{-6}$	50	150	50
Aerosol relaxation rate	$m\ s^{-1}$	0.001	50	150	50
Wet scavenging coefficient, HNO_3	s^{-1}	$9.\ 10^{-6}$	0	200	100
Wet scavenging coefficient, aerosols	s^{-1}	$1.3.\ 10^{-5}$	30	1000	100
Wet scavenging coefficient, sulphur dioxide	s^{-1}	$1.\ 10^{-6}$	0	200	100
Wet scavenging coefficient, NH_3	s^{-1}	$9.\ 10^{-6}$	20	100	-50
Reaction rate, $NO + O_3 \rightarrow NO_2 + O_2$		Appendix 1	80	120	-20
Reaction rate, $OH + NO_2 (+ M) \rightarrow HNO_3 (+ M)$		Appendix 1	70	130	-30
Reaction rate, $SO_2 + OH \rightarrow SO_4$		Appendix 1	20	100	-50
Reaction rate, $SO_2 \rightarrow SO_4$		Appendix 1	50	200	100
Reaction rate, $SO_4 + 2NH_3 \rightarrow (NH_4)_2SO_4$		Appendix 1	30	1000	100
Reaction rate, $NH_3 + HNO_3 \rightarrow NH_4NO_3$		Appendix 1	30	1000	100
Reaction rate, $NO_2 + h\nu \rightarrow NO + O$		Appendix 1	50	125	25
Reaction rate, $NO_2 + O_3 \rightarrow NO_3 + O_2$		Appendix 1	50	200	100
Reaction rates gaseous species with aerosols		Appendix 1	50	200	100
[OH]		STOCHEM field	50	200	100
$[CH_3COO_2]$		STOCHEM field	50	200	100
$[NO_3]$		STOCHEM field	50	200	100
$[O_3]$	ppb	34	80	120	20
Fraction sulphur released as sulphur trioxide or sulphate		0.05	60	140	-40
Seeder feeder factor on wet deposition rate		2	50	150	-50
Seeder feeder factor on SO_2 oxidation rate			70	130	-30
Seeder feeder effect cut in level	mm/year	800	75	125	-25
Ammonia emissions		Inventory	50	150	-50
Hydrogen chloride emission		Inventory	80	120	-20
Oxides of nitrogen emissions		Inventory	80	120	-20
Boundary layer height	m	800	80	120	20

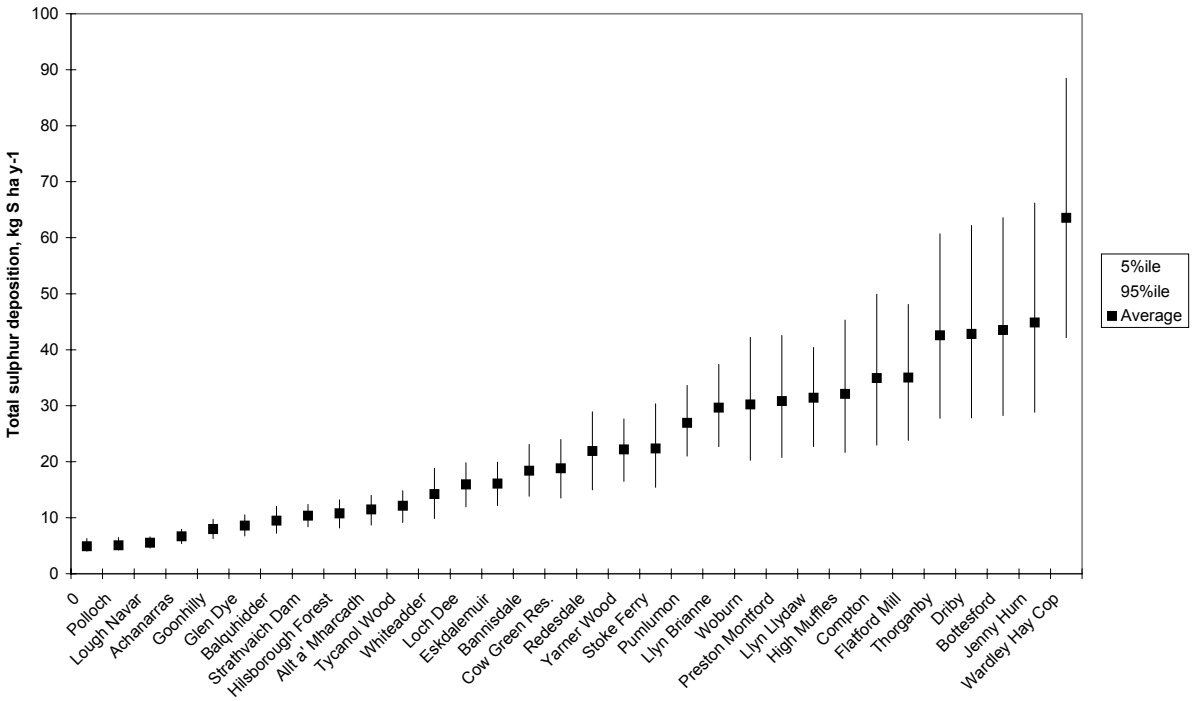

Figure 4.14 Predicted sulphur deposition at grid cells containing monitoring sites, TRACK with 1990 emissions: mean, 5th %ile and 95th %ile predictions from Monte Carlo analysis

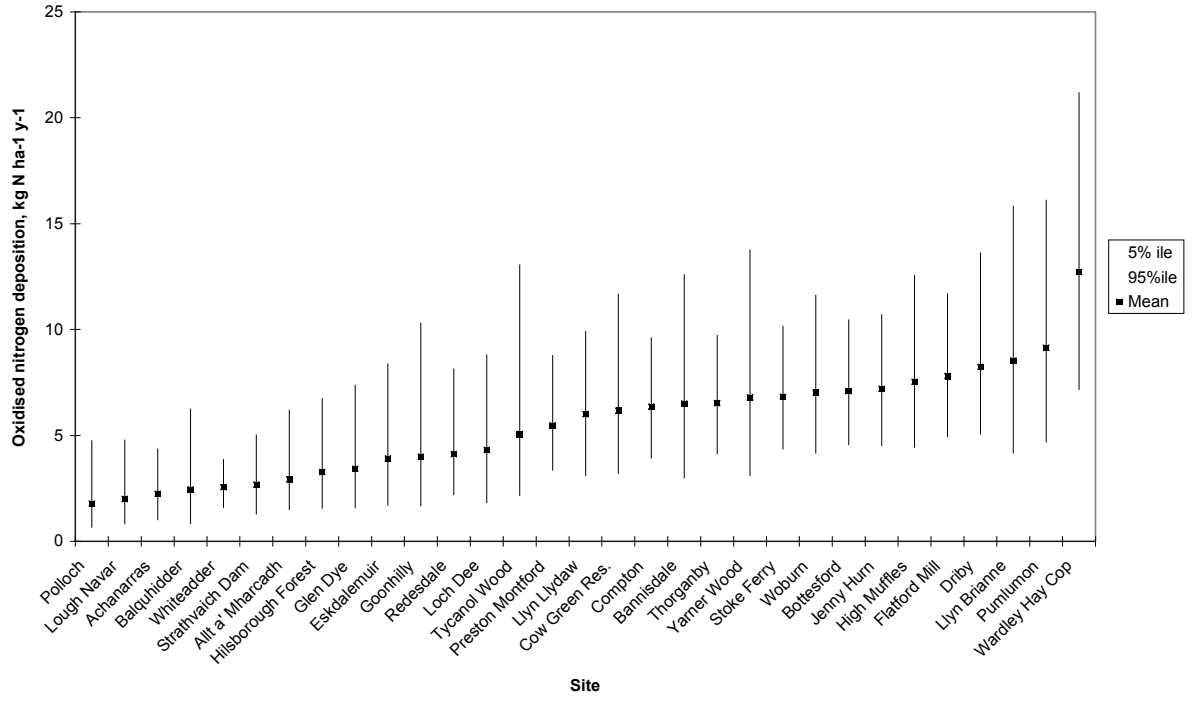

Figure 4.15 Predicted oxidised nitrogen deposition at grid cells containing monitoring sites, TRACK with 1990 emissions: mean, 5th %ile and 95th %ile predictions from Monte Carlo analysis

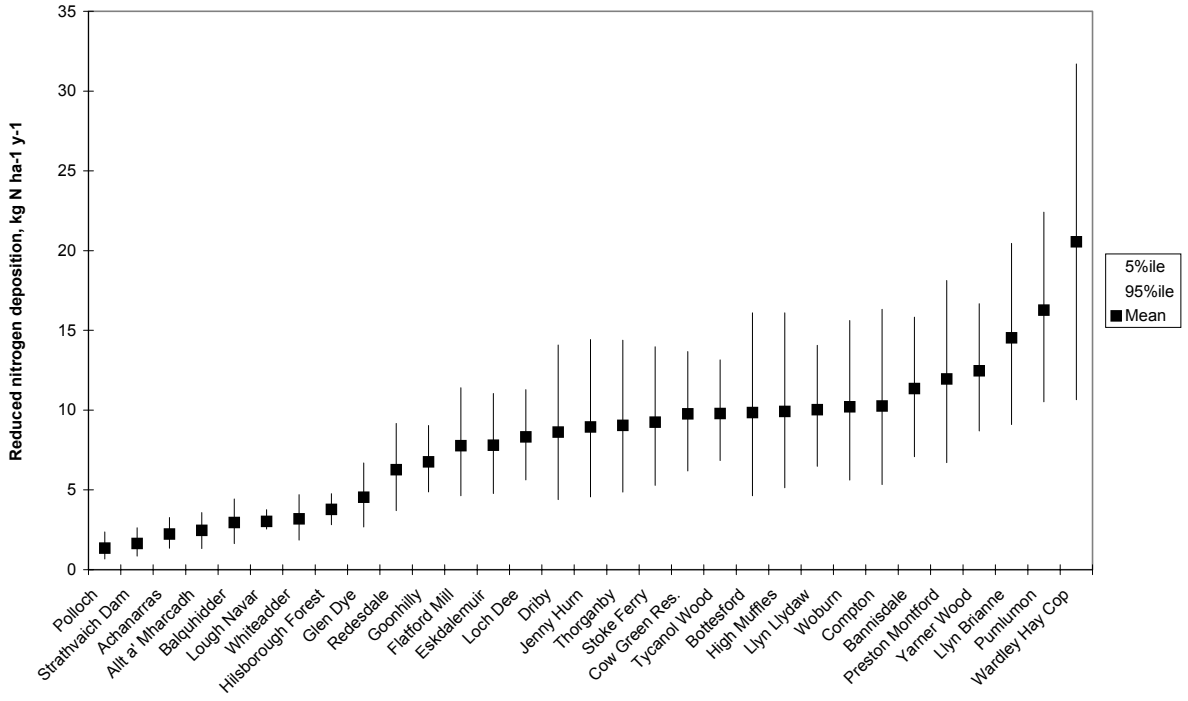

Figure 4.16 Predicted reduced nitrogen deposition at grid cells containing monitoring sites, TRACK with 1990 emissions: mean, 5th %ile and 95th %ile predictions from Monte Carlo analysis

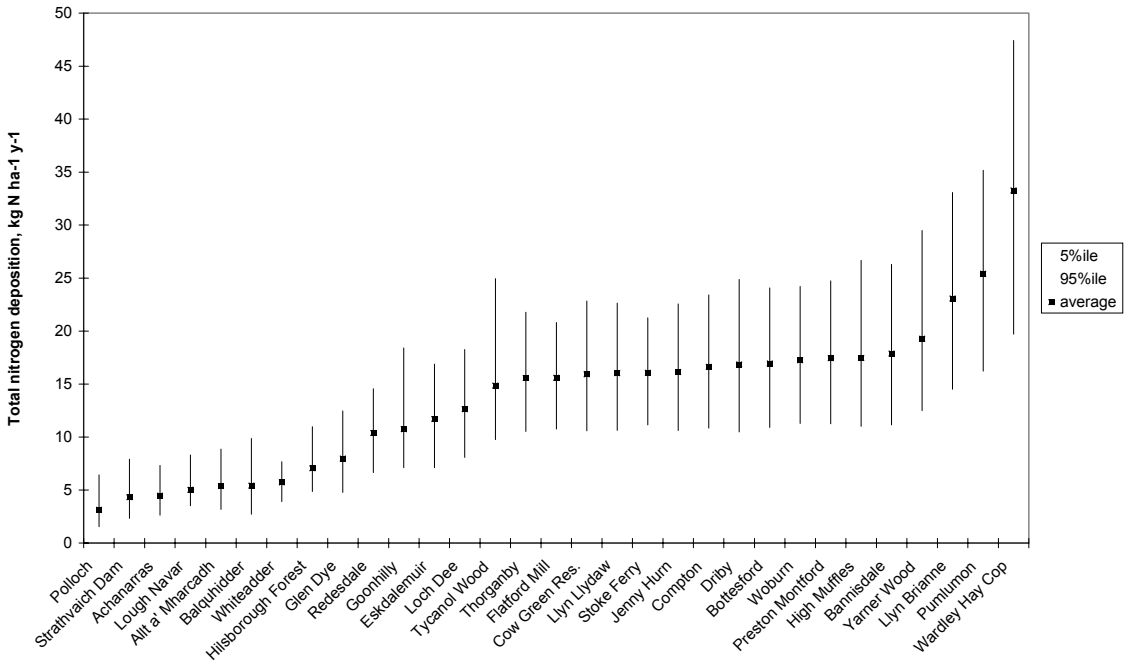

Figure 4.17 Predicted total (oxidised plus reduced) nitrogen deposition at grid cells containing monitoring sites, TRACK with 1990 emissions: mean, 5th %ile and 95th %ile predictions from Monte Carlo analysis

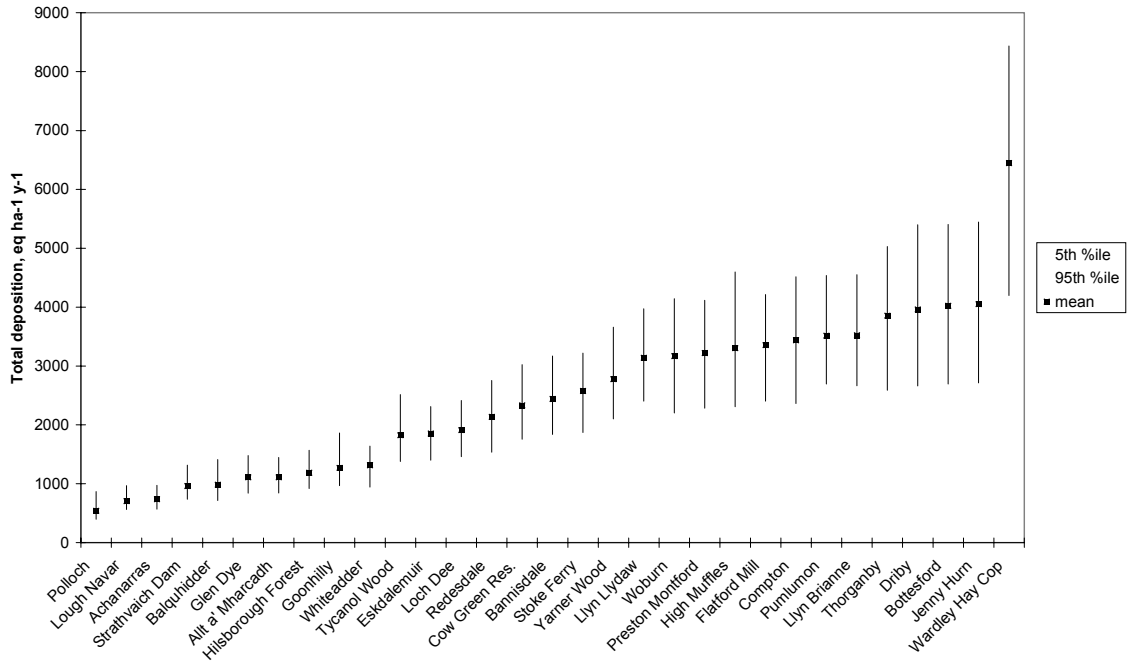

Figure 4.18 Predicted total (oxidised, nitrogen, reduced nitrogen and sulphur) deposition at grid cells containing monitoring sites, TRACK with 1990 emissions: mean, 5th %ile and 95th %ile predictions from Monte Carlo analysis

Figures 4.19 to 4.21 show the cumulative probability of predicted sulphur, oxidised and reduced nitrogen depositions at the Jenny Hurn site. In each case, the distribution is approximately log-normal over the 5th to 95th %ile range.

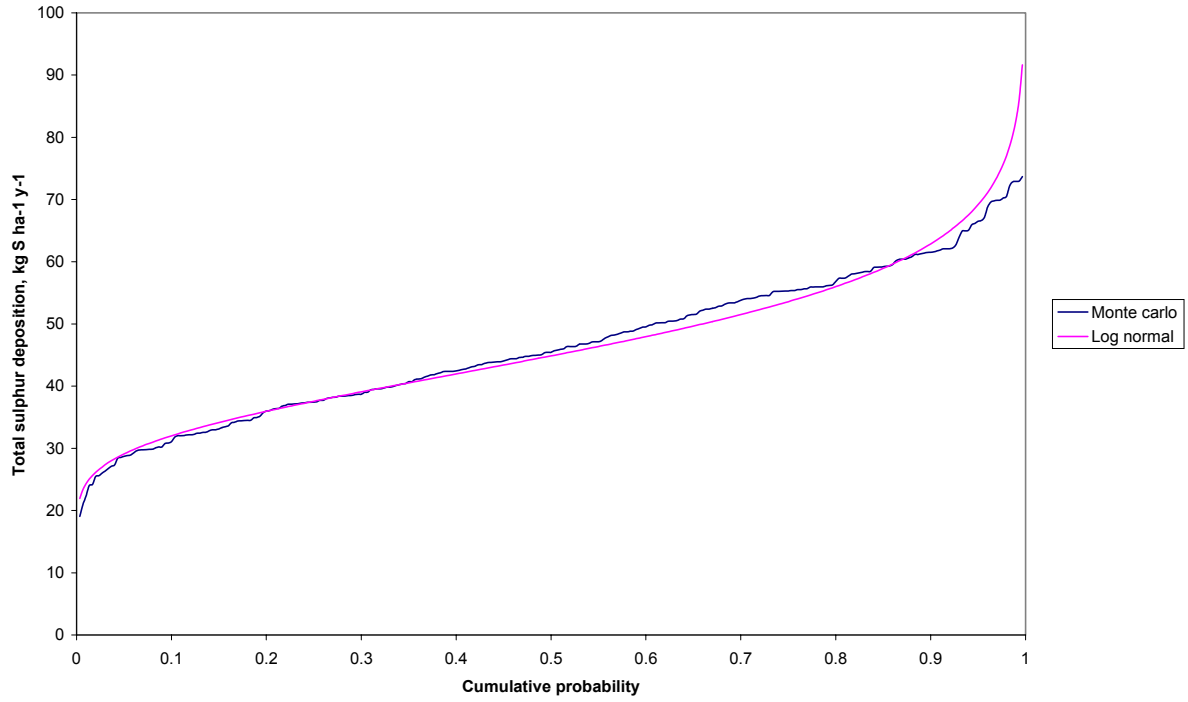

Figure 4.19 Cumulative probability distribution of sulphur deposition: TRACK model, 1990 emissions, Jenny Hurn

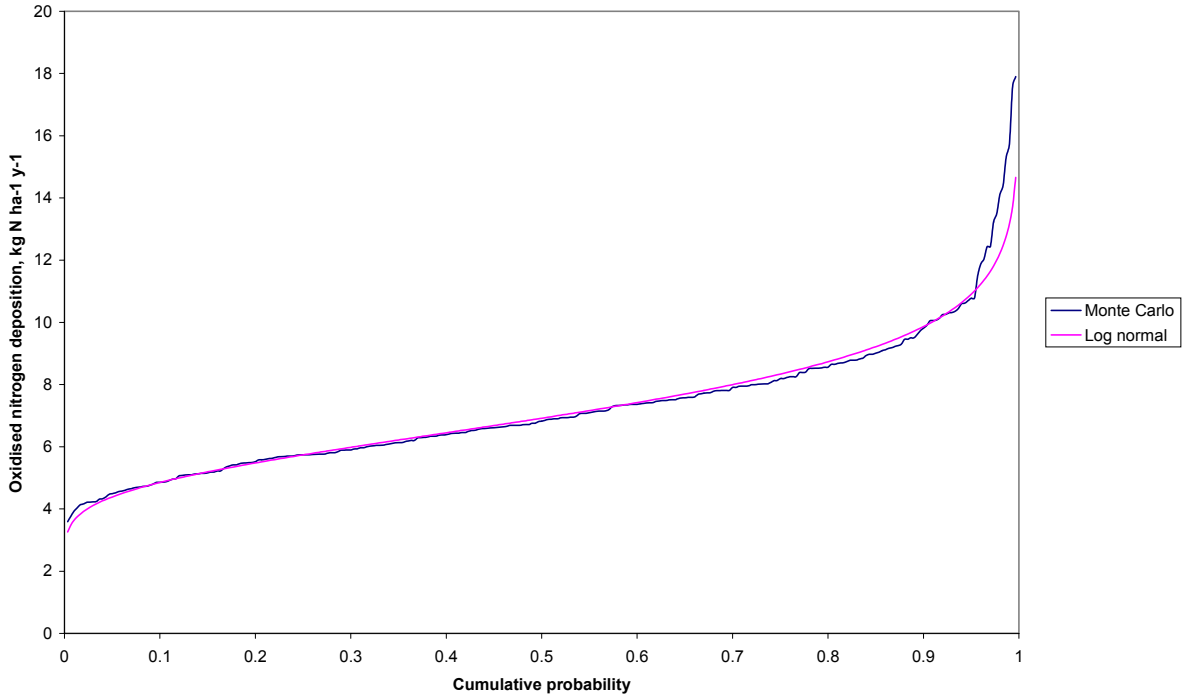

Figure 4.20 Cumulative probability distribution of oxidised nitrogen deposition: TRACK model, 1990 emissions, Jenny Hurn

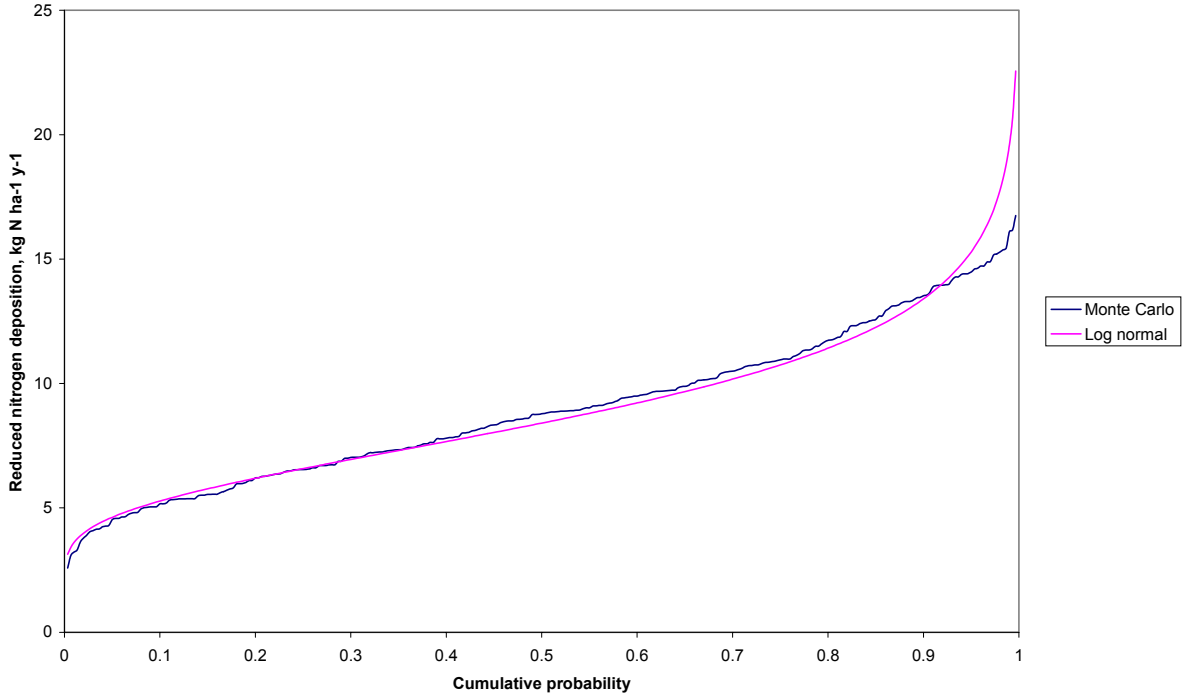

Figure 4.21 Cumulative probability distribution of reduced nitrogen deposition: TRACK model, 1990 emissions, Jenny Hurn

4.4.2 First order analysis

For the first order analysis, the input parameters were varied one at a time from the baseline value. Table 4.3 shows the incremental changes in the input parameters. The average of the distribution of the rates of deposition was then estimated from:

$$\phi_{av} = \phi_0 + \sum \frac{\Delta\phi}{\Delta p}.(p_{av} - p_0)$$

where ϕ is the natural logarithm of the rate of deposition;
p is the parameter value and the summation is over parameter values;
$\Delta\phi$ is the incremental change in the logarithm of the deposition resulting from an incremental change Δp in the input parameter p;
subscript *0* refers to the baseline;
subscript *av* refers to the average value.

The variance, V(ϕ), of the log distribution was estimated from:

$$V(\phi) = \sum \left(\frac{\Delta\phi}{\Delta p} \right)^2 V(p)$$

where V(p) is the variance of the input parameters.

The 5th and 95th percentile of the distribution were estimated, assuming a log normal distribution, from:

$$\phi_{0.05} = \phi_{av} - 1.65\sqrt{V(\phi)}$$
$$\phi_{0.95} = \phi_{av} + 1.65\sqrt{V(\phi)}$$

Figure 4.22 shows the predicted average, 5th percentile and 95th percentile sulphur deposition at grid cells containing the Acid Deposition Network sites. It also shows the values derived from the Monte Carlo simulation for comparison. In each case the first order analysis has provided predictions of sulphur deposition approximately 30% greater than those provided by the Monte Carlo analysis.

Figure 4.23 shows the predicted average, 5th percentile and 95th percentile oxidised nitrogen deposition at grid cells containing the Acid Deposition Network sites. It also shows the values derived from the Monte Carlo simulation for comparison. In each case the first order analysis has provided predictions of oxidised nitrogen deposition similar to those provided by the Monte Carlo analysis.

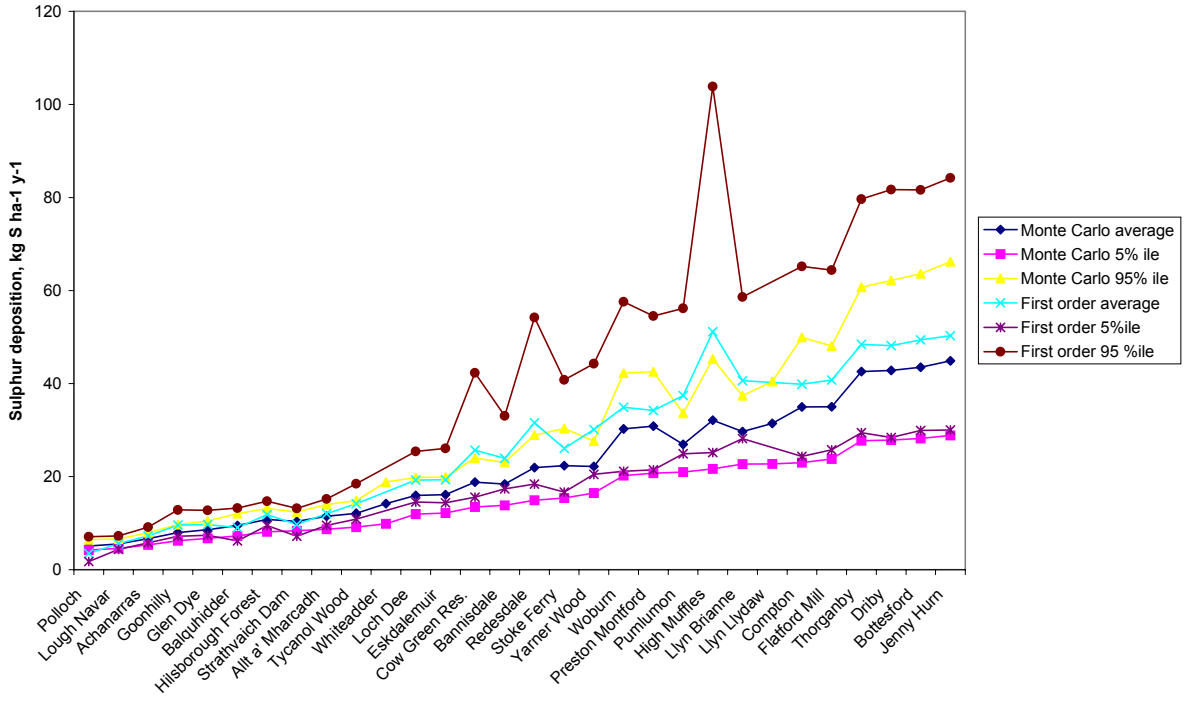

Figure 4.22 Average, 5 percentile and 95th percentile sulphur deposition predicted using TRACK, 1990 emissions: Monte Carlo analysis and first order error analysis

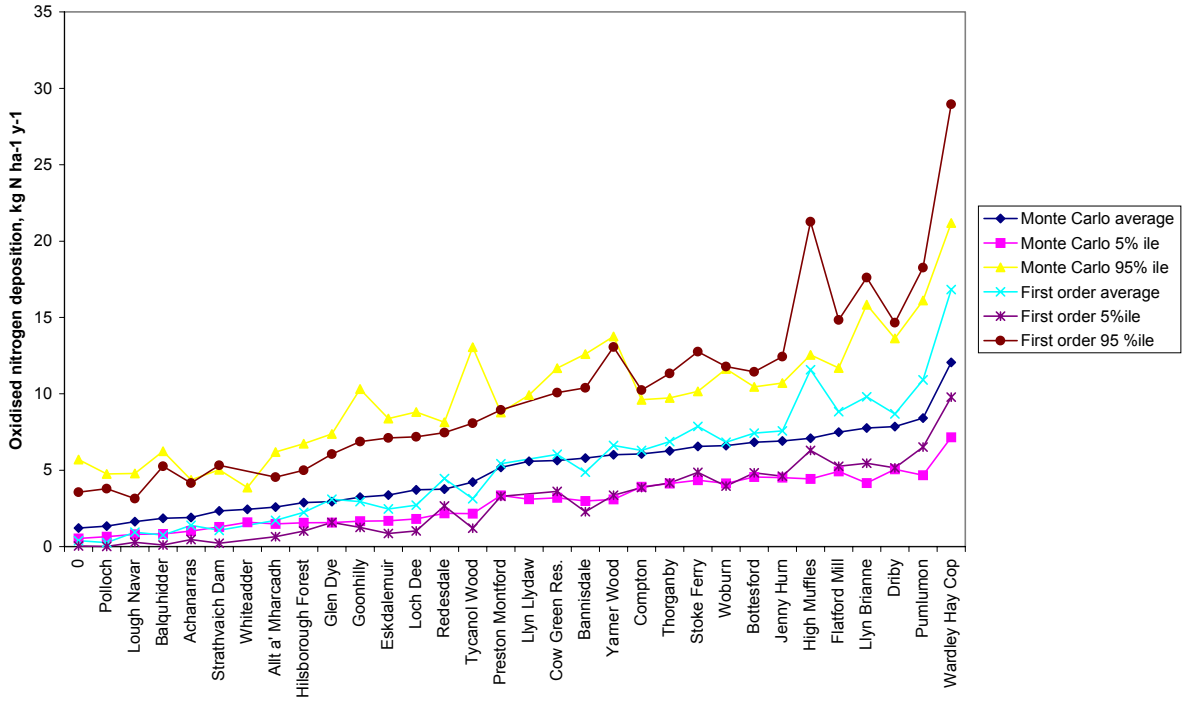

Figure 4.23 Average, 5th percentile and 95th percentile oxidised nitrogen deposition predicted using TRACK, 1990 emissions: Monte Carlo analysis and first order analysis

Figure 4.24 shows the predicted average, 5th percentile and 95th percentile reduced nitrogen deposition at grid cells containing the Acid Deposition Network sites. It also shows the values derived from the Monte Carlo simulation for comparison. The first order analysis has provided predictions of average and 5th percentile reduced nitrogen deposition similar to those provided by the Monte Carlo analysis. The 95th percentile value was typically 50% greater than that provided by the Monte Carlo analysis.

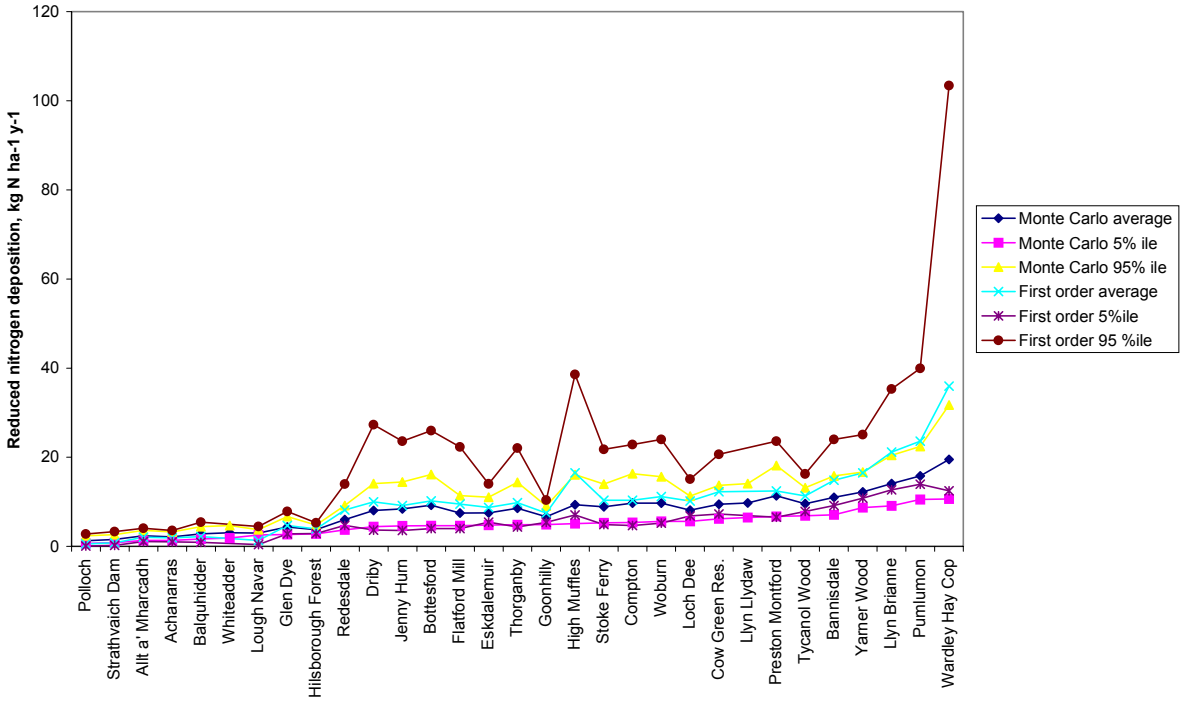

Figure 4.24 Average, 5th percentile and 95th percentile reduced nitrogen deposition predicted using TRACK, 1990 emissions: Monte Carlo analysis and first order analysis

The results have shown that first order analysis can provide reasonable estimates of the uncertainty in the acid deposition models resulting from the uncertainty in the input parameters. However the method does not take account of any non-linearity in the models with respect to individual parameters. The response of the model to many of the input parameters is non-linear: in consequence the predicted values of the 95th and 5th percentiles will depend on the size of the increment in the input values. Furthermore, interactions between parameters may compound the non-linear effects.

4.5 TRACK Model - Impact of an additional point source

4.5.1 Monte Carlo simulation

The model was run with an additional point source emitting 150 kt per annum of oxides of nitrogen (equivalent to approximately two power stations of the size of Drax) at OS grid reference (5100, 3100) (near Peterborough). Three hundred model runs were carried out with the same values of the input parameters used in the baseline assessment. The incremental impact of the additional source was determined for each

model run by subtracting the baseline deposition from the total deposition. The incremental deposition from the source was calculated at receptors on a trajectory passing through the point source in a direction 330^{o} from north (i.e. towards the northwest of Scotland). Figure 4.25 shows the 5th percentile, average and 95th percentile incremental contribution from the source to oxidised nitrogen deposition at increasing distances from the source. The contribution generally decreases with distance from the source, although local variations in dry deposition velocity and rainfall have some influence on the predicted values. The 95th percentile value is typically approximately twice the average value: the 5th percentile is approximately half the average value.

Figure 4.25 also shows for comparison the polar analytical solution from Appendix 3 for the excess ammonia case. The input parameters were as for the baseline case in Table 4.2 except that a wind direction frequency of 0.086 was used with a wind sector size of 45^{o} corresponding to the wind direction from 135-180^{o} taken from Table 3.6. Although the comparison does not provide a comprehensive test of the analytical solution, it does suggest that the analytical solution provides a reasonable surrogate for the numerical models for the purposes of uncertainty analysis.

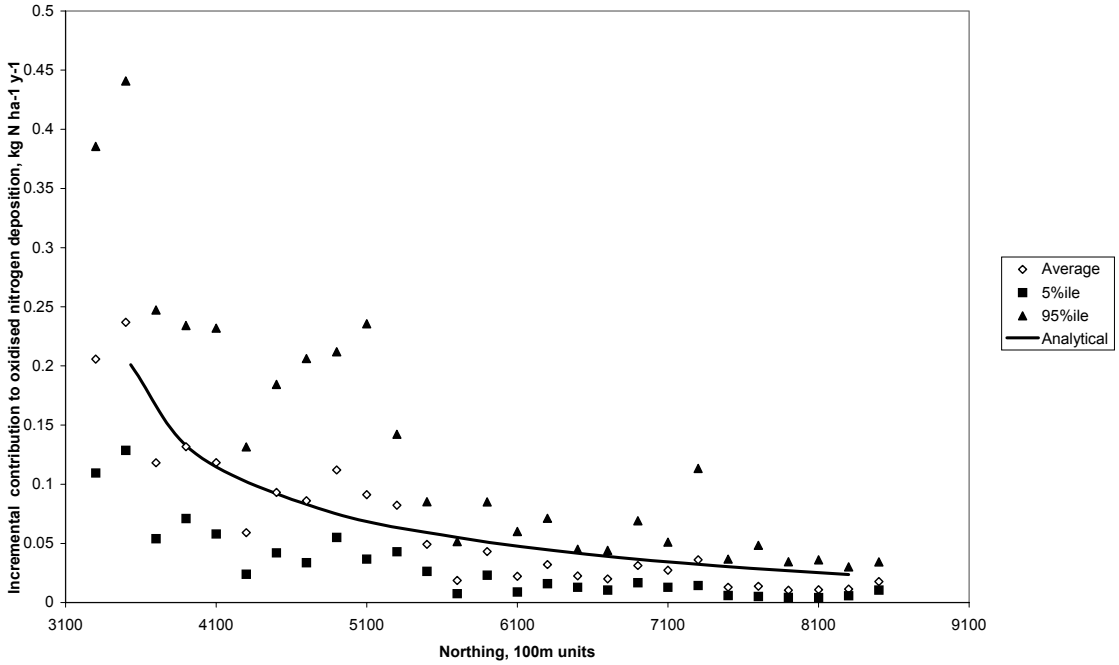

Figure 4.25 Incremental contribution to oxidised nitrogen deposition from a point source at (5100, 3100) emitting 150 kt oxides of nitrogen per year, TRACK model, 1990 base emissions, Monte Carlo analysis. Results from the analytical model assuming excess ammonia are also shown

Model runs were also carried out for a source emission of 75 kt per annum (i.e. half of 150 kt). Figure 4.26 shows the 150kt:75 kt ratios of the 5th percentile, average and 95th percentile rates of deposition. Far from the source, the predicted contribution to deposition from the additional source is approximately proportional to the rate of emission. Closer to the source, the contribution for the 150 kt emission is around 1.8 times that for the 75 kt emission indicating that there is some non-linearity in the

predicted deposition. The extent of the non-linearity is not great compared to the uncertainty arising from the uncertainty in the input parameters. For example, the predicted contribution to oxidised nitrogen deposition 80km from a 75 kt source was 0.07 kg N $ha^{-1}y^{-1}$. Simply doubling this rate for a 150 kt emission gives a rate of deposition of 0.14 kg N $ha^{-1}y^{-1}$ which may be compared with the 5 to 95th percentile range of 0.07 to 0.24, average 0.13 kg N $ha^{-1}y^{-1}$ shown in Figure 4.25 for the 150 kt source.

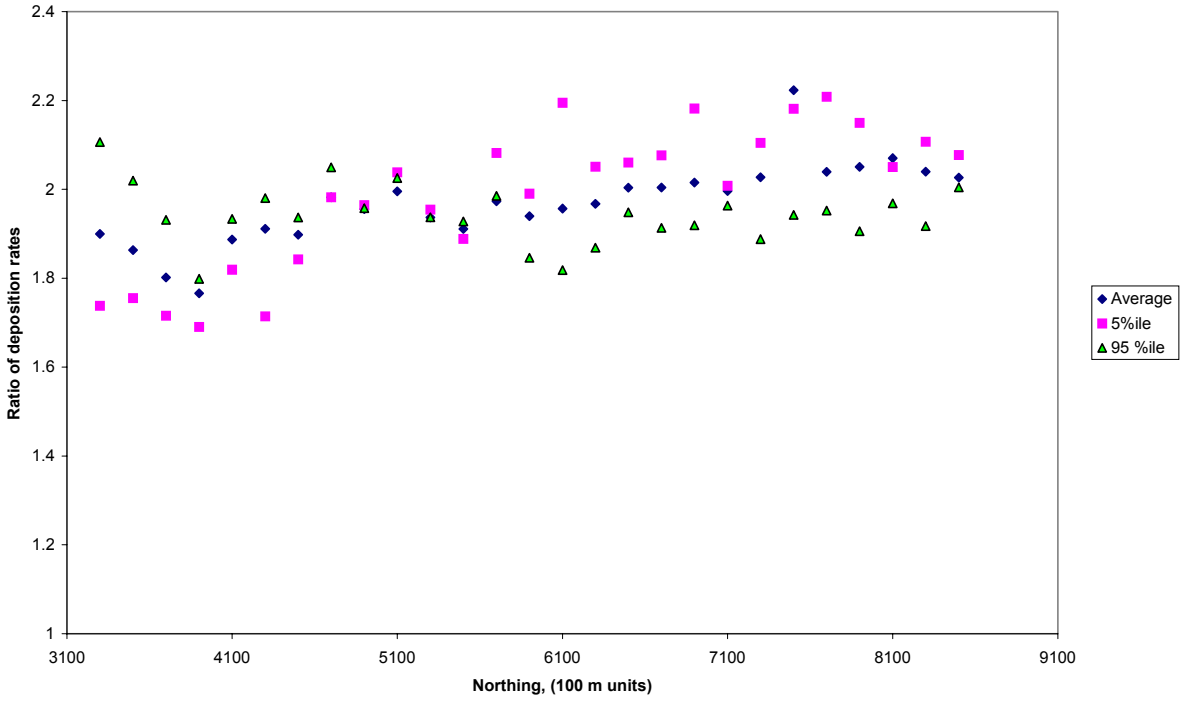

Figure 4.26 Ratio of contribution to rates of oxidised nitrogen deposition for sources emitting 150 kt and 75 kt per annum of oxides of nitrogen (as NO2): TRACK model 1990 background emissions: source at (5100, 3100)

4.6 HARM Model - Baseline predictions

4.6.1 Sampling based on Latin Squares

The HARM model was used to predict oxidised and reduced nitrogen deposition for the baseline scenario for input parameters in ranges identified in the assessment described in Section 3. The baseline scenario was based on the 1997 emissions inventory for the UK and for the EMEP grid. The input ranges for each parameter are shown in Table 4.4. (Table 4.4 also shows the increment size used in the first order error analysis referred to below). Values of each parameter were sampled at random from the range assuming a uniform distribution using a sampling strategy based on a Latin Square. Twelve model runs were carried out. Values of the 8th and 92nd percentile rates of deposition were estimated from the minimum and maximum modelled results (1/12~8%).

Figure 4.27 shows the predicted mean and 8th and 92nd percentile rates of oxidised nitrogen deposition at grid squares containing the Acid Deposition Network sites throughout the United Kingdom. The 92nd percentile value is typically around 1.5 times

the average: the average is typically around 1.5 times the 8 th percentile. The predicted rates of deposition are broadly similar to those predicted using the TRACK model (Figure 4.15) with average rates of deposition generally agreeing within a factor of two at each of the grid squares containing the Network sites.

Figure 4.28 shows the predicted mean and 8th and 92nd percentile rates of reduced nitrogen deposition at Acid Deposition Network sites throughout the United Kingdom. The 92nd percentile value is typically around 1.5 times the average: the average is typically around 1.5 times the 8th percentile.

Table 4.4 Input ranges of parameters used in Latin Square simulation and first order error analysis for the HARM model

Parameter	Units	Baseline	Range, % of baseline		Increment, % of baseline
			Lower limit	Upper limit	
Dry deposition velocity, NO_2		Land use dependent	30	170	33
Dry deposition velocity, HNO_3			50	200	50
Wet scavenging coefficient, aerosols	s^{-1}	$1.3.\ 10^{-5}$	30	1000	100
Ratio of reaction rates, $NO + O_3 \rightarrow NO_2 + O_2$ and $NO_2+hv \rightarrow NO+O \rightarrow NO+O3$		Appendix 1	0	200	50
Reaction rate, $OH + NO_2 (+ M) \rightarrow HNO_3 (+ M)$		Appendix 1	70	170	50
Reaction rate, $NO_2 + O_3 \rightarrow NO_3 + O_2$		Appendix 1	70	130	50
Reaction rate, $NH_3 + HNO_3 \rightarrow NH_4NO_3$		Appendix 1	50	200	50
Reaction rates nitric acid with aerosols	s^{-1}	$3.\ 10^{-5}$	30	1000	100
Ammonia emissions		Inventory	50	200	50
Sulphur dioxide emission		Inventory	50	200	50
Oxides of nitrogen emissions		Inventory	80	120	20
Boundary layer height	m	800	80	120	12.5

Figure 4.29 and Figure 4.30 show the cumulative probability of predicted oxidised and reduced nitrogen depositions at the Jenny Hurn site. In both cases, the distribution is approximately log-normal over the 8th to 92nd % ile range.

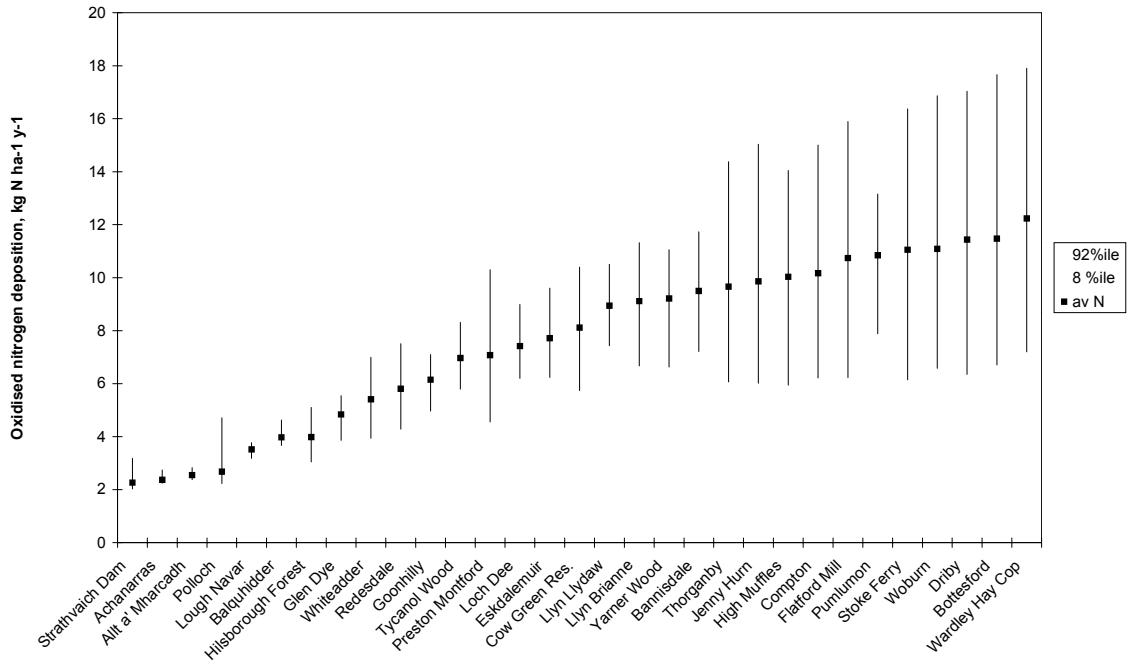

Figure 4.27 Predicted oxidised nitrogen deposition at monitoring sites, HARM with 1997 emissions: mean, 8th %ile and 92nd %ile predictions from Latin Square analysis.

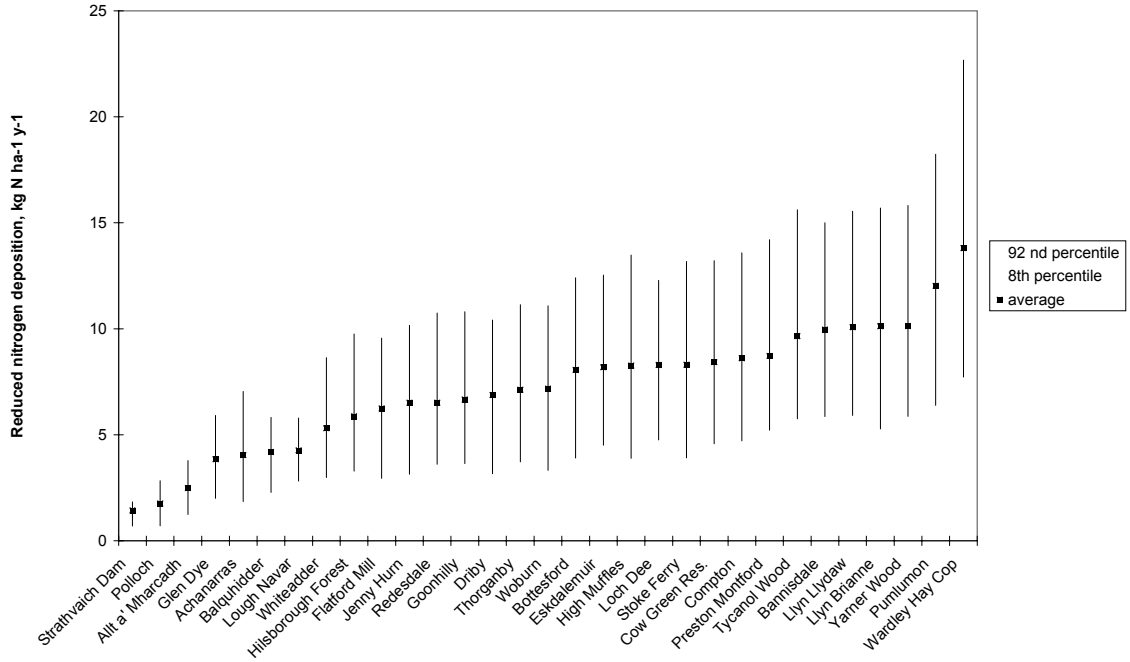

Figure 4.28 Predicted reduced nitrogen deposition at monitoring sites, HARM with 1997 emissions: mean, 8th %ile and 92nd % ile predictions from Latin Square analysis.

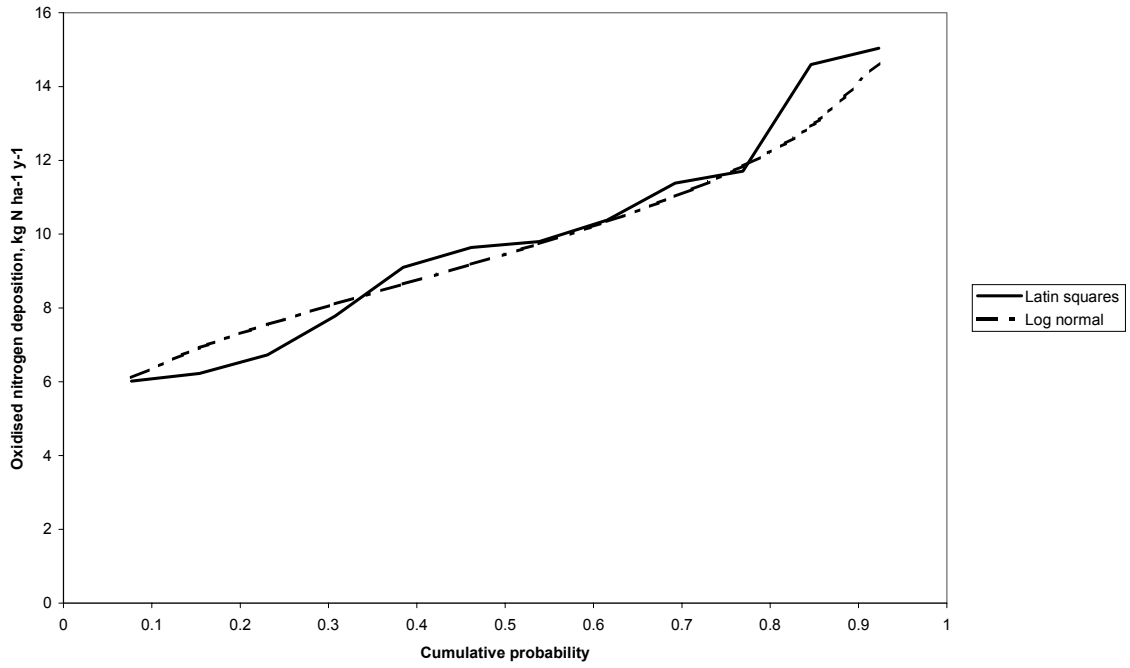

Figure 4.29 Cumulative probability distribution of oxidised nitrogen deposition: HARM model, 1997 emissions, Jenny Hurn

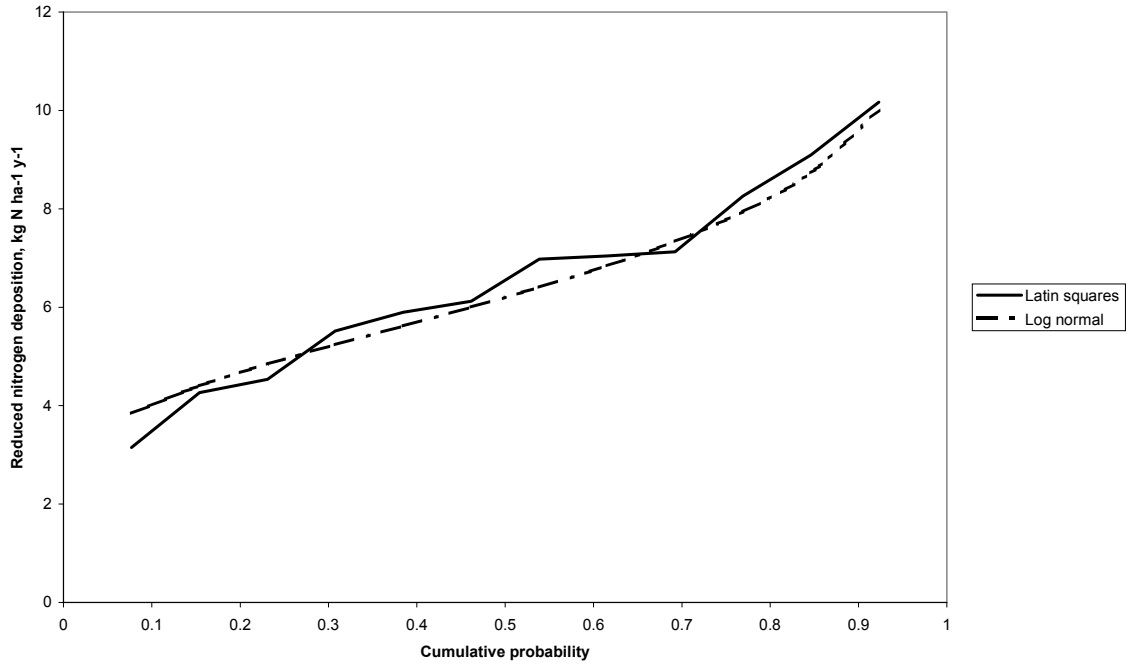

Figure 4.30 Cumulative probability distribution of reduced nitrogen deposition: HARM model, 1997 emissions, Jenny Hurn

4.6.2 First order error analysis

For the first order analysis, the input parameters were varied one at a time from the baseline value. The final column in Table 4.4 shows the chosen incremental changes in the input parameters. The average, 5th percentile and 95th percentile rates of deposition were calculated as described in Section 4.4.2.

Figure 4.31 shows the predicted average, 5th percentile and 95th percentile oxidised nitrogen deposition at the Acid Deposition Network sites. It also shows the values derived from the Latin Square simulation for comparison. In each case, the first order analysis has provided predictions of oxidised nitrogen deposition similar to those provided by the Latin Square sampling analysis.

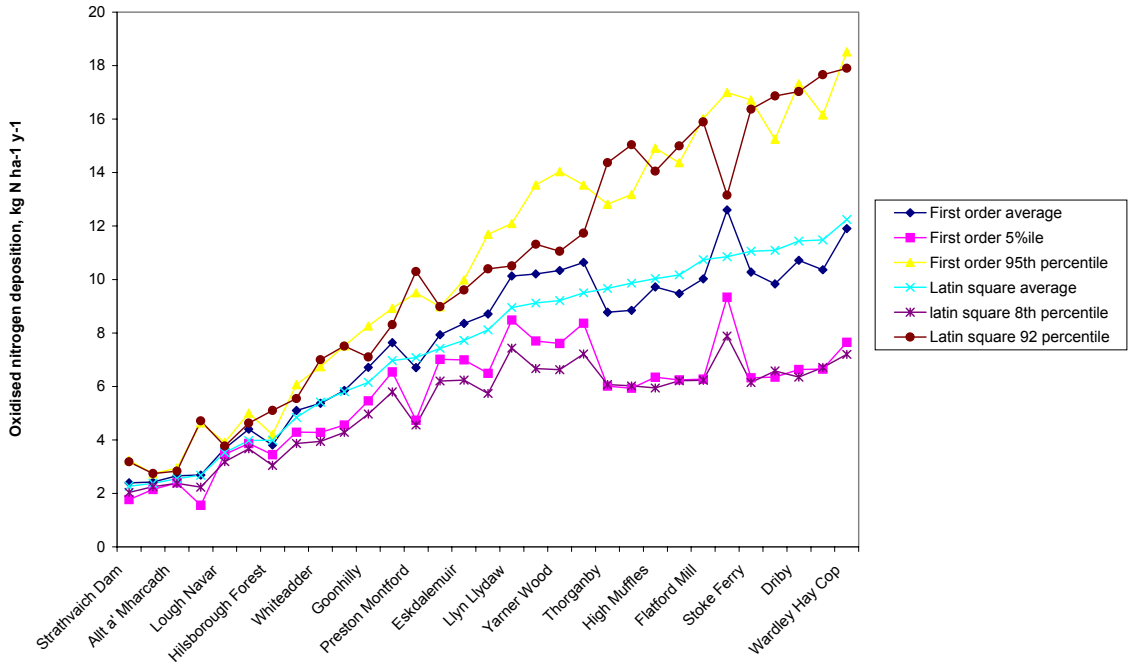

Figure 4.31 Average, 5th percentile and 95th percentile oxidised nitrogen deposition predicted using HARM, 1997 emissions: Latin Square and first order error analysis

Figure 4.32 shows the predicted average, 5th percentile and 95th percentile reduced nitrogen deposition at the Acid Deposition Network sites. It also shows the values derived from the Latin Square sampling simulation for comparison. The first order analysis has provided predictions of average and 5th percentile reduced nitrogen deposition similar to those provided by the Latin Square sampling. The 95th percentile value was typically 30% greater than that provided by the Latin Square sampling.

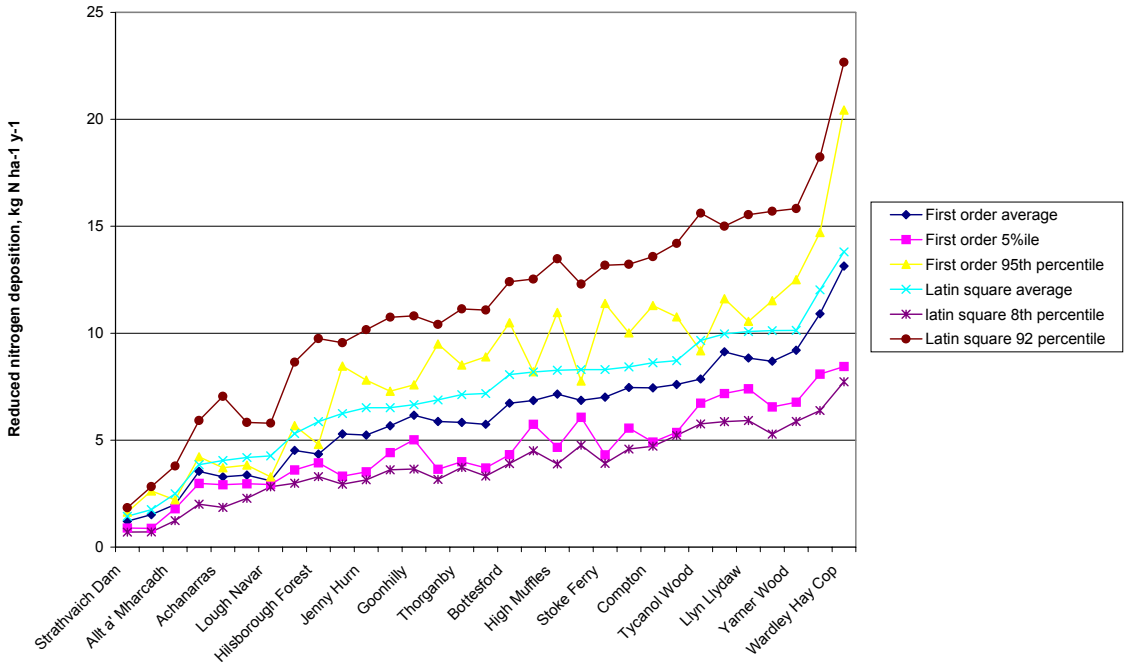

Figure 4.32 Average, 5 percentile and 95th percentile reduced nitrogen deposition predicted using HARM, 1997 emissions: Latin Square and first order error analysis

4.6.3 Spatial expression of changes in model input parameters

The impact of changes in the input parameters set out in Table 4.4 will vary in both magnitude and spatial pattern. Parameters which relate to dry deposition might be expected to have the greatest effect in source regions, while those associated with aerosol production and washout rates will affect wet deposition and might be expected to be more influential in remote areas. Some of these issues are discussed further in Appendix 7.

4.7 HARM Model - Impact of an additional point source

4.7.1 First order error analysis

The model was run with an additional point source emitting 150 kt per annum of oxides of nitrogen (equivalent to approximately two power stations of the size of Drax) at OS grid reference (5100, 3100) (near Peterborough). The input parameters were varied one at time using the values used for the first order analysis of the baseline. The impact of this additional source in terms of the UK budget is summarised in Table 4.5. When the source is emitting 150 kt NO_x, total deposition of oxidised N across the UK is calculated to increase by 1.9%.

Table 4.5 HARM modelled UK deposition budgets with and without additional source

	Dry S	Wet S	Total S	Dry NO_y-N	Wet NO_y-N	Total NO_y-N	Dry NH-N	Wet NH-N	Total NH-N
Base	89.6	120.2	209.8	47.2	106.6	153.8	56.0	71.9	127.9
75 kt	89.6	120.2	209.8	48.5	107.2	155.7	56.0	72.0	128.0
150 kt	89.6	120.2	209.8	49.4	107.4	156.8	56.0	72.0	128.0

The incremental impact of the additional source was determined for each model run by subtracting the baseline deposition from the total deposition. The incremental deposition from the source was calculated at receptors on a trajectory passing through the point source in a direction 330^{o} from north (i.e. towards the northwest of Scotland). Figure 4.33 shows the 5th percentile, average and 95th percentile incremental contribution from the source to oxidised nitrogen deposition at increasing distances from the source. The contribution generally decreases with distance from the source, although local variations in dry deposition velocity and rainfall have some influence on the predicted values. The 95th percentile value is typically approximately 1.4 times the average value: the 5th percentile is approximately 0.7 times the average value. Figure 4.33 shows some areas where the rate of deposition increases with distance from the source: the areas of increased deposition broadly correspond to the Yorkshire Dales, Southern Uplands and Scottish Highlands reflecting the enhanced deposition in upland areas.

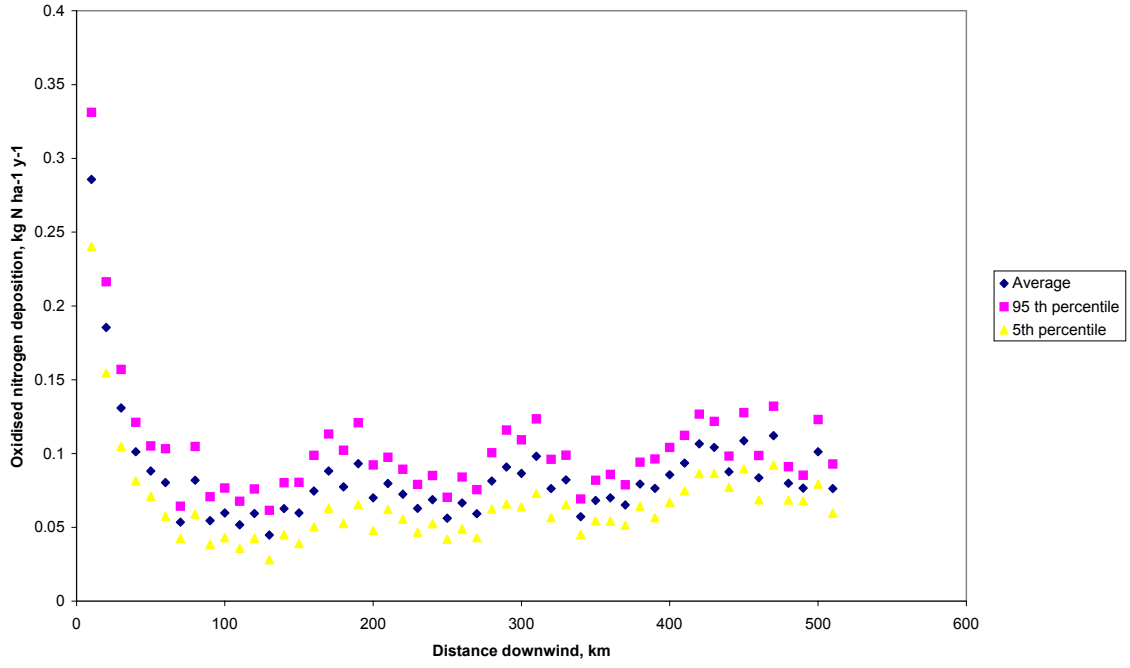

Figure 4.33 Incremental contribution to oxidised nitrogen deposition from a point source at (5100,3100) emitting 150 kt oxides of nitrogen per year, HARM model, 1997 base emissions, first order analysis

4.8 FRAME

4.8.1 Sampling based on Latin Square

The FRAME model was used to predict reduced nitrogen deposition for the baseline scenario for input parameters in ranges identified in the assessment described in Section 3. The baseline scenario was based on the 1997 emissions inventory for the UK and for the EMEP grid. The input ranges for each parameter are shown in Table 4.6. Values of each parameter were sampled at random from the range assuming a uniform distribution using a sampling strategy based on a randomised Latin Square. Twelve model runs were carried out with randomised input variables. The model experienced some stability problems when relatively extreme values of the input parameters were used, particularly for dry deposition velocities and wet scavenging coefficients. The stability problems were resolved by reducing the model time step: however, the time required to carry out the model runs was considered excessive. Consequently all randomised model runs were carried out with these parameters set to their baseline values.

Figure 4.34 shows the predicted mean and 8th and 92nd percentile rates of reduced nitrogen deposition at Acid Deposition Network sites throughout the United Kingdom. The mean values are a little larger than those predicted by the TRACK and HARM models. The 92nd percentile value is typically around twice the average: the average is typically around twice times the 8th percentile.

Table 4.6 Input ranges of parameters used in the Latin Square simulation and first order error analysis for the FRAME model

Parameter	Units	Baseline	Range, % of baseline		Increment%
			Lower limit	Upper limit	
Dry deposition velocity of ammonia		Land use and time variable	10^{+}	2000^{+}	100
Dry deposition of HNO3	mm s^{-1}	40	50^{+}	200^{+}	50
Dry deposition aerosols	mm s^{-1}	1	0^{+}	100^{+}	-50
Sulphur dioxide emission		Inventory	50	200	50
Ammonia emissions		Inventory	50	200	50
Oxides of nitrogen emissions		Inventory	80	120	20
Ammonium nitrate equilibrium factor		Appendix 1	50	200	-50
Vertical dispersion coefficient		Default value	50	200	100
Boundary layer height	m	800	80	120	20
Wind speed	m s^{-1}	7.5	75	125	10
$^{+}$ Baseline value only used for Latin Square sampling					

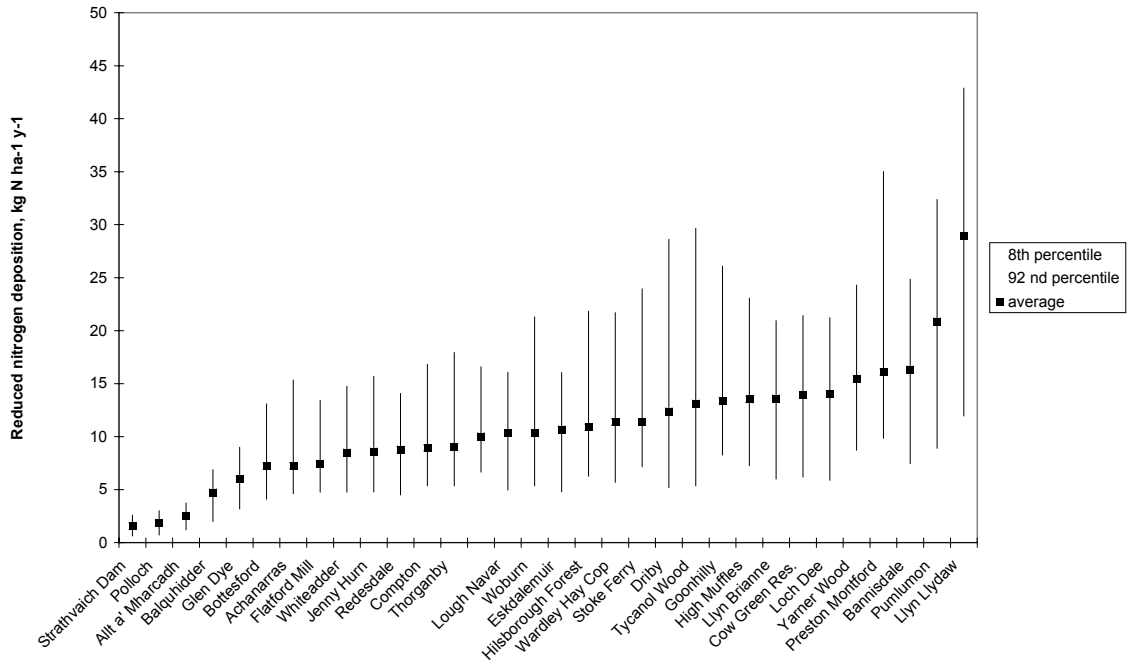

Figure 4.34 Predicted reduced nitrogen deposition at monitoring sites, FRAME with 1997 emissions: mean, 8th %ile and 92nd %ile predictions from the Latin Square analysis.

Figure 4.35 shows the cumulative probability of predicted reduced nitrogen depositions at the Jenny Hurn site.

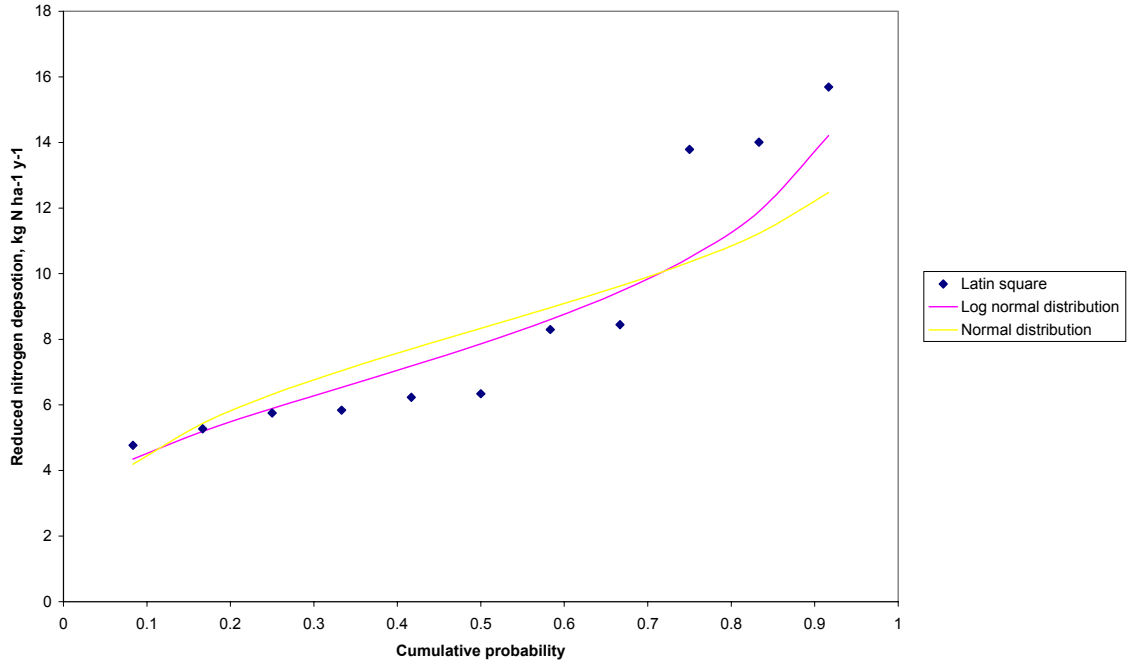

Figure 4.35 Cumulative probability distribution of reduced nitrogen deposition: FRAME model, 1997 emissions, Jenny Hurn

4.8.2 First order error analysis

For the first order error analysis, the input parameters were varied one at a time from the baseline value. The final column in Table 4.6 shows the chosen incremental changes in the input parameters. The variance of the log distribution of predicted rates of reduced nitrogen deposition was calculated as described in Section 4.4.2. The contribution to the variance from each of the input parameters is shown in Table 4.7 for a selection of sites.

Table 4.7 Contribution to variance from each of the input parameters

	Contribution to variance from input parameters %				
	Polloch	Stathvaich Dam	Yarner Wood	Flatford Mill	Jenny Hurn
Dry deposition velocity ammonia	16	15	0	8	2
Dry deposition velocity nitric acid	0	0	0	0	0
Dry deposition velocity aerosols	0	0	0	0	0
Sulphur dioxide emission	0	0	0	0	0
Ammonia emission	22	10	59	40	56
Oxides of nitrogen emission	0	0	0	0	0
Ammonium nitrate equilibrium factor	0	0	0	0	0
Vertical dispersion coefficient	0	0	0	0	1
Boundary layer height	2	4	3	6	5
Wind speed	59	70	38	46	36
$V(\varphi)$	1.11	1.60	0.36	0.49	0.48

Table 4.7 shows that the uncertainty in the dry deposition velocity of ammonia, the ammonia emission rates and the wind speed make the greatest contributions to the uncertainty in the predicted rates of reduced nitrogen deposition. The uncertainty in other parameters, such as the vertical dispersion coefficient, make much smaller contributions to the overall uncertainty.

5 UNCERTAINTY IN CRITICAL LOADS

5.1 Introduction

Having undertaken detailed analysis of the likely uncertainties in estimates of acid deposition over the U.K., it is appropriate to consider the uncertainty in the environmental objectives with which the deposition will be compared. The formal definition of a critical load is: "a quantitative estimate of an exposure to one or more pollutants below which significant harmful effects on specified sensitive elements of the environment do not occur according to present knowledge" (Nilsson and Grennfelt, 1988). This definition was elaborated at a workshop at Skokloster in Sweden in 1988, and has been used to develop policy within the UNECE, and more recently the EU, ever since. The underlying notion is that of a threshold: if deposition is below the threshold there are no problems; if it is above the threshold, harm is being done to the environment. This is the way the concept is explained to policymakers: it therefore appears to make sense to reduce deposition below the critical load as quickly as possible, in order to avoid further harm.

But defining "significant harmful effects" for sensitive elements of the environment on a European scale is a formidably difficult task. The natural environment is immensely complex, constantly changing, and not well understood. There are millions of species of animals, plants and micro-organisms interacting in an inconceivably vast number of ways with each other and with the physical environment. The response of only a few of these species to only a few pollutants is known over only a small range of conditions. Even for these, pollutant effects may be modified e.g. by interaction with other pollutants, or by different physical conditions. Even then, species sometimes have geographically distinct ecotypes with a different response to pollutants; there is invariably a range of responses between individuals. Over large areas such as Europe, there are pronounced gradients in physical conditions that change the relative importance of ecosystem processes. Even if the response of species or ecosystems to pollutants were known with certainty, data on species distribution and physical characteristics of the environment would still need to be known at a fine scale. These difficulties are of course not unique to the critical loads approach: they apply to the setting of any sort of scientifically-based environmental quality standard. The critical load approach attempts to overcome them by concentrating on certain species that are known to be sensitive to pollutant deposition, or chemical substitutes for these, in the hope that this will also protect every other component of the ecosystem. It is clear then that the critical load threshold, if there is one, is likely to be very fuzzy.

Appendix 4 is a literature review of the analysis of uncertainty in critical loads. It contains a summary of the methods used to estimate critical loads, a description of previous uncertainty analyses for critical loads and a discussion of the issues associated with the validation of critical loads estimation methods and other factors contributing to the uncertainty. The aim of Appendix 4 is to summarize current knowledge about the uncertainties entailed in estimating critical loads. Only an outline of critical load

methodology is given: full details will be found in the official UNECE Mapping Manual (UBA, 1996), in reports from the UK National Focal Centre at Monks Wood (Hall *et al.* 1997, 1998, 2001a) and in publications of the Co-ordinating Centre for Effects (CCE) in the Netherlands (Posch *et al*. 1995, 1997, 1999, 2001).

The UK calculates critical loads for 6 ecosystems: acid grasslands; calcareous grasslands; heathlands; coniferous woodland; deciduous woodland and freshwaters. For each of these, four critical loads are calculated corresponding to the nodes on the critical loads function (Figure 5.1). These are the maximum critical load for sulphur ($CL_{max}S$); the maximum critical load for nitrogen ($CL_{max}N$); the minimum critical load for N ($CL_{min}N$); and the critical load for nutrient N ($CL_{nut}N$).

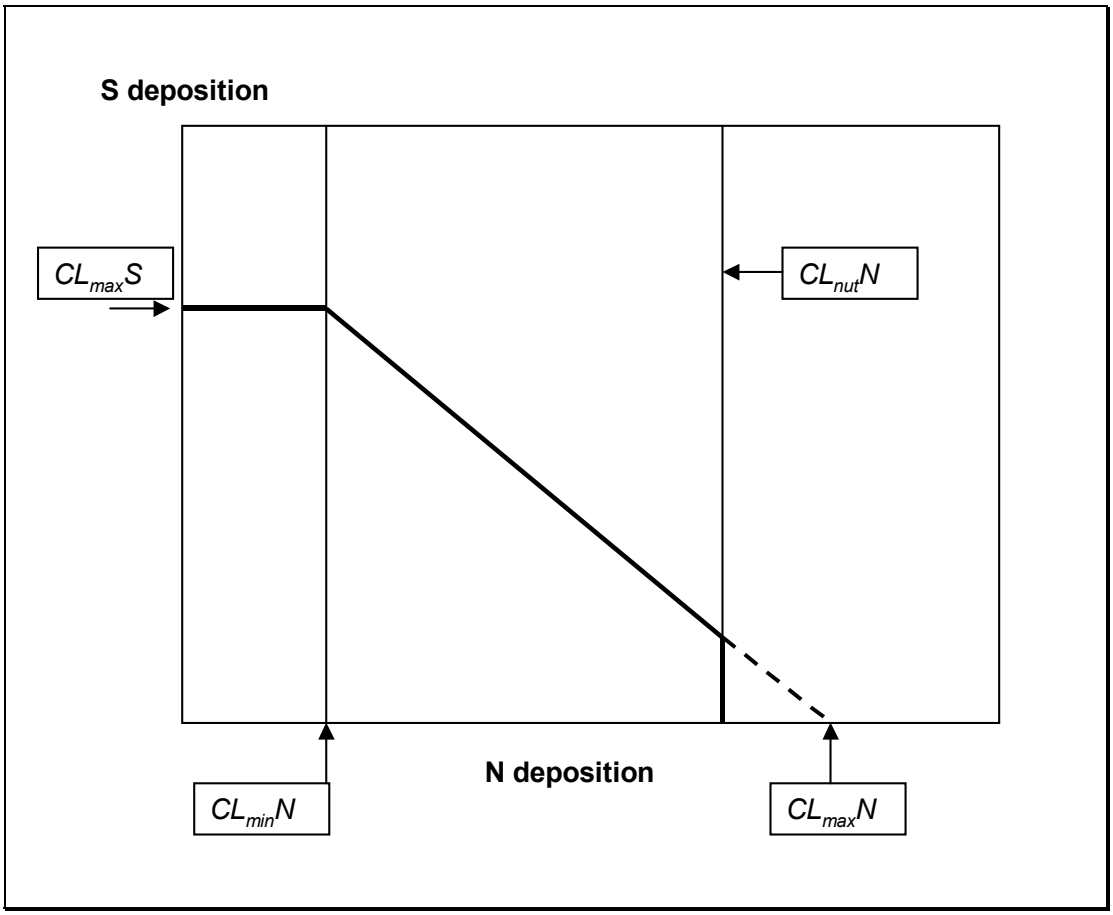

Figure 5.1 The critical load function.

The thick line represents the critical load for a hypothetical ecosystem as a function of S and N deposition. The $CL_{max}S$ represents the critical load for acidity when nitrogen deposition is zero. The critical load is equal to $CL_{max}S$, whilst all nitrogen deposition is taken up by the catchment, hence the horizontal portion of the critical load function. $CL_{min}N$ is the deposition-independent critical load of acidity due to nitrogen removal processes alone (nitrogen uptake, immobilization, and denitrification). $CL_{max}N$ is the critical load for acidity when S deposition is zero. $CL_{nut}N$ is the critical load for nutrient nitrogen, intended to protect against non-acidifying effects of N deposition. In this example, $CL_{nut}N$ is less than $CL_{max}N$, truncating the function, but this is not necessarily the case.

Appendix 4 describes the theoretical background, the methods the U.K. uses for calculation, and the major uncertainties in the methods for each type of critical load.

The critical load will vary from site to site. Hence it is not practical in this study to estimate in a general way the uncertainty in the critical load function. However soils in forested areas are particularly sensitive to acidification and therefore would represent an important case study. The uncertainty in the estimation of critical loads for these areas was investigated by means of a case study for a coniferous forest area at Liphook in the south of England. Appendix 5 contains details of the case study. It is summarised below.

5.2 Uncertainty in critical load function, Liphook case study

The value of $CL_{max}S$ was estimated by repeated evaluation of the Steady State Soil Mass Balance equation for a range of input values:

$$CL_{\max}(S) = BC^{*}_{dep} - Cl^{*}_{dep} + BC_w - BC_u + \left(1.5 \times \frac{Bc_{dep} + Bc_w - Bc_u}{(Bc/Al)_{crit}}\right) + Q^{2/3} \times \left(1.5 \times \frac{Bc_{dep} + Bc_w - Bc_u}{(Bc/Al)_{crit} \times K_{gibb}}\right)^{1/3}$$

where BC is the flux of base cations ($Na^+ + K^+ + Ca^{2+} + Mg^{2+}$), and the suffixes represent:
dep- deposition
w - weathering (i.e. release of base cations from soil minerals or rock minerals)
u - uptake by plants into perennial tissues;
* represents non-marine;
Bc (distinct from *BC*) is the flux of base cations other than Na. The evaluation considered Ca^{2+} only, following U.K. practice (see Appendix 4 Section 2.4.2);
$(Bc/Al)_{crit}$ is the critical base cation/Al ratio defined by the user;
Q is effective rainfall/runoff;
K_{Gibb} is the Gibbsite coefficient, expressing the ratio between Al and H^+ concentrations in the soil solution.

All fluxes are expressed in equivalence units e.g. keq ha^{-1} y^{-1} or meq m^{-2} y^{-1}.

The minimum critical load of nitrogen represents the critical load of acidity due solely to nitrogen removal processes in soil:

$$CL_{min}N = N_u + N_i + N_{de}$$

where N_u is the nitrogen uptake;
N_I is the nitrogen immobilisation; and
N_{de} is the denitrification.

For woodland ecosystems, N_u is set at 7 kg N ha^{-1} yr^{-1}. The value of N_i is either 1 or 3 kg N ha^{-1} y^{-1} depending on soil type, and likewise the value of N_{de} is 1, 2 or 4 kg N ha^{-1} y^{-1} depending on soil type. (Note 1 kg N ha^{-1} y^{-1} = 1/14 keq ha^{-1} y^{-1}).

For terrestrial ecosystems,

$$CL_{max}N = CL_{max}S + CL_{min}N$$

Values of the input parameters were selected at random from a plausible range of input values for the site. One thousand evaluations were carried out using the proprietary software package Crystal Ball. Appendix 5 describes the range and distribution of input parameters used in the analysis.

Figures 5.2 to 5.4 show the cumulative probability distribution for $CL_{max}S$, $CL_{min}N$ and $CL_{max}N$. The figures show the normal distribution curve fitted to the Monte Carlo predictions.

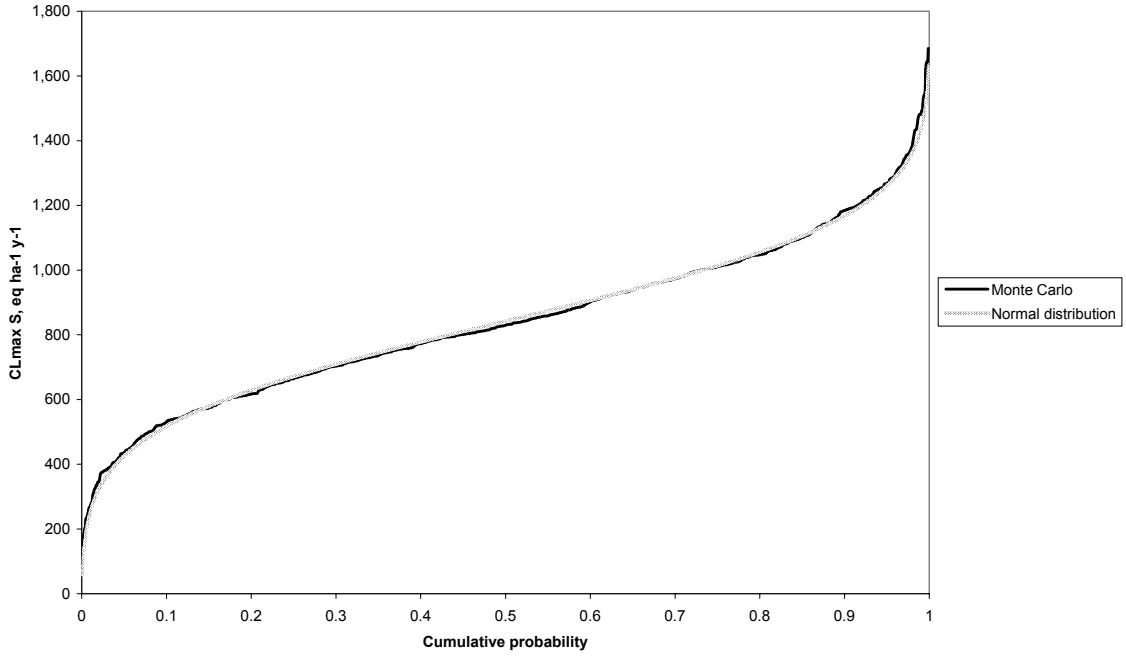

Figure 5.2 Cumulative probability distribution of the critical load parameter $CL_{max}S$ for the Liphook site

Table 5.1 shows the means, standard deviations and coefficients of variation of the predicted critical load function parameters.

Table 5.1 Mean standard deviation and coefficient of variation of the predicted critical load function parameters

	Mean, eq ha^{-1} y^{-1}	Standard deviation, eq ha^{-1} y^{-1}	Coefficient of variation, %
$CL_{min}N$	775	172	22
$CL_{max}S$	848	244	29
$CL_{max}N$	1613	220	14

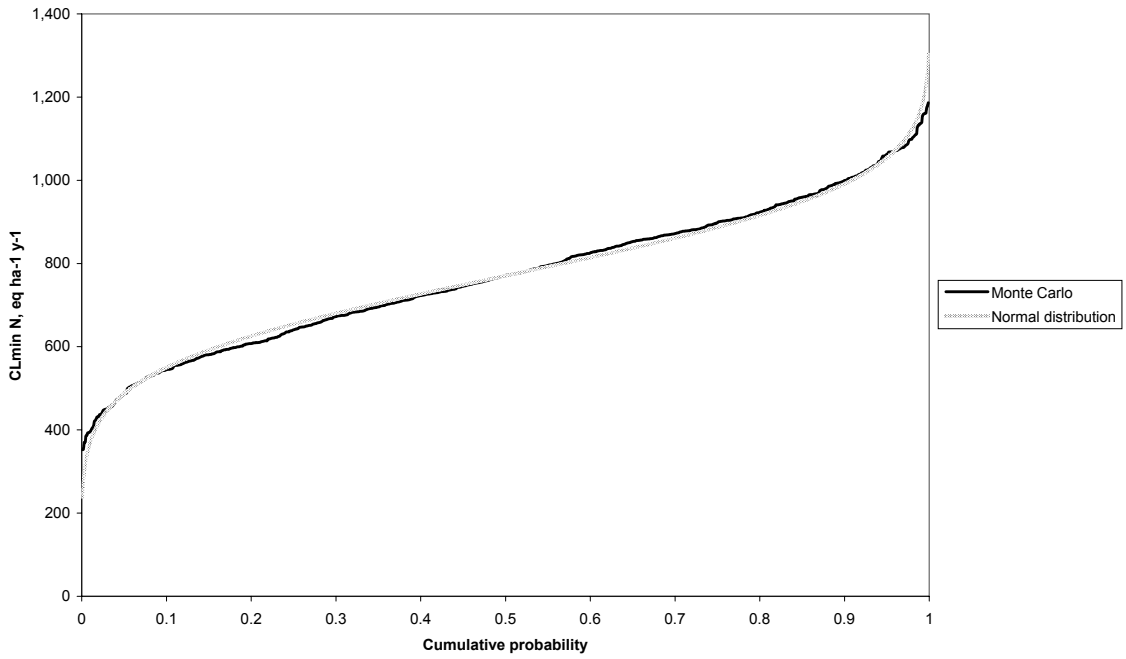

Figure 5.3 Cumulative probability distribution of the critical load parameter $CL_{min}N$ for the Liphook site

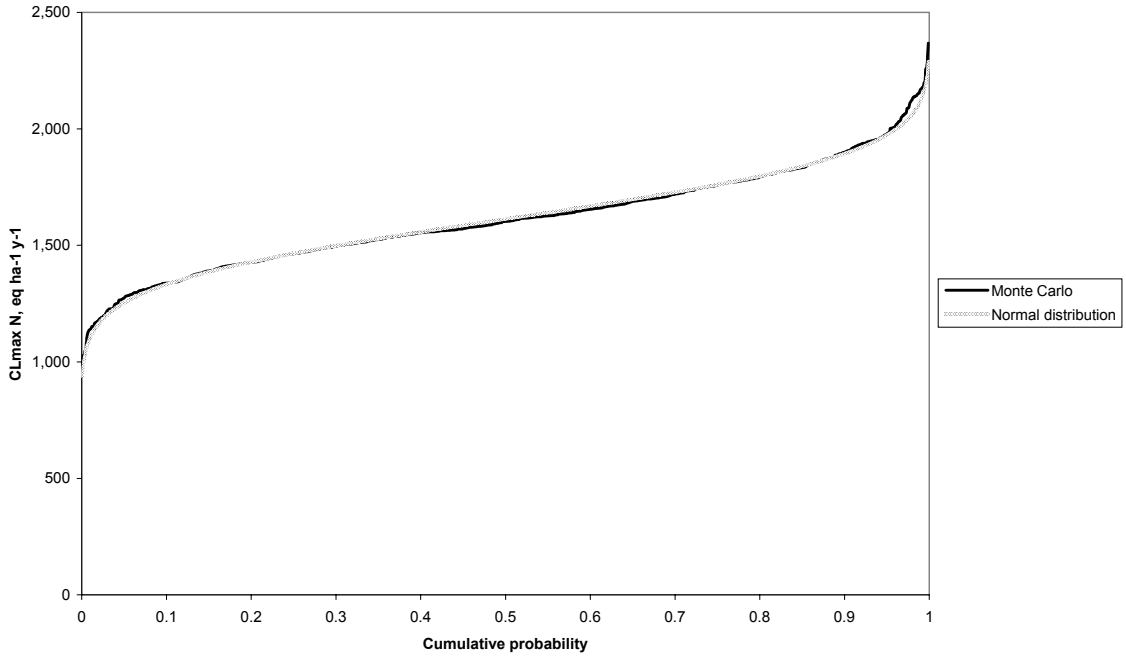

Figure 5.4 Cumulative probability of critical load parameter $CL_{max}N$ for the Liphook site

6 OVERALL UNCERTAINTY IN THE PREDICTION OF CRITICAL LOAD EXCEEDENCES

6.1 Introduction

The critical load exceedence, the extent to which the deposition exceeds the critical load defined by the critical load function, provides a measure of the extent to which the rate of deposition predicted by the acid deposition models exceeds the estimated critical load at a particular site. It provides an indication of the likely potential for harm caused by acid deposition and the extent to which deposition should be reduced to prevent harm. The overall uncertainty in the exceedence prediction depends on the uncertainty in the predictions of deposition and the estimates of the critical load. The combined overall uncertainty in exceedence for the case study site at Liphook is investigated in this section.

6.2 Calculation of exceedence

The exceedence was calculated from:

$$E = S_{dep} - CL_{\max} S \qquad \text{when } N_{dep} < CL_{\min} N$$

$$E = N_{dep} + S_{dep} - CL_{\max} N \qquad \text{when } N_{dep} \geq CL_{\min} N$$

which hold for the special case

$$CL_{max}N = CL_{max}S + CL_{min}N$$

where S_{dep} is the total wet and dry deposition of sulphur, eq ha^{-1} y^{-1}, and
N_{dep} is the total wet and dry deposition of oxidized and reduced nitrogen, eq ha^{-1} y^{-1}.

The probability distribution of the exceedence was developed from the probability distributions of the critical loads and the predicted rates of deposition by Monte Carlo simulation. For each of the 1000 joint estimates of $CL_{max}S$, $CL_{min}N$ and $CL_{max}N$ (see Section 5.2) a joint estimate of S_{dep} and N_{dep} was sampled at random from the 300 randomized TRACK model runs (see Section 4.4.1). Figure 6.1 shows the probability distribution of the predicted exceedence at the Liphook site for the TRACK predictions using the 1990 emissions inventory. It shows that the probability that the rate of deposition was less than the critical load was less than 0.1% i.e. there is a high degree of confidence that the critical load was exceeded.

Consideration was then given to the situation resulting from a reduction in the rates of deposition following a global reduction in emissions of sulphur dioxide and oxides of nitrogen. Figures 6.2 to 6.5 show the cumulative distribution of exceedence for predicted rates of deposition of 0.5, 0.2, 0.1 and 0.05 times the predicted rates for the 1990 emission inventory. Note that the predicted rates of deposition are approximately log-normally distributed (see Section 4.4.1).

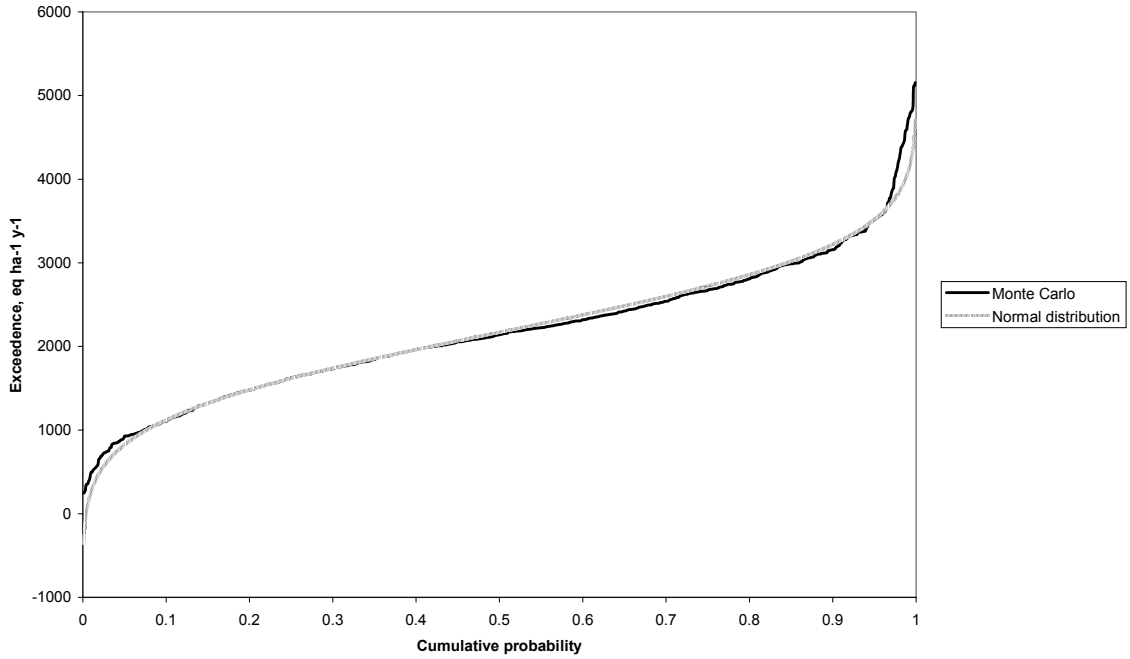

Figure 6.1 Cumulative probability distribution of predicted exceedence at Liphook, 1990 emissions. Note the position of exceedence = 0 on the y axis.

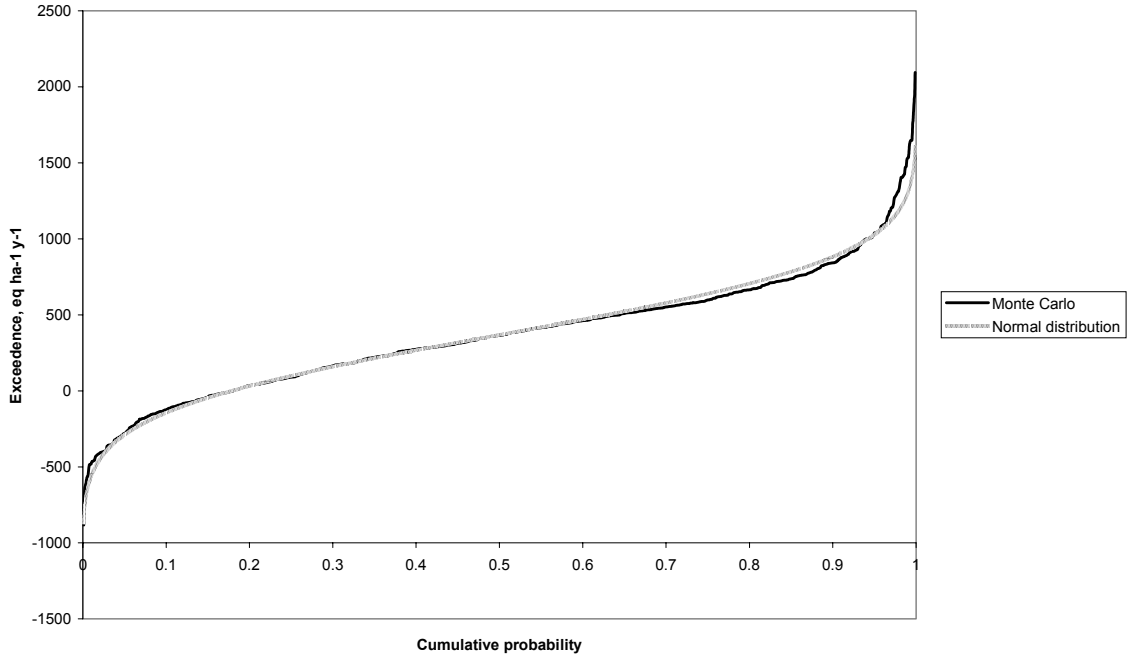

Figure 6.2 Cumulative probability distribution of predicted exceedence at Liphook, assuming deposition equals half that for 1990 emissions. Note the position of exceedence = 0 on the y axis.

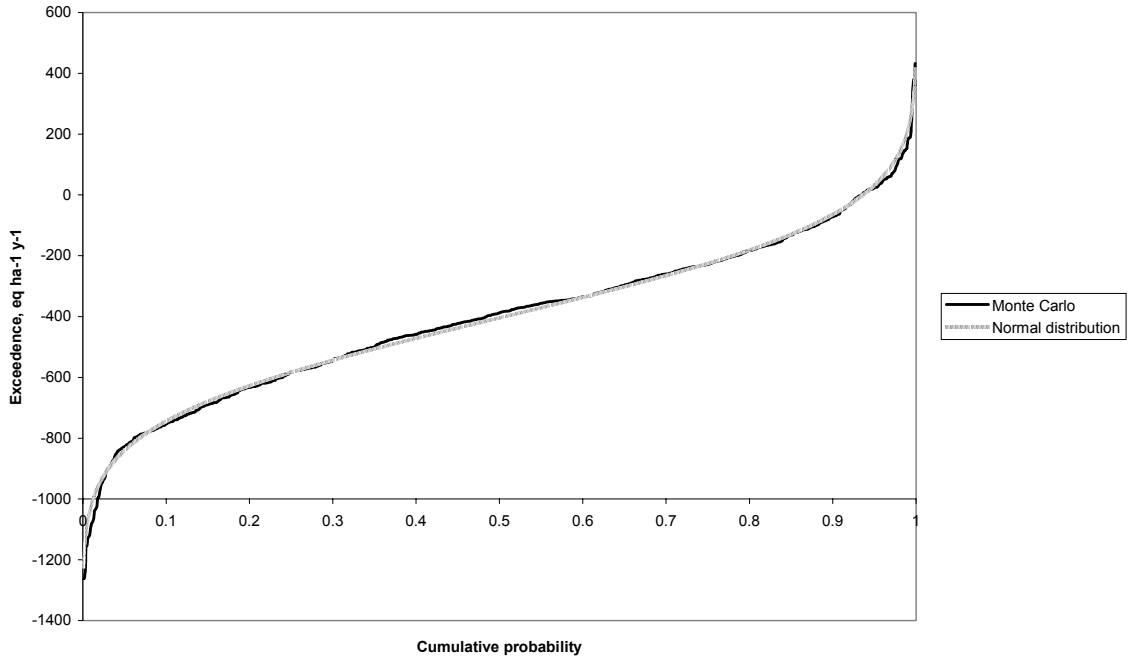

Figure 6.3 Cumulative probability distribution of predicted exceedence at Liphook, deposition 20% of that for 1990 emissions. Note the position of exceedence = 0 on the y axis.

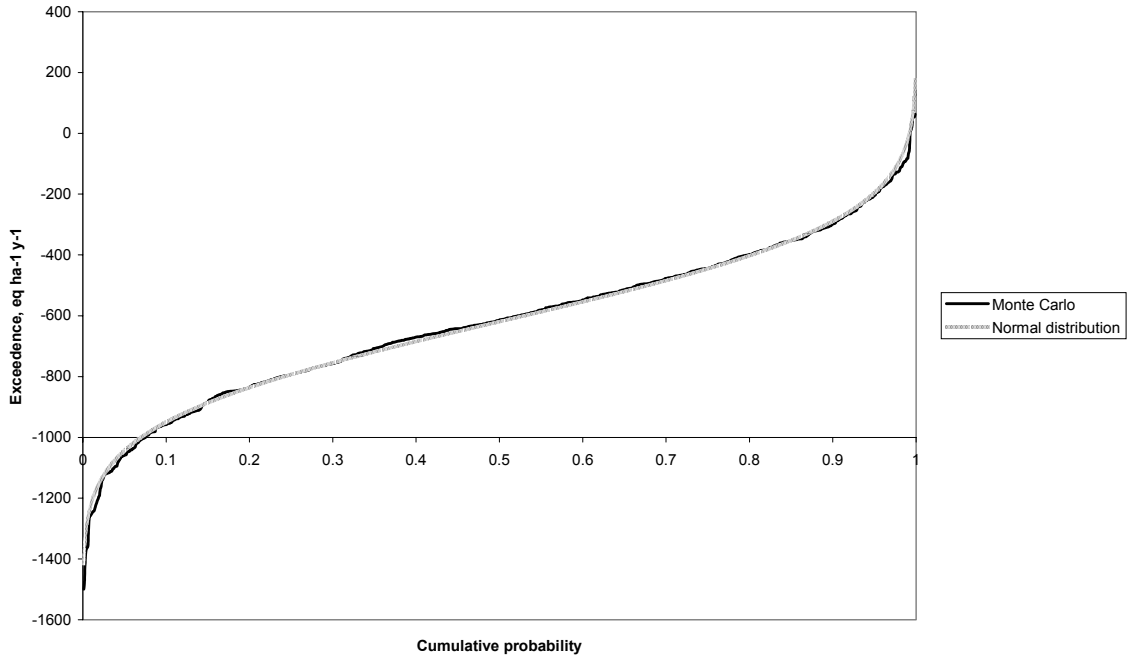

Figure 6.4 Cumulative probability distribution of predicted exceedence at Liphook, deposition 10% of that for 1990 emissions. Note the position of exceedence = 0 on the y axis.

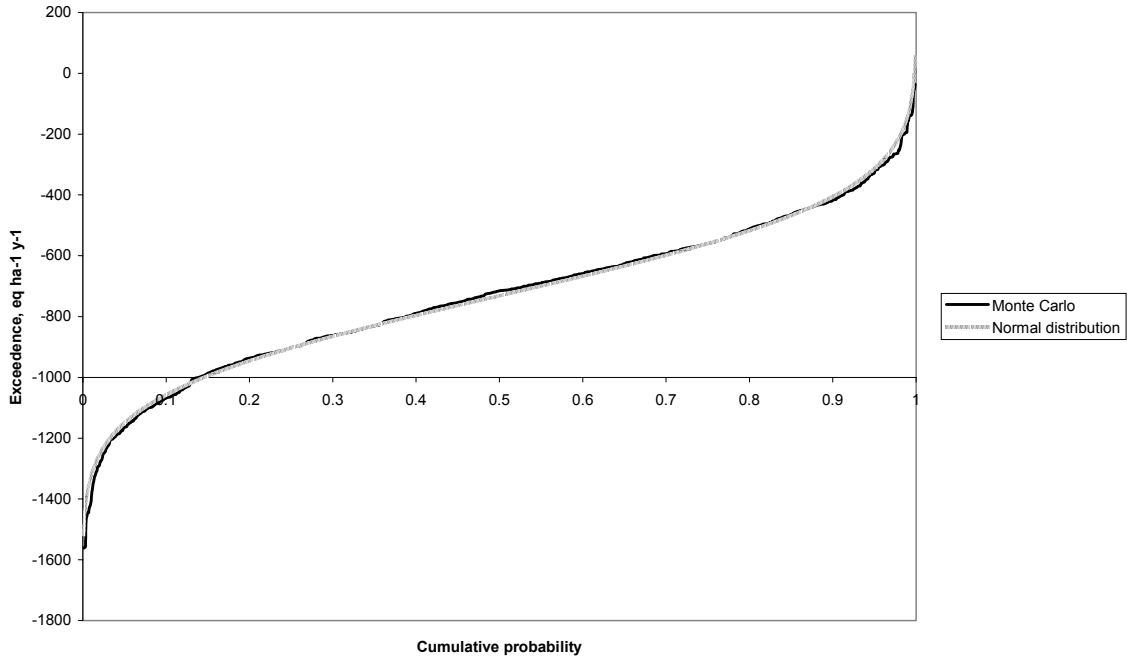

Figure 6.5 Cumulative probability distribution of predicted exceedence at Liphook, deposition 5% of that for 1990 emissions. Note the position of exceedence = 0 on the y axis.

Table 6.1 shows the standard deviation of the exceedence and the probability of exceedence for each of the sampled scenarios. Note that the standard deviation of the exceedence falls to values similar to the standard deviation of the critical loads (see Table 5.1) as the probability of exceedence decreases. One would expect this, as in this range the acid deposition is generally comparable or less than the critical load function.

Table 6.1 Effect on the standard deviation of exceedence and probability of exceedence as the rate of deposition is reduced.

Deposition attenuation factor (applied to sulphur and nitrogen deposition)	Standard deviation, eq ha^{-1} y^{-1}	Probability of exceedence, %
1	771	>99.9
0.5	400	83
0.37	308	50
0.2	268	7
0.1	259	0.6
0.05	253	<0.1

Examination of Table 6.1 indicates that meeting the critical load as a limit value might be achieved if the rate of deposition was reduced to slightly less than 40% of the 1990 predictions (accepting a probability of 50%). Reducing the rate of deposition to less

than 20% of the 1990 predictions would lead to a high degree of confidence (with a probability of 95%) that the critical load was not exceeded. Table 6.1 shows that the risk of exceeding the critical load at Liphook decreases from very high to very low as the rate of deposition decreases from 1990 levels to 5% of 1990 levels. This suggests that a probabilistic approach to the critical load and regional or national scale deposition models can be applied to regional scale emissions policy development.

The effect of an increase in deposition from an additional source on the risk of exceedence may be assessed as follows. Take for example, a 150 kt per annum emission of NO_x, corresponding to a very large power station. Figure 4.25 for TRACK and Figure 4.33 for HARM indicate that the rate of deposition of oxidised nitrogen 50 km from the source would be of the order of 0.1 kg N ha^{-1} y^{-1} or 7 eq ha^{-1} y^{-1}. This incremental increase may be compared with Figures 6.1 to 6.5. The incremental source will increase the risk of exceedence of the critical load by approximately 1% or less in each case. This example would suggest that the critical load methodology and regional scale acid deposition models have limited application for assessing the impact of individual emission sources of oxides of nitrogen at individual receptor sites, because the likely changes in the risk of exceedence are marginal.

For sulphur dioxide, Metcalfe and Whyatt(2000) have predicted the incremental increase in sulphur deposition from emissions from Drax power station at receptors throughout the UK. Maximum predicted rates of deposition were of the order of 2.25 kg S ha^{-1} y^{-1}: the predicted rate of deposition at Liphook was approximately 1 kg S ha^{-1} y^{-1}. These values correspond to 141 eq ha^{-1} y^{-1} and 63 eq ha^{-1} y^{-1} respectively. Referring to Figs 6.1 to 6.5, this additional deposition will increase the risk of exceedence of the critical load by approximately 10% and 5 % respectively. This example would suggest that the critical load methodology and regional scale acid deposition models may be more useful for assessing the impact of individual emission sources of sulphur dioxide (rather than oxides of nitrogen) at individual receptor sites, because the likely changes in the risk of exceedence appear significant .

6.3 Integration of observed rates of deposition

The above assessment has assumed that the acid deposition model does not overestimate the rates of deposition. In practice, the predicted rates of deposition may be compared with observed or independently estimated rates of deposition at Secondary Network sites throughout the United Kingdom. An integrated assessment approach would allow the performance of the model at these sites to be taken into account when estimating the likelihood of exceedence of the critical load at other sites. The integration of observed data with model predictions is outside the scope of this project. However, the following approach is suggested for further investigation. It relies on the assumption that exceedence of the critical load at the location of interest is independent of the ability of the model to predict rates of deposition at the observation sites.

For each model run, i , with input parameters x_{ij} , let the probability p_i that the model does not overestimate the observed rate of deposition be:

$$p_i = \frac{k_i}{n+1}$$

where k_i is the number of sites at which the predicted rate of deposition is less than or equal to the observed rate for the parameter set x_{ij}; i equals 1 to n, where n is the number of sites, and j spans the range of parameters.

Then the overall probability for all m model runs that the model does not overestimate the observed rate of deposition is:

$$P(Not) = \frac{\sum_{i=1}^{m} p_i}{m+1}$$

Then the joint probability for all m model runs that the critical load is exceeded and the model does not overestimate the rates of deposition is estimated to be:

$$P(Ex \cap Not) = \frac{\sum_{i=1}^{m} p_i \delta_i}{m+1}$$

where $\delta_i = 0$ if the predicted acid deposition is less than or equal to the critical load, and $\delta_i = 1$ otherwise.

Then assuming that exceedence of the critical load is independent of the performance of the model at the observation sites, the probability of exceedence is:

$$P(Ex) = \frac{P(Ex \cap Not)}{P(Not)}$$

While this approach seems inherently reasonable and simple to apply, giving greatest weight to those model runs where exceedence is predicted and the model underestimates observed rates of deposition, doubts remain about its statistical rigour.

7 CONCLUSIONS AND RECOMMENDATIONS

This report has been prepared as the result of successful collaboration between a number of groups and is a model for further successful co-operation. The acid deposition models HARM, FRAME and TRACK are simple trajectory models employing broadly similar chemical reaction schemes. They have many common features and might be expected to demonstrate similar behaviour. The model equations are to some extent amenable to analytical solution. Analytical solutions have been developed as part of this project and have been used to help identify the critical input parameters and to develop methods of data analysis.

The main variables in the equations within the models are:

1. Chemical reaction rate constants:
2. Dry deposition velocities;
3. Wet scavenging coefficients (including enhancement in high rainfall areas) ;
4. Background concentrations of chemical species;
5. Wind speed;
6. Frequency of winds from each wind direction sector;
7. Boundary layer height;
8. Emissions;
9. Speciation of emitted sulphur dioxide and oxides of nitrogen.

Plausible ranges of these input parameters have been identified based on literature surveys, current practice and expert judgement. The uncertainty in some of the input parameters, such as the rate of reaction of simple gaseous species is quite small; the uncertainty in other parameters, such as the rate of reaction of gases with particulate matter may be quite large, approaching an order of magnitude.

A systematic sensitivity analysis of the uncertainty in the national emissions leads to some estimates, notably for sulphur and nitrogen oxides, which are substantially lower than those which would have been estimated by expert judgement. It is not within this study to explore alternative methodologies, but it is recognised that Monte Carlo analysis is not able to treat uncertainties in processes, which are unknown. In addition uncertainties in individual processes are treated as independent variables.

The basis of uncertainty assessment is to make multiple calculations using plausible range of parameter values. The uncertainty in sulphur deposition was investigated by Monte Carlo analysis of the analytical model with the values of input parameters selected from their plausible ranges. Maximum rates of sulphur deposition were predicted close to the source. The 95^{th} percentile of the predicted deposition rates was approximately a factor of 2 times the average value and the 5^{th} percentile was approximately half the average value.

The analytical model was also used to carry out a first order error analysis of the uncertainty in sulphur deposition, in which each of the input variables was changed one variable at a time. The first order analysis explained 95% of the overall variance

throughout the range of prediction. The major contributor to the overall variance of predicted values was the uncertainty in the dry deposition velocity for sulphur dioxide in the vicinity of the receptor. Other significant contributors to the variance were the uncertainties in the rate of emission, boundary layer height, wind speed, frequency of the wind direction in the relevant sector and the wet deposition coefficient for sulphur dioxide. At 800 km from the source, the largest contributors to the variance in the predicted total sulphur deposition rate at receptors were the uncertainties in the dry deposition velocity for sulphur dioxide both upwind and local to the receptor.

The analytical model was used to compare the performance of Monte Carlo simulation with that of more limited sampling based on the use of a Latin Square with only 13 model runs. The Latin Square sampling strategy provided a reasonable estimate of the distribution derived from the Monte Carlo analysis in the cumulative probability range between 0.1 and 0.9, but provided little information at the extremes of the distribution. In both cases, the predicted distribution approximated to log-normal.

Results from the Monte Carlo simulations have possible implications for other studies, particularly those where the number of computer runs is restricted by practical considerations. Table 7.1 summarises the advantages and disadvantages of the alternative sampling strategies in terms of the criteria affecting sensitivity analysis, such as number of runs and ease of application. These may be important for future studies.

Monte Carlo analysis of the analytical model for nitrogen deposition was also carried out. The 95^{th} percentile of the predicted rates of deposition was approximately twice the mean value and the 5^{th} percentile was approximately one third of the mean value. Approximately 10 to 30% of the variance is not explained by first order analysis and is associated with more complex interactions between parameters. The largest contributors to the variance in the predicted rates of deposition were the background concentration of the hydroxyl radical, the wet deposition of the aerosols, the frequency of the wind direction, the wind speed, the rate constant for the formation of nitrogen pentoxide, the rate of emission, and the rate constant for the formation of nitric acid.

Monte Carlo simulations of sulphur, oxidised nitrogen and reduced nitrogen deposition using the TRACK model showed that: (a) the 95^{th} percentile of predicted rates of sulphur deposition at a range of sites throughout the UK (the Secondary Network sites) was typically 1.3 times the mean value predicted at each site: the mean was typically around 1.45 times the 5^{th} percentile, (b) the 95^{th} percentile of predicted rates of oxidised nitrogen deposition was typically around 1.9 times the average: the average was typically around 2 times the 5^{th} percentile, and (c) the 95^{th} percentile of predicted rates of reduced nitrogen deposition was typically around 1.5 times the average: the average is typically around 1.7 times the 5^{th} percentile. The probability distributions of predicted rates of sulphur, oxidised and reduced nitrogen deposition were approximately log-normal.

Table 7.1 Comparison of sampling strategies

Criterion	Monte Carlo	Latin Square	First order
Number of model runs	Large numbers of model runs required	Minimum number of model runs required	Minimum number of model runs required
Interactions between variables	Allows all interactions between variables to be taken into account	Allows many interactions between variables to be taken into account	Does not consider interactions between variables
Non-linearity	Allows the non-linearity in models to become apparent	Allows the non-linearity in models to become apparent	Does not take non-linearity into account
Shape of the input distributions	Allows the shape of the input distribution to be taken into account	Allows the shape of the input distribution to be taken into account	Does not take account of the shape of the input distributions
Sampling process	Sampling from input distributions is straightforward	Requires some additional work	Minimal effort required
Shape of the output distribution	Provides detailed information	Provides some information: little information provided about the extremes of the distribution	Provides no information
Relative contribution to variance from input parameters	Regression analysis provides a first order assessment of the contribution to variance from each of the input parameters	Provides no useful information	First order assessment provided by simple calculation

First order error analysis of model uncertainties in which the input parameters were varied one variable at a time was also carried out using the TRACK model. The predicted average, 5th percentile and 95th percentile rates of sulphur deposition were approximately 30% greater than those provided by the Monte Carlo analysis. Predictions of the range of nitrogen deposition rates were similar to those provided by the Monte Carlo analysis. Predictions of average and 5th percentile reduced nitrogen deposition were similar to those provided by the Monte Carlo analysis. The 95th percentile value was typically 50% greater than that provided by the Monte Carlo analysis.

The uncertainty in the estimates made by TRACK of the incremental impact of an additional 150 kt per annum source of oxides of nitrogen was also investigated using Monte Carlo analysis. The 95th percentile of the additional oxidised nitrogen deposition

was approximately twice the average value: the 5th percentile was approximately half the average value.

The non-linearity of predictions of the incremental impact of additional sources was investigated using the TRACK model. Far from the source, the incremental contribution from a 75 kt source of oxides of nitrogen was half that for a 150 kt source i.e. the predictions varied linearly with emission. Closer to the source, the predictions were slightly sublinear: the deposition of oxidised nitrogen associated with a 150 kt source was only 1.8 times that for a 75 kt source.

The uncertainty in predictions of nitrogen deposition made by the HARM model was investigated using a Latin Square sampling strategy. This approach required fewer model runs than Monte Carlo simulation. The 92nd percentiles of the predicted rates of oxidised and reduced nitrogen were typically around 1.5 times the mean values: averages were typically around 1.5 times the 8th percentiles. The probability distributions of predicted rates of deposition approximated to log-normal.

First order error analysis of the uncertainty in HARM model predictions of oxidised and reduced nitrogen was also carried out. The first order error analysis provided predictions of oxidised nitrogen deposition similar to those provided by the Latin Square sampling analysis. Average and 5th percentile predictions of reduced nitrogen deposition were similar to those determined by Latin Square sampling: the 95th percentile value was typically 30% greater than that provided by the Latin Square sampling.

To balance the uncertainty estimates in the calculation of deposition a review of the literature on the uncertainty in critical loads was carried out. The review concluded that further work was required to quantify the uncertainty in critical loads estimates. A case study for Liphook, a forested area in the south of England, was therefore carried out in order to investigate the uncertainty in the critical load estimate at a well-documented site. The case study involved the standard procedure for estimating the critical load at this site, but also conducting a Monte Carlo simulation, selecting input values from plausible ranges for this well-documented site. The coefficients of variation of $CL_{min}N$, $CL_{max}S$ and $CL_{max}N$, the main parameters describing the critical load function at this site, were 22%, 30% and 14 % respectively. The probability distribution of the critical loads approximated to a normal distribution.

The uncertainty in the prediction of exceedence of the critical load i.e. deposition minus critical load, at the Liphook site was investigated. Estimates of critical loads sampled from the case study Monte Carlo simulation were randomly matched with estimates of the rate of acid deposition sampled from the TRACK Monte Carlo simulation. The simulation indicated that there was a high probability (>99.9%) that the critical load was exceeded at the site based on 1990 emissions. Reducing the rates of deposition to around 40% of that for 1990 emissions would reduce the probability of exceedence to around 50%. It would be necessary to reduce acid deposition to approximately 20 % of that predicted from 1990 emissions in order to have a high degree of confidence (95%) that the critical load was not exceeded at this site. This example suggests that the critical load and deposition model methodology could, if required, be adapted to provide a probabilistic assessment tool for emissions policies at the regional scale, despite the uncertainties in the critical loads function and rates of deposition.

The incremental contribution to sulphur and nitrogen deposition from a large point source was compared to the uncertainty in the exceedence at the Liphook site. For the example considered, the incremental contribution to nitrogen deposition would increase the risk of exceedence of the critical load by around 1%. Similarly, the incremental contribution to sulphur deposition would increase the risk of exceedence of the critical load by approximately 10 to 20%. The example suggests that the uncertainties in the critical load methodology and regional scale deposition models are too large for the impact of individual sources of oxides of nitrogen at specific receptor sites to be assessed with confidence. The method may be more effective for assessing the impact of sulphur dioxide emissions.

The assessment of uncertainty carried out in this study does not take account of measured rates of deposition. In practice, the predicted rates of deposition may be compared with observed, or independently estimated rates of deposition at Secondary Network sites throughout the United Kingdom. An integrated assessment approach would allow the comparison of the model estimates with measurements at these sites to be taken included, improving the reliability of estimates of exceedence of the critical load at other sites. A probabilistic method for incorporating measured deposition rates in the assessment of uncertainty is suggested.

The following recommendations are made:

- The uncertainty in the prediction of rates of deposition resulting from the uncertainty in input parameters may be assessed by Monte Carlo analysis.
- Latin Square sampling or first order error analysis should provide useful estimates of the uncertainty where Monte Carlo analysis is not practical because it would not be practical to make the number model runs The distribution of predicted rates of deposition may be approximated by a log-normal distribution.
- The uncertainty in acid deposition models resulting from the uncertainty in the input parameters may be broadly described as within a “factor of two”. Any estimate could be within a factor of two larger or smaller than the “best” prediction.
- Analytical deposition models may be used to test Monte Carlo techniques. Their real value may arise in their flexibility to optimise input parameters when comparing predictions against observations, using for example Bayesian Monte-Carlo methods.
- The uncertainty in prediction of critical loads resulting from uncertainties in input parameters may be assessed by Monte Carlo analysis.
- The uncertainty in predicting exceedence of critical loads may be obtained by sampling from the probability distributions of the predicted critical loads and rates of acid deposition.
- Further investigations should be carried out to integrate measurements of rates of deposition into the analysis of uncertainty. The suggested probabilistic method would provide a practical means of investigation.

Given the extent of the inaccuracy in assessments of exceedence, which would probably not be regarded as unexpected by the user community, a number of issues are raised concerning the critical loads methodology. The bounds on uncertainty in deposition are comparable to the bandings associated with critical loads categories. These broadly span

factors of two, so that the uncertainty in deposition could be interpreted as equivalent to incorrectly assessing the critical load at a site by allocating the site to a wrong category, either one category more or less sensitive.

Estimates of future exceedence, in NEGTAP (2001) for example, suggest that the area of exceedence of critical loads in the UK exceeds over 71% of sensitive ecosystems over the period 1995-7, and this is expected to decline to 46% by 2010. Critical loads for eutrophication (NEGTAP, 2001) exceeded 25% of the UK with sensitive grasslands in 1995-7, and 55% of the UK with heathland. These fractions are expected to decline to circa 20% and 40% respectively in 2010. Reduced ammonia is the main contributor. These predicted fractions are based on estimates using the HARM model for sulphur and nitrogen oxides and the FRAME model for reduced nitrogen. These estimates are based on ensuring that the "best" estimate of the deposition is less than the "best" estimate of the critical load (or appropriate critical load function). The intention of future policy measures enacted through the Large Combustion Plant Directive and the Gothenburg Protocol is to bring about the emissions reductions producing these declines.

It is apparent that if the exceedence of critical loads is expressed in probabilistic terms, as developed in this study, the estimated improvement as a result of emissions reductions may be different to those previously forecast, even though the same models are applied. The consequence of no longer applying absolute criteria to critical load exceedences is not part of this study. However some general comments about the benefits of emissions control can be made. Without absolute criteria, the percentage reduction in area exceeded cannot be used as the measure of improvement. Improvement will still occur as a result of emissions reductions and percentages may still be one way of summarising the improvement. However an attempt to reduce the fractional area of the country where critical loads are exceeded to a very low percentage will be sensitive to the way an exceedence is defined in probabilistic terms. The example shown in Chapter 6 (Figures 6.1 to 6.2) shows that a decision must be made as to what would be regarded as an acceptably low probability of exceedence, conventionally about 0.05. This probability will never be zero, and as the figures and Table 6.1 show a very low probability of exceedence is very hard to achieve. As the deposition declines one approaches a region of diminishing returns, if one were to require a very low probability of exceedence.

The uncertainty in estimates of exceedence also has important implications for the strategy to be adopted for environmental improvement. Broadly, improvement requires the exceedence of critical loads to be minimised. One might therefore expect that if critical load exceedence cannot be assessed with great accuracy, as implied by this study, detailed improvements plans based on detailed source reduction plans in specific areas, might not represent a justifiable optimal objective. Instead a more general strategy based on national or regional reductions across the board might be all that could be justified with any confidence, given the accuracy of the critical load exceedence estimates.

8 REFERENCES

Charles, D., Jones, B.M.R., Salway, A.G., Eggleston, H.S. and Milne, R., 1998. *Treatment of Uncertainties for National Estimates of Greenhouse Gas Emissions*, AEA Technology, Report No AEAT-2688.

Clarke R.H., 1979. *A model of the short and medium range dispersion of radionuclides released to the atmosphere. The first report of a working group on atmospheric dispersion*. National Radiological Protection Board. NRPB-R91

Derwent R.G., G.J. Dollard and S.E. Metcalfe, 1988. *On the nitrogen budget for the United Kingdom and Northwest Europe*. Q.J.R Meteorol. Soc., 114**,** 1127-1152.

Derwent R.G. and A.R. Curtis, 1998. *Sensitivity and uncertainty analysis of the long range transport and deposition of nitrogen and sulphur compounds in Europe.: a Howgood application*. AERE Report R13284.

Finlayson-Pitts B.J. and J.N. Pitts, 2000. *Chemistry of the upper and lower atmosphere.* Academic Press.

Goodwin, J.W.L., Salway, A.G., Murrells, T.P., Dore, C.D., Passant, N.R., King, K.R., Coleman, P.J., Hobson, M.M., Pye, S.T., & Watterson, J.D., 2002. UK *Emissions of Air Pollutants* 1970-1999, AEA Technology plc, Report No. AEAT/ENV/R/0798.

Hall, J. R., 1993. *Critical loads mapping at the UK Critical Loads Mapping Centre - data requirements and presentation.* In Hornung, M. and Skeffington, R. A. *Critical Loads: Concept and Applications.* ITE Report 28, 74-78 London, HMSO

Hall, J., Hornung, M., Freer-Smith, P., Loveland, P., Bradley, I., Langan, S., Dyke, K., Gascoigne, J., and Bull, K., 1997. *Current status of UK critical loads data - December 1996* Report to UK Dept of the Environment, Institute of Terrestrial Ecology, Monks Wood, Cambs.

Hall, J., Bull, K., Bradley, K., Curtis, C., Freer-Smith, P. H., Hornung, M., Howard, D., Langan, S., Loveland, P., Reynolds, B., Ulyett, J., and Warr, T., 1998. *Status of UK critical loads and Exceedences January 1998. Part 1 - critical loads and critical load maps* Report to UK Department of the Environment, Institute of Terrestrial Ecology, Monks Wood, Cambs.

Hall, J., Hornung, M., Kennedy, F., Reynolds, B., Curtis, C., Langan, S., and Fowler, D. , 2001a. *Status of UK critical loads and Exceedences: Part 1 Critical loads and critical load maps, update to January 1998 report*, CEH, Monks Wood, Cambridge.

Hall, J., Reynolds, B., Aherne, J. and Hornung, M., 2001b. *The importance of selecting appropriate criteria for calculating critical loads for terrestrial ecosystems using the simple mass balance equation*. Water, Air and Soil Pollution, Focus, 1, 29-41.

Hall, J., Hornung, M., Kennedy, F., Langan, S., Reynolds, B. and Aherne, J., 2001c. *Investigating the uncertainties in the Simple Mass Balance equation for acidity critical loads for terrestrial ecosystems*. Water, Air and Soil Pollution, Focus, 1, 43-56.

IPCC (Intergovernmental Panel on Climate Change), 2000. *Good Practice Guidance and Uncertainty Management* in National Greenhouse Gas Inventories, IPCC.

J.A. Jones, 1983. *Models to allow for the effects of coastal sites, plume rise and buildings on dispersion of radionuclides and guidance on the value of deposition velocity and washout coefficients*. National Radiological Protection Board Fifth Report of a Working Group on Atmospheric Dispersion. NRPB R157.

D.S. Lee, R.D. Kingdon, M.E. Jenkin and J.A. Garland, 2000. *Modelling the atmospheric oxidised and reduced nitrogen budgets for the UK with a Lagrangian multi-layer long-range transport model*. Environmental modelling and assessment, 5, 83-104.

S.E. Metcalfe, J.D. Whyatt and R.G. Derwent, 1995. *A comparison of model and observed network estimates of sulphur deposition across Great Britain for 1990 and its likely source attribution.* Q.J.R Meteorol. Soc., 121**,** 1387-1411.

Metcalfe S.E. and Whyatt J.D., 2000. *Linearity of sulphur chemistry in the HARM atmospheric transport and deposition model.* Environment Agency R&D Technical Report P275.

National Expert Group on Transboundary Air Pollution (NEGTAP), 2001. Transboundary air pollution: Acidification, eutrophication and ground-level ozone in the U.K. CEH Edinburgh Report ISBN 1 870393 619

Nilsson, J and Grennfelt, P., 1988. *Critical loads for sulphur and nitrogen* Report 1988:15, Nordic Council of Ministers, Copenhagen.

Pasquill F. and F.B. Smith., 1983. *Atmospheric diffusion. Third edition*. Ellis Horwood Limited.

Posch, M., de Smet, P. A. M., Hettelingh, J.-P., and Downing, R. J., 1995. *Calculation and Mapping of Critical Thresholds in Europe* 259101004, RIVM, Bilthoven, The Netherlands.

Posch, M., Hettelingh, J.-P., de Smet, P. A. M., and Downing, R. J., 1997. *Calculation and Mapping of Critical Thresholds in Europe* 259101007, RIVM, Bilthoven, The Netherlands.

Posch, M., de Smet, P. A. M., Hettelingh, J.-P., and Downing, R. J., 1999. *Calculation and Mapping of Critical Thresholds in Europe* 259101009, RIVM, Bilthoven, The Netherlands.

Posch, M., de Smet, P. A. M., Hettelingh, J.-P., and Downing, R. J., 2001. *Modelling and mapping of critical thresholds in Europe: Status Report 2001,* RIVM Report 259101010, RIVM, Bilthoven, The Netherlands.

Posch, M.and Hettelingh, J.-P., 2001. From critical loads to dynamic modelling. In Posch, M., de Smet, P. A. M., Hettelingh, J.-P., and Downing, R. J. *Modelling and mapping of critical thresholds in Europe: Status Report 2001*. RIVM Report 259101010, pp 33-39 RIVM Bilthoven, The Netherlands,.

Salway, A.G., Murrells, T.P., Milne, R., and Ellis, S., 2001. UK Greenhouse Gas Inventory, 1990 to 1999, AEA Technology plc, Report No. AEAT/ENV/R/0524

R. Singles, 1996. Ph. D. Thesis. University of Edinburgh.

R. Singles, M.A. Sutton and K.J. Weston, 1998. *A multi-layer model to describe the atmospheric transport and deposition of ammonia in Great Britain*. Atmospheric Environment, 32, 393-399.

UBA, 1996. *Manual on Methodologies and Criteria for Mapping Critical Levels / Loads and Geographical Areas where they are Exceeded.* Texte 71:96, Umweltbundesamt, Berlin.

Underwood B. Y., 2001. *Review of deposition velocity and washout coefficient*. AEA Technology, Harwell.

US Environmental Protection Agency, 2001. *Compilation of air pollution emission sources*. AP42. [www.epa.gov/ttn/chief/ap42/index.html]

Appendices

CONTENTS

1 TRACK, HARM and FRAME model chemistry

CONTENTS

Table 1: Chemical Mechanisms Used in the HARM and TRACK Acid Deposition Models

(a) The HARM Model Chemistry [Metcalfe *et al.* (R(1))]

Reaction	Model Rate Expression[(a)]	Latest Rate Expression[(a)]	Uncertainty	Ref.	Note
$NO + O_3 \rightarrow NO_2 + O_2$	$1.8 \times 10^{-12} \exp(-1370/T)$	$2.0 \times 10^{-12} \exp(-1400/T)$ $1.8 \times 10^{-12} \exp(-1370/T)$	$\Delta E = \pm 200$; f(298 K) = 1.1[(b)] $\Delta \log k(298) = \pm 0.08$; $\Delta E = \pm 200$[(c)]	R(2) R(3)	H(A)
$NO_2 + h\nu \rightarrow NO + O$	$1.45 \times 10^{-2} \exp(-0.4 \sec\theta)\ s^{-1}$	$1.165 \times 10^{-2} (\cos\theta)^{0.244} \exp(-0.279 \sec\theta)\ s^{-1}$	Factor of 2, see note (d)	R(4)	H(A) H(B)
$O + O_2 + M \rightarrow O_3 + M$	$5.6 \times 10^{-34} (T/300)^{-2.8}$ [M]	$6.0 \times 10^{-34} (T/300)^{-2.3}$ [M] $6.0 \times 10^{-34} (T/300)^{-2.8}$ [M], M = O_2 $5.6 \times 10^{-34} (T/300)^{-2.8}$ [M] , M = N_2	$\Delta k = \pm 0.5$; $\Delta n = \pm 0.5$[(e)] $\Delta \log k(298) = \pm 0.05$; $\Delta n = \pm 0.5$ [(c)] $\Delta \log k(298) = \pm 0.05$; $\Delta n = \pm 0.5$ [(c)]	R(2) R(3)	H(A)
$OH + NO_2 + M \rightarrow HNO_3 + M$	1.5×10^{-11}	$k_0(T) = 2.5 \times 10^{-30} (T/300)^{-4.4}$ [M] $k_\infty(T) = 1.6 \times 10^{-11} (T/300)^{-1.7}$ $F_c = 0.6$ (fixed) $k_0(T) = 2.6 \times 10^{-30} (T/300)^{-2.9}$ [M] $k_\infty(T) = 6.7 \times 10^{-11} (T/300)^{-0.6}$ $F_c = 0.43$	$\Delta k_0 = \pm 0.1$; $\Delta n = \pm 0.3$[(e)] $\Delta k_\infty = \pm 0.2$; $\Delta m = \pm 0.2$[(e)] $\Delta \log k_0(298) = \pm 0.1$; $\Delta n = \pm 0.3$ [(c)] $\Delta \log k_\infty(298) = \pm 0.1$; $\Delta n = \pm 0.5$ [(c)]	R(2) R(3)	H(C)
$NO_2 + O_3 \rightarrow NO_3 + O_2$	$1.2 \times 10^{-13} \exp(-2450/T)$	$1.2 \times 10^{-13} \exp(-2450/T)$ $1.2 \times 10^{-13} \exp(-2450/T)$	$\Delta E = \pm 150$; f(298 K) = 1.15 [(b)] $\Delta \log k(298) = \pm 0.06$; $\Delta E = \pm 150$[(c)]	R(2) R(3)	-
$NO_3 + h\nu \rightarrow NO_2 + O$	$8.94 \times 10^{-2} \exp(-0.06 \sec\theta)\ s^{-1}$	$1.747 \times 10^{-1} (\cos\theta)^{0.261} \exp(-0.288 \sec\theta)\ s^{-1}$	see note (d)	R(4)	H(B)
$NH_3 + HCl \rightarrow NH_4Cl$	1.0×10^{-14}	-	-	R(1)	H(D)
$NH_3 + HNO_3 \rightarrow NH_4NO_3$	1.0×10^{-14}				

Reaction	Model Rate Expression[(a)]	Latest Rate Expression[(a)]	Uncertainty	Ref.	Note
$HNO_3 \rightarrow$ aerosol	3.0×10^{-5} s^{-1}	-	-	R(1)	H(E)
$NO_3 + NO_2 \rightarrow N_2O_5$	$2.3 \times 10^{-13} \exp(-1000/T)$	$k_0(T) = 2.2 \times 10^{-30} (T/300)^{-3.9}$ [M] $k_\infty(T) = 1.5 \times 10^{-12} (T/300)^{-0.7}$ $F_c = 0.6$ (fixed) $k_0(T) = 2.7 \times 10^{-30} (T/300)^{-3.4}$ [M] $k_\infty(T) = 2.0 \times 10^{-12} (T/300)^{+0.2}$ $F_c = [\exp(-T/250) + \exp(-1050/T)]$	$\Delta k_0 = \pm 0.5$; $\Delta n = \pm 1.0$[(e)] $\Delta k_\infty = \pm 0.8$; $\Delta m = \pm 0.4$[(e)] $\Delta \log k_0(298) = \pm 0.1$; $\Delta n = \pm 0.5$ [(c)] $\Delta \log k_\infty(298) = \pm 0.2$; $\Delta n = \pm 0.6$ [(c)]	R(2) R(3)	H(C)
$N_2O_5 \rightarrow$ aerosol	3.0×10^{-5} s^{-1}	-	-	R(1)	H(E)
$SO_2 \rightarrow SO_4$	2.8×10^{-6} s^{-1}	-	Uncertainty = ±50% [R(1)]	R(1)	H(F)

(b) The TRACK Model Chemistry [Lee *et al.* (R(6) and R(7))]

Reaction	Model Rate Expression (a)	Latest Rate Expression (a)	Uncertainty	Ref.	Note
$NO + O_3 \rightarrow NO_2 + O_2$	$1.8 \times 10^{-12} \exp(-1370/T)$	$2.0 \times 10^{-12} \exp(-1400/T)$ $1.8 \times 10^{-12} \exp(-1370/T)$	$\Delta E = \pm 200$; f(298 K) = 1.1 [(b)] $\Delta \log k(298) = \pm 0.08$; $\Delta E = \pm 200$ [(c)]	R(2) R(3)	T(A)
$NO_2 + h\nu \rightarrow NO + O$	$1.1 \times 10^{-2} (\cos\theta)^{0.397} \exp(-0.183 \sec\theta)$ (1.0 - 0.5 C) s^{-1} [R(5)]	$1.165 \times 10^{-2} (\cos\theta)^{0.244} \exp(-0.279 \sec\theta)\ s^{-1}$	Factor of 2, see note (d)	R(4)	T(A)
$O + O_2 + M \rightarrow O_3 + M$	Assumed instantaneous	$6.0 \times 10^{-34} (T/300)^{-2.3}$ [M] $6.0 \times 10^{-34} (T/300)^{-2.8}$ [M], M = O_2 $5.6 \times 10^{-34} (T/300)^{-2.8}$ [M] , M = N_2	$\Delta k = \pm 0.5$; $\Delta n = \pm 0.5$ [(e)] $\Delta \log k(298) = \pm 0.05$; $\Delta n = \pm 0.5$ [(c)] $\Delta \log k(298) = \pm 0.05$; $\Delta n = \pm 0.5$ [(c)]	R(2) R(3)	T(A)
$OH + NO_2 (+ M) \rightarrow HNO_3 (+ M)$	$1.33 \times 10^{-11} (T/300)^{-2.0}$	$k_0(T) = 2.5 \times 10^{-30} (T/300)^{-4.4}$ [M] $k_\infty(T) = 1.6 \times 10^{-11} (T/300)^{-1.7}$ $F_c = 0.6$ (fixed) $k_0(T) = 2.6 \times 10^{-30} (T/300)^{-2.9}$ [M] $k_\infty(T) = 6.7 \times 10^{-11} (T/300)^{-0.6}$ $F_c = 0.43$	$\Delta k_0 = \pm 0.1$; $\Delta n = \pm 0.3$ [(e)] $\Delta k_\infty = \pm 0.2$; $\Delta m = \pm 0.2$ [(e)] $\Delta \log k_0(298) = \pm 0.1$; $\Delta n = \pm 0.3$ [(c)] $\Delta \log k_\infty(298) = \pm 0.1$; $\Delta n = \pm 0.5$ [(c)]	R(2) R(3)	T(B)
$NO_2 + O_3 \rightarrow NO_3 + O_2$	$1.2 \times 10^{-13} \exp(-2450/T)$ (only at night)	$1.2 \times 10^{-13} \exp(-2450/T)$ $1.2 \times 10^{-13} \exp(-2450/T)$	$\Delta E = \pm 150$; f(298 K) = 1.15 [(b)] $\Delta \log k(298) = \pm 0.06$; $\Delta E = \pm 150$ [(c)]	R(2) R(3)	-
$NO_3 + h\nu \rightarrow NO_2 + O$	Assumed instantaneous during the day	$1.747 \times 10^{-1} (\cos\theta)^{0.155} \exp(-0.125 \sec\theta)\ s^{-1}$	Factor of 2, see note (d)	R(4)	T(C)
$NH_3 + HNO_3 \rightarrow NH_4NO_3$	1.0×10^{-14}	-	-	-	T(D)

Reaction	Model Rate Expression (a)	Latest Rate Expression (a)	Uncertainty	Ref.	Note
$NH_3 + HCl \rightarrow NH_4Cl$	1.0×10^{-14}	-	-	-	T(D)
$HNO_3 \rightarrow$ aerosol	Jaenicke Scheme 2.3×10^{-4} s^{-1} Marine 9.1×10^{-4} s^{-1} Rural	-	-		T(E)
$NO_3 + NO_2 \rightarrow N_2O_5$	Assumed instantaneous at night	$k_0(T) = 2.2 \times 10^{-30} (T/300)^{-3.9}$ [M] $k_\infty(T) = 1.5 \times 10^{-12} (T/300)^{-0.7}$ $F_c = 0.6$ (fixed) $k_0(T) = 2.7 \times 10^{-30} (T/300)^{-3.4}$ [M] $k_\infty(T) = 2.0 \times 10^{-12} (T/300)^{+0.2}$ $F_c = [\exp(-T/250) + \exp(-1050/T)]$	$\Delta k_0 = \pm 0.5$; $\Delta n = \pm 1.0$ [(e)] $\Delta k_\infty = \pm 0.8$; $\Delta m = \pm 0.4$ [(e)] $\Delta \log k_0(298) = \pm 0.1$; $\Delta n = \pm 0.5$ [(c)] $\Delta \log k_\infty(298) = \pm 0.2$; $\Delta n = \pm 0.6$ [(c)]	R(2) R(3)	T(F)
$N_2O_5 \rightarrow$ aerosol	Jaenicke Scheme 1.1×10^{-4} s^{-1} Marine 2.2×10^{-4} s^{-1} Rural				T(E)
$SO_2 + OH \rightarrow SO_4$	$9.8 \times 10^{-13} (T/300)^{-1.4}$	$k_0(T) = 3.0 \times 10^{-31} (T/300)^{-3.3}$ [M] $k_\infty(T) = 1.5 \times 10^{-12} (T/300)^{-0}$ $F_c = 0.6$ (fixed) $k_0(T) = 4.0 \times 10^{-31} (T/300)^{-3.3}$ [M] $k_\infty(T) = 2.0 \times 10^{-12}$ $F_c = 0.45$	$\Delta k_0 = \pm 1.0$; $\Delta n = \pm 1.5$ [(e)] $\Delta k_\infty = \pm 0.5$; $\Delta m = +0,-2$ [(e)] $\Delta \log k_0(298) = \pm 0.3$; $\Delta n = \pm 1.0$ [(c)] $\Delta \log k_\infty(298) = \pm 0.3$ [(c)]	R(2) R(3)	T(G)
$SO_2 \rightarrow SO_4$	2.0×10^{-6} s^{-1}				T(H)
$SO_4 + 2NH_3 \rightarrow (NH_4)_2SO_4$	3.3×10^{-15}				Estimate

Reaction	Model Rate Expression (a)	Latest Rate Expression (a)	Uncertainty	Ref.	Note
$OH + NO (+ M) \rightarrow HONO (+ M)$	$9.36 \times 10^{-12} (T/300)^{-2.0}$	$k_0(T) = 7.0 \times 10^{-31} (T/300)^{-2.6}$ [M] $k_\infty(T) = 3.6 \times 10^{-11} (T/300)^{-0.1}$ $F_c = 0.6$ (fixed) $k_0(T) = 7.4 \times 10^{-31} (T/300)^{-2.4}$ [M] $k_\infty(T) = 4.5 \times 10^{-11}$ $F_c = 0.9$	$\Delta k_0 = \pm 1.0$; $\Delta n = \pm 0.3$ [(e)] $\Delta k_\infty = \pm 0.2$; $\Delta m = \pm 0.5$ [(e)] $\Delta \log k_0(298) = \pm 0.1$; $\Delta n = \pm 0.3$ [(c)] $\Delta \log k_\infty(298) = \pm 0.2$ [(c)]	R(2) R(3)	T(I)
$HONO + h\nu \rightarrow OH + NO$	$2.48 \times 10^{-3} (\cos \theta)^{0.431} \exp(-0.194 \sec\theta) (1.0 - 0.5\ C)\ s^{-1}$ [R(5)]	$2.644 \times 10^{-3} (\cos \theta)^{0.261} \exp(-0.288 \sec\theta)\ s^{-1}$	Factor of 2, see note (d)	R(4)	-
$HONO \rightarrow$ nitrite aerosol	Jaenicke Scheme $0.9 \times 10^{-4}\ s^{-1}$ Marine $3.2 \times 10^{-4}\ s^{-1}$ Rural				T(E)
$NO_2 \rightarrow HONO$	$5.6 \times 10^{-6} (100/h)\ s^{-1}$				T(J)
$NO_2 + CH_3COO_2 + M \rightarrow PAN + M$	$1.05 \times 10^{-11} (T/300)^{-0.9}$	$k_0(T) = 9.7 \times 10^{-29} (T/300)^{-5.6}$ [M] $k_\infty(T) = 9.3 \times 10^{-12} (T/300)^{-1.5}$ $F_c = 0.6$ (fixed) $k_0(T) = 2.7 \times 10^{-28} (T/300)^{-7.1}$ [M] $k_\infty(T) = 1.2 \times 10^{-11} (T/300)^{-0.9}$ [M] $F_c = 0.3$	$\Delta k_0 = \pm 3.8$; $\Delta n = \pm 2.8$ [(e)] $\Delta k_\infty = \pm 0.4$; $\Delta m = \pm 0.3$ [(e)] $\Delta \log k_0(298) = \pm 0.4$; $\Delta n = \pm 2$ [(c)] $\Delta \log k_\infty(298) = \pm 0.2$; $\Delta m = \pm 1$ [(c))]	R(2) R(3)	T(K)
$PAN + M \rightarrow NO_2 + CH_3COO_2 + M$	$2.53 \times 10^{16} \exp(-13530/T)\ s^{-1}$	see note (f) $k_0(T) = 4.9 \times 10^{-3} \exp(-12100/T)$ [M] $k_\infty(T) = 1.2 \times 10^{-11} (T/300)^{-0.9}$ [M] $F_c = 0.3$	see note (e) $\Delta \log k_0(298) = \pm 0.4$; $\Delta E = \pm 1000$ [(c)] $\Delta \log k_\infty(298) = \pm 0.2$; $\Delta m = \pm 1$ [(c))]	R(2) R(3)	T(K)

(c) The FRAME Model Chemistry [Singles, 1996; Bartnicki, Olrndrzynski, Jonson, Berge and Unger;Tsyro, 2001)]

Reaction	Model Rate Expression (a)	Latest Rate Expression (a)	Uncertainty	Ref.	Note
$NO + O_3 \rightarrow NO_2 + O_2$	$2.1 \times 10^{-12} \exp(-1450/T)$	$2.0 \times 10^{-12} \exp(-1400/T)$ $1.8 \times 10^{-12} \exp(-1370/T)$	$\Delta E = \pm 200$; f(298 K) = 1.1 [(b)] $\Delta \log k(298) = \pm 0.08$; $\Delta E = \pm 200$ [(c)]	R(2) R(3)	T(A)
$NO_2 + h\nu \rightarrow NO + O$	$1.0 \times 10^{-2} \exp(-0.39 \sec\theta)$ (1.0 - 0.5 C) s^{-1}	$1.165 \times 10^{-2} (\cos\theta)^{0.244} \exp(-0.279 \sec\theta)\ s^{-1}$	Factor of 2, see note (d)	R(4)	T(A)
$O + O_2 + M \rightarrow O_3 + M$	Assumed instantaneous	$6.0 \times 10^{-34} (T/300)^{-2.3}$ [M] $6.0 \times 10^{-34} (T/300)^{-2.8}$ [M], M = O_2 $5.6 \times 10^{-34} (T/300)^{-2.8}$ [M] , M = N_2	$\Delta k = \pm 0.5$; $\Delta n = \pm 0.5$ [(e)] $\Delta \log k(298) = \pm 0.05$; $\Delta n = \pm 0.5$ [(c)] $\Delta \log k(298) = \pm 0.05$; $\Delta n = \pm 0.5$ [(c)]	R(2) R(3)	T(A)
$OH + NO_2 (+ M) \rightarrow HNO_3 (+ M)$	1.1×10^{-11}	$k_0(T) = 2.5 \times 10^{-30} (T/300)^{-4.4}$ [M] $k_\infty(T) = 1.6 \times 10^{-11} (T/300)^{-1.7}$ $F_c = 0.6$ (fixed) $k_0(T) = 2.6 \times 10^{-30} (T/300)^{-2.9}$ [M] $k_\infty(T) = 6.7 \times 10^{-11} (T/300)^{-0.6}$ $F_c = 0.43$	$\Delta k_0 = \pm 0.1$; $\Delta n = \pm 0.3$ [(e)] $\Delta k_\infty = \pm 0.2$; $\Delta m = \pm 0.2$ [(e)] $\Delta \log k_0(298) = \pm 0.1$; $\Delta n = \pm 0.3$ [(c)] $\Delta \log k_\infty(298) = \pm 0.1$; $\Delta n = \pm 0.5$ [(c)]	R(2) R(3)	T(B)
$NO_2 + O_3 \rightarrow NO_3 + O_2$	$1.2 \times 10^{-13} \exp(-2450/T)$ (only at night)	$1.2 \times 10^{-13} \exp(-2450/T)$ $1.2 \times 10^{-13} \exp(-2450/T)$	$\Delta E = \pm 150$; f(298 K) = 1.15 [(b)] $\Delta \log k(298) = \pm 0.06$; $\Delta E = \pm 150$ [(c)]	R(2) R(3)	-
$NO_3 + h\nu \rightarrow NO_2 + O$	Assumed instantaneous during the day	$1.747 \times 10^{-1} (\cos\theta)^{0.155} \exp(-0.125 \sec\theta)\ s^{-1}$	Factor of 2, see note (d)	R(4)	T(C)
$NH_3 + HNO_3 \rightarrow NH_4NO_3$	Assumed instantaneous if favoured by equilibrium	-	-	-	F(A)

Reaction	Model Rate Expression (a)	Latest Rate Expression (a)	Uncertainty	Ref.	Note
$HNO_3 \rightarrow NO_3^- + H^+$	1.0×10^{-5} s^{-1}	-	Estimate		
$NO_3^- + H^+ \rightarrow HNO_3$	0.5×10^{-5} s^{-1}		Estimate		
$NO_3 + NO_2 \rightarrow N_2O_5$	Assumed instantaneous	$k_0(T) = 2.2 \times 10^{-30} (T/300)^{-3.9}$ [M] $k_\infty(T) = 1.5 \times 10^{-12} (T/300)^{-0.7}$ $F_c = 0.6$ (fixed) $k_0(T) = 2.7 \times 10^{-30} (T/300)^{-3.4}$ [M] $k_\infty(T) = 2.0 \times 10^{-12} (T/300)^{+0.2}$ $F_c = [\exp(-T/250) + \exp(-1050/T)]$	$\Delta k_0 = \pm 0.5$; $\Delta n = \pm 1.0$ [(e)] $\Delta k_\infty = \pm 0.8$; $\Delta m = \pm 0.4$ [(e)] $\Delta \log k_0(298) = \pm 0.1$; $\Delta n = \pm 0.5$ [(c)] $\Delta \log k_\infty(298) = \pm 0.2$; $\Delta n = \pm 0.6$ [(c)]	R(2) R(3)	T(F)
$N_2O_5 \rightarrow$ aerosol	Assumed instantaneous				T(E)
$SO_2 \rightarrow SO_4$	Documentation inadequate, probably around 2.8×10^{-6} s^{-1} but may include diurnal variation				T(H)

Reaction	Model Rate Expression (a)	Latest Rate Expression (a)	Uncertainty	Ref.	Note
$SO_4 + 1.5NH_3 \rightarrow (NH_4)_{1.5}SO_4$	Assumed instantaneous if reactants available				
$NO_2 + CH_3COO_2 + M \rightarrow PAN + M$	3.2×10^{-12}	$k_0(T) = 9.7 \times 10^{-29} (T/300)^{-5.6}$ [M] $k_\infty(T) = 9.3 \times 10^{-12} (T/300)^{-1.5}$ $F_c = 0.6$ (fixed) $k_0(T) = 2.7 \times 10^{-28} (T/300)^{-7.1}$ [M] $k_\infty(T) = 1.2 \times 10^{-11} (T/300)^{-0.9}$ [M] $F_c = 0.3$	$\Delta k_0 = \pm 3.8$; $\Delta n = \pm 2.8$ [(e)] $\Delta k_\infty = \pm 0.4$; $\Delta m = \pm 0.3$ [(e)] $\Delta \log k_0(298) = \pm 0.4$; $\Delta n = \pm 2$ [(c)] $\Delta \log k_\infty(298) = \pm 0.2$; $\Delta m = \pm 1$ [(c))]	R(2) R(3)	T(K)
$PAN + M \rightarrow NO_2 + CH_3COO_2 + M$	$7.94 \times 10^{14} \exp(-12530/T)\ s^{-1}$	see note (f) $k_0(T) = 4.9 \times 10^{-3} \exp(-12100/T)$ [M] $k_\infty(T) = 1.2 \times 10^{-11} (T/300)^{-0.9}$ [M] $F_c = 0.3$	see note (e) $\Delta \log k_0(298) = \pm 0.4$; $\Delta E = \pm 1000$ [(c)] $\Delta \log k_\infty(298) = \pm 0.2$; $\Delta m = \pm 1$ [(c))]	R(2) R(3)	T(K)

(d) Comments on the HARM Chemical Mechanism

H(A) These three reactions define the photochemical stationary state, which is established within minutes during daylight hours. In the HARM model, these are treated explicitly.

H(B) Photolysis rates were derived as a function of solar zenith angle using the PHOTOL model [R(10)] for the following conditions - 500 m above a land surface, clear sky conditions and an ozone column of 350 DU above 24 km. Equation (1) was used to represent the dependence of the photolysis rates on solar zenith angle:

$$J(X) = l \exp[-n \sec(X)] \qquad (1)$$

H(C) Rate coefficient taken from Baulch *et al.* [R(11)].

H(D) This is represented as a bimolecular gas-phase reaction forming an aerosol product. The rate coefficient is said to be an estimate [R(1)].

H(E) This reaction represents the uptake of a gaseous component into the aerosol phase. The rate coefficient is said to be an estimate [R(1)].

H(F) The gas- and aqueous-phase oxidation of sulphur dioxide is represented by a simple first order rate expression.

(e) Comments on the TRACK Chemical Mechanism

T(A) These three reactions define the photochemical stationary state, which is established within minutes during daylight hours. In the TRACK model, the formation of ozone from $O(^3P)$ is assumed to be instantaneous so that its rate is equal to the rate of photolysis of NO_2.

T(B) The rate expression quoted was obtained by calculating the bimolecular rate coefficient for one atmosphere pressure and fitting the functional form $k(T) = k(300)(T/300)^n$ to the rate coefficients for the temperature range 270-320 K.

T(C) NO_3 has two photolysis channels:

$$NO_3 + h\nu \rightarrow NO_2 + O(^3P)$$

$$NO_3 + h\nu \rightarrow NO + O_2$$

The model only uses channel (2) as the first channel leads to a null cycle.

$$NO_3 + h\nu \rightarrow NO_2 + O(^3P)$$

$$O(^3P) + O_3 + M \rightarrow O_3 + M$$

$$NO_3 + O_3 \rightarrow NO_3 + O_3$$

Channel (2) can be assumed to be instantaneous as NO_3 has a lifetime of seconds during the day.

T(D) This is represented as a bimolecular gas-phase reaction forming an aerosol product. The rate coefficient is an estimate and is therefore highly uncertain.

T(E) The observed concentrations of nitrate in precipitation are imply that there are other removal processes of gas-phase NO_y, in addition to that of HNO_3. In particular, NO_2, HNO_3 and N_2O_5 may react with seasalt aerosol:

$$NaCl + 2\ NO_2 \rightarrow NaNO_3 + ClNO_2$$

$$NaCl + HNO_3 \rightarrow NaNO_3 + HCl$$

$$NaCl + N_2O_5 \rightarrow NaNO_3 + ClNO_2$$

For these reactions, the rate of the first order uptake of the gas on the aerosol surface has been treated using the model of Fuchs and Sutugin [R(8)] for typical rural and marine aerosols. These aerosols have been represented as three log normal distributions, the parameters of which were taken from Jaenicke [R(9)]. The uptake rate depends on the accommodation coefficient, α, which have been taken from the NASA Evaluation [R(2)] for HNO_3 and N_2O_5.

T(F) This is the only loss process for NO_3 at night. The rate limiting step in the sequence

$$NO_2 + O_3 \rightarrow NO_3 + O_2$$

$$NO_2 + NO_3 + M \rightarrow N_3O_5 + M$$

is the formation of NO_3. The rate of formation of N_3O_5 is equal to the rate of formation of NO_3, which explains why this reaction is described as instantaneous.

T(G) This is a simplified representation of the following gas-phase reaction sequence:

$$OH + SO_2 + M \rightarrow HOSO_2 + M$$

$$HOSO_2 + O_2 \rightarrow SO_3 + HO_2$$

$$SO_3 + H_2O \rightarrow H_3SO_4$$

The rate expression quoted was obtained by calculating the bimolecular rate coefficient for one atmosphere pressure and fitting the functional form $k(T) = k(300)\ (T/300)^n$.

T(H) The aqueous-phase oxidation of sulphur dioxide is presumed to be dominated by its reaction with H_2O_2 for the pH range typically observed (2-6). The oxidation process is represented as a first order reaction. The value of the rate coefficient has been chosen so that the overall rate coefficient for the gas and aqueous-phase oxidation routes is 2.8

x 10^{-6} s^{-1}. The effective gas-phase oxidation rate coefficient is 8 x 10^{-7} s^{-1} for an OH radical concentration of 8 x 10^5 molecule cm^{-3}.

T(I) The rate expression quoted was obtained by calculating the bimolecular rate coefficient for one atmosphere pressure and fitting the functional form $k(T) = k(300)(T/300)^n$ to the rate coefficients. The pressure dependent rate coefficients were taken from the IUPAC Evaluation [R(2)].

T(J) Taken from Harrison *et al.* [R(11)]. The expression is based about field measurements of HONO fluxes.

T(K) Rate coefficients used are based on the recommendations of Lightfoot *et al.* [R(12)], which have been incorporated into the more recent evaluations. The uncertainty factors are likely to be comparable to those quoted.

(f) Comments on the FRAME Chemical Mechanism

F(A) Ammonium nitrate is formed if :

$$\left([HNO_3]+[NO_3^-]\right)\left([NH_3]+[NH_4^+]\right) \geq K_p$$

where K_p is an equilibrium coefficient. The value of K_p is calculated from a semi-empirical expression for solid particulates in dry weather conditions [Stelson and Seinfeld, 1982]:

$$\ln K_{rh<rhd} = 70.78 - \frac{24220}{T} - 6.1 \ln \frac{T}{298} \qquad \text{where K is in ppm}^2$$

The equilibrium constant decreases slowly once the ambient relative humidity exceed the relative humidity of deliquescence.

$$\ln(rhd) = \frac{856.23}{T} + 1.2306 \qquad \text{where } rhd \text{ is in percent}$$

When the ambient humidity approaches saturation there is a marked decrease in the equilibrium constant.

(g) Notes

(a) Units are cm^3 $molecule^{-1}$ s^{-1}, unless otherwise stated.

(b) The uncertainty factor f(298 K) gives the upper and lower bound (corresponding to ~ 1σ) of the rate coefficient at 298 K. The uncertainty factor at other temperatures can be found using equation (2) (note the absolute value). The upper and lower bounds are obtained by multiplying and dividing the rate coefficient at that temperature by the factor f(T).

$$f(T) = f(298\ K) \exp \left| \frac{\Delta E}{R} \left(\frac{1}{T} - \frac{1}{298} \right) \right| \qquad (2)$$

(c) An estimate of the uncertainty in the rate coefficient is given by equation (3) (note the absolute value).

$$\Delta \log k(T) = \Delta \log k(298\ K) + 0.4343 \exp \left| \frac{\Delta E}{R} \left(\frac{1}{T} - \frac{1}{298} \right) \right| \qquad (3)$$

(d) The photodissociation rate J_Y of a species Y is the product of the spherically integrated (actinic) photon flux with the absorption cross section σ and the quantum yield ϕ of the species integrated over all wavelengths λ

$$J_Y(X) = \int_0^\infty \Phi(\lambda,X)\ \sigma(\lambda)\ \phi(\lambda)\ d\lambda) \qquad (4)$$

The factors affecting the photolysis rates are:

- the solar flux incident on the earth's atmosphere [WMO 16, 1986]
- surface albedo
- cloud cover
- atmospheric aerosol content
- stratospheric oxygen and ozone columns
- tropospheric oxygen and ozone profiles
- height above surface
- solar zenith angle

Of these, only the solar zenith angle and the cloud cover vary diurnally; the rest have characteristic timescales of a year. The solar zenith angle governs the amount of atmosphere through which the solar beam must pass and hence the amount of attenuation that affects the radiation. The instantaneous value of the solar zenith angle X can be calculated from a knowledge of the latitude, longitude and time of day (t in seconds).

For daylight hours (i.e. for solar zenith angles less than 90°), the time-of-the-day dependence of the photolysis rates was described by calculating the instantaneous solar zenith angle, X, and using expressions of the form below, to estimate the photolysis rate, J(X), for a particular photochemical process:

$$J(X) = l\,[\cos(X)]^m \exp[-n \sec(X)] \qquad (5)$$

During the night (i.e. for solar zenith angles greater than 90°), photolysis frequencies are zero.

The coefficients l, m and n were determined for each process by fitting the J-values calculated using the UVFLUX model [R(13) and R(14)] to the functional form given in equation (5). The difference between the fitted and calculated photolysis frequencies was less than 0.5% for solar zenith angles close to 30° but increased to 5% for a solar zenith angle of 70°. The difference was significantly larger for those photolysis processes having a strong dependence on the solar zenith angle. In these cases however, the photolysis frequencies calculated for solar zenith angles close to 90° were many orders of magnitude smaller than those calculated for smaller zenith angles. With such low photolysis frequencies, these processes will make a negligible contribution to the overall photochemistry.

The uncertainty in the instantaneous photolysis rate will be species dependent and vary with the quality of the absorption cross-section and quantum yield data. In addition, depending on the model application, the photolysis rate may be a diurnally- or long-term averaged value. It is therefore difficult to identify a specific value. Indeed, the IUPAC evaluation [R(3)] states that the panel do not feel justified in assigning error limits to the parameters reported for photochemical reactions given the scarcity of reliable data.

One measure of the uncertainty can be gained from the spread in the photolysis rates calculated by different radiative-transfer models. An inter-comparison of numerical models which calculate photolysis frequencies has been undertaken under the auspices of the Intergovernmental Panel on Climate Change [R(15)]. A reference case was defined for noon on 1st July at 45°N assuming that vertical profiles of relevant quantities were specified by the US Standard Atmosphere. The spread in the photolysis rates calculated for the photolysis process: $O_3 + h\nu \rightarrow O(^1D) + O_2$ using a number of different models was ±30% for this particular photolysis process. In general, an uncertainty of a factor of 2 is not unrealistic.

(e) Third-order rate coefficients show both a dependence on temperature and pressure (represented generically as M or specifically O_2 or N_2). The effective second-order rate coefficient is parameterised in terms of limiting low pressure (k_0) and high pressure (k_∞) rate coefficients and a curvature factor (F_c), given by

$$k(T) = \left(\frac{k_0(T)M}{1 + k_0(T)M/(k_\infty(T))} \right) F \qquad (6)$$

$$\log_{10} F = \log_{10} F_c \Big/ \left[1 + \left(\log_{10}(k_0 / k_\infty) \right)^2 \right]$$

The temperature dependencies of the limiting low pressure (k_0) and high pressure (k_∞) rate coefficients are given by

$$k_0(T) = [k_0(300\ K) \pm \Delta k_0(300\ K)]\ (T/300)^{\ n\pm\Delta n} \qquad (7)$$

and

$$k_\infty(T) = [k_\infty(300\ K) \pm \Delta k_\infty(300\ K)]\ (T/300)^{\ m\pm\Delta m} \qquad (8)$$

(f) The rate coefficient is determined from the reverse reaction and the equilibrium constant $K(T)$ where $K(T) = 9.0 \times 10^{-29} \exp(14{,}000/T)$ [B =14,000 K]. The uncertainty is calculated using the same approach as given for second-order rate coefficients i.e.

$$f(T) = f(298\ K) \exp \left| \frac{\Delta B}{R} \left(\frac{1}{T} - \frac{1}{298} \right) \right| \qquad (9)$$

with f(298 K) = 2.0 and $\Delta B = 200$.

(h) References

R(1) S E Metcalfe, J D Whyatt and R G Derwent (1995) *A comparison of Model and Observed Network Estimates of Sulphur Deposition across Great Britain for 1990 and its likely Source Attribution.* Quarterly Journal of the Meteorological Society, 121, 1387-1411.

R(2) W B DeMore, S P Sander, D M Golden, R F Hampson, M J Kurylo, C J Howard, A R Ravishankara, C E Kolb and M J Molina (1997) *NASA Panel for Data Evaluation. Chemical Kinetic and Photochemical Data for Use in Stratospheric Modelling: Evaluation Number 12,* Rep. JPL 97-4, Jet Propulsion Laboratory, Pasadena, California, USA.

R(3) R Atkinson, D L Baulch, R A Cox, R F Hampson, J A Kerr, M J Rossi and J Troe (1997) *Evaluated Kinetic and Photochemical Data for Atmospheric Chemistry: Supplement V*. Journal of Physical and Chemical Reference Data, 26, 521-1011.

R(4) M E Jenkin, G D Hayman, R G Derwent, S M Saunders and M J Pilling (1997) *Tropospheric Chemistry Modelling: Improvements to Current Models and Application to Policy Issues*. Annual Report (Reference AEA/RAMP/20150/001 Issue 1) prepared for the Department of the Environment on Contract EPG 1/3/70.

R(5) M E Jenkin, C E Johnson, R G Derwent, S M Saunders and M J Pilling (1994) *Tropospheric Chemistry Modelling: Improvements to Current Models and Application to Policy Issues.* Annual Report (Reference AEA/CS/18360008/001) prepared for the Department of the Environment on Contract PECD 7/12/149.

R(6) D S Lee, R D Kingdon, M E Jenkin and J A Garland (2000) *Modelling the Atmospheric Oxidised and Reduced Nitrogen Budgets for the UK with a Lagrangian Multi-layer Long-range Transport Model.* Environmental Modelling and Assessment, 5, 83-104.

R(7) D S Lee, R D Kingdon, M E Jenkin and A Webster (2000) *Modelling the Contribution of Different Sources of Sulphur to Atmospheric Deposition in the United Kingdom.* Environmental Modelling and Assessment, 5, 105-118.

R(8) N A Fuchs and A G Sutigin (1971) *High-dispersed Aerosols*. International Review of Aerosol Physics and Chemistry, 2, 1-60.

R(9) R Jaenicke (1988) *Properties of Atmospheric Aerosols* in *Numerical Data and Functional Relationships in Science and Technology* Landolt-Bornstein New Series, V: Geophysics and Space Research, 4: Meteorology (G. Fischer, ed.) b: Physical and Chemical Properties of the Air. 391-457, Springer, Berlin.

R(10) A M Hough (1988**)** *The Calculation of Photolysis Rates for Use in Global Tropospheric Modelling Studies*. AERE Report R-13259, HMSO, London [ISBN 0-7058-1259-6].

R(11) D L Baulch, R Atkinson, R A Cox, R F Hampson, J A Kerr and J Troe (1984) *Evaluated Kinetic and Photochemical Data for Atmospheric Chemistry: Supplement II.* Journal of Physical and Chemical Reference Data, 13, 1259-1380.

R(11) R M Harrison, J D Peak and G M Collins (1996) *The Tropospheric Cycle of Nitrous Acid.* Journal of Geophysical Research, 101, 14429-12239.

R(12) P D Lighhtfoot, R A Cox, J N Crowley, M Destriau, G D Hayman, M E Jenkin, G K Moortgat and F Zabel (1992) *Organic Peroxy Radicals: Kinetics, Spectroscopy and Tropospheric Chemistry.* Atmospheric Environment, 26A, 1805-1964.

R(13) G D Hayman (1997) *Effects of Pollution Control on UV Exposure.* Final project report (AEA\RFIN\22525001\R\ 002 Issue 2) prepared for the Department of Health on contract 121/6377 (1997).

R(14) G D Hayman, S Espenhahn and J A Garland (1998**)** *Effects of Air Pollution Control on UV Exposure.* Project report (AEAT-3937\20467001\001 Issue 1) prepared for the Department of Health on contract 121/6703.

R(15) IPCC (1995) *Climate Change 1994 - Radiative Forcing of Climate Change and an Evaluation of the IPCC IS92 Emission Scenarios.* Edited by J T Houghton, L G Meira Filho, J Bruce, H Lee, B A Callendar, E Haites, N Harris and K Maskell, Cambridge University Press: Cambridge, UK.

2 Analytical model for sulphate deposition

CONTENTS

(a) Introduction

The TRACK, HARM and FRAME models all employ similar schemes of differential equations to describe the processes affecting the rate of sulphur deposition. The differential equations may be solved analytically if a number of simplifying assumptions are made. An analytical solution for sulphate deposition is presented in this Appendix.

(b) Sulphur dioxide oxidation

The oxidation of sulphur dioxide emitted from a point source as the parcel of air travels along the trajectory from the source to the receptor is represented in the HARM and TRACK single layer models by:

$$\frac{d[SO_2]}{dt} = -\left(k_1[OH] + k_2 + \frac{V_{d,SO_2}}{h} + \Lambda_{SO_2}\right)[SO_2]$$

$$\Rightarrow \frac{d[SO_2]}{dt} = -\left(\lambda_{SO_2}(t)\right)[SO_2]$$

$$\Rightarrow [SO_2] = [SO_2]_0 \exp\left(-\int \lambda_{SO_2}(t)dt\right)$$

$$\Rightarrow [SO_2] = [SO_2]_0 \exp\left(-(\lambda_{SO_2})_{av} t\right)$$

where $[SO_2]_0 = \frac{Q(1-f)\psi}{Whu}$

The above equations allow for the variation in the rates of reaction and wet and dry deposition rates with time as the parcel of air travels along the trajectory. The solution shows that the variation in the parameters with time may be represented by a simple arithmetic average value.

(c) Total sulphate deposition

Sulphuric acid formed as the result of sulphur dioxide oxidation and subsequent reaction with atmospheric moisture reacts with atmospheric ammonia to form ammonium sulphate. The reactions may be represented by:

$$\frac{d[SO_4^{2-}]}{dt} = \left(k_1[OH] + k_2\right)[SO_2] - r\left([NH_3],[SO_4^{2-}]\right) - \left(\frac{V_{dSO_4^{2-}}}{h} + \Lambda_{SO_4}\right)[SO_4^{2-}]$$

$$\frac{d[AS]}{dt} = r\left([NH_3],[SO_4^{2-}]\right) - \left(\frac{V_{dAS}}{h} + \Lambda_{AS}\right)[AS]$$

If the dry deposition velocity and the wet scavenging coefficient are the same for sulphuric acid and for ammonium sulphate (as assumed in practice by all the models) then it is possible to write the following expression for total sulphate concentration ($[SO_4]+[AS]=[TS]$):

$$\frac{d[TS]}{dt} = (k_1[OH] + k_2)[SO_2]_0 \, exp(-\lambda_{SO_2} t) - \left(\frac{V_{dTS}}{h} + \Lambda_{TS}\right)[TS]$$

substituting for $[SO_2]$:

$$\frac{d[TS]}{dt} = (k_1[OH] + k_2)[SO_2]_0 \exp(-\lambda_{SO_2} t) - \left(\frac{V_{dTS}}{h} + \Lambda_{TS}\right)[TS]$$

Solving:

$$[TS] = (k_1[OH] + k_2)[SO_2]_0 \exp(-\lambda_{TS} t)\left(\frac{[SO_4^{2-}]_0}{(k_1[OH] + k_2)[SO_2]_0} - \frac{1}{(\lambda_{TS} - \lambda_{SO_2})} + \frac{\exp((\lambda_{TS} - \lambda_{SO_2})t)}{(\lambda_{TS} - \lambda_{SO_2})}\right)$$

where $[SO_{4_2}^{2-}]_0 = \dfrac{Qf\psi}{Whu}$

and $\lambda_{TS} = \dfrac{V_{dTS}}{h} + \Lambda_{TS}$

The total rate of sulphur deposition in the vicinity of a receptor is then given by:

$$[TS]_{dep} + [SO_2]_{dep} = [TS](V_{dTS} + h\Lambda_{TS})_{local} + [SO_2](V_{dSO_2} + h\Lambda_{SO_2})_{local}$$

where the dry deposition velocity V_d and the wet scavenging coefficient Λ_d are representative of the area around the receptor. The local deposition velocity and wet scavenging coefficient may be independent of the trajectory average values.

The models are also commonly used to predict the total deposition over the UK land mass. The total deposition from a single source may be estimated (following integration of the deposition rates with respect to distance) from:

$$[TS]_{dep-total} + [SO_2]_{dep-total} = \frac{(V_{dTS} + \Lambda_{TS}h)(k_1[OH] + k_2)[SO_2]_0 u}{(\lambda_{TS} - \lambda_{SO_2})} \left(\frac{\left(1 - \exp(-\lambda_{SO_2} \frac{x}{u}\right)}{\lambda_{SO_2}} - \frac{\left(1 - \exp(-\lambda_{TS} \frac{x}{u}\right)}{\lambda_{TS}} \right)$$

$$+ \frac{[SO_4]_0 u(V_{dTS} + \Lambda_{TS}h)}{\lambda_{TS}} \left(1 - \exp(-\lambda_{TS} \frac{x}{u})\right) + \frac{[SO_2]_0 u(V_{dSO_2} + \Lambda_{SO_2}h)}{\lambda_{SO_2}} \left(1 - \exp(-\lambda_{SO_2} \frac{x}{u})\right)$$

(d) Vertical dispersion

TRACK (multi-level mode) and FRAME allow for the dispersion in the vertical dimension of the emitted sulphur dioxide and the reaction products. No allowance is made for dispersion in the horizontal dimension other than the initial dispersion across the width of the trajectory.

However, in practice, sulphur dioxide emissions from a point source are dispersed throughout the boundary layer depth within about 6 km, under neutral atmospheric conditions. The initial dispersion of the emission in the vertical dimension ceases to be important beyond this distance, which is small compared to the range over which the models apply. The models all assume a constant trajectory width greater than 5 km. The plume from a point source expands in the horizontal dimension at the rate of approximately 10% of the distance travelled downwind: the plume will not expand to the box width until the air parcel has travelled more than 50 km.

At around 7.5 m s^{-1} wind speed, dispersion in the vertical dimension over the initial 6 km corresponds to a mixing time constant of the order of 10^{-3} s^{-1} (~7.5/6000). This value may be compared to the time constant for dry deposition of the most reactive sulphur species, sulphur dioxide (V_d/h) of 10^{-5} s^{-1}. It is concluded that mixing of the depositing total sulphate and sulphur dioxide throughout the boundary layer is much faster than their rate of depletion by dry deposition and so the concentration gradient away from the surface will be small. It is therefore unlikely that vertical dispersion will have a significant effect on the rates of sulphur deposition.

(e) Polar co-ordinates

The analysis presented above has assumed that the pollutant is contained in a parcel of air of constant width. This follows the general approach taken by the HARM and FRAME models. For a single point source, it is more appropriate to allow for the parcel width to increase with increasing distance from the source to allow for horizontal dispersion and for statistical variations in wind direction. However, the sulphate deposition equations are linear with respect to the rate of emission and so the average rate of deposition at distance x from the source across a wind direction sector taking account of the increase in sector width may be calculated by putting:

$$W = x\theta$$

in the above equations, where θ is the sector width in radians.

(f) Nomenclature

Concentrations

$[SO_2]$	concentration of sulphur dioxide
$[SO_4^{2-}]$	concentration of sulphuric acid
[AS]	concentration of ammonium sulphate
[OH]	concentration of OH
[TS]	concentration of total sulphate = ammonium sulphate plus sulphuric acid

Other parameters

k_{s1}	gas phase reaction rate of sulphur dioxide with OH
k_{s2}	aqueous phase oxidation rate of sulphur dioxide
Q	emission rate of sulphur dioxide
f	proportion of emission as sulphur trioxide
x	distance downwind
W	width of trajectory
h	boundary layer height
u	wind speed
V_d	dry deposition velocity
λ	characteristic frequency
Λ	wet scavenging coefficient
Ψ	frequency of wind in direction
θ	wind sector angle

3 Analytical model for nitrogen deposition

The TRACK, HARM and FRAME models all employ similar schemes of differential equations to describe the processes affecting the rate of nitrogen deposition. The differential equations may be solved analytically if a number of simplifying assumptions are made. An analytical solution for nitrogen deposition is presented in this Appendix.

There are however some differences in the reaction schemes employed by the TRACK, HARM and FRAME models. For this analysis, a simplified reaction scheme has been investigated that represents the major features of the reaction schemes employed in the numerical models,

For the purposes of the analytical assessment, the mass balance of the oxidised nitrogen species has been represented by the following equations. These equations involve some simplification but broadly represent the most significant reactions considered in the acid deposition models.

$$\frac{d[NO]}{dt} = J_1[NO_2] - k_1[NO][O_3] + q\frac{E}{h}$$

$$\frac{d[NO_2]}{dt} = -J_1[NO_2] + k_1[NO][O_3] + (1-q)\frac{E}{h} - k_4[OH][NO_2] - k_5[O_3][NO_2] + J_2[NO_3] -$$

$$k_{10}[NO_3][NO_2] - \frac{v_{dNO_2}}{h}[NO_2]$$

$$\frac{d[O_3]}{dt} = -\frac{v_{dO_3}}{h}([O_3] - [O_3]_0) - k_1[NO][O_3] + J_1[NO_2] - k_5[NO_2][O_3] + J_2[NO_3]$$

$$\frac{d[NO_3]}{dt} = k_5[O_3][NO_2] - J_2[NO_3] - k_{10}[NO_3][NO_2]$$

$$\frac{d[N_2O_5]}{dt} = k_{10}[NO_3][NO_2] - k_{11}[N_2O_5]$$

Further reactions then take place involving nitric acid, ammonia, oxidised nitrogen aerosol and ammonium aerosol. The path of these reactions depends on whether ammonia is present. In the absence of ammonia, the mass balance equations for nitric acid and oxidised nitrogen aerosol are:

$$\frac{d[HNO_3]}{dt} = k_4[OH][NO_2] - k_9[HNO_3] - (\frac{v_{dHNO_3}}{h} + \Lambda_{HNO_3})[HNO_3]$$

$$\frac{d[N_{ox}aer]}{dt} = k_{11}[N_2O_5] + k_9[HNO_3] - (\frac{v_{daer}}{h} + \Lambda_{aer})[N_{ox}aer]$$

If there is excess ammonia present, the nitric acid reacts quickly (effectively instantaneously) with the ammonia to form ammonium aerosol (cf. FRAME). The mass balance equations are then:

$$\frac{d[N_{ox}aer]}{dt} = k_4[OH][NO_2] + k_{11}[N_2O_5] - (\frac{v_{daer}}{h} + \Lambda_{aer})[N_{ox}aer]$$

$$\frac{d[NH_4aer]}{dt} = k_4[OH][NO_2] - (\frac{v_{daer}}{h} + \Lambda_{aer})[NH_4aer]$$

$$\frac{d[NH_3]}{dt} = -k_4[OH][NO_2] - (\frac{v_{dNH_3}}{h} + \Lambda_{NH_3})[NH_3]$$

The mass balance equations for NO, NO_2, NO_3, O_3 and N_2O_5 contain non-linear reaction terms. For additional regulated sources, the equations can be linearised about the operating point:

$$[NO] = [NO]_0 + [NO]'$$

etc.

where $[NO]_0$ is the baseline concentration and [NO]' is the contribution from the additional sources. The mass balance equations may then be written in terms of the incremental change in the concentrations e.g.

$$\frac{d[NO]'}{dt} = J_1[NO_2]' - k_1[O_3]_0[NO]' - k_1[NO]_0[O_3]' + q\frac{E'}{h}$$

The linearised mass balance equations representing the response to the incremental additional source may then be presented in terms of their Laplace transforms (dropping the prime notation for convenience):

$$(\lambda_{NO} + s)[NO](s) = q\frac{E}{h}(s) + J_1[NO_2](s) - k_1[NO]_0[O_3](s)$$

$$(\lambda_{NO_2} + s)[NO_2](s) = (1-q)\frac{E}{h}(s) + k_1[O_3]_0[NO](s) + \left(k_1[NO]_0 - k_5[NO_2]_0\right)[O_3](s) +$$

$$\left(J_2 - k_{10}[NO_2]_0\right)[NO_3](s) \qquad (A)$$

$$(\lambda_{O_3} + s)[O_3](s) = -k_1[O_3]_0[NO](s) + \left(J_1 - k_5[O_3]_0\right)[NO_2](s) + J_2[NO_3](s)$$

$$(\lambda_{NO_3} + s)[NO_3](s) = \left(k_5[O_3]_0 - k_{10}[NO_3]_0\right)[NO_2](s) + k_5[NO_2]_0[O_3](s)$$

$$(\lambda_{N_2O_5} + s)[N_2O_5](s) = k_{10}[NO_3]_0[NO_2](s) + k_{10}[NO_2]_0[NO_3](s) \qquad (B)$$

In the absence of ammonia:

$$(\lambda_{HNO_3} + s)[HNO_3](s) = k_4[OH][NO_2](s)$$

$$(\lambda_{N_{ox}aer} + s)[N_{ox}aer](s) = k_{11}[N_2O_5](s) + k_9[HNO_3](s)$$

For excess ammonia:

$$(\lambda_{N_{ox}aer} + s)[N_{ox}aer](s) = k_4[OH][NO_2](s) + k_{11}[N_2O_5](s)$$
$$(\lambda_{NH_4aer} + s)[NH_4aer](s) = k_4[OH][NO_2](s)$$
$$(\lambda_{NH_3} + s)[NH_3](s) = -k_4[OH][NO_2](s)$$

The characteristic frequencies, λ, are given by:

$$\lambda_{NO} = k_1[O_3]_0$$
$$\lambda_{NO_2} = J_1 + k_4[OH] + k_5[O_3]_0 + k_{10}[NO_3]_0 + \frac{v_{dNO_2}}{h}$$
$$\lambda_{O_3} = k_1[NO]_0 + k_5[NO_2]_0 + \frac{v_{dO_3}}{h}$$
$$\lambda_{NO_3} = J_2 + k_{10}[NO_2]_0$$
$$\lambda_{N_2O_5} = k_{11}$$
$$\lambda_{HNO_3} = k_9 + \frac{v_{dHNO_3}}{h} + \Lambda_{HNO_3}$$
$$\lambda_{N_{ox}aer} = \frac{v_{daer}}{h} + \Lambda_{aer}$$
$$\lambda_{NH_4aer} = \frac{v_{daer}}{h} + \Lambda_{aer}$$
$$\lambda_{NH_3} = \frac{v_{dNH_3}}{h} + \Lambda_{NH_3}$$

The use of the Laplace transform method implies that the baseline concentrations $[O_3]_0$, $[NO]_0$, $[NO_3]_0$ and $[NO_2]_0$, dry deposition velocities, wet scavenging coefficients and reaction rate constants do not change. This is a reasonable approximation for the purposes of investigating system dynamics and uncertainties. However, in practice these parameters will vary with time and location: these effects can only be investigated by means of numerical models although the analytical solution may be applied piecewise if these parameters do not change rapidly.

The Laplace transform of each species concentration in terms of s may be obtained by algebraic elimination. In principal, the concentration as a function of time may be obtained as the inverse Laplace transform of the resulting expressions. However, this is rather tedious. Some simplification follows from frequency-response analysis of the expression for $[NO_2](s)$ and $[N_2O_5](s)$. The analysis involves substituting $s=j\omega$ where $j=\sqrt{(-1)}$ and calculating the amplitude ratio as the modulus of the resulting expression. The analysis is simplified for overdamped systems i.e. where each of the characteristic frequencies is real and positive as here. The frequency-response diagram shows the amplitude ratio plotted against frequency, ω. Fig. A3.1 shows a plot for $h[NO_2](s)/E(s)$ for typical parameter values over the range 10^{-7}-2 x 10^{-3} s^{-1}. This range is appropriate for the investigation of regional scale and national scale deposition corresponding to time scales greater than about 10 minutes up to more than 100 hours. System responses that take place over shorter timescales will be damped,

rapidly approaching a localised equilibrium: those that require longer timescales will not progress substantially.

Fig. A3.1 shows the shape of the frequency response for a typical set of input parameters. The general shape of the plot closely resembles that for a first order system with a characteristic frequency (the corner frequency) of approximately 5 10^{-5} s^{-1}. The frequency response for other sets of input parameters (40 model runs) covering their expected ranges was very similar with characteristic frequencies between 5.10^{-6} and 2.10^{-4}.

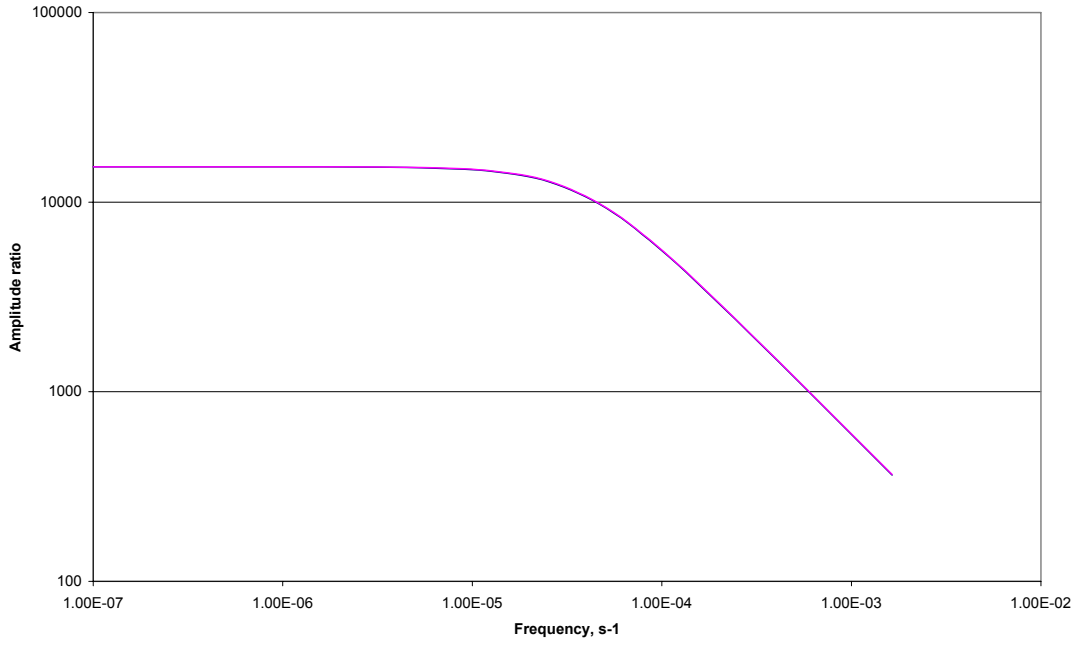

Fig.A3.1: Frequency response plot for h[NO_2](s)/E(s) for typical input parameters

The system has therefore been simplified by replacing (A) above with:

$$(\lambda^*_{NO_2} + s)[NO_2](s) = k^* \frac{E}{h}(s)$$

where

$$\lambda^*_{NO_2} = \frac{10^{-3}.Amplitude\_ratio(\omega = 10^{-3})}{Amplitude\_ratio(\omega = 10^{-7})}$$

$$k^* = 10^{-3}.Amplitude\_ratio(\omega = 10^{-3})$$

The values of λ_{NO2} and k must be evaluated for each set of input parameters. Parameters such as those characterising the reaction of nitric oxide with ozone (e.g. baseline ozone and nitric oxide concentrations, k_1), which takes place relatively

rapidly, influence the magnitude of λ_{NO2} and k because they determine localised equilibrium states.

Fig.A3.1 also shows the pseudo-first order amplitude ratio: the amplitude ratio for the pseudo-first order expression is not significantly different from that for (A).

Similarly the right hand side of (B) has been replaced by:

$$(\lambda^{''} + s)(k_{10}[NO_3]_0[NO_2](s) + k_{10}[NO_2]_0[NO_3](s)) = k^{''}\frac{E}{h}(s)$$

Substituting into (B) and rearranging gives:

$$(\lambda^{**} + s)(\lambda_{N_2O_5} + s)[N_2O_5](s) = k^{**}\frac{E}{h}(s)$$

Species concentrations for a point source were then obtained by inverse Laplace transforms. For the ammonia absent case:

$$[NO_2] = \frac{Q\psi k^*}{Whu}\exp\left(-\lambda^*_{NO_2}t\right)$$

$$[HNO_3] = \frac{Q\psi k^*}{Whu}k_4[OH]\frac{\left\{\exp\left(-\lambda^*_{NO_2}t\right)-\exp\left(-\lambda_{HNO_3}t\right)\right\}}{\left\{\lambda_{HNO} - \lambda^*_{NO_2}\right\}}$$

$$[N_{ox}aer] = \frac{Q\psi}{Whu}\left[\begin{array}{l} k^{**}k_{11}\dfrac{\left\{(\lambda_{N_2O_5}-\lambda_{N_{ox}aer})\exp\left(-\lambda^{**}t\right)+(\lambda_{N_{ox}aer}-\lambda^{**})\exp\left(-\lambda_{N_2O_5}t\right)+(\lambda^{**}-\lambda_{N_2O_5})\exp\left(-\lambda_{N_{ox}aer}t\right)\right\}}{\left\{(\lambda^{**}-\lambda_{N_2O_5})(\lambda_{N_2O_5}-\lambda_{N_{ox}aer})(\lambda_{N_{ox}aer}-\lambda^{**})\right\}} \\ + k^*k_9k_4[OH]\dfrac{\left\{(\lambda_{HNO_3}-\lambda_{N_{ox}aer})\exp\left(-\lambda^*_{NO_2}t\right)+(\lambda_{N_{ox}aer}-\lambda^*_{NO_2})\exp\left(-\lambda_{HNO_3}t\right)+(\lambda^*_{NO_2}-\lambda_{HNO_3})\exp\left(-\lambda_{N_{ox}aer}t\right)\right\}}{\left\{(\lambda^*_{NO_2}-\lambda_{HNO_3})(\lambda_{HNO_3}-\lambda_{N_{ox}aer})(\lambda_{N_{ox}aer}-\lambda^*_{NO_2})\right\}} \end{array}\right]$$

For the ammonia-rich case:

$$[NO_2] = \frac{Q\psi k^*}{Whu}\exp\left(-\lambda^*_{NO_2}t\right)$$

$$[N_{ox}aer] = \frac{Q\psi}{Whu}\left[\begin{array}{l} k^{**}k_{11}\dfrac{\left\{(\lambda_{N_2O_5}-\lambda_{N_{ox}aer})\exp\left(-\lambda^{**}t\right)+(\lambda_{N_{ox}aer}-\lambda^{**})\exp\left(-\lambda_{N_2O_5}t\right)+(\lambda^{**}-\lambda_{N_2O_5})\exp\left(-\lambda_{N_{ox}aer}t\right)\right\}}{\left\{(\lambda^{**}-\lambda_{N_2O_5})(\lambda_{N_2O_5}-\lambda_{N_{ox}aer})(\lambda_{N_{ox}aer}-\lambda^{**})\right\}} \\ + k^*k_4[OH]\dfrac{\left\{\exp\left(-\lambda^*_{NO_2}t\right)-\exp\left(-\lambda_{N_{0x}aer}t\right)\right\}}{\left\{\lambda_{N_{ox}aer}-\lambda^*_{NO_2}\right\}} \end{array}\right]$$

$$[NH_4aer] = \frac{Q\psi}{Whu}k^*k_4[OH]\frac{\left\{\exp\left(-\lambda^*_{NO_2}t\right)-\exp\left(-\lambda_{NH_4aer}t\right)\right\}}{\left\{\lambda_{NH_4aer}-\lambda^*_{NO_2}\right\}}$$

$$[NH_3] = -\frac{Q\psi}{Whu}k^*k_4[OH]\frac{\left\{\exp\left(-\lambda^*_{NO_2}t\right)-\exp\left(-\lambda_{NH_3}t\right)\right\}}{\left\{\lambda_{NH_3}-\lambda^*_{NO_2}\right\}}$$

The total rate of oxidised nitrogen deposition is then given by ;

$$[NO_2]_{dep}+[HNO_3]_{dep}+[N_{ox}aer]_{dep} = [NO_2]v_{dNO_2}+[HNO_3]\left(v_{dHNO_3}+\Lambda_{HNO_3}h\right)+[N_{ox}aer]\left(v_{daer}+\Lambda_{aer}h\right)$$

The analysis presented above has assumed that the pollutant is contained in a parcel of air of constant width. This follows the general approach taken by the HARM and FRAME models. For a single point source, it is more appropriate to allow for the parcel width to increase with increasing distance from the source to allow for horizontal dispersion and for statistical variations in wind direction. However, the linearised deposition equations are necessarily linear with respect to the rate of emission and so the average rate of deposition at distance x from the source across a wind direction sector taking account of the increase in sector width may be calculated by putting:

$$W = x\theta$$

in the above equations, where θ is the sector width in radians.

NOMENCLATURE

Molecular concentrations

$[HNO_3]$	total or incremental concentration of nitric acid
$[NH_3]$	total or incremental concentration of ammonia
$[NH_4aer]$	total or incremental concentration of ammonium aerosol (NH_4^+ in ammonium nitrate)
[NO]	total or incremental concentration of nitric oxide
$[NO_2]$	total or incremental concentration of nitrogen dioxide
$[NO_3]$	total or incremental concentration of nitrate radical
$[N_2O_5]$	total or incremental concentration of nitrogen pentoxide
$[N_{ox}aer]$	total or incremental concentration of oxidised nitrogen aerosol (NO_3^- in ammonium nitrate plus products of nitric acid and nitrogen pentoxide reactions with atmospheric aerosols)
$[O_3]$	total or incremental concentration of ozone
[OH]	total or incremental concentration of OH radical

subscript $_0$ refers to baseline conditions
superscript ' refers to incremental concentration (dropped in Laplace transform equations)

Reaction rates

k_1	rate constant $NO+O_3 \rightarrow NO_2+O_2$
k_4	rate constant $NO_2+OH \rightarrow HNO_3$
k_5	rate constant $NO_2+O_3 \rightarrow NO_3+O_2$
k_9	rate constant $HNO_3 \rightarrow$aerosol
k_{10}	rate constant $NO_2+NO_3 \rightarrow N_2O_5$
k_{11}	rate constant $N_2O_5 \rightarrow$ aerosol
J_1	rate constant $NO_2 \rightarrow NO+O_3$
J_2	rate constant $NO_3 \rightarrow NO_2+O$

Other parameters

v_d	dry deposition velocity for each species
Λ	wet scavenging coefficient for each species

h	boundary layer height
q	proportion NOx as NO
t	time
λ	characteristic frequencies
Q	rate of emission of NOx
W	trajectory width
u	wind speed
ψ	frequency of wind in trajectory direction

Appendix 4 Analysis of Uncertainty in Critical Loads: Literature Review

EXECUTIVE SUMMARY

The critical loads approach has been developed as an aid to the regulation of acidifying gas emissions, both within the UK and internationally. The critical load is broadly defined as the amount of pollutant deposition a part of the environment can tolerate without harm. To make effective use of the concept, it is important that regulatory agencies understand the limitations and uncertainties associated with the critical loads approach. This Appendix forms part of a larger report, which is aimed at defining and quantifying the uncertainties involved. The aim of this report is to summarise current knowledge about the uncertainties entailed in estimating critical loads themselves.

Each method used for estimating critical loads in the UK is reviewed. For each method, the theory is outlined; the way it is used in the UK is described; and comments made on the uncertainties involved, quantitatively if possible. The methods covered are: empirical and mass balance critical loads for nutrient nitrogen; empirical and mass balance critical loads for soil acidity; and for freshwaters the Steady State Water Chemistry Model, the Diatom Model, and the First Order Acid Balance Model. Comments are also made on the derivation of the Critical Loads Function.

Progress in the use of dynamic models for assessment of acidification effects is also described. Dynamic models are easier to validate than critical load models, fit better with economic analyses, and give more realistic impressions to policymakers. They are however more demanding of data. In spite of their use of more parameters, there is no real evidence that they are subject to more uncertainty than orthodox critical load models.

The literature on uncertainty analysis of critical load estimation is reviewed. The uncertainty of critical load estimates is narrower than what might be intuitively be assumed, coefficients of variation being typically 25-40%. This may be the result of optimistic assumptions about input data, however, and some methods give wider limits. Sensitivity analyses show that the range of critical loads generated by reasonable changes in some input parameters was >100% of the central value. Considering all input parameters together narrows uncertainty because of a “compensation of errors” mechanism. Applying different models to the same site and altering model structures within the limits of theoretical knowledge also generates a wide range of critical load outcomes. There is much uncertainty about uncertainty, and more work is needed to make quantitative estimates.

The steady state nature of critical load models means they are very difficult to validate. There is a vague correspondence between critical load exceedence by deposition and areas of known damage. The UK’s practice in calculating critical loads is in line with that of other European countries, which is in any case very varied.

The uncertainty in the experimental data behind the two most commonly used critical limits (base cation: aluminium ratios for soils and acid neutralising capacity for waters) is reviewed. Critical limits are effectively the environmental quality standards the critical load is trying to achieve. In both cases the response of the target organisms is probabilistic rather than all-or-nothing. The range between zero and 100% response is very wide, and choice of a critical limit is largely a matter of choosing the desired degree of precaution or acceptance of damage.

Identifying the location of the ecosystem types for which critical loads are calculated is not a trivial task. In the UK, the accuracy of land use identification from satellite data is said to be 80-85%, but this is reduced by translation into the categories used for critical load calculation.

The methods for aggregation of data from more to less detailed scales pose further problems. For most aggregation methods, this process reduces the area of low critical loads and probably reduces calculated exceedence. The "average accumulated exceedence" approach provides a method for using more of the information about exceedence in a given grid square. Other probabilistic methods could be used in the calculation and presentation of critical loads.

CONTENTS

List of Figures

List of Tables

1 Introduction

The formal definition of a critical load is: "a quantitative estimate of an exposure to one or more pollutants below which significant harmful effects on specified sensitive elements of the environment do not occur according to present knowledge" (Nilsson and Grennfelt, 1988). This definition was elaborated at a workshop at Skokloster in Sweden in 1988, and has been used to develop policy within the UNECE, and more recently the EU, ever since. The underlying notion is that of a threshold: if deposition is below the threshold there are no problems; if it is above the threshold, harm is being done to the environment. This is the way the concept is explained to policymakers: it therefore appears to make sense to reduce deposition below the critical load as quickly as possible, in order to avoid further harm.

But defining "significant harmful effects" for sensitive elements of the environment on a European scale is a formidably difficult task. The natural environment is immensely complex, constantly changing, and not well understood. There are millions of species of animals, plants and micro-organisms interacting in an inconceivably vast number of ways with each other and with the physical environment. The response of only a few of these species to only a few pollutants is known over only a small range of conditions. Even for these, pollutant effects may be modified e.g. by interaction with other pollutants, or by different physical conditions. Even then, species sometimes have geographically distinct ecotypes with a different response to pollutants; there is invariably a range of responses between individuals. Over large areas such as Europe, there are pronounced gradients in physical conditions, which change the relative importance of ecosystem processes. Even if the response of species or ecosystems to pollutants were known with certainty, data on species distribution and physical characteristics of the environment would still need to be known at a fine scale. These difficulties are of course not unique to the critical loads approach: they apply to the setting of any sort of scientifically-based environmental quality standard. The critical load approach attempts to overcome them by concentrating on certain species, which are known to be sensitive to pollutant deposition, or chemical substitutes for these, in the hope that this will also protect every other component of the ecosystem. It is clear then that the critical load threshold, if there is one, is likely to be very fuzzy.

The aim of this report is to summarise current knowledge about the uncertainties entailed in estimating critical loads. Only an outline of critical load methodology can be given here: full details will be found in the official UNECE Mapping Manual (UBA, 1996), in reports from the UK National Focal Centre at Monks Wood (Hall *et al.* 1997, 1998, 2001a) and in publications of the Co-ordinating Centre for Effects (CCE) in the Netherlands (Posch *et al*. 1995, 1997, 1999, 2001).

2 Methods for determining critical loads

The UK calculates critical loads for 6 ecosystems: acid grasslands; calcareous grasslands; heathlands; coniferous woodland; deciduous woodland and freshwaters. For each of these, four critical loads are calculated corresponding to the nodes on the critical loads function (Fig. 2.1). These are the maximum critical load for sulphur ($CL_{max}S$); the maximum critical load for nitrogen ($CL_{max}N$); the minimum critical load for N ($CL_{min}N$); and the critical load for nutrient N ($CL_{nut}N$).

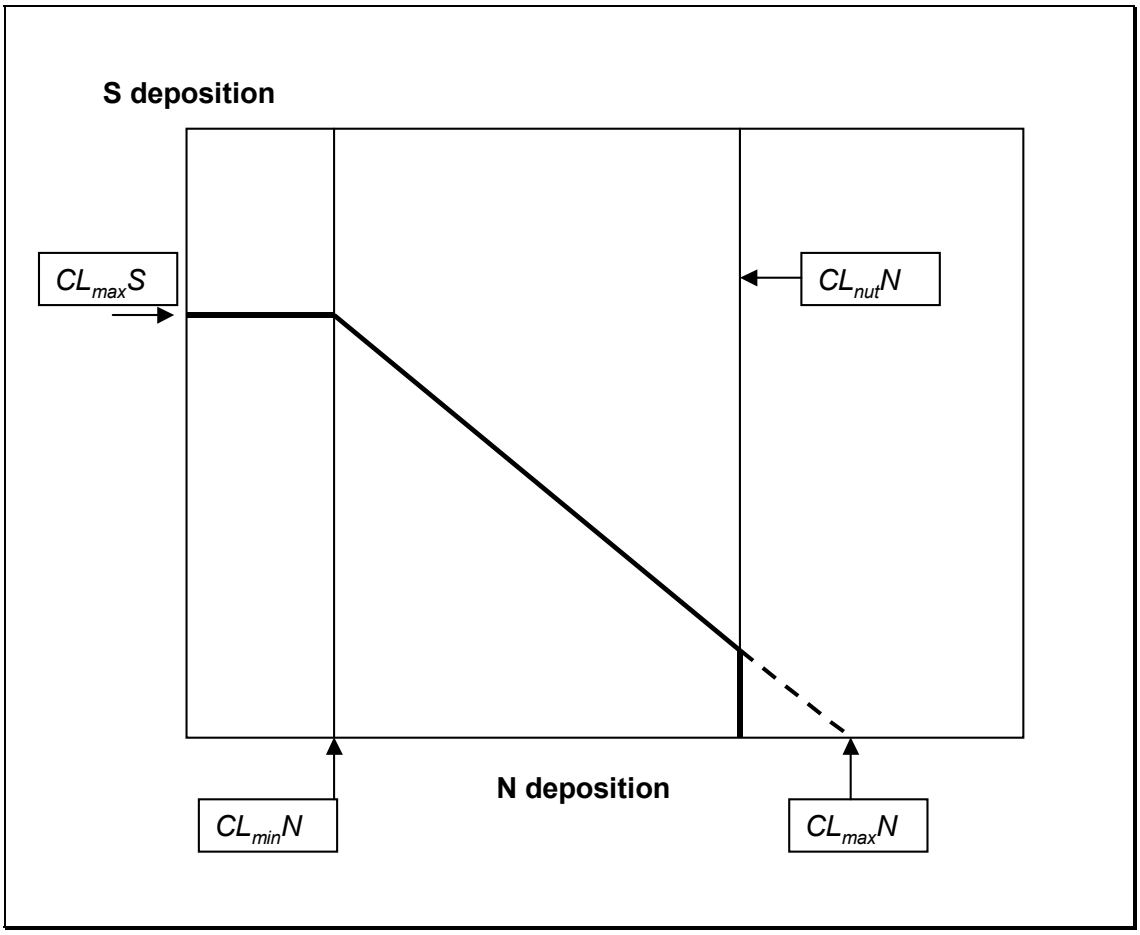

Figure 2.1: The critical load function.

The thick line represents the critical load for a hypothetical ecosystem as a function of S and N deposition. The $CL_{max}S$ represents the critical load for acidity when nitrogen deposition is zero. The critical load is equal to $CL_{max}S$ whilst all nitrogen deposition is taken up by the catchment, hence the horizontal portion of the critical load function. $CL_{min}N$ is the deposition-independent critical load of acidity due to nitrogen removal processes alone (nitrogen uptake, immobilization, and denitrification). $CL_{max}N$ is the critical load for acidity when S deposition is zero. $CL_{nut}N$ is the critical load for nutrient nitrogen, intended to protect against non-acidifying effects of N deposition. In this example, $CL_{nut}N$ is less than $CL_{max}N$, truncating the function, but this is not necessarily the case.

For each type of critical load, the next section describes the theoretical background, the methods the UK uses for calculation, and the major uncertainties in the methods.

Critical loads for nutrient nitrogen are described first, as they are easier to treat in isolation from the others.

2.1 Critical Loads for Nutrient Nitrogen

The general definition of a critical load was modified somewhat for nitrogen to "a quantitative estimate of an exposure to deposition of nitrogen as NH_x and/or NO_y below which significant harmful effects in ecosystem structure and function do not occur according to present knowledge" (Grennfelt and Thörnelöf, 1988). The addition of the terms "structure" and "function" recognises that ecosystems may be visibly damaged (e.g. by loss of species) or damaged in their capacity to fulfil functions (such as absorption of N). Deposition of combined nitrogen from the atmosphere has two major, potentially harmful effects: acidification and "eutrophication". Acidification effects are dealt with in conjunction with the acidifying effects of S (see below), but eutrophication effects are specific to N and have to be considered separately. Eutrophy (literally "good nutrition") has acquired connotations of a harmful effect in relation to lakes: in the context of N critical loads it means an increase in the N status of an ecosystem to such an extent that an effect considered to be harmful is likely to appear. The resulting critical load is the critical load for nutrient nitrogen $CL_{nut}N$. There are two methods in common use for estimating the critical load for nutrient nitrogen: the empirical method and the mass balance method.

2.1.1 Theoretical background – empirical critical loads for nutrient N

The empirical method is based on observations of the N deposition at which changes to ecosystem structure and function occur, either in the field or in experiments. The current official values are given by Bobbink *et al.* (1996) and reproduced in Table 2.1. An example of a documented change in ecosystem function is generation of nutrient imbalances in coniferous trees (critical load 10-15 kg N ha^{-1} y^{-1}); a typical change in ecosystem structure is the replacement of heather by grassland in the Netherlands (critical load 15-20 kg N ha^{-1} y^{-1}). Bobbink et al. (1996) provide estimates of the reliability of each critical load: both the above are regarded as "reliable" (with 2 others - there are 9 rated as "quite reliable" and 6 as "expert judgement" i.e. an informed guess). Absolute values of the critical loads range from 5 kg N ha^{-1} y^{-1} (ombrotrophic bogs and arctic heaths) to 35 kg N ha^{-1} y^{-1} (calcareous grasslands). Note that there are a number of different critical loads for the same ecosystem, depending on the ecological effect of concern or the characteristics of the ecosystem (e.g. high/low nitrification).

The UNECE Expert Workshop on Chemical Criteria and Critical Limits, held at York in March 2001, proposed a few changes, mostly in a downward direction, and these are also shown in Table 2.1. There are likely to be more changes, however, resulting from a proposed workshop on empirical nitrogen critical loads in autumn 2002.

Table 2.1: Empirical Critical Loads for Nitrogen Deposition

Ecosystem	[1]Critical Load (kg N ha^{-1} y^{-1})	Indication of Exceedence
Coniferous trees (acidic)	10-15##	Nutrient imbalance (low nitrification)
Coniferous trees (acidic)	20-30#	Nutrient imbalance (moderate-high nitrification)
Deciduous trees	15-20#	Nutrient imbalance (increased shoot/root ratio)
Acidic coniferous forests	7-20##	Changes in ground flora & mycorrhizas; increased leaching
Acidic deciduous forests	10-20#	Changes in ground flora & mycorrhizas
Calcareous forests	15-20(#)	Changes in ground flora
Acidic natural forests	7-15(#)	Changes in ground flora & leaching
Forests in humid climates	5-10(#)	Decline in lichens, increase in free-living algae
Lowland dry heathlands	15-20##	Transition heather to grass, functional change (litter production, flowering)
Lowland wet heathlands	17-22#	Transition heather to grass
Species rich heaths/grassland	10-15#	Decline in sensitive species
Upland Calluna heaths	10-20(#)	Decline in heather dominance, mosses & lichens, N accumulation
Arctic & alpine heaths	5-15(#) [5-10##]	Decline in lichens, mosses, evergreen dwarf shrubs
Calcareous grasslands	15-35# [15-25#]	Increased mineralization, N accumulation, leaching, tall grass; change in diversity
Neutral - acidic grasslands	20-30#	Increase in tall grass, change in diversity
Montane-subalpine grassland	10-15(#)	Increase in tall graminoids, change in diversity
Mesotrophic fens	20-35#	Increase in tall graminoids, decline in diversity
Ombrotrophic bogs	5-10# [##]	Decrease in typical mosses, increase in tall graminoids, N accumulation
Shallow soft water bodies	5-10##	Decline in isoetid species
[Dune grasslands]	[10-20#]	[None mentioned]

Notes: [1]confidence indicated as: ## reliable; # quite reliable; (#) expert judgement. Square brackets [] indicate changes proposed at the UNECE Workshop on Chemical Criteria and Critical Limits. Modified from Bobbink *et al.* (1996).

2.1.2 Empirical nitrogen methods used by the UK

The methods used in the UK are based on the values in Table 2.1, and apply to the five terrestrial ecosystems for which the UK calculates critical loads (Hall *et al.*, 1998, 2001a). Although the methodology exists to calculate $CL_{nut}N$ values for freshwaters, the UK does not use it on the grounds that most UK upland waters are likely to be phosphorus limited, and hence N eutrophication is not likely to be a relevant issue. A stepwise approach is taken dependent on the soil and ecosystem types present within each category (Table 2.2).

Table 2.2: Empirical Nitrogen Critical Loads used in the UK

Ecosystem	Critical Load (kg N ha^{-1} y^{-1})
Acid grassland	25
Acid grassland if montane sub-alpine grassland present	12.5
Acid grassland if peat soils dominate	10
Calcareous grassland	50
Heathland	17
Heathland with upland *Calluna* moorland	15
Heathland with arctic-alpine heath	10
Heathland with peat soils	10
Deciduous woodland	17
Coniferous woodland	13

2.1.3 Uncertainties in empirical N critical loads

The empirical method has the merit of being based on observation, but has a number of disadvantages. Vegetation changes observed in the field normally have multiple causes (e.g. management changes; climatic fluctuation; pathogen attacks) and are not necessarily due entirely to N deposition. Changes due to experimental manipulation can be attributed to N with more certainty, but often have low resolution. For instance, if an effect is seen at 40 kg N ha^{-1} y^{-1}, but not at 5 kg N ha^{-1} y^{-1} (a fairly typical experimental spread - scientists like to see results) then the critical load could be set at 5 (precautionary approach) or 40 (lowest observed effect level) or somewhere in between. UNECE workshops (Hornung et al., 1994; UBA, 1996) have called for higher resolution experiments. This is one reason for quoting empirical critical loads as a range; other reasons are to take some account of ecosystem diversity and environmental conditions. The UNECE Mapping Manual (UBA, 1996) provides guidelines for choosing which parts of a range to represent on a map, but this inevitably involves more "expert judgement". At present, critical loads for oxidised and reduced N deposition are not distinguished, though there is evidence that reduced N deposition is more damaging to most ecosystems. Finally it is difficult with the empirical method to take account of effects which may appear in the long-term, after ecosystems have accumulated N to a threshold value, and there is some evidence that this is a credible damage mechanism (see below). This was one reason for the development of the mass balance method.

2.2 Critical Loads for Nutrient Nitrogen – Mass Balance Method

The UK uses the mass balance method, as well as the empirical method, to calculate $CL_{nut}N$ for the two woodland ecosystems only.

2.2.1 Theoretical background for mass balance critical loads

The mass balance approach is based on calculation of all significant outputs and inputs of N to each ecosystem. Inputs equal outputs plus accumulation:

$$N_{dep} + N_{fix} = N_i + N_u + N_{de} + N_{ad} + N_{fire} + N_{eros} + N_{vol} + N_{le} \quad (1)$$

where the suffices represent:

dep	atmospheric deposition of combined N;
fix	N fixation (reduction of atmospheric N_2 to NH_3 and incorporation into other N species);
i	immobilisation into soil organic matter;
u	uptake by plants and animals;
de	denitrification (reduction of NO_3^- to N_2 or N_2O, and release to the atmosphere)
ad	adsorption (typically of NH_4^+ onto clays);
fire	N loss during combustion (in accidental or deliberate fires);
eros	erosion (of what is not stated, but probably it means soil which would include particulate N, which is not otherwise accounted for);
vol	volatilisation (of NH_3, from alkaline soils);
le	leaching (of NO_3^-, NH_4^+, and dissolved organic N).

To set the critical load, each term in equation (1), except N_{dep}, must be specified, assumed to be negligible, or given an "acceptable" value. The Mapping Manual (UBA, 1996) suggests default values for many important ecosystems for use in the absence of measurements (the usual situation). N_{vol} is assumed to be negligible - a reasonable assumption except on calcareous soils, or where there are large populations of grazing animals. N_{ad} is assumed to be zero for different reasons; it is a sink of a finite size and therefore cannot contribute indefinitely to the critical load calculation (it is likely to be a small sink for most soils). N_{eros} is generally assumed to be small, except following disturbance, such as fire or clear cutting of a forest. Default values for these events are provided, which are intended to be divided by the time interval between events: these could be significant for some ecosystems (e.g. 4 - 7.5 kg N ha^{-1} y^{-1} for a heathland burnt every 20 years), but it is not clear that they have ever been used in critical load calculations. Similar arguments apply to N_{fire}, important in *Calluna* heathland management in the UK and in Mediterranean *maquis* vegetation. Generally, however, these 4 parameters are set to zero and attention concentrated on the remaining 5.

N_{fix} is usually assumed to be between 0 and 3 kg N ha^{-1} y^{-1}, e.g. the UK originally used 0 for calcareous grassland, 1 for acid grassland and 3 for all forests. N_{fix} will be much greater (30-100 kg N ha^{-1} y^{-1}) in sites with nitrogen-fixing plants, but the authors are not aware that these systems have been considered in critical load calculations. Since 1998, however, the UK has not taken nitrogen fixation into account.

Nitrogen uptake N_u into plant or animal is a more important parameter. Only biomass which is harvested or leaves the system in some way should be considered. Some elaborate calculation methods are suggested in the Mapping Manual (UBA, 1996), based on estimates of tree growth limited by either physical conditions or base cation availability or both. The UK does not believe the data are available to perform these calculations reliably, and simply uses a single value for all woodlands. This comes in for some mild criticism in the latest report from the CCE (Posch *et al.* 2001).

N immobilisation N_i can occur at high rates, but the problem for calculating critical loads is deciding what is sustainable in the long term. Since the last glaciation, woodland soils in Northern Europe have accumulated N at the rate of about 1-2 kg N ha^{-1} y^{-1}. In experiments, however, some forests have been able to accumulate N in soil at much higher rates. At Aber in N Wales for instance the forest was able to assimilate virtually all

the experimentally applied input of NH_4^+ - N at 17.5 kg N ha^{-1} y^{-1} for at least 6 years in spite of being classed as being N saturated, with no obvious deleterious effects. Eventually, however, it is assumed that the C:N ratio of the forest floor would decrease to the point where N mineralisation and leaching would start to occur. Dynamic models are required to assess how long it would take to reach this point. If N deposition increases productivity, then C assimilation should also increase, potentially increasing the ability to immobilise N without decreasing the C:N ratio. The assumption that N_i should be limited to the historical rate in N-limited systems is thus very much a worst-case assumption. The Mapping Manual recommends 0.5 – 1 kg N ha^{-1} y^{-1}: the UK uses 1 or 3 kg N ha^{-1} y^{-1} depending on soil type.

Denitrification N_{de} is characteristic of anoxic conditions and thus heavily dependent on soil type and moisture conditions. It is also dependent on the supply of NO_3^- - N, and thus on N_{dep}. Two methods are suggested in the Mapping Manual (UBA, 1996): the simplest assumes that a constant fraction of the expression (N_{dep}- N_i - N_u) is denitrified. This is known as the *denitrification fraction* f_{de} which varies between 0.1 and 0.8 depending on soil type. A more complex expression relates denitrification in a non-linear fashion to soil moisture, temperature and pH, giving a perhaps more realistic curve shape, but on the basis of a very small amount of experimental data. Again long-term rates are small: 1-3 kg N ha^{-1} y^{-1} being recommended for forest systems. The UK uses neither of these methods: it assumes the rate is 1, 2 or 4 kg N ha^{-1} y^{-1} depending on soil type.

The final term to be calculated is N_{le}. As N leaching is a natural process, and always occurs even in pristine conditions, an acceptable N leaching $N_{le(acc)}$ is defined as the rate observed in similar ecosystems in pristine environments. Recommended values (UBA, 1996) range from 0.5 to 4 kg N ha^{-1} y^{-1}: the UK uses 6 kg N ha^{-1} y^{-1}.

2.2.2 Nitrogen mass balance methods used by the UK

The UK uses a simplified mass balance equation for the nutrient nitrogen critical load $CL_{nut}N$:

$$CL_{nut}N = N_u + N_i + N_{le(acc)} + N_{de} \quad (2)$$

where
- N_u is nitrogen uptake;
- N_i is nitrogen immobilisation;
- $N_{le(acc)}$ is the acceptable level of nitrogen leaching;
- N_{de} is denitrification.

For both woodland ecosystems, N_u is set at 7 kg N ha^{-1} y^{-1}, and $N_{le(acc)}$ at 6 kg N ha^{-1} y^{-1}. The value of N_i is either 1 or 3 kg N ha^{-1} y^{-1} depending on soil type, and likewise the value of N_{de} is 1, 2 or 4 kg N ha^{-1} y^{-1} depending on soil type. The lower of the empirical and mass balance N critical loads is the value mapped. As the empirical critical load for coniferous woodlands is inevitably lower than the mass balance, this is the value mapped (hence all coniferous woodlands have the same $CL_{nut}N$ value of 13 kg N ha^{-1} y^{-1} in the UK). For deciduous woodlands, the UK maps show a mixture of empirical and mass balance values.

2.2.3 Uncertainties in mass balance N critical loads

Clearly, with much uncertainty over individual terms in equations (1) and (2), the overall result will also be uncertain. The method has been parameterised with nitrogen-limited northern coniferous forests in mind: N_{le} for instance has a low value, not because of any deleterious effects of N leaching in the receiving water, but because natural northern forests cycle N very tightly. A higher value for N_{le} would be ecologically acceptable for more nitrophilous systems. Immobilisation is currently capable of absorbing more N in most current systems than the default values indicate: the N_i parameter is adjusted to what might be the long-term sustainable value. It follows that the mass balance method does not necessarily represent the present response of ecosystems, most of which can probably immobilise more N without deleterious effects. Only dynamic modelling can estimate when deleterious effects might start to appear. The UK has clearly made choices for models and parameters, which in some cases lie outside the recommended ranges. This reflects expert knowledge of UK ecosystems, but is also an indication of uncertainty.

2.3 Empirical Critical Loads for Acidity: Soils

The other nodes on the Critical Load Function are calculated using different models for the various ecosystems. The models for calculating acidity critical loads are therefore described first, followed by a description of their application to the Critical Load Function for the different ecosystems in Sections 2.9 to 2.11. The empirical critical load for soils for the UK was the first to be calculated.

2.3.1 Empirical critical loads for acidity for soils: theoretical background

The empirical method of calculating critical loads for forest soils was originally developed at the Skokloster Workshop (Nilsson and Grennfelt, 1988). It is based on assignments of mineral weathering rates to various soil-forming minerals, as mineral weathering is the principal process opposing acidification in terrestrial ecosystems. These weathering rates are then modified by site factors, such as slope, soil depth and drainage. The method was modified for use in the UK by Hornung *et al.* (1995); the original mineral classifications being changed considerably to take UK conditions into account, especially in relation to lowland clay soils. Soil characteristics were obtained from soil maps and in underlying databases at the Soil Survey of England and Wales and the Macaulay Land Use Research Institute in Scotland. Results are mapped in classes, which are intended to give some indication of the uncertainties involved. Class intervals were (in keq ha^{-1} y^{-1}): <0.2; 0.2-0.5; 0.5-1.0; 1.0-2.0; and >2.0. These class intervals were chosen under pressure at the Skokloster Conference (Cresser, 2000), but they have stood the test of time and are widely used. The result (Hornung *et al.* 1995) is an intuitively satisfying map (of course it may be intuitively satisfying because it is based partly on intuition). Nevertheless, the sensitive areas are where they might be expected to be, in the uplands of the north and west, and on base poor sandstones in the south.

The UK introduced another innovation: critical loads for peat soils. The Skokloster method cannot be applied to these, as they have essentially no weatherable minerals. Cresser and his colleagues (Skiba and Cresser, 1989; Smith *et al.* 1993) devised a method which is based on laboratory experiments with small peat pellets. From the results of these experiments, and a large number of assumptions, they were able to calculate the acid load required to reduce peat in the field by an arbitrary 0.2 pH units. The procedure

was criticised by Skeffington *et al.* (1995) and Wilson *et al.* (1995) on the basis of their own experiments with peat, but they have yet to come up with a viable alternative. Jenkins and Reynolds (2000) discuss some of the problems, but in the meantime the empirical critical load method devised by Cresser and colleagues is used for UK peats.

2.3.2 Uncertainties in empirical acidity critical loads

The empirical soils method has an element of arbitrariness about it, and depends on expert knowledge of the mineralogy of UK soils. This is particularly so in England and Wales, where mapped soil series do not necessarily have the same mineralogy everywhere. The modifying factors are also essentially arbitrary. Setting the critical load equal essentially to the weathering rate implies that it is acceptable for already acidified soils to remain acidified. The fact that the results are reported in classes causes some difficulties. Similar soils may differ in calculated critical load by a factor of 2 or more, if one is judged to be on one side of a class boundary and the other on the other. Deciding how to represent the class for modelling purposes (e.g. for calculating exceedence) introduces another arbitrary choice. Should it be the lower bound (precautionary), the central value (moderation) or the upper bound (conservative)? Such considerations led to the mass balance approaches, which are referred to within UNECE as “Level 1” approaches, as opposed to the disparaging epithet “Level 0” applied to the empirical method.

2.4 Mass Balance Critical Loads for Acidity: Soils

2.4.1 Theoretical background to soil mass balance methods

The aim of the acidity mass balance methods is similar to that of the N mass balance: to calculate all the significant inputs and outputs of acidity, and to link the results to some chemical criterion of "harm" to enable a critical load to be calculated. The mass balance for S is considered to be:

$$S_{le} = S_{dep} - S_{ad} - S_u - S_i - S_{re} - S_{pr} \quad (3)$$

where the subscripts represent:

le	leaching
dep	deposition
ad	adsorption (typically onto sesquioxides or similar soil minerals)
u	uptake (into plants)
i	immobilisation
re	reduction
pr	precipitation (i.e. as a chemical compound)

For forest soils, uptake, immobilisation, precipitation and reduction of S are considered to be insignificant. Some of this is arguable: S uptake is perhaps 10% of base cation uptake, and soils which are sufficiently anaerobic to reduce S, are not uncommon in the landscape as a whole. Sulphate adsorption is an admittedly significant process, but because soils are considered to have a finite capacity, it too is ignored, since the system is assumed to be in steady state. All S leaching is assumed to be SO_4^{2-} (not too unreasonably). Hence the S mass balance reduces simply to:

$$SO_4^{2-}{}_{le} = S_{dep} \quad (4)$$

A consequence of these assumptions is that the S mass balance does not necessarily represent the behaviour of catchments at the present time. It is very much a worst case, and in the short term (which may be several centuries for strongly sulphate-adsorbing soils) SO_4^{2-} leaching could be very much less than deposition.

Having obtained mass balances for S and N, these are linked to a definition of "harm" by considering the leaching of Acid Neutralising Capacity (ANC), which requires a mass balance of all the other significant ions in the system. This yields:

$$BC_{le} + NH_4^+{}_{le} - SO_4^{2-}{}_{le} - NO_3^-{}_{le} - Cl^-{}_{le} = ANC_{le} \quad (5)$$

where:

BC	base cations ($Na^+ + K^+ + Ca^{2+} + Mg^{2+}$)
le	leaching
ANC	Acid Neutralising Capacity.

All fluxes are expressed in equivalence units e.g. keq ha^{-1} y^{-1}.

The mass balances expressed by equations (1), (3) and (4) can be combined with other assumptions to generate the basic mass balance equation (see Posch et al., 1995). These assumptions are: (1) chloride inputs equal chloride outputs; (2) base cation sources (deposition and weathering) equal base cation sinks (leaching and uptake); and (3) all leaching from terrestrial catchments is in the form of NO_3^-. Substitution then gives:

$$S_{dep} + N_{dep} - BC_{dep} + Cl^-{}_{dep} = BC_w - BC_u + N_i + N_u + N_{de} - ANC_{le} \quad (6)$$

where the symbols represent:

BC	base cations ($Na^+ + K^+ + Ca^{2+} + Mg^{2+}$)
ANC	Acid Neutralising Capacity
dep	deposition
le	leaching
w	weathering (i.e. release of base cations from soil minerals)
u	uptake into plants
i	immobilisation in soil organic matter
de	denitrification.

It is customary to use "non-marine" deposition fluxes in these calculations (symbolised by *). This makes little difference to the mass balance, as marine ($S_{dep} + Cl^-{}_{dep}$) ≈ marine BC_{dep}. This is the Simple Mass Balance Equation (SMB), so called because it is recognised that there are a number of simplifying assumptions. It is also known as the Steady State Mass Balance Equation (SSMB). Critical loads for S and N can be derived from this equation, given that values are assigned to all the other parameters and an "acceptable" value of ANC_{le} is defined.

There are several ways of calculating an acceptable ANC_{le}, but by far the most widely-used is the critical base cation : aluminium ratio. This states that the ratio of ($K^+ + Ca^{2+} + Mg^{2+}$) to Al in the soil solution should not exceed a certain value (usually 1). This criterion is derived from work on toxicity of Al^{3+} to tree roots, showing that Ca^{2+} (and with rather less certainty Mg^{2+} and K^+) exerts some protection against Al toxicity (see

Sverdrup and Warfvinge 1993). Sodium is considered to offer no protection, the three protective base cations ($K^+ + Ca^{2+} + Mg^{2+}$) being abbreviated to *Bc*. This ratio is discussed further in Section 5.1.

To calculate the critical ANC leaching, use is made of another (equivalent) formulation of ANC:

$$ANC_{le} = - Al_{le} - H_{le} = -Q\,([Al_{le}] + [H_{le}]) \qquad (7)$$

where quantities in square brackets are concentrations as opposed to fluxes, and Q is the effective precipitation (precipitation - evaporation). Base cation concentrations are calculated from the base cation mass balance, and application of the required Bc/Al ratio gives the Al term in equation (7) directly. The H^+ term has to be calculated by assuming equilibrium with aluminium hydroxide (Gibbsite). Different apparent equilibrium constants for Gibbsite are given in the Mapping Manual (UBA 1996) depending on the organic matter content of the soil. The critical load for S deposition alone ($CL_{max}S$ - see Section 2.9) can then be calculated by assuming that the N sink terms in equation (6) can account for all N deposition, and hence the S critical load is:

$$CL_{max}(S) = BC^*_{dep} - Cl^*_{dep} + BC_w - BC_u + \left(1.5 \times \frac{Bc_{dep} + Bc_w - Bc_u}{(Bc/Al)_{crit}}\right)$$
$$+ Q^{2/3} \times \left(1.5 \times \frac{Bc_{dep} + Bc_w - Bc_u}{(Bc/Al)_{crit} \times K_{gibb}}\right)^{1/3} \qquad (8)$$

where *BC* is the flux of base cations ($Na^+ + K^+ + Ca^{2+} + Mg^{2+}$), and the suffices represent:
dep deposition
w weathering (i.e. the release of base cations from soil minerals or rock minerals)
u uptake by plants into perennial tissues;
* represents non-marine;
Bc (as distinct from *BC*) is the flux of base cations other than Na;
$(Bc/Al)_{crit}$ is the critical base cation/Al ratio defined by the user;
Q is effective rainfall/runoff;
K_{Gibb} is the Gibbsite coefficient, expressing the ratio between Al and H^+ concentrations in the soil solution.
All fluxes are expressed in equivalence units e.g. keq ha^{-1} y^{-1} or meq m^{-2} y^{-1}.

The *Bc* fluxes must be total and not non-marine, as plants cannot distinguish between marine- and non-marine-derived cations. This makes a large difference to calculated critical loads in countries, which have a heavy sea-salt deposition, like the UK.

2.4.2 Soil mass balance methods used by the UK

In the UK, a variant of equation (8) is used in which the *Bc* terms represent only Ca^{2+}, rather than $K^+ + Ca^{2+} + Mg^{2+}$. If all three base cations are used then the critical loads calculated for the UK are high, largely because the deposition of marine Mg^{2+} elevates the numerator of the equation. There is then little exceedence even in areas known to be sensitive to acidification (Reynolds, 2000), and this was deemed unacceptable. As an example, Reynolds (2000) calculated critical loads from 20 forest sites in Wales. At all

sites, acid deposition exceeded the empirical critical loads for acidity, which were in the range 0.2-0.5 keq ha^{-1} y^{-1}. *No* sites were exceeded if critical loads were calculated with the SSMB equation with Sitka spruce as the biological target (BC/Al=0.4); critical loads were in the range 2.3-9.8 keq ha^{-1} y^{-1}. Critical loads were directly proportional to sea-salt deposition, with r^2 of 0.97. This may however reflect biological reality: as pointed out earlier (Skeffington 1999), the SSMB is calculating whether the growth of some target plant (e.g. Norway spruce) will be affected in the long term, not a generalised sensitivity to acidification. The evidence that these areas are sensitive derives mostly from effects on freshwaters. It may well be correct that they can continue to grow Norway spruce at high acid deposition levels. Roberts *et al*. (1989) showed that Type I Norway spruce decline as seen in Germany could never occur in the UK, because of the supply of marine magnesium. The UK claims that the use of a Ca^{2+}: Al ratio is better founded than the Bc:Al ratio, which is true, though the Bc:Al ratio is better supported than many other parameters in the chain of critical load calculation, and other countries continue to use it.

The UK also introduces another minor modification left over from an earlier version of the SSMB equation. There is a minimum calcium concentration of 2 μeq l^{-1} in the soil solution, and this value, converted into a flux, is subtracted from the numerators of the expressions involving *Bc*.

The mass balance critical load maps for the terrestrial ecosystems look rather different to the empirical map (Hall *et al.* 2001a). There is a trend for Western areas to be less sensitive, particularly obvious in the Lake District and the Scottish Highlands. On the other hand, the large sensitive area south-west of London becomes less sensitive on the mass balance maps.

2.4.3 Uncertainties in the soil mass balance equations

The number of parameters in the SSMB equation tends to increase uncertainty. Hall *et al.* (2001b) conducted a sensitivity analysis of the Ca : Al ratio and K_{gibb} parameters (see Section 3.2 below) and found wide variations induced by the possible ranges of values. They also tested different critical limits, with similar results.

Measurement of weathering rates is problematic. The UK uses values in the SSMB model derived in the same way as for the empirical method. Other countries use the PROFILE model (Warfvinge and Sverdrup (1992). After a study of weathering rate calculation by PROFILE, Hodson *et al.* (1997) estimated the uncertainty range as ±250%.

Base cation uptake is not only difficult to estimate on a country-wide basis, it is not clear whether it should be included at all. A natural ecosystem will tend to recycle its base cations *in situ*. A natural forest, for example, will take up cations from the soil as the trees grow, but these will be returned to the soil when the trees die and decay. Cations are only removed from the system when the trees are harvested by man. It seems reasonable to assume that foresters will grow their tree crop in a sustainable fashion, or to require that they do so, by replacing those base cations that they remove in the harvested timber just as farmers use fertilisers to replace nutrients used by crops. If this view is accepted, the BC_u parameter should not be included in equation (8). This would increase critical loads substantially in many areas.

2.5 Critical Loads for Freshwaters: Steady State Water Chemistry Method

There are three methods in use for determining critical loads for freshwaters. For submissions to DEFRA and CCE, the UK National Focal Centre at Monks Wood uses the most recent: the First Order Acid Balance, or FAB Model. However, FAB is based on the older Steady State Water Chemistry (SSWC) Model, as is the other model used in the UK, the Diatom Model. The Forestry Commission still use the SSWC model in their regulatory work. It is clearer therefore to describe the models in the order which they were developed. Discussion of uncertainties is left until all three models have been described (Section 2.7.3).

2.5.1 The SSWC Model: theoretical background

The Steady State Water Chemistry Method (UBA, 1996) is based on the idea that catchments should be able to supply enough base cations to maintain the acid neutralising capacity (ANC) of a lake at a given criterion value. The most common criterion value is 20 μeq l^{-1}, though the UK currently uses zero. Since ANC can be approximately defined as:

$$[ANC] = [*BC] - [*SO_4^{2-}] - [NO_3^-] \quad (9)$$

where brackets denote concentrations in μeq l^{-1}, then if a critical ANC (ANC_{crit}) is chosen, the allowable SO_4^{2-} and NO_3^- concentrations will be:

$$[*SO_4^{2-}]_{crit} + [NO_3^-]_{crit} = [*BC]_0 - [ANC]_{crit} \quad (10)$$

where $[*BC]_0$ is the concentration of non-marine base cations in a given lake under pristine conditions. The problem is then to estimate $[*BC]_0$. The SSWC Method uses the current non-marine base cation concentration $[*BC]_t$ as an estimator. It is recognised, however, that $[*BC]_t$ usually incorporates base cations leached from the soil ion exchange complex by acid deposition. These elements have therefore to be subtracted from $[*BC]_t$ to obtain $[*BC]_0$. The relationship between changes in SO_4^{2-} + NO_3^- and non-marine base cations in surface waters is expressed by the F-factor:

$$F = \Delta [*BC] / \Delta ([*SO_4^{2-}] + [NO_3^-]) \quad (11)$$

F is estimated by an empirical relationship with current base cation concentrations observed in Norwegian lakes (Brakke *et al*., 1990). If the pristine sulphate concentration $[*SO_4^{2-}]_0$ in a lake is known, the pristine base cation concentration $[*BC]_0$ can therefore be calculated. $[*SO_4^{2-}]_0$ is estimated by yet another empirical relationship observed in Norwegian lakes, in areas unaffected by acid deposition:

$$[*SO_4^{2-}]_0 = 15 + 0.16\,[*BC]_t \quad (12)$$

$[*BC]_0$ can now be calculated as:

$$[*BC]_0 = [*BC]_t - F \times ([*SO_4^{2-}]_t + [NO_3^-]_t - [*SO_4^{2-}]_0 - [NO_3^-]_0) \quad (13)$$

The critical $SO_4^{2-} + NO_3^-$ concentration can now be calculated from equation (10). The critical load for S and N can be obtained by multiplying by the runoff, Q.

$$(*S + N)_{crit} = Q([*BC]_0 - [ANC]_{crit}) \quad (14)$$

Henriksen *et al*. (1995) give this as the critical load for acidity. The Mapping Manual (UBA, 1996) however, gives:

$$CL(Ac) = Q\ ([*BC]_0 - [ANC]_{crit}) - *BC_{dep} + BC_u \quad (15)$$

The inclusion of the terms for deposition and uptake allows the critical load to be independent of current base cation deposition. The equation is often quoted without the base cation uptake term, which in any case applies only to managed forests. Though it appears counter-intuitive that base cation deposition should reduce the critical load, equation (15) recognises that base cation deposition also contributed to the pristine base cation concentration $[BC_0]$. In calculating exceedence with equation (15), base cation deposition needs to be added back. In many Scandinavian catchments virtually all the incoming S passes through the catchment, whereas most of the incoming N is adsorbed. N can thus be accounted for approximately by assuming the present catchment uptake is constant in time, and defining a parameter N_{leach} operationally as the measured inorganic N concentration in runoff, and conceptually as N deposition minus all the N sinks in the catchment. Critical load *exceedence* then becomes:

$$Ex(Ac) = *S_{dep} + N_{leach} - BC*_{dep} - CL(Ac) \quad (16)$$

To make the method even more involved, a variable ANC_{crit} value is now used in Norway and Sweden. The rationale for this (Henriksen *et al*., 1995) is that in areas of low acid deposition the probability of acid episodes leading to fish kills is lower and thus a low ANC_{crit} can be accepted. In areas subject to high acid deposition a higher ANC_{crit} is needed to protect against acid episodes. The ANC_{crit} is now set to zero in areas of zero deposition, increasing linearly to 50 μeq l^{-1} at acid depositions of 0.2 keq ha^{-1} y^{-1} or greater. This will make the critical loads even lower than the standard ANC_{crit}= 20 μeq l^{-1} for all areas where acid deposition is greater than 80 meq m^{-2} y^{-1}. The choice of values for this function appears to be completely arbitrary. In spite of being made dependent on deposition, the ANC_{crit} is then treated as characteristic of the lake once set, i.e. it does not change even if deposition changes. The logic of this is hard to understand.

2.5.2 Use of the SSWC in the UK

The SSWC is still used for research purposes in the UK (e.g. White *et al.* 2000) and for regulatory purposes by the Forestry Commission (Nisbet, 2001). Exceedence of the SSWC critical load by 1986-8 sulphur deposition is used as a screening technique to identify sensitive areas. Planting proposals in those areas have to be accompanied by a more detailed assessment, which is based on a water sample at high flow and the use of equation (14). Currently there are proposals (Nisbet, pers. comm.) to use more up-to-date (1995-7) deposition data for assessment, and to consider nitrate as well as sulphate in calculating the critical load exceedence (i.e. to use equation (16)). There are no plans to use the FAB Model at present.

2.6 Critical Loads for Freshwaters: the Diatom Model

2.6.1 Diatom model: theoretical background

The Diatom Method is a variant of the SSWC Method, which uses changes in diatom populations, rather than a critical ANC, as the criterion response. The species composition history of diatom populations in lakes, which is strongly affected by water chemistry, can be inferred from palaeolimnological studies of sediment cores (e.g. Battarbee *et al*., 1996). Whether a lake has acidified or not can thus be judged by examining sediment cores. Battarbee *et al*. (1996) found that acidified and non-acidified lakes can be separated optimally by a relationship between current lake Ca concentration and current S deposition :

$$[Ca] = 94 \times {}^{*}S_{dep} \qquad (17)$$

where $[Ca]$ is expressed in μeq l^{-1} and ${}^{*}S_{dep}$ in keq ha^{-1} y^{-1}. Calcium concentration can be taken as a measure of the neutralising power of the catchment, and hence this relationship could be used to set a critical load. However, acid deposition has probably increased the [Ca] currently found in lakes. As a rough approximation of the original neutralising power of the catchment, the original Ca concentration of the lake $[Ca^{2+}]^{*}_{0}$ is estimated in the same way as in the SSWC Method, replacing $^{*}BC$ with $^{*}Ca^{2+}$ as appropriate. A critical load for S can then be calculated from equation (17). The method has been adapted to produce a critical load for acidity in a similar way to the SSWC Method, by assuming that the current N sinks in the catchment are stable, and that the catchment adsorbs no S, so that the fraction of nitrogen deposition contributing to acidification a_N is:

$$a_N = ({}^{*}S_{dep} / N_{dep}) / ({}^{*}[SO_4^{2-}]_t / [NO_3^{-}]_t) \qquad (18)$$

If the model is recalibrated using this equation, the Ca:deposition ratio reduces slightly, to 89:1, leaving the critical load for acidity as:

$$CL(A) = [{}^{*}Ca^{2+}]_0 / 89 \qquad (19)$$

where the critical load is expressed in keq ha^{-1} y^{-1}, and $[{}^{*}Ca^{2+}]_0$ in μeq l^{-1}.

Exceedence is defined as:

$$CL(A)_{ex} = CL(A) - {}^{*}S_{dep} - a_N N_{dep} \qquad (20)$$

2.6.2 Use of the Diatom Model in the UK

The Diatom Model is used primarily for research purposes, e.g. Kernan *et al.* (2001) and Ulyett *et al.* (2001) used it to calculate critical loads for comparison with catchment characteristics. The parameterisation of the model has not altered since Battarbee *et al.* (1996).

2.7 Critical Loads for Freshwaters: the FAB Model

The First Order Acid Balance (FAB) Model is the method of choice for calculating critical loads in the UK and continental Europe, partly because it is the only one which can be used to generate the critical loads function as it treats S and N independently. Apart from critical loads, it can also be used to predict future sulphate and nitrate concentrations in surface waters.

2.7.1 The FAB Model: theoretical background

The FAB Method is the aquatic analogue of the SSMB Method, in which an attempt is made to take into account in-lake processes, which can be very effective in producing alkalinity. As with the SSMB method, a combination of charge balance and mass balance equations leads to:

$$*S_{dep} + N_{dep} = fN_u + (1 - r)(N_i + N_{de}) + rN_{ret} + rS_{ret} + *BC_{le} - ANC_{le} \qquad (21)$$

where:

dep	deposition (all fluxes in acid equivalents ha^{-1} y^{-1})
f	fraction of catchment area which is forested
N_u	N uptake into forest trees
r	fraction of catchment area occupied by lakes
N_i	N immobilisation in soil organic matter
N_{de}	denitrification in the catchment soils
N_{ret}	in-lake retention of N
S_{ret}	in-lake retention of S
BC_{le}	leaching of base cations ($Na^+ + K^+ + Ca^{2+} + Mg^{2+}$)
ANC_{le}	Acid Neutralising Capacity leaching.

Equation (21) differs from that in the Mapping Manual (UBA, 1996) in having non-marine rather than total $*S_{dep}$ and $*BC_{le}$, but equation (21) is the correct formulation (Reynolds and Skeffington 1999). It is not clear whether this is universally appreciated.

The soil parameters (N uptake and immobilisation, and denitrification) are estimated as for the SSMB Model (Section 2.3). Note however that N uptake is only counted if it goes into forest biomass, as it will then be harvested and removed from the system instead of recycled *in situ*. Immobilisation and denitrification are scaled to the land surface area.

The parameters rN_{ret} and rS_{ret} model N and S retention by lakes in the catchment. Lakes are powerful generators of alkalinity which can not be ignored when acidification effects are being considered. The principal processes are S and N reduction in the lake sediments, and the rates of these two processes are estimated as follows. In-lake retention of N is assumed to be proportional to the net input of N i.e. N deposition less immobilisation, uptake and denitrification:

$$rN_{ret} = \rho_N(N_{dep} - fN_u - (1-r)(N_i + N_{de})) \qquad (22)$$

where the factor ρ_N is modelled by a kinetic equation derived from work on lakes in Norway and sub-arctic Canada:

$$\rho_N = S_N / (S_N + (Q / r)) \quad (23)$$

The factor S_N is a mass transfer coefficient for N with units of velocity (m y^{-1}).

Sulphur retention is treated in an exactly analogous way:

$$rS_{ret} = \rho_S S_{dep} \quad (24)$$

where the factor ρ_S is modelled by a kinetic equation based on the same lakes:

$$\rho_S = S_S / (S_S + (Q / r)) \quad (25)$$

where the factor S_S is a mass transfer coefficient for S with units of velocity.

The parameters $*BC_{le}$ - ANC_{le} are modelled using exactly the same methods as for the SSWC Model (equations 10-14).

The FAB critical load equation then becomes:

$$a_N CL(N) + a_S CL(S) = b_1 N_u + b_2 N_i + Q ([*BC]_0 - [ANC]_{crit}) \quad (26)$$

equivalent to:

$$a_N CL(N) + a_S CL(S) = b_1 N_u + b_2 N_i + L_{crit} \quad (27)$$

where the coefficients are dimensionless and depend on lake and catchment properties alone:

$$a_N = (1-f_{de}(1-r))(1-\rho_N)$$
$$a_S = 1-\rho_S$$
$$b_1 = f(1-f_{de})(1-\rho_N)$$
$$b_2 = (1-f_{de})(1-r)(1-\rho_N)$$

where ρ_N and ρ_S are defined in equations (23) and (25), and f_{de} is the denitrification fraction, and L_{crit} is the critical leaching, defined as $Q([*BC]_0 - [ANC]_{crit})$. If deriving these expressions, note that the denitrification fraction is calculated differently for forested and non-forested land.

2.7.2 Use of the FAB Model in the UK

The use and parameterisation of FAB in the UK is described by Curtis *et al.* (1998, 2000). As always, the model has been adapted for British conditions. N uptake is parameterised as a single value of 0.279 keq ha^{-1} y^{-1}: unlike the value for terrestrial woodland systems it was not increased to 0.5 keq ha^{-1} y^{-1} for 2001. Only coniferous forest uptake of N is counted when calculating freshwater critical loads. Deciduous forest is discounted on the grounds that it is not likely to be harvested (hence removing N from the system), and other ecosystems are not considered at all. This is also inconsistent with the methods for terrestrial ecosystems which all include parameterisation of N uptake.

Nitrogen immobilisation and denitrification are parameterised as for the terrestrial ecosystems, i.e. as fixed values dependent on soil type. The Mapping Manual (UBA, 1996) suggests that denitrification should be proportional to deposition (as in the coefficients of equation (27)) and that the fraction of net N deposition (deposition after removal by other sink processes) which is denitrified (f_{de}) should be:

$$f_{de} = 0.1 + 0.7 f_{peat} \quad (28)$$

where f_{peat} is the fraction of peat soils in the catchment. However it was considered that this would lead to unrealistically high N removal rates for British upland conditions, up to 30 kg N ha^{-1} y^{-1} as opposed to the 1 – 4 kg N ha^{-1} y^{-1} actually used. As yet unpublished results from a subsequent research project (the CLAM Project) are said to confirm the lower values.

Default values are used for the in-lake retention parameters. The UK critical loads are estimated from a single water sample taken, in the autumn or spring of 1992-4, from what was considered to be the most sensitive lake in each 10 km grid square (20 km grid square in lowland areas). If no lake was available, a first-order stream was used. The in-lake retention parameters were set to zero if the sample was taken from a stream, although whether this should be so is another topic which is currently being researched.

In the UK, ANC_{crit} is set to zero, though there are proposals to make it +20 μeq l^{-1}. This would bring the UK into line with some other countries in Europe, but would produce unrealistic critical loads for a proportion of lakes. The current freshwater critical load maps produced by the UK contain some errors in that some waters in the South and Midlands have very low critical loads. These are usually lowland waters with an indigenous source of sulphate, which should have been eliminated from the dataset, but were not owing to an oversight.

2.7.3 Uncertainties in freshwater critical load methods

All three water methods are related, and all are highly empirical. All require the estimation of the pre-industrial base cation concentration through a chain of empirical equations which are validated with data from the Nordic countries. Where the physical environment differs from that in these countries, the empirical relationships are likely to be different. Indeed, R. Harriman (pers. communication) has long considered that equation (12) exaggerates pre-industrial sulphate concentrations in the UK, and uses $[^*SO_4^{2-}]_0 = 7 + 0.05\ [^*BC]_t$ instead on the basis of measurements in Scottish lochs in relatively pristine areas. Kämäri *et al.* (1993) performed an uncertainty analysis on the SSWC Model for lakes in Finland, using Monte Carlo methods. This suggested an overall standard deviation on the critical load of ±10%. There is also some as yet unpublished work in Norway on uncertainties in the SSWC Model.

The assumption that the F-factor (equation (11)) is a constant is not consistent with current biogeochemical knowledge: it should change with the acidification state of the soil. Henriksen (1995) evaluated the effect of changing F on critical load *exceedence*. The effect was small in Norway, reflecting the sensitivity of Norwegian lakes, but larger in Sweden and Finland. For instance, substituting F = 0 in equation (11) reduced exceedence from 29.7% in Norwegian lakes to 27.2%, but from 29.6% to 16.4% of Swedish lakes.

The Diatom Model has the same uncertainties as the SSWC Model except for the uncertainty involved in defining the ANC limit. This is a major advantage of the Diatom Model: there is no constraint to a fixed ANC, and thus some of the individual characteristics of lakes are in theory taken into account. However, it uses an additional empirical relationship, between S deposition and [Ca], which may not be applicable outside the UK and which may alter with time. Use of the pristine calcium concentration in equation (19) is precautionary, as the point at which acidification is initiated will lie somewhere between $[*Ca^{2+}]_0$ and current $[Ca^{2+}]$.

The FAB Model has the same uncertainties as the SSWC Model and a number of others. Curtis *et al.* (2000) discuss some of them. The fraction of the catchment which is forested has to be identified from satellite photographs or other data. Estimates of N uptake, immobilisation and denitrification have to be provided, usually from default values. Deposition and runoff data have to be interpolated onto a catchment area from grid-based model outputs, which are themselves uncertain. The in-lake retention parameters are based on data from sub-arctic regions with lower temperatures and hence slower reaction rates than those found in the UK. Rivers are given zero S and N retention, which in many cases will ignore a significant process. There is also some uncertainty about how to calculate the critical loads function (Sections 2.10 and 2.11).

2.8 Application of Dynamic Models

Dynamic models are not routinely being used to calculate critical loads, although there is a lot of ongoing work on dynamic modelling in this context both in the UK and in Europe. However dynamic models have the potential to be very useful for regulatory purposes. In some senses they are more complex than the steady-state models, but they avoid some of the uncertainties inherent in the latter. Jenkins and Reynolds (2000) have recently reviewed dynamic models for the assessment of acidification for the Environment Agency, and there would be little point in repeating that work here. Their report contains a description of the MAGIC Model and a review of some of the uncertainty and validation studies which have been applied to it. There are shorter descriptions of the SMART and SAFE models. These three models are those likely to be used for dynamic modelling in UK and European applications. This section therefore concentrates on a review of current thinking of how dynamic models might be *applied* in a regulatory context.

2.8.1 Advantages of dynamic models

The characteristic of dynamic models is that they calculate the values of environmental variables as a function of *time*. These variables may be chemical values familiar from the critical loads methods, such as ANC or Bc : Al ratio. They could also be used to generate more detailed chemistry, which could be used as input to biological response models. An example might be the use of Al, Ca and pH to predict fish status, or ion exchange models to predict plant growth, as discussed by Jenkins and Reynolds (2000). Though the biological response models introduce additional uncertainty, they focus attention on the ultimate target, the part of the system that public and policymakers are really interested in. The calculation of ANC is of interest to chemists, but the aim of policy is to protect aquatic organisms.

As discussed below, dynamic models are easier to validate against measurement data than steady state critical load models, because they make predictions which should be true at a certain time. Steady state critical load models are predicting an equilibrium state which may occur at some future time, possibly centuries hence. Dynamic models can make predictions, which come within the time horizon of current policymakers (although the actions necessary to achieve environmental targets within a few years may come as something of a shock).

In a cost-benefit framework, dynamic models (calculating environmental benefits) interface better with economic models (calculating costs). Economic models are typically dynamic, at least in the sense that future expenditure is discounted. Schmieman and Van Ierland (1999) provide an example of linked dynamic environmental and economic models, which came to the conclusion that the critical loads approach had provided a sub-optimal solution to the same problem.

Dynamic models escape the uncertainties associated with the damage threshold concept which underlies critical loads. Critical loads as calculated are not really thresholds (Skeffington, 1999) nor do such unequivocal thresholds really exist in the natural environment. The use of dynamic models can obviate the need to define thresholds, and concentrate attention instead on the response over time of chemical and biological entities. The addition of the time dimension adds another choice for the policymaker. This choice may be unwelcome, but gives further scope for balancing costs and benefits.

2.8.2 Developments in dynamic modelling

Dynamic modelling has been discussed for a long time, but it is now really making progress. There are several reasons for this. Firstly, the technology is becoming available. Computing power continues to increase, and GIS systems are able to transform and process these data and present the results in the form of maps. Secondly, models (e.g. deposition models) are becoming more sophisticated and can produce outputs on a finer scale, and environmental data can be obtained on national and European scales. Thirdly, the infrastructure has already been developed under UNECE, and in national critical loads programmes. The people who have developed and run these programmes can apply their experience to dynamic modelling.

The UNECE Working Group on Effects has set up a Joint Expert Group on dynamic modelling, which met in October 2000 and November 2001 in Ystad, Sweden. The location is not entirely insignificant, because the meetings were organised and funded by the Swedish International and National Abatement Strategies for Transboundary Air Pollution (ASTA) Programme, which is headed by Jan Nilsson, original promoter of the critical load concept. The two meeting reports show that real progress is being made. The EU is funding the RECOVER:2010 programme, which is currently modelling the response of sensitive waters to reductions of acid deposition in seven European countries, including the UK. Four countries now have fine-scale regional dynamic assessments of the response of soil to deposition reductions. Dynamic models are being applied to soils in a subset of the EU/UNECE forest plots. CCE have prepared a draft Dynamic Modelling Manual analogous to the Mapping Manual. The USA and Canada are both developing regional dynamic assessments. The intention is to use dynamic

models in the reviews of the Gothenburg Protocol and the Emission Ceilings Directive in the middle of the decade, and the structures for doing this are being prepared.

Dynamic model applications to single sites are well established, and a lot of the effort within UNECE is being devoted to the problems of applying them on a wider (European) scale. In particular, thought is being given to applying them within the existing structure of integrated assessment models (Posch and Hettelingh 2001). Dynamic models are too complex and data-demanding to be run *within* the structure of the RAINS Model, which claims to produce cost-optimised solutions to controlling emissions in Europe. It is possible that simplified versions could be used within RAINS, as happened with the EMEP ozone model, though it is not certain that simplified versions of the dynamic models, which capture the essentials of their behaviour are in fact possible. More realistically, dynamic models could be run to determine target loads, e.g. the maximum deposition which would allow the attainment of a certain environmental goal (e.g. ANC concentration) within a given time. These target loads could be fitted into the existing integrated assessment framework. Another possibility is described by Posch and Hettelingh (2001) as "recovery isolines", which show recovery times as a function of deposition reduction and year of implementation. These could be pre-run and used within a probabilistic optimisation framework as with the Gothenburg Protocol. (There is clearly something wrong with this diagram, which implies that emission reductions in certain years would lead to recovery before the reductions were implemented).

Treatment of dynamic models within the UK has no need to be so elaborate. A start has already been made on the use of dynamic models to predict acidification status on a broad scale. Jenkins *et al.* (1997) and Jenkins and Cullen (2001) applied MAGIC to data from some of the 22 sites in the UK Acid Waters Monitoring Network. The earlier study modelled the effect of the Second Sulphur Protocol to the year 2041. The later study used fewer sites but had the benefit of more data for calibration and a version of MAGIC with improved N dynamics. It modelled the effect of the Gothenburg Protocol up to 2020. In both cases most sites showed some recovery in ANC, though not always to the UK criterion value of 0 μeq l^{-1}. Up to 2020, best-case and worse-case assumptions about nitrate made only minor differences to ANC predictions. Comparing FAB predictions (Curtis *et al.* 1998) from the same sites, however, indicated that increasing nitrate leaching could make a very large difference indeed to ANC concentrations. This study illustrates some of the value to be obtained from dynamic modelling: it indicates a general pattern of behaviour of sensitive sites, can generate uncertainty bands, and points to research directions.

Another style of modelling is to run dynamic models in probabilistic mode. For a regional application, input variables are randomly sampled from defined frequency distributions based on observed data for the region as a whole. Models are run many times, Monte-Carlo fashion, and outputs are in the form of statistical distributions of parameters for the region as a whole. This approach sacrifices locational information about sites *within* the region, but enables statistical statements to be made about the region as a whole. The approach is compatible with targets such as "90% of lakes within this region should have ANC> 20 μeq l^{-1} by the year 2020". An example from the UK is a regional model for Wales, which was used by Sefton and Jenkins (1998) to show that an 80-85% reduction in deposition (based on 1990) would be necessary if 95% of acid-sensitive Welsh waters were to achieve ANC > 0 μeq l^{-1} by the year 2030.

A heroic attempt at modelling individual sites on a wide scale was that of Evans *et al.* (1998), who applied MAGIC to 1027 sites in Great Britain using water quality data derived from the critical loads sample survey, and soil and deposition databases. Since this uses a single spot value to represent the annual mean water chemistry, it was to be expected that there would be some difficulty in calibrating the model at some sites, and there was, particularly at sites with high sea-salt inputs. Nevertheless satisfactory calibration was achieved at 698 sites, and the reduction in deposition due to the Second S Protocol was modelled until 2050. The authors produced some statistics showing regional recovery trends, with some sites still with ANC <0 in 2050, and average recovery of ANC compared to the calculated pristine value was about 15-30%, depending on region. The study could have been used for scenario analysis, but the authors are clearly aware of its limitations and suggest some improvements in methodology. Nevertheless it demonstrates that meaningful results can be produced by this approach provided the data are available and a critical approach is adopted.

Water quality modelling usually concentrates on headwater catchments, but very often the important biological resources are lower down in larger streams and rivers. Here mixing of waters from different sources has to be taken into account, and there is spatial connectivity between catchments, which is not captured on the usual gridded maps. Cooper *et al.* (2000) devised a procedure for modelling recovery in these catchments by identifying landscape types, which were assumed to behave as homogenous units, and mixing the waters resulting from modelled changes in the landscape types. This procedure was developed in the Towy catchment in Wales, but it proved possible to transfer it to other UK catchments with varying degrees of success.

2.8.3 Uncertainties in dynamic models

Jenkins and Reynolds (2000) review some uncertainty analyses for dynamic models, and produce error bounds on predictions. In this section, the authors consider the question "Are dynamic models more uncertain than orthodox steady-state critical load models?". There are no quantitative, objective analyses which address this question. The answer will of course depend on which models are chosen for comparison, but some general statements can be made about the commonly used models.

Dynamic models require more parameters than steady-state models, usually a cause of greater uncertainty. Some of the parameters required are the same, weathering rate for instance, but the dynamic models also require the variation of some parameters over time, including variation in past centuries and predicted variation in future. Set against this, dynamic models are usually calibrated against current conditions, which constrains the range of possible outcomes. It is much harder to do this with the steady-state models, which inherently predict conditions at some indefinite time in future (see Section 4). On the other hand there are several examples in which a dynamic model was calibrated to present conditions in more than one way, leading to very different future predictions. But there again there is no need in the dynamic models for the long chain of empirical relationships used in the freshwater critical load models to estimate pre-industrial base cation concentration. From first principles, all that can be said is that there is no evidence that dynamic models are more or less uncertain than the steady-state models. Some quantitative work on this question might be worthwhile.

2.9 Maximum Critical Loads of Sulphur ($CL_{max}S$)

For terrestrial ecosystems, $CL_{max}S$ (Fig. 2.1) is based on the acidity critical load values but also takes into account non-marine base cation and chloride deposition to the soil, and base cation removal from the system:

$$CL_{max}S = CL(A) + {}^*BC_{dep} - {}^*Cl_{dep} - BC_u \quad (29)$$

where:

$CL(A)$	acidity critical load
${}^*BC_{dep}$	non-marine base cation deposition
${}^*Cl_{dep}$	non-marine chloride deposition
BC_u	base cation uptake by vegetation.

For the acid grassland, calcareous grassland and heathland ecosystems, $CL(A)$ is the empirical critical load for soils (Section 2.3). For the deciduous and coniferous woodland ecosystems $CL(A)$ in equation (29) is the mass balance critical load (equation (8)).

For aquatic ecosystems, $CL_{max}S$ is given by:

$$CL_{max}(S) = L_{crit} / (1-\rho_S) \quad (30)$$

where ρ_S is defined as in equation (25) and L_{crit} as in equation (27). This is the critical load for acid leaching modified by S retention in lakes. Hence for aquatic ecosystems, S retention is taken into account while base cation deposition is not (at least directly), while for terrestrial ecosystems the reverse is the case. The justification for this difference is debatable.

2.10 Minimum Critical Loads of Nitrogen ($CL_{min}N$)

The calculation of $CL_{min}N$ for terrestrial ecosystems is closely related to the mass balance model for $CL_{nut}N$, and similar comments apply. The minimum critical load of nitrogen represents the critical load of acidity due solely to nitrogen removal processes in soil:

$$CL_{min}N = N_u + N_i + N_{de} \quad (31)$$

where:

N_u	nitrogen uptake
N_i	nitrogen immobilisation
N_{de}	denitrification

This equation applies only if it is assumed that all N deposition which is not taken up, immobilised or denitrified is leached as nitrate. In the UK, N_i and N_{de} depend solely on soil type and are restricted to a few discrete values. Immobilisation is either 0.0714 or 0.2143 keq ha^{-1} y^{-1}, and denitrification is either 0.0714, 0.2143 or 0.2857 keq ha^{-1} y^{-1}. (These are whole numbers when expressed in kg N ha^{-1} y^{-1}; see Section 2.2.2). The 5 terrestrial ecosystems are assumed to have different uptake values. Acid grasslands are assigned a value of 0.0714 keq ha^{-1} y^{-1}; calcareous grasslands, 0.714 keq ha^{-1} y^{-1};

heathlands, 0.290 keq ha^{-1} y^{-1} and deciduous and coniferous woodlands, 0.5 keq ha^{-1} y^{-1}. Uncertainties are the same as those discussed in relation to the mass balance approach to $CL_{nut}N$, except that an acceptable leaching does not have to be assumed.

$CL_{min}N$ values for aquatic ecosystems are calculated using the FAB Model (see Section 2.7). The formula used in the UK (Curtis *et al.* 2000) is:

$$CL_{min}N = fN_u + (1\text{-}r)(N_i + N_{de}) \quad (32)$$

with parameters defined as in equation (21).

This represents the N absorbed by the terrestrial catchment, and differs somewhat from the formula in the Mapping Manual (UBA, 1996). N uptake is parameterised as a single value of 0.279 keq ha^{-1} y^{-1} and applies only to coniferous forests. Note the value is lower than the 0.5 keq ha^{-1} y^{-1} used for terrestrial ecosystems.

2.11 Maximum Critical Loads of Nitrogen ($CL_{max}N$)

For terrestrial ecosystems,

$$CL_{max}N = CL_{max}S + CL_{min}N \quad (33)$$

This relationship would not hold if the treatment of denitrification recommended by the Mapping Manual (UBA, 1996) were followed, where it is a function of deposition. The UK's adoption of a deposition-independent value simplifies the situation.

For aquatic ecosystems, the UK uses the formula, derived from FAB:

$$CL_{max}N = CL_{min}N + L_{crit} / (1\text{-}\rho_N) \quad (34)$$

where values are defined as in equations (23) and (27).

This takes into account the N absorbed by the catchment and the lake, as well as the critical ANC. This is logical, but as with $CL_{min}N$ it differs from the formula in the Mapping Manual.

3 Previous uncertainty analyses for critical loads

There have been a number of attempts to establish the range of uncertainty of critical loads in recent years. This may be as a result of pressure from policymakers and industrial groups concerned about expensive policies being implemented as a result of calculations which cannot be trusted. For the latest submission of data to the Co-ordination Centre for Effects (CCE), national centres were asked to include an estimate of uncertainty (though few did).

This section reviews the use of various techniques for estimating uncertainty.

3.1 Uncertainty Analyses

Uncertainty analyses are here defined as studies in which there is a systematic attempt to explore the range of variation in critical loads generated by quantified uncertainty in data inputs and model parameters. Ideally this should include all such inputs and parameters: in practice this is rarely done with complex models, and has never been attempted for critical loads.

The most frequently utilised technique for uncertainty analysis is Monte Carlo simulation. The data input or model parameter values are sampled from a frequency distribution. The nature of the distribution reflects knowledge of the particular parameter: it may be known to be approximately normal or log-normal, for instance. More often in ecological modelling there is little or no knowledge of the parameter distribution, and in these cases a triangular distribution is used where it is felt a central value is more likely, or a uniform distribution if there is no clear information. The choice of distribution thus introduces a subjective element into the analysis. Parameter values are chosen at random from the appropriate distribution, and the model is run many times, typically hundreds or thousands, with a new set of parameters each time. This generates a distribution of output values. Values can be discarded if they do not meet a set of criteria, if there is some knowledge or expectation of what the output values ought to be. Otherwise the range and distribution of output values are taken to reflect the uncertainty of the model outputs. Monte Carlo analysis only addresses errors in data inputs and their propagation through the model, not errors in model structure. Moreover, the simple analysis described above does not preserve the covariance structure of input parameters (Barkman 1997) i.e. input parameters may be correlated with each other. If this is taken into account the uncertainty in the output may increase or decrease. Simple Monte Carlo simulation is thus a best case approach to uncertainty analysis.

The most comprehensive set of uncertainty analyses for critical load models are those of Barkman and colleagues at the University of Lund, Sweden (Barkman *et al.* 1995, Barkman 1997, Barkman and Alveteg 2001a,b). These studies consist of an uncertainty analysis of the PROFILE Model as used to determine critical loads in Southern Sweden. Critical load determination by PROFILE is in principle the same as by the Steady State Mass Balance Method, PROFILE providing a mechanism for calculating the weathering rates and some of the nutrient cycling parameters required by the SSMB Model. Barkman used Monte Carlo analysis on two sets of data from forest plots in southern Sweden. For the first analysis (Barkman *et al.* 1995) values were sampled from triangular or regular distributions of 30 of the model's 100 input variables (see

shortened version in Table 3.1). The model was applied 500 times to each of the 128 sites, and the distribution of output uncertainties of 100 of these was approximately normal and thus suitable for the application of parametric statistics. The pooled standard deviation of the critical load for all 100 sites was 0.19 keq ha^{-1} y^{-1} on a median of about 1.0 keq ha^{-1} y^{-1}, though individual means and standard deviations varied considerably. The pooled standard deviation of the exceedence was 0.31 keq ha^{-1} y^{-1} on a median of about 1.5 keq ha^{-1} y^{-1}. The major interest of this study is however that it allowed estimates of the uncertainties of critical load exceedence to be made on a regional basis.

In the second study, Barkman (1997) studied 67 forested sites in a small area (392 km^2) of southern Sweden. Monte Carlo analysis was applied to PROFILE as before, using slightly different uncertainty ranges and allowing for some covariance in deposition. For coniferous forests, the pooled standard deviation of the critical load was 0.32 keq ha^{-1} y^{-1} (range 0.13 – 0.61) on a median of 0.9 keq ha^{-1} y^{-1}. The standard deviation clearly increased with the mean, implying a roughly constant coefficient of variation (CV) of about 36%. For deciduous forests, the pooled standard deviation of the critical load was 0.45 keq ha^{-1} y^{-1} (range 0.15 – 0.72) on a median of 1.8 keq ha^{-1} y^{-1}, though here the CV was less constant at 20-30%. For exceedence the standard deviation was again higher at about 0.5 keq ha^{-1} y^{-1} for both forest types.

Table 3.1 Ranges Used in Uncertainty Studies of the SSMB

Parameter	**Range (± percentage of mean)**			
Author[1]	**Zak**	**Barkman**	**Suutari (G)**	**Suutari (A)**
$*BC_{dep}$	-[2]	20	20	30
$*Cl_{dep}$	-	20	20	30
BC_w	[3]20	[3]20-100	20	40
BC_u	-	20	15	20
Bc_{dep}	-	20	20	30
Bc_w	[3]20	[3]20-100	20	40
Bc_u	-	20	15	20
$(Bc/Al)_{crit}$	-	-	10	-
Q	-	30	15	50
$logK_{gibb}$	5	0.3[4]	20	20
N_i	-	-	5	-
N_u	-	20	20	20
N_{de}	-	-	[5]20	-

Notes: [1]Zak *et al.* (1997); Barkman (1997); Suutari *et al.* (2001) – "G" and "A" refer to German and Austrian data; [2] kept constant during the analysis; [3]derived from PROFILE, dependent on mineral type; [4]range in absolute value; [5]denitrification fraction.

Barkman and Alveteg (2001a) investigated the sources of data uncertainty in weathering rates, critical loads and exceedances for 1883 forest sites in Sweden using Monte Carlo analysis and the PROFILE Model. Monte Carlo analysis was performed on the whole data set, and compared with a repeated analysis with a subset of input parameters held constant. There were six subsets covering atmospheric deposition; stand characteristics such as base cation uptake; soil mineral content; soil physical properties; soil solution chemistry and solution chemistry but including uncertainty in the critical limit. Soil physical properties were the dominant contributor to uncertainty in weathering rate, but for critical load and exceedence calculations the major source of uncertainty was the critical limit i.e. the assumed Bc/Al ratio. This was especially true in the north of Sweden, but in the south, atmospheric deposition and stand characteristics tended to be most important. The authors suggest that a practical strategy for reducing critical load uncertainties should concentrate on narrowing uncertainty in deposition and nutrient cycling, because the critical limit is intrinsically difficult to evaluate.

In a related study, Barkman and Alveteg (2001b) considered the effects of uncertainty on a nationwide critical load assessment. Grouping their site data into 150km EMEP grid cells, they calculated median and 95% confidence intervals for each grid cell using Monte Carlo analysis of the individual sites. At 95% confidence, the critical loads of most grid cells were not distinguishable – in fact the only significant differences among the 35 grid cells were between two cells with low critical loads and two cells with high critical loads. (In the UK, with its more varied geology, probably no cells would be significantly different). Re-aggregation onto the EMEP 50km grid made it possible to differentiate the critical loads on more squares, but even so on 70% of the grid squares it was uncertain whether the critical load was exceeded, or not within the confidence intervals calculated.

However Barkman and Alveteg realised that, if uncertainties were not included, the 95-percentile would be a site-specific value (the most sensitive site if there were up to 40 sites in the grid square) and hence vulnerable to the random inclusion or omission of a single site. They argued that since the uncertainty analysis showed that many sites could in fact be the fifth percentile, it was more robust to construct confidence limits on the percentiles rather than the individual sites. Since this is an important mechanism for narrowing confidence intervals on the whole critical load assessment process (see Suutari *et al.*, 2001, below), and the explanation in Barkman and Alveteg is much clearer, it is worth quoting exactly how this was done. "…the results from the Monte Carlo simulation are transferred to a matrix with as many columns as there are sites, and as many rows as there are replicate runs. The ordinary cumulative distribution function (CDF) with site-specific uncertainties is created by sorting each column to determine the median value and the confidence interval for each site….The modified CDF, on the other hand, is created by first sorting each *row* from low to high, thereby changing the interpretation of a column from site-specific to percentile-specific values. Each column is then sorted from low to high to determine the median value and the confidence interval for each percentile" (Barkman and Alveteg, 2001b). This modification reduced the median critical load for all the EMEP 150 squares, and narrowed the confidence interval for 90% of them, sometimes considerably. The 95-percentile exceedence was increased on all but three of the grid squares, and the confidence intervals of exceedence were reduced on all squares.

Zak *et al*. (1997) and Zak and Beven (1999) also performed an uncertainty analysis of critical load estimation using PROFILE, but with very different results. They used a technique called Generalised Likelihood Uncertainty Estimation (GLUE) which is based on Monte Carlo techniques and was originally developed to assess the predictive capability of distributed hydrological models. GLUE recognizes that it is not possible to identify unequivocally a set of parameters as being optimal for an environmental model. Quite different sets of parameters might be essentially equivalent as simulators of a system, a concept which they call *equifinality*. Hence GLUE does not attempt to optimise on a single set of parameters, but a set of behavioural criteria (not specified very clearly in the papers). Zak *et al.* (1997) calculated the uncertainty of the critical load for a small catchment at the Plynlimon research site in mid-Wales. Monte Carlo variation was applied to 10 sets of parameters within the PROFILE model. Distributions were uniform ± 20%. The best 20% of 60,000 simulations were retained. The median critical load was 1.07 keq ha^{-1} y^{-1}, and the 90% confidence range was 0.27 to 1.87 keq ha^{-1} y^{-1}. This range is similar to the range in the geographical variation in total S deposition to the UK (NEGTAP, 2001). A set of 6 field measurements was compared with the range of estimates derived from the model: only 3 of the 6 fell within the uncertainty ranges in the simulation. Zak *et al.* (1997) concluded from this that there were significant deficiencies in the model structure, or the boundary conditions applied, or both.

Zak and Beven (1999) re-applied the GLUE methodology to critical load estimation by PROFILE at the same catchment but varied a wider range of parameters, and also applied it to a further 4 research catchments. The median and 90% confidence range altered a little to 1.20 (0.24 – 1.82) keq ha^{-1} y^{-1}. Corresponding figures (in keq ha^{-1} y^{-1}) for the other sites were 0.92 (0.32 – 1.34) for Aber in North Wales; 3.12 (2.60 – 3.58) at Uhlirska in the Czech Republic; and 0.80 (0.29 – 1.34) at Fårahall in Sweden. The official critical loads for coniferous forest in the area round Aber were estimated to be about 2.1 keq ha^{-1} y^{-1} in 1998 (quoted in Zak and Beven, 1999), but in the 1.0 to 2.0 range in 2001 (Hall *et al.* 2001a). For the fifth site (Alice Holt Lodge in Hampshire) none of the 60,000 Monte Carlo runs gave an acceptable simulation of the data, showing that PROFILE was inappropriately structured or parameterised for this site. The site has a clay soil, and PROFILE has been observed to give poor results for such soils in other studies (e.g. Van der Salm, 2001).

It is perhaps discouraging that such a wide uncertainty range in critical load results from application of fairly narrow uncertainty bands to only about 10% of model parameters, especially given that these are research catchments where many input variables are known with greater certainty than is generally the case. However, GLUE has been criticised as a methodology and normally gives wider limits than other such methods.

An interesting Monte Carlo analysis of SSMB critical loads from some sites in China was performed by Larssen *et al.* (2000). The parameter ranges chosen and resultant critical loads with 90% confidence intervals are shown in Table 3.2. The critical loads are very high, partly because of large amounts of base cation deposition. It is not possible to calculate coefficients of variation from the data presented, but using the statistic in the bottom row of the table (which will be a little higher than a conventional CV) the variation ranges from 27 to 50% of the median. Larssen *et al.* (2000) also modelled these sites using the MAGIC model, and using only parameter ranges which gave acceptable simulations in MAGIC to re-run the Monte Carlo analysis of the SSMB

Model (final two columns of Table 3.2) reduced the 90 percentile range at one site (LGC) but not the other (TSP).

The paper by Larssen *et al.* (2000) also contains a Monte Carlo analysis of the dynamic model MAGIC as applied to the LCG and TSP catchments. The median hindcast soil base saturation was about 28%, with an absolute range of 21-34%. Although MAGIC was not used to calculate critical loads in the paper, this range would probably lead to considerable differences.

Table 3.2 Monte Carlo Analysis of Some Sites in China

Parameter	**Range (keq ha^{-1} y^{-1})**						
Site	**Conghua**	**LCG**	**Leigong**	**Simian**	**TSP**	**LCG Recalc[1]**	**TSP Recalc[1]**
BC_{dep}	0.67-2.7	2.0-7.4	0.74-3.0	0.81-3.2	4.2-12.0	3.3-7.4	5.5-9.7
BC_w	0.3-7.1	0.01-1.6	0.13-3.7	0.06-1.8	0.04-2.6	0.09-0.52	0.19-0.55
BC_u	0.1-1.0	0.1-1.0	0.1-1.0	0.1-1.0	0.1-1.0	0.18-0.59	0.1-0.25
$LogK_{gibb}$	7.70-9.18	8.17-9.18	7.70-9.18	7.70-9.18	7.70-8.94	8.17-9.18	7.70-8.94
Q mm y^{-1}	550-750	567-693	550-850	450-750	550-770	567-693	550-770
S_{dep}	1.9-4.4	3.3-7.5	0.63-2.5	0.63-2.5	5.0-8.8	3.3-7.5	6.6-8.6
Median C Load	11.6	8.3	6.6	4.7	15.2	9.4	15.2
90% CI	8.5-14.7	5.0-11.6	3.3-9.9	2.5-6.8	10.0-20.3	6.6-11.8	10.0-20.1
CI/Med[2]	27%	40%	50%	46%	35%	27%	33%

After Larssen *et al.* (2000). [1]Recalculated using parameters which gave an acceptable MAGIC simulation. [2]Half the 90-percentile range divided by the median critical load

A contrasting uncertainty analysis is that of Suutari *et al.* (2001), which was undertaken as part of an analysis of the uncertainty of the whole integrated assessment process, used in the negotiation of national emission limits. Suutari *et al.* (2001) applied Monte Carlo analysis to most of the parameters in the SSMB equation, using the ranges specified in Table 3.1. These ranges were derived from estimates by the German and Austrian national focal centres (for critical load calculation). How these ranges were estimated were not stated. After 2000 Monte Carlo runs, the CVs of the $CL_{max}S$ values were 22% for the German data and 25% for the Austrian. The CVs for $CL_{min}N$ were 7.5% and 8.8%, and for $CL_{max}N$ 12.5% and 17.5% respectively. These results illustrate a phenomenon Suutari *et al.* (2001) call *compensation of errors*, because the range of uncertainty of the results is narrower than the uncertainty range of most of the input parameters. This occurs when it is assumed that the input parameters are uncorrelated (as they were in this case apart from base cation and nitrogen uptake). The phenomenon leads to remarkably (unbelievably?) narrow uncertainty ranges for the whole integrated assessment process (see Suutari *et al.* 2001, Posch *et al.* 2001).

The study by Suutari *et al.* (2001) illustrates some important questions that need to be asked about such uncertainty analyses. How are the ranges in input variables derived? Though unstated in any of the papers reviewed, the answer appears to be "expert judgement" i.e. a guess, rather than any objective process. Attempts in the literature to evaluate the uncertainty ranges of some of these parameters tend to result in much wider ranges than those used. For instance, Suutari *et al.* (2001) used an uncertainty of ± 10% for the $(Bc/Al)_{crit}$ parameter (i.e. the range used in the Monte Carlo analysis was probably 0.9 to 1.1). Cronan and Grigal (1995) reviewed the use of this indicator, and suggested that a range of 1.0±50% would give 50% confidence of vegetation damage. Weathering rates provide another example. The German national focal centre estimated the range in weathering rates as ±20% and the Austrian ±40%. After a study of the weathering rate calculation by PROFILE, Hodson *et al.* (1997) estimated the uncertainty range as ±250%. Van der Salm (2001) found the PROFILE model overestimated weathering on some Dutch soils by a factor of 7 when not calibrated on laboratory data, and by a factor of 95 when it was calibrated. A range of ±40% seems small compared to these estimates.

Another important question arises when the uncertainty analysis is being applied to anything other than a reasonably homogeneous entity i.e. when there is real variation in the input parameter, which is due to the varied nature of the thing in question. For instance, the unit for critical load calculations on an international level is currently the 50 km grid square. A 50 km grid square will typically contain a number of soil types, and weathering rates might easily vary by 2 orders of magnitude – from quartzites to limestones, say. Is the range term in the Monte Carlo analysis meant to include this variation? It clearly does not in the Suutari *et al.* (2001) study, but probably does in the Larsen *et al.* (2000) work. Or is the range intended to be the uncertainty for a given ecosystem, and if so how is the uncertainty generated by the variation within the square taken into account? The spatial scale of uncertainty analyses needs to be made very explicit. Many of the parameters in the SSMB equation will have similar ranges of natural variation to that of weathering rate.

The only uncertainty study known to the author performed on freshwater critical load models is that of Kämäri *et al.* (1993). They performed an uncertainty analysis on the SSWC Model for lakes in Finland, using Monte Carlo methods. This suggested an overall standard deviation on the critical load of ±10%.

Heywood *et al.* (2002, in press) studied the influence of uncertainties in S and N deposition alone on UK critical load exceedence, using Monte Carlo analysis. Deposition was assumed to vary by ±40%, and S and N were analysed together and separately. This variation had a considerable, non-linear effect on exceedence with the area exceeded in the year 2010 varying from +35% and -50% of the deterministic value. Accumulated exceedence (see Section 7.2) varied within wider limits, between +100 and –75% of the deterministic value. Although the medians of these distributions were lower than the deterministic values (i.e. a smaller area of exceedence) use of a 95% confidence interval would lead to more pessimistic estimates than those currently used by policymakers; a 35% increase in area exceeded, for example.

3.2 Sensitivity analyses

In contrast to uncertainty analyses, sensitivity analyses look at the sensitivity of the output variable to changes in one input variable, usually with the others held constant. Sensitivity analyses should be part of an uncertainty analysis, but are more common than the latter because they are less technically demanding. Hall *et al.* (2001b) conducted a limited sensitivity analysis of the SSMB equation as used in the UK. Reducing the $(Ca/Al)_{crit}$ value from 1.5 to 1.0 to 0.5 altered the mean critical load from 1.77 to 1.96 to 3.11 keq ha^{-1} y^{-1} respectively, and doubled the range between the absolute maxima and minima. In a parallel investigation, Hall *et al.* (2001c) investigated the effect of altering the Gibbsite equilibrium constant K_{gibb} on SSMB critical loads. K_{gibb} governs the relationship between H^+ and Al concentrations and thus has a strong effect on base cation/aluminium ratios. Altering K_{gibb} through the range recommended in the Mapping Manual (UBA, 1996) for different soil types altered the mean UK critical load from 3.2 to 1.8 keq ha^{-1} y^{-1}. Hall *et al.* (2001bc) also studied the effect of using different critical load criteria on critical loads calculated by the SSMB. These criteria are all used by different European countries (Hall *et al.* 2001c) as critical chemical values. The mean value of UK critical loads for coniferous woodland was 1.96 keq ha^{-1} y^{-1} using $(Ca/Al)_{crit}$ as the criterion, 2.83 keq ha^{-1} y^{-1} using a critical Al concentration of 200 μeq l^{-1}; and 3.17 keq ha^{-1} y^{-1} using a critical pH of 4.2. There is no reason why these should be the same, but it highlights the need for a careful choice of critical chemical value in relation to the receptor, and some of the reasons for differing critical loads between European countries. Critical loads derived from a critical pH of 4.2 are particularly sensitive to the chosen value of K_{gibb}, UK mean values varying from 1.28 to 20.3 keq ha^{-1} y^{-1} when K_{gibb} was varied over the range of acceptable values (Hall *et al.* 2001bc).

Wilby (1995) investigated the sensitivity of critical loads to climate change, which he did by altering the amount of annual runoff assumed in the critical load model (which was MAGIC), using observed values for the Beacon Hill Catchment near Loughborough for each of the 6 years between 1984 and 1990. The calculated critical load for the wettest year (0.60 keq ha^{-1} y^{-1}) was almost double that of the driest (0.35 keq ha^{-1} y^{-1}). This is possibly an unusually wide range, as the critical load model used (attainment of a target Al concentration in surface waters) is strongly non-linear, and the catchment has a low runoff/rainfall ratio compared to most upland catchments.

Thomas and Reynolds (1998) investigated the sensitivity of critical loads as calculated by the SSMB to changes in all input parameters, using data ranges characteristic of the Welsh uplands. They observed what they called instabilities, regions of the parameter space where critical loads changed very rapidly in response to small input parameter changes. Typically these responses were non-linear and occurred just past a zero response threshold. Though not strictly unstable, the critical load response may be surprisingly large if changing a parameter caused one of these regions to be crossed.

Two studies by the Stockholm Environment Institute (Kuylenstierna *et al.* 2001ab) examined the effects of alternative assumptions about the values of critical loads derived from measurements of weathering rates and soil parameters, using a low range and a high range of twice the value, and similar assumptions about base cation deposition. Kuylenstierna *et al.* (2001a) applied this methodology to critical loads and exceedences on a global scale, showing that it made a considerable difference to

exceedence in Asia in particular (because of the base cation deposition). Kuylenstierna *et al.* (2001b) applied the same approach to Asian countries alone, providing some more quantitative results. The difference in area exceeded between the best case scenario (high critical loads, base cation deposition, low emissions) and worst case (the converse) was 54%. These results obviously depend on the values chosen, but illustrate the range of results generated by credible assumptions.

There are various other sensitivity analyses which deal with the effect of input parameters on key elements in critical load calculation, rather than critical loads themselves. For instance, Zak *et al.* (1997) performed a sophisticated sensitivity analysis of base cation/aluminium ratio calculation by PROFILE, showing at the Plynlimon site that it was very sensitive to K_{gibb} but not much to other parameters. Goulding and Blake (1993) showed that K_{gibb} had a large effect on soil acidification calculated by PROFILE. The weathering calculation is affected by a number of soil physical parameters, being sensitive particularly to assumed mineral surface area (Hodson *et al.* 1997). Hodson and Langan (1999ab) considered the uncertainty with which current weathering rates are known or can be calculated, and concluded that it was currently impossible to derive accurate critical loads for acidity as weathering rates were so uncertain. A full survey of such studies would probably not be very illuminating in the present context, as it is the combination of uncertainties and sensitivities which is really critical.

3.3 Multiple model applications

Another approach to evaluating uncertainties is to apply different critical load models to the same site, or range of sites. Holdren *et al.* (1993) pioneered this approach, applying several versions of the SSWC Model and MAGIC to 762 lakes from the north east USA. The models showed the same general trends but differed quantitatively, the maximum difference observed being 1.71 keq ha^{-1} y^{-1}, roughly comparable to the maximum S deposition in this area. Holdren *et al.* (1993) used two different methods of calculating the F-factor for the SSWC Model (see Section 2.5): the resulting critical loads were essentially uncorrelated. Holdren *et al.* concluded that risk managers, rather than risk assessors, should make the decisions about the magnitude and timing of emission reductions i.e. that it was not just a problem in applied mathematics.

Anderson *et al.* (1998) applied different methods to the Gårdsjön experimental area in Sweden. Six different methods were applied to the coniferous forest at the site – the resulting range in critical loads for acidity was 0.20 – 1.07 keq ha^{-1} y^{-1}. Nine different methods were applied to the lake: the resulting range was 0.02 – 0.74 keq ha^{-1} y^{-1}. Some of this variation was due to the use of different criteria for estimating endpoints. This is one of the few sites where there is enough field evidence to estimate the "true" critical load for acid deposition to waters at least, which was 0.1 – 0.44 keq ha^{-1} y^{-1}.

Kurz *et al.* (2001) applied SAFE (the dynamic version of PROFILE) to 600 forest sites in Switzerland, and compared the results from those with steady-state models. The scenario run was the Gothenburg Protocol, and the critical limit a Bc/Al of 1. According to the RAINS assessment (performed on a scale of 150km) this will reduce the percentage of Swiss forest ecosystems with exceeded critical loads from 41% to 4% by the year 2010. These figures are 63% to 16% if the assessment is performed on a 1km scale using the SSMB Model. The dynamic model however predicts 45% exceedence in

1995 reducing to only 39% by 2010 and 32% by 2100. The implication is that most of these soils will eventually reach the critical limit, but not for a very long time (perhaps millennia).

3.4 Changes in model structure

Van der Salm and de Vries (2001) investigated the effect of some changes in the structure of the SSMB to critical loads in The Netherlands. Weathering was made pH dependent. This is theoretically more correct, but means the equation can only be solved iteratively. This modification increased the median critical load from 0.23 keq ha^{-1} y^{-1} to 0.45 keq ha^{-1} y^{-1}. The increase was especially marked for clay soils, which acquired much higher (and more credible) weathering rates. The Gibbsite equilibrium was replaced by empirically observed relationships between Al and pH differentiated by soil type. It has long been known that the Gibbsite equilibrium does not describe field data very well, and modification has often been suggested, but this is the first practical application of this. This modification alone increased the median critical load for forest soils from 0.27 to 0.39 keq ha^{-1} y^{-1}. Another criterion was added to the model, so that soils were also protected against a reduction in base saturation. This hardly affected the median critical load in The Netherlands, but decreased its value on the more base rich soils considerably. For instance, the 95-percentile critical load decreased from 15.4 to 5.5 keq ha^{-1} y^{-1}. This study illustrates that theoretically reasonable changes to critical load model structures can cause very large alterations in critical load.

Tao and Feng (2000ab; 2001) developed a new sensitivity classification, which they claimed was more suitable for the sub tropics, and applied it to China. They noted that although some areas were the same, the distribution of sensitivity was very different to that calculated by the RAINS-ASIA Model, which is based on the SSMB Model.

3.5 Conclusions on uncertainty

It is fair to say that there are conflicting views on the uncertainties which should be attached to critical loads. Some authors (e.g. Hodson and Langan, 1999a,b) believe that it is impossible to derive critical loads with any useful degree of accuracy, while estimates of key underlying processes such as weathering rates are so uncertain. Others (e.g. Suutari *et al.* 2001) derive coefficients of variation of 25% (for $CL_{max}S$) and 10% (for $CL_{\min}N$), probably by underestimating the uncertainty in the input variables. However, compensation of errors and aggregating estimates on a wide spatial scale will reduce uncertainties below what would be expected intuitively. Reasonably objective Monte Carlo analyses in areas with good data give CVs in the range of 25-50%. GLUE analysis gives wider limits. Using alternative but still reasonable models can produce large differences in critical loads. There is a lot of uncertainty about uncertainties, and more work is needed to define them objectively.

4 Validation

Validation involves a comparison of the behaviour predicted by models with observed behaviour. Ideally, areas with exceeded critical loads should correspond with areas in which acidification and/or eutrophication has occurred. A quantitative correspondence would constitute validation. Unfortunately, the steady-state nature of the concept precludes this simple approach, as illustrated in Fig. 4.1.

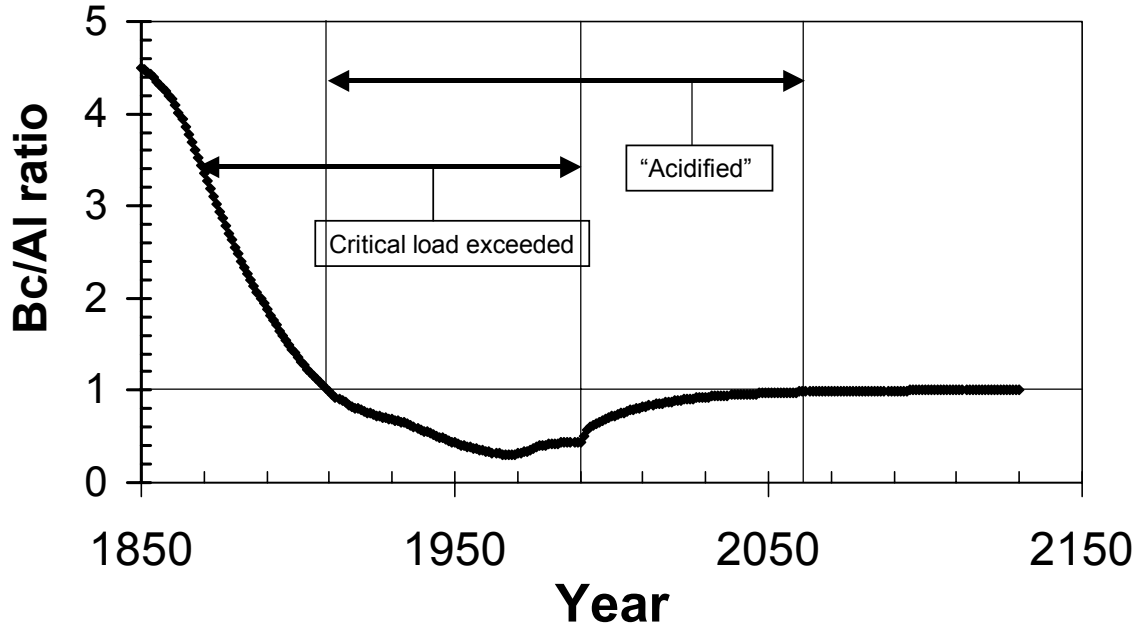

Figure 4.1: The difficulty of validating critical loads

Figure 4.1 shows a MAGIC run with a realistic model ecosystem, which was subjected to a deposition pattern similar to that of the UK, increasing until about 1968 and then declining. In 1990, deposition was decreased to the calculated SSMB critical load, assumed to be the deposition which generates a BC/Al ratio of 1.0 at steady state. Figure 4.1 illustrates a number of points:

- The critical load was first exceeded in 1870, but delays in the system mean that the critical limit (BC/Al=1) was not violated until 1910. Posch and Hettelingh (2001) call this period the *damage delay time*.
- Conversely, the critical load was attained in 1990, but the critical limit remained violated until about 2060. Posch and Hettelingh (2001) call this period the *damage recovery time.*
- Deposition at the critical load does not imply recovery to pristine conditions (hence "acidified" in quotes).
- This model ecosystem was constructed to give a relatively rapid recovery – more typical recovery times would be centuries.

From Fig. 4.1 it should be clear why it is difficult to validate critical loads against observations. During the damage delay time the critical load is exceeded, but there is no damage. During the damage recovery time the critical load is not exceeded, but there is

damage. Moreover, the system can be acidifying when the critical load is not exceeded, as in 1850-70, and recovering when the critical load is exceeded, as in 1970-90. The time scales of these responses are long compared to the time available for observation.

An example of the difficulty was the Liphook Forest Fumigation Experiment, where trees on the same soil (critical load <0.2 keq ha^{-1} y^{-1}) were subjected to one of three S deposition treatments. Deposition in the highest treatment exceeded the critical load by a factor of about 30, but the trees grew perfectly well (McLeod and Skeffington 1995). This does not invalidate the site critical load, however, because it is essentially a prediction that sometime in future tree growth *would* be affected. Indeed the BC/Al ratio at Liphook was well above 1, though decreasing, showing the plots to be in the "damage delay time" stage.

Nevertheless, there is a vague correspondence between critical load exceedence and known areas of damage, both in the UK and Europe as a whole. To see a quantitative relationship between critical load exceedence and damage, however, it would be necessary either to make observations for a long time, or choose ecosystems in steady state. As an example of the former, Reynolds *et al.* (1998) studied the responses of a number of manipulated ecosystems in the NITREX Project. These long-term ecosystem experiments showed responses which were consistent with some calculated critical load exceedences, in that nitrate leaching was positively correlated with exceedence of $CL_{nut}N$.

Southern Norway is somewhere that might be close to steady state in many places, given thin soils, high rainfall, and a long history of relatively high deposition. Henriksen *et al.* (1999) claimed that there was a good relationship between fish population status in Norwegian lakes and critical loads exceedence, though the ranges of exceedence for the fish population categories: "extinct", "reduced" and "unaffected", were in fact very similar. Nevertheless, they could be statistically distinguished. Southern Norway also supplied one of the few instances in which tree defoliation correlated with critical load exceedence (Nelleman and Frogner 1994). It is hard to find other examples.

Critical loads therefore have some relationship to ecosystem sensitivity, but are never likely to be validated quantitatively and unequivocally. This is one of their disadvantages compared to dynamic models, which can be used to generate predictions, which can be tested against data on a reasonable timescale.

5 Uncertainty associated with chemical criteria

The chemical criteria, or critical chemical values, used to determine critical loads are themselves associated with considerable uncertainties. Most of the criteria have been subjected to extensive debate, though some of the empirical nutrient nitrogen critical loads have perhaps not been debated quite as hotly. It is not the intention here to review or comment on those debates, but rather to estimate the uncertainties associated with the two most commonly used criteria: BC/Al ratio for soils, and ANC for waters.

5.1 Base cation : aluminium criterion

The use of a BC/Al ratio to assess toxicity goes back to the work of Ulrich (1983), and is based on two generally-accepted propositions: that high concentrations of inorganic aluminium are toxic to many plants, and that this toxicity can be alleviated by calcium. The use of certain Bc/Al ratios for individual species derives from a meta analysis by Sverdrup and Warfvinge (1993). They plotted growth responses of a number of species in experiments against the (Ca + Mg + K) / Al ratio, obtaining a sigmoid curve. A Bc/Al of 1 represented approximately a 20% growth reduction on the mean curve. Of more relevance to uncertainty analysis, however, is the spread of values. The curve covers four orders of magnitude in BC/Al ratio, from 0.01 to 100, between 100% growth reduction and no effect. More significantly, the lowest Bc/Al ratio with no growth reduction was 0.6, and the highest with some growth reduction was 20. Given the sensitivity of critical loads to this parameter (Section 3.2) this is a very large range. This covers all species, but the species most investigated (Norway spruce) shows a similar spread.

The use of the Bc/Al ratio has generated an enormous amount of controversy (e.g. Högberg and Jensén, 1994; Løkke *et al.* 1996) because it is usually uncorrelated with damage in the field; takes no account of nutrient uptake from the humus layer, where Al is likely to be complexed and not toxic and so on. However, it has proved difficult to devise a critical chemical value which is obviously better. Cronan and Grigal (1995) reviewed over 300 papers on the use of the Ca/Al ratio as an indicator of stress in forest ecosystems and concluded that it was reasonable to use it as a risk parameter. They concluded that a ratio below 1.0 indicated a 50% risk of adverse impacts on tree growth and nutrition, a ratio below 0.5 indicated a 75% risk, and a ratio below 0.2 almost a 100% risk. The uncertainty on each of these ratios they estimated to be approximately ±50%. These uncertainty estimates were arrived at by subjective processes, inevitably in view of the diversity of experimental approaches in the papers they reviewed. These estimates are however the best indication available of the uncertainty to be attached to the Ca/Al ratio. Note that Cronan and Grigal did not review the Bc/Al ratio proposed by Sverdrup and Warfvinge (1993). That is presumably more uncertain still.

5.2 ANC criterion

The use of acid neutralising capacity (ANC) as a criterion to assess damage to aquatic populations has also proved controversial. Aquatic organisms should not respond to ANC, as it is not a substance but the result of a titration (Skeffington, 1999). It is however correlated to the substances that organisms do respond to, particularly H^+, Ca^{2+} and inorganic Al, and provides a convenient surrogate which takes various aspects of water chemistry into account, and is relatively easy to measure and calculate. The best

evidence for determining the appropriate value of ANC to use as a critical limit comes from studies in Norway (Lien *et al.* 1996). These authors were able to correlate the fish and invertebrate status of large numbers of lakes with ANC (and other parameters). The results, plotted as cumulative frequency diagrams, give an estimate of the uncertainty due to natural variation in these waters. For brown trout, for instance, the ANC above which there was no damage to fish populations was about 35 μeq l^{-1}. At an ANC concentration of 20 μeq l^{-1} about 10% of populations were reduced. At an ANC of 0 μeq l^{-1} about 50% of populations were reduced, including 15% which were extinct. All populations were reduced, and 75% extinct, at an ANC of –30 μeq l^{-1}. All brown trout were absent at ANC < -50 μeq l^{-1}. Brown trout was the second most sensitive species, Atlantic salmon being more sensitive but living in rivers rather than lakes. The Norwegians thus originally chose +20 μeq l^{-1} ANC as their critical limit, accepting a 10% probability of damage but avoiding the setting of unrealistic targets for lakes with naturally low ANC. (Even so, many lakes would naturally have ANC < 20 μeq l^{-1} in Norway).

It is clear that there is quite a wide range over which a reasonable critical limit could be set, from 0 μeq l^{-1} accepting approximately 50% damage probability but ensuring no lakes had an unrealistic target, to +50 μeq l^{-1} on the precautionary side. This is illustrated by those countries which submitted data on freshwater critical loads to the CCE in 2001. Belgium and Finland used 20 μeq l^{-1} as their critical limit; Norway used 20-50 μeq l^{-1} depending on deposition; Sweden used 20 μeq l^{-1}, where the pre-industrial base cation concentration [$*BC_0$] was estimated to be less than 25 μeq l^{-1}, and 0.75[$*BC_0$] otherwise, and the UK used 0 μeq l^{-1}. These limits are all based on the same data set of Lien *et al.* (1996). The Swedish approach is an attempt to avoid the problem of lakes with naturally low ANC, and appears worth investigating for transfer to the UK.

A further source of uncertainty is the extent to which these limits are transferable to other countries with different hydrochemical settings, and possibly organisms with different sensitivities. Ormerod (1993) found relationships between the abundance of various aquatic organisms and ANC in Wales, although trout populations were not quite extinct in the ANC –50 to –200 class. The work of Ormerod (1993) and co-workers also shows very clearly that species richness increases steadily with ANC. There is no threshold or step change in toxicity.

6 UK practice compared to other countries

The methods used for calculating critical loads in the UK differ from those of other European countries, but then these all differ from each other. Hall *et al.* (2001c) surveyed the 19 countries submitting data to the CCE in 1999 and discovered they used 15 different critical limits and combinations of limits for forest ecosystems. In 2001, the number of variants increased, with the Netherlands having the most elaborate system based both on maintaining a BC/Al ratio and negligible change in soil base and aluminium status. The Mapping Manual (UBA 1996) imposes a certain amount of standardisation, but still leaves wide choices of both methods and parameters. Some concern is expressed in the latest CCE report (Posch *et al.* 2001) about this, as it must impact on the fairness in sharing the burden of emission control between countries in international negotiations. To some extent, however, the different methods reflect the different environmental conditions and receptors across Europe, as well as national idiosyncrasies.

The UK differs from most countries in using a Ca/Al ratio as the SSMB critical limit for forest ecosystems instead of a Bc/Al ratio, though two other countries do so and two further countries use Ca/Al in conjunction with other criteria. It is also unusual, but not unique, in submitting data for heathland and distinguishing between different types of grassland. The critical limit used for assessing lake acidification varies between countries, as noted in Section 5.2, the UK's limit being lower than other countries, generating higher critical loads. Otherwise the UK's methods for calculating critical loads fall within the envelope of methods used in Europe as a whole.

7 Uncertainties due to mapping limitations

Some uncertainty for the practical user of critical loads is generated from limitations generated by parts of the assessment process other than the theory and calculation of critical loads. These are briefly discussed below, quoting quantitative limits where possible.

7.1 Identification of Land Use Types

The UK calculates critical loads for five terrestrial ecosystems and also for freshwaters. Critical loads for waters are calculated on the basis of field measurements of specific lakes or streams (Section 2.7.2) and catchment areas are digitised from topographic maps: the freshwater ecosystem of concern can therefore be identified unequivocally. The lake sampled is meant to represent the most sensitive water in the 10 km square surveyed, and some uncertainty is introduced here, as it may not be the most sensitive. Application of the FAB Model requires the identification of the proportion of coniferous forest in the catchment of each lake (see terrestrial ecosystems, below) but otherwise ecosystem identification is not an issue.

The land cover for the terrestrial ecosystems on the other hand is derived from the 1990 ITE Land Cover Map of Great Britain (Fuller *et al.* 1994). This was produced using data from the Landsat Thematic Mapper satellite. The map is based on a 25m grid and consists of 25 cover types, including inland water, arable land, and 18 types of semi-natural vegetation. Landsat images from both winter and summer were used to improve the classification. Northern Ireland and the Isle of Man lie outside the range of the map, so the less-detailed CORINE land cover map is used in those areas (see Hall *et al.* 1998).

A comparison of cover types identified in the Land Cover Map (LCM) with independent ground reference data showed a correspondence of 67% (Fuller *et al.* 1994). This may not seem very good – one third of the identifications in the LCM are wrong – and indeed some field workers have been disappointed in the map data. However, as Fuller *et al.* (1994) point out, it is not simply a question of comparing map predictions with "ground truth" which can be identified in the field without error. Landscape patterns are actually a continuum, and their mapping into discrete classes imposes an artificial classification on a continuously varying pattern. Different surveyors attempting to apply the same classification will obtain somewhat different results, since the choice of where to place the boundaries is fairly arbitrary. At what point does a heathland with scattered trees turn into a woodland with a heathland under-storey? Problems also arose when cover type boundaries crossed a 25 x 25 m data pixel, which was about 40% of cases, as the pixel has to be assigned to one category or another. Temporal change between the satellite image and ground survey accounted for more variation. Overall, Fuller *et al.* (1994) estimate the accuracy of their LCM at 80 to 85%, though they note (probably in response to criticism from users) that this is an average figure and there will be areas where the classification is much better, and areas where it is much worse.

Transfer of the LCM categories into the five ecosystems used for critical load mapping introduces more uncertainty. The process is described by Hall *et al.* (1998, 2001a). Data on both the LCM and the critical load maps is presented on a 1km square basis. Land

cover types which appear in <5% of a 1 km square are discounted for critical load purposes, as some slight defence against misclassification. LCM classes do not precisely correspond to the critical load ecosystem types. "Acid grassland" is an amalgam of eight LCM types including felled forest, bracken and lowland and upland bog types. "Calcareous grassland" corresponds to two LCM types representing pasture, meadow and amenity grass, but also identified as having species-rich calcareous grassland in data from the Biological Records Centre at Monks Wood. "Heathland" is an amalgam of four LCM classes and "deciduous woodland" of two. Only "coniferous woodland" has one-to-one class correspondence with the LCM.

The result of these uncertainties is that it is easy to see areas on the critical load maps, where an ecosystem type which exists on the ground, is missing. Although the calcareous grassland map picks calcareous areas in the south of England quite well, limestone areas round Llangollen and in south Wales are missing, the Yorkshire Dales look under-represented, and there is no calcareous grassland in Scotland. The large areas of what the author would describe as heathland south west of London are mostly recorded as coniferous forest. Such problems are inevitable when dealing with a quarter of a million data points per ecosystem and highlight the fact that ecosystem identification is not a trivial task. There is now a new land cover map (LCM2000) with data categories corresponding to "Broad Habitats" as defined by the UK's Biodiversity Action Plan. These may correspond more closely with the categories on the critical load maps, though there are no plans to use it at present.

7.2 Choice of Grid Size and Averaging Technique

The spatial variability of the natural environment also causes problems when generating spatial databases or presenting data on maps. Entities in the natural environment cover a huge range of spatial scales, from the μm scale occupied by bacteria and soil particles, to the km+ scale occupied by some geological formations. If the scale is small enough, some effect even of minute amounts of pollution will be seen. Every grain of sand has its own weathering rate and hence acid neutralising capacity, and this may be of vital importance to an individual nematode, for example. To be manageable for policy purposes, small-scale data need to be aggregated into larger units, and this requires a thorough understanding of the purposes for which the data are to be used. Environmental pressure groups tend to assume that the correct value of the critical load is that of the most sensitive entity on the most detailed mapping scale available, but this is not necessarily the case. This would probably result in uniformly low critical loads over the UK, obviating one of the purposes of using critical loads, which is to recognise that some *areas* are more sensitive than others and hence deserving of more protection.

At present in the UK (and in Europe generally) the finest scale on which critical load data are available is the 1 km square. It could be argued that this is rather coarse, since rock, soil, vegetation and deposition can vary considerably within a square, especially within the diverse UK environment. However, the amount of data needs to be kept manageable, and the provenance of the input data also needs to be considered. Soil data, for instance, will rarely be a measured value even at 1km scale but will have been interpolated from soil maps which were produced for other purposes (Hornung *et al.* 1995). Modelled deposition data is currently available only down to a 5km scale. The 1km scale is therefore a compromise taking into account all these considerations.

The calculation of empirical critical loads in classes also means that choices have to be made as to how to represent classes as a single number. Originally, the UK used the upper bound of the class, as a conservative assumption. Later, the central point of the range was used (Hall *et al.* 1998), reflecting increasing confidence about the values but in the process depressing critical load values used for regulatory purposes significantly.

Aggregation of data to larger scales requires more decisions. For use with European policymaking, critical load data were aggregated to a 150km scale to match the EMEP grid, to be reduced to 50 km in subsequent applications. It was realised early on that the choice of a single number to present on an aggregated map posed problems. Hall (1993) presented maps of the minimum, mean, median and mode of UK empirical soil critical loads for acidity at 10 km scale, to show the very different patterns and values which resulted. The problems of aggregation were graphically illustrated in 1996, when the UK submitted three quite different sets of critical loads at 150km scale to the CCE, based on different models and assumptions (Hall *et al.* 1997). These submissions used the 5 percentile critical load, derived from ranking the critical loads and normalising by area. This averaging technique therefore calculates the value which will protect 95% of the area of ecosystems on a grid square. As a technique for generating a single number it has the advantage of avoiding dominance of the value by a few very sensitive ecosystems. However, it effectively "writes off" 5% of the ecosystem area, and takes no account of the rest of the distribution. For instance the 94% of ecosystems remaining could be totally insensitive or not very much less sensitive than the 5 percentile ecosystem, but the number would be exactly the same. These difficulties were at the root of the UK's problems with producing credible 150km critical load maps in 1996.

An elegant approach to this problem was the "accumulated exceedence" technique developed during the negotiation of the Gothenburg Protocol (Posch *et al.* 1999, 2001). The accumulated exceedance (AE) is defined as:

$$AE = \Sigma A_i Ex_i, \qquad (35)$$

where A_i is area and Ex_i is exceedence of the critical load for ecosystems i =1…N in a given grid square.

Average accumulated exceedence (AAE) is this quantity normalised by area:

$$AAE = AE/\Sigma A_i \qquad (36)$$

The aim of emission control policy then became the reduction of a certain proportion of AAE on each grid square. This then enables the entire distribution of exceedence to be taken into account, and not just exceedence of the 5^{th} percentile critical load. The approach also has technical advantages in providing a smooth damage function for optimisation procedures.

A statistical approach to presenting critical load data, for instance as cumulative distribution functions, gives more information than a bare number. Examples on both a national basis and a grid square basis can be found in Posch *et al.* (2001). This approach loses the impact of maps with coloured squares representing a single number, however.

Experiments with representing critical load data on different spatial scales show clearly that the more detailed the scale, the greater the area of low critical loads, and the greater the area of high exceedence. This should be true for any aggregating technique unless the aggregated map shows the minima of the more detailed scales. Hall (1993) demonstrated this for the UK with maps at 1, 10 and 20 km scale, and Posch *et al.* (2001) with a comparison of European maps at 50 and 150 km scale. Figure 7.1 shows the proportions of the critical load classes, which appeared in the original empirical soils critical load databases at 1 km and 10 km scales.

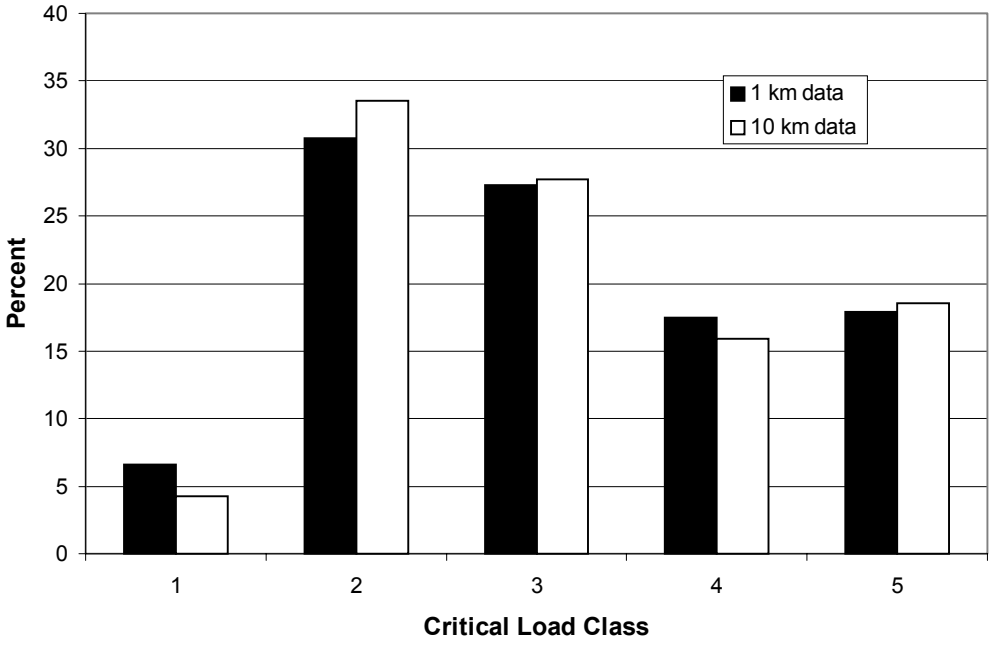

Figure 7.1. The proportions of critical load classes at two different scales

The figure shows the percentages of each of the standard critical load classes in the original empirical soils database, displayed at either 1 km and 10 km resolution. Data from ITE (now CEH).

It can be seen that at the 10km scale, the proportion of the most sensitive class is considerably less. Again, what must be considered is the appropriateness of the scale of presentation or calculation, given the policy purposes for which it is to be used.

8 Conclusions

The recent interest shown in defining the uncertainties to be attached to critical loads has borne some fruit. Uncertainty analyses have been able to place some limits on some critical load models in some circumstances. These limits usually consider only the propagation of errors in input variables through the models, rather than errors in model structure. Though these can be identified, they are much more difficult to quantify. There is still much uncertainty about the uncertainty to be attached to critical loads.

Other parts of this study (see Appendices 5 and 6) will consist of an uncertainty analysis applied to a real ecosystem. It will be possible to test some hypotheses that have developed during this literature survey.

9 References

Andersson, B.I., Skeffington, R.A., Hultberg, H. and Sverdrup, H.U. (1998) *Assessment of critical loads for coniferous forests and surface waters at Lake Gårdsjön in South-West Sweden*. In Experimental Reversal of Acid Rain Effects: the Gårdsjön Roof Project (Eds Hultberg, H. and Skeffington, R. A.), pp. 411-431. John Wiley and Sons Ltd, Chichester, England.

Barkman, A. (1997) *Applying the critical loads concept: constraints induced by data uncertainty* Reports in Ecology and Environmental Engineering 1997:1, University of Lund, Lund, Sweden.

Barkman, A. and Alveteg, M. (2001a) *Identifying potentials for reducing uncertainty in critical load calculations using the PROFILE model*. Water Air and Soil Pollution, **125**, 33-54.

Barkman, A. and Alveteg, M. (2001b) *Effects of data uncertainty in the Swedish critical load assessment for forest soils*. Water Air and Soil Pollution, **125**, 133-156.

Barkman, A., Warfvinge, P. and Sverdrup, H. (1995) *Regionalization of critical loads under uncertainty*. Water Air and Soil Pollution, **85**, 2515-2520.

Battarbee, R. W., Allott, T. E. H., Juggins, S., Kreiser, A. M., Curtis, C. and Harriman, R. (1996) *Critical loads of acidity to surface waters: an empirical diatom-based palaeolimnological model*. Ambio, **25**, 366-369.

Bobbink, R., Hornung, M., and Roelofs, J. G. M. (1996) *In Manual on Methodologies and Criteria for Mapping Critical Levels / Loads and Geographical Areas where they are Exceeded* Texte 71:96, Umweltbundesamt, Berlin.

Brakke, D.F., Henriksen, A. and Norton, S.A. (1990) *A variable F-factor to explain changes in base cation concentrations as a function of strong acid deposition.* Verhandlungen der Internationale Vereinigung für Theoretische und Angewandte Limnologie, **24**, 146-149.

Cooper, D.M., Jenkins, A., Skeffington, R.A. and Gannon, B. (2000) *Catchment-scale simulation of stream water quality by spatial mixing: theory and application*. Journal of Hydrology, **233**, 121-137.

Cresser, M.S. (2000) *The critical loads concept: milestone or millstone for the new millennium?* Science of the Total Environment, **249**, 51-62.

Cronan, C.S. and Grigal, D.F. (1995) *Use of calcium/aluminum ratios as indicators of stress in forest ecosystems*. Journal of Environmental Quality, **24** , 209-226.

Curtis, C., Allott, T., Hall, J., Harriman, R., Helliwell, R., Hughes, M., Kernan, M., Reynolds, B. and Ullyett, J. (2000) *Critical loads of sulphur and nitrogen for freshwaters in Great Britain and assessment of deposition reduction requirements with the First-Order Acidity Balance (FAB) Model*. Hydrology and Earth System Sciences, **4**, 125-140.

Curtis, C.J., Allott, T.E.H., Reynolds, B. and Harriman, R. (1998) *The prediction of nitrate leaching with the first-order acidity balance (FAB) model for upland catchments in Great Britain.* Water Air and Soil Pollution, **105**, 205-215.

Evans, C.D., Jenkins, A., Helliwell, R.C. and Ferrier, R. (1998) *Predicting regional recovery from acidification; the MAGIC Model applied to Scotland, England and Wales*. Hydrology and Earth System Sciences, **2**, 543-554.

Fuller, R.M., Groom, G.B. and Jones, A.R. (1994) *The Land Cover Map of Great Britain: an automated classification of Landsat Thematic Mapper data.* Photgrammetric Engineering and Remote Sensing, **60**, 553-562.

Goulding, K. W. T.and Blake, L. (1993) *Testing the PROFILE Model on long-term data*. In Hornung, M. and Skeffington, R. A. Critical loads: concept and applications. ITE Report 28, pp 68-73 London, HMSO.

Grennfelt, P. and Thörnelöf, E. (1992) *Critical loads for nitrogen - report from a workshop held at Lokeberg*, Sweden. Nordic Council of Ministers, Copenhagen.

Hall, J. R. (1993) *Critical loads mapping at the UK Critical Loads Mapping Centre - data requirements and presentation*. In Hornung, M. and Skeffington, R. A. Critical Loads: Concept and Applications. ITE Report 28, 74-78 London, HMSO

Hall, J., Hornung, M., Freer-Smith, P., Loveland, P., Bradley, I., Langan, S., Dyke, K., Gascoigne, J., and Bull, K. (1997) *Current status of UK critical loads data - December 1996 Report to UK Dept of the Environment,* Institute of Terrestrial Ecology, Monks Wood, Cambs.

Hall, J., Bull, K., Bradley, K., Curtis, C., Freer-Smith, P. H., Hornung, M., Howard, D., Langan, S., Loveland, P., Reynolds, B., Ulyett, J., and Warr, T. (1998) *Status of UK critical loads and exceedances January 1998. Part 1 - critical loads and critical load maps* Report to UK Department of the Environment, Institute of Terrestrial Ecology, Monks Wood, Cambs.

Hall, J, Hornung, M., Kennedy, F., Reynolds, B., Curtis, C., Langan, S., and Fowler, D. (2001a) *Status of UK critical loads and exceedances: Part 1 Critical loads and critical load maps, update to January 1998* report, CEH, Monks Wood, Cambridge.

Hall, J., Reynolds, B., Aherne, J. and Hornung, M. (2001b) *The importance of selecting appropriate criteria for calculating critical loads for terrestrial ecosystems using the simple mass balance equation*. Water, Air and Soil Pollution, Focus 1, 29-41.

Hall, J., Hornung, M., Kennedy, F., Langan, S., Reynolds, B. and Aherne, J. (2001c) *Investigating the uncertainties in the Simple Mass Balance equation for acidity critical loads for terrestrial ecosystems.* Water, Air and Soil Pollution, Focus 1, 43-56.

Henriksen, A., Fjeld, E. and Hesthagen, T. (1999) *Critical load exceedance and damage to fish populations*. Ambio, **28**, 583-586.

Henriksen, A., Posch, M., Hultberg, H. and Lien, L. (1995) *Critical loads of acidity for surface waters - can the ANC(limit) be considered variable?* Water Air and Soil Pollution, **85**, 2419-2424.

Hodson, M.E., Langan, S.J. and Wilson, M.J. (1997) *A critical evaluation of the use of the PROFILE Model in calculating mineral weathering rates.* Water, Air and Soil Pollution, **98**, 79-104.

Hodson, M.E. and Langan, S.J. (1999a) *Considerations of uncertainty in setting critical loads of acidity of soils: the role of weathering rate determination.* Environmental Pollution, **106**, 73-81.

Hodson, M.E. and Langan, S.J. (1999b) *The influence of soil age on calculated mineral weathering rates.* Applied Geochemistry, **14**, 387-394.

Högberg, P. and Jensen, P. (1994) *Aluminium and uptake of base cations by tree roots - a critique of the model proposed by Sverdrup et al*. Water Air and Soil Pollution, **75**, 121-125.

Holdren, G. R., Strickland, T. C., Shaffer, P. W., Ryan, P. F., Ringold, P. L. and Turner, R. S. (1993) *Sensitivity of critical load estimates for surface waters to model selection and regionalization schemes.* Journal of Environmental Quality, **22**, 279-289.

Hornung, M., Bull, K. R., Cresser, M., Hall, J. R., Langan, S. J., Loveland, P. J. and Smith, C. (1995) *An empirical map of critical loads of acidity for soils in Great Britain.* Environmental Pollution, **90**, 301-310.

Hornung, M., Sutton, M. A., and Wilson, R. B. (1994) *Mapping and modelling of critical loads for nitrogen - a workshop report,* Institute of Terrestial Ecology, Edinburgh, Scotland.

Jenkins, A. and Cullen, J.M. (2001) *An assessment of the potential impact of the Gothenburg Protocol on surface water chemistry using the dynamic MAGIC model at acid sensitive sites in the UK.* Hydrology and Earth System Sciences, **5**, 529-541.

Jenkins, A., .Renshaw, M., Helliwell, R. C., Sefton, C., Ferrier, R. C., and Swingewood, P. J (1997) *Modelling surface water acidification in the UK.* IH Report 131 Wallingford, Oxon.

Jenkins, A. and Reynolds, B. (2000) *Review of dynamic models for catchment and surface water acidification R and D* Technical report P246, Environment Agency, Bristol.

Kämäri, J., Forsius, M. and Posch, M. (1993) *Critical loads of sulphur and nitrogen for lakes II: Regional extent and variability in Finland.* Water, Air and Soil Pollution, **66**, 77-96.

Kernan, M., Hall, J., Ullyet, J. and Allott, T. (2001) *Variation in freshwater critical loads across two upland catchments in the UK: implications for catchment scale management.* Water Air and Soil Pollution, **130**, 1169-1174.

Kurz, D., Rihm, B., Alveteg, M. and Sverdrup, H. (2001) *Steady-state and dynamic assessment of forest soil acidification in Switzerland.* Water Air and Soil Pollution, **130**, 1217-1222.

Kuylenstierna, J.C.I., Hicks, W.K., Cinderby, S. , Vallack, H.W. and Engardt, M. (2001a) *Variability in mapping acidification risk scenarios for terrestrial ecosystems in Asian countries.* Water Air and Soil Pollution, **130**, 1175-1180.

Kuylenstierna, J.C.I., Rodhe, H., Cinderby, S. and Hicks, K. (2001b) *Acidification in developing countries: ecosystem sensitivity and the critical load approach on a global scale.* Ambio, **30**, 20-28.

Larssen, T., Schnoor, J.L., Seip, H.M. and Dawei, Z. (2000) *Evaluation of different approaches for modeling effects of acid rain on soils in China*. Science of the Total Environment, **246**, 175-193.

Lien, L., Raddum, G. G., Fjellheim, A. and Henriksen, A. (1996) *A critical limit for acid neutralizing capacity in Norwegian surface waters, based on new analyses of fish and invertebrate responses.* The Science of the Total Environment, **177**, 173-193.

Løkke, H., Bak, J., Falkengren-Grerup, U., Finlay, R. D., Ilvesniemi, H., Nygaard, P. H. and Starr, M. (1996) *Critical loads of acidic deposition for forest soils: is the current approach adequate?* Ambio, **25**, 510-516.

McLeod, A. R. and Skeffington, R. A. (1995) *The Liphook Forest Fumigation Project - an overview.* Plant, Cell and Environment, **18**, 327-335.

Nellemann, C. and Frogner, T. (1994) *Spatial patterns of spruce defoliation - relation to acid deposition, critical loads, and natural growth conditions in Norway.* Ambio, **23**, 255-259.

Nilsson, J and Grennfelt, P. (1988) *Critical loads for sulphur and nitroge*n Report 1988:15, Nordic Council of Ministers, Copenhagen.

Nisbet, T.R. (2001) *The role of forest management in controlling diffuse pollution in UK forestry.* Forest Ecology and Management, **143**, 215-226.

Ormerod, S. J. (1993) *Assessing critial loads for stream organisms using empirical data.* In Hornung, M. and Skeffington, R. A. *Critical loads: concept and applications*. ITE Report 28, 115-118 London, HMSO.

Posch, M., de Smet, P. A. M., Hettelingh, J.-P., and Downing, R. J. (1995) *Calculation and Mapping of Critical Thresholds in Europe* 259101004, RIVM, Bilthoven, The Netherlands.

Posch, M., Hettelingh, J.-P., de Smet, P. A. M., and Downing, R. J. (1997) *Calculation and Mapping of Critical Thresholds in Europe* 259101007, RIVM, Bilthoven, The Netherlands.

Posch, M., de Smet, P. A. M., Hettelingh, J.-P., and Downing, R. J. (1999) *Calculation and Mapping of Critical Thresholds in Europe* 259101009, RIVM, Bilthoven, The Netherlands.

Posch, M., de Smet, P. A. M., Hettelingh, J.-P., and Downing, R. J. (2001) *Modelling and mapping of critical thresholds in Europe*: Status Report 2001 RIVM Report 259101010, RIVM, Bilthoven, The Netherlands.

Posch, M.and Hettelingh, J.-P. (2001) *From critical loads to dynamic modelling.* In Posch, M., de Smet, P. A. M., Hettelingh, J.-P., and Downing, R. J. *Modelling and mapping of critical thresholds in Europe: Status Report 2001*. RIVM Report 259101010, pp 33-39 RIVM Bilthoven, The Netherlands,.

Reynolds, B. (2000) *An evaluation of critical loads of soil acidity in areas of high sea salt deposition.* Science of the Total Environment, **253**, 169-176.

Reynolds, B., Wilson, E. J. and Emmett, B. A. (1998) *Evaluating critical loads of nutrient nitrogen and acidity for terrestrial systems using ecosystem-scale experiments (NITREX).* Forest Ecology and Management, **101**, 81-94.

Reynolds, B. and Skeffington, R.A. (1999) *Developments in critical loads. Progress* in Environmental Science, **1**, 371-381.

Roberts, T.M., Skeffington, R.A. and Blank, L.W. (1989*) Causes of Type 1 spruce decline in Europe.* Forestry, **62**, 179-222.

Schmieman, E.C. and Van Ierland, E.C. (1999) *Dynamics of soil acidification: an economic analysis.* Ecological Economics, **31**, 449-462.

Sefton, C.E.M. and Jenkins, A. (1998) *A regional application of the MAGIC Model in Wales: calibration and assessment of future recovery using a Monte-Carlo approach*. Hydrology and Earth System Sciences, **2**, 521-531.

Skeffington, R.A. (1999) *The use of critical loads in environmental policymaking: a critical appraisal.* Environmental Science and Technology, **33**, 245A-252A.

Skeffington, R. A., Wilson, E. J., Immirzi, P., and Maltby, E. (1995) *Setting a critical load for dystrophic peat.* In Hydrology and Hydrochemistry of British Wetlands (Eds Hughes, J. and Heathwaite, A. L.), pp 183-198. John Wiley and Sons, Ltd, Chichester, UK.

Skiba, U. and Cresser, M. (1989) *Prediction of long-term effects of rainwater acidity on peat and associated drainage water chemistry in upland areas.* Water Research, **23**, 1477-1482.

Smith, C.M.S., Cresser, M.S. and Mitchell, R.D.J. (1993) *Sensitivity to acid deposition of dystrophic peat in Great Britain*. Ambio, **22**, 22-26.

Suutari, R., Amann, M., Cofala, J., Klimont, Z., Posch, M., and Schöpp, W. (2001) *From economic activities to ecosystem protection in Europe. An uncertainty analysis of the RAINS integrated assessment model* CIAM/CCE Report 1/2001, IIASA, Laxenburg, Austria.

Sverdrup, H. and Warfvinge, P. (1993) *Soil Acidification Effect on Growth of Trees, Grasses and Herbs Expressed by the (Ca + Mg + K)/Al Ratio*. Technical Report, University of Lund, Lund, Sweden.

Tao, F.L. and Feng, Z.W. (2001) *Critical loads of acid deposition for ecosystems in south China - derived by a new method.* Water Air and Soil Pollution, **130**, 1187-1192.

Tao, F.L. and Feng, Z.W. (2000) *Critical loads of SO2 dry deposition and their exceedance in south China.* Water Air and Soil Pollution, **124**, 429-438.

Tao, F.L. and Feng, Z.W. (2000) *Terrestrial ecosystem sensitivity to acid deposition in south China.* Water Air and Soil Pollution, **118**, 231-243.

Thomas, A.H. and Reynolds, B.R. (1998) *Numerical stability considerations in the simple mass balance calculation of critical loads of acidity.* The Science of the Total Environment, **217**, 257-264.

UBA (1996) *Manual on Methodologies and Criteria for Mapping Critical Levels / Loads and Geographical Areas where they are Exceeded* Texte 71:96, Umweltbundesamt, Berlin.

Ullyett, J.M., Hall, J.R., Hornung, M. and Kernan, M. (2001) *Mapping the potential sensitivity of surface waters to acidification using measured freshwater critical loads as an indicator of acid sensitive areas.* Water Air and Soil Pollution, **130**, 1235-1240.

Ulrich, B. (1983) *Soil acidity and its relations to acid deposition. In Effects of accumulation of air pollutants in forest ecosystems* (Eds Ulrich, B. and Pankrath, J.), pp 23-47 D. Reidel, Dordrecht, The Netherlands.

Van Der Salm, C. (2001) *Assessment of the regional variation in weathering rates of loess and clay soils in The Netherlands.* Water Air and Soil Pollution, **131**, 217-243.

Van Der Salm, C. and De Vries, W. (2001) *A review of the calculation procedure for critical acid loads for terrestrial ecosystems.* Science of the Total Environment, **271**, 11-25.

Warfvinge, P. and Sverdrup, H. (1992) *Calculating critical loads of acid deposition with PROFILE - a steady-state soil chemistry model.* Water, Air and Soil Pollution, **63**, 119-143.

White, C.C., Smart, R. and Cresser, M.S. (2000) *Spatial and temporal variations in critical loads for rivers in NE Scotland: a validation of approaches.* Water Research, **34**, 1912-1918.

Wilby, R. L. (1995) *Critical loads' sensitivity to climate change*. Environmental Conservation, **22**, 363-365.

Wilson, E.J., Skeffington, R.A., Maltby, E., Immirzi, P., Swanson, C. and Proctor, M.C. (1995) *Towards a new method of setting a critical load of acidity for ombrotrophic peat.* Water, Air and Soil Pollution, **85**, 2491-2496.

Zak, S.K., Beven, K. and Reynolds, B. (1997) *Uncertainty in the estimation of critical loads: a practical methodology.* Water, Air and Soil Pollution, **98**, 297-316.

Zak, S.K. and Beven, K.J. (1999) Equifinality, sensitivity and predictive uncertainty in the estimation of critical loads. Science of the Total Environment, **236**, 191-214.

Appendix 5 Liphook Critical Loads Case Study

CONTENTS

1 DESCRIPTION OF PARAMETERS USED IN MONTE CARLO ANALYSIS FOR CRITICAL LOADS

The results of the Monte Carlo analysis depend critically on the means, ranges and distribution types chosen for each parameter. Attempts were made to produce the best possible estimates, given knowledge of the Liphook site in southern England, as described below.

Abbreviations and descriptions of terms

Concentrations and fluxes are expressed in equivalence units, e.g. keq ha^{-1} y^{-1} (mol_c ha^{-1} y^{-1}).

*	refers to the non-marine contribution
dep	deposition of the substance in question, e.g.:
S_{dep}	sulphur deposition
$NO_3^-{}_{dep}$	nitrate deposition
$NH_4^+{}_{dep}$	ammonium deposition
N_{dep}	$NO_3^-{}_{dep} + NH_4^+{}_{dep}$
BC_{dep}	base cation ($Na^+ + K^+ + Ca^{2+} + Mg^{2+}$) deposition
ANC_w	acid neutralising capacity generated by weathering
Ca_w	calcium released from soil minerals by weathering
BC_u	base cation uptake into plants
Ca_u	uptake of calcium into plants
Q	runoff or effective rainfall
$[BC]_l$	limiting concentration below which plants are considered to be unable to take up base cations
Ca/Al_{crit}	critical ratio of Ca to Al in the soil solution, defining the damage threshold
K_{gibb}	Gibbsite equilibrium constant, defining the relationship between H^+ and Al concentrations in soil solution
N_i	immobilisation of nitrogen (into soil organic matter)
N_u	uptake of nitrogen into plants
N_{de}	denitrification (conversion of inorganic N into N_2 or N_2O

1.1 Sulphur Deposition

Deposition of S, N, and non-marine Cl was estimated using TRACK modelling based on 1990 emissions. Measured values are available from the site for the years 1986-90 (Skeffington and Sutherland, 1995). The TRACK estimate of dry deposition was close to that observed in net throughfall, but the wet deposition estimate from TRACK was about double that observed S in bulk precipitation. S deposition in 1990 was therefore taken to be the modelled estimate of dry deposition, plus measured wet deposition. The mean, standard deviation and distribution were obtained by re-sampling from a distribution generated from the revised means and standard deviation. Deposition in 1997 was generated by reducing deposition according to regional modelling in NEGTAP (2001), wet deposition by 41% and dry by 53%, giving an overall reduction of 48.8%. The standard deviation was reduced proportionately to the mean.

Nitrogen Deposition
A similar procedure was used to calculate nitrate and ammonium deposition. In these cases there were no measurements of dry deposition, so the TRACK estimate was used. TRACK estimates of wet deposition of both species were high compared to measured bulk precipitation values, which were used instead to calculate 1990 values. The mean, standard deviation and distribution were obtained by re-sampling from a distribution generated from the revised means and standard deviation, this time producing a log-normal distribution. To calculate deposition in 1997, estimates from NEGTAP were used, resulting in no change in wet deposition of oxidised N and a 32% decrease in dry deposition; a 15% decrease in wet reduced N deposition and 5% decrease in dry. These generated overall reductions of 17.4% and 7.7% for oxidised and reduced N respectively. Again the standard deviations were reduced in proportion.

Non-marine Chloride Deposition
The value produced by TRACK modelling (46 eq ha^{-1} y^{-1}) was close to the observed mean value (67 eq ha^{-1} y^{-1}), so a mean value of the two was used with an arbitrary standard deviation. In the absence of evidence, the deposition was not altered in 1997, though it may have declined slightly.

Total Chloride Deposition
Chloride deposition, largely derived from sea-salt, was based on the mean measured value from 1986-90. The actual mean and standard deviation employed were derived by re-sampling as above.

Base Cation Deposition
The parameters above have been assumed to be independent of each other. But base cation deposition is largely sea-salt and thus strongly correlated with total chloride deposition. It would be misleading to allow these parameters to vary independently in the Monte Carlo analysis. The relationship between the two was derived from annual bulk precipitation values at Liphook as BC = Cl*1.18; r^2=0.997, expressed in eq ha^{-1} y^{-1}. Dry deposition of base cations needed to be included to match dry deposition of the acidic species. This is a very uncertain area: an estimate of 375 eq ha^{-1} y^{-1} was obtained from maps in Draajers *et al.*1997, and hence the equation became BC = Cl*1.18 + 375. A range of ±50% was estimated for the variation of this estimate and converted to a distribution by sampling as before. The correlation coefficient used in the Monte Carlo analysis was 0.99.

Calcium Deposition
Calcium deposition was estimated from the Liphook data by an identical procedure. The equation was Ca = Cl * 0.136; r^2 = 0.991. This gave an estimate of total Ca deposition greater than that in Draajers *et al.* (1997), so no dry deposition was added. Again an estimated variation of ±50% was converted into a log-normal distribution by sampling, and a correlation coefficient of 0.99 with chloride deposition was used in the analysis.

Weathering Rates
The mineralogy of the site was investigated by S. Langan and M. Hodson with a view to calculating weathering rates with the PROFILE Model (pers. comm.). The soil proved so short of weatherable minerals that a rate close to zero was calculated. The UK empirical critical load map puts the site in the 0-200 eq ha^{-1} y^{-1} category: hence a value of 100 eq ha^{-1} y^{-1} for ANC_w was adopted. The range was adopted from that suggested by

Hodson and Langan (1999) to represent uncertainties in weathering rates. Calcium weathering was estimated to be 70% of ANC_w. Since the two are clearly correlated a correlation coefficient of 0.90 was adopted for the analysis.

Base Cation Uptake
The appropriate value here is the long-term mean over the life cycle of the forest. Since this is unmeasurable in the short-term, the default value used for coniferous tree uptake in the UK of 250 eq ha^{-1} y^{-1} was used ±50% to represent variation. Ca uptake was estimated from measurements of the trees at Liphook (Shaw and McLeod, 1995) to be 50% of this. The two uptake parameters are clearly strongly correlated, and a value of 0.99 was again employed.

Runoff
The value of *Q*, the long-term mean runoff or effective rainfall, is considered to be known within 10% under UK conditions. The absolute value was obtained from the MORECS database.

Limiting Base Cation Concentration
This is meant to represent the minimum concentration of calcium in the leaching solution which plants can absorb. This concept is not supported by any experimental evidence, but a value of 2 μeq l^{-1} is universally used, and an uncertainty range of 0-2 μeq l^{-1} has been adopted.

Critical Ca:Al ratio
This is the critical limit below which damage occurs. Cronan and Grigal (1995) suggested that a value of 1.0 ± 50% would give a 50% chance of damage, and this mean and range have been adopted here.

Gibbsite Equilibrium Constant
This expresses the relationship between dissolved H^+ and Al^{3+}. The Mapping Manual (UBA, 1996) gives the range for the Liphook soil type as 300 – 3000 m^6 eq^{-2}, which is based on a certain amount of experimental evidence. This range is therefore used converted to a log-normal distribution to weight towards low values. This range is perhaps rather narrow in view of the wide range observed in field situations (corresponding to about 10 to 10,000 m^6 eq^{-2}) though these are on a variety of soil types.

Nitrogen Immobilisation
The three N sink parameters are intended as long-term sustainable sinks rather than measurable values. Immobilisation values used in the UK (Hall *et al.* 2001) are either 71 or 214 eq ha^{-1} y^{-1} dependent on soil type. For this application the range has been extended to 350 eq ha^{-1} y^{-1} to account for some uncertainty, and because current immobilisation rates are likely to be higher.

Denitrification
The well-drained sandy soil at Liphook is unlikely to denitrify to any great extent, and hence a range of ± 50% centred on the lowest value used in UK calculation (71 eq ha^{-1} y^{-1}) has been used.

Nitrogen Uptake
As with base cation uptake, the appropriate value is the long-term mean over the life cycle of the forest. Since this is unmeasurable in the short-term, the default value used for coniferous tree uptake in the UK of 500 eq ha^{-1} y^{-1} was used, with ±50% to represent variation. As N uptake and base cation uptake are closely related to growth rates they are well correlated, and a correlation coefficient of 0.99 was used in the analysis.

2 CALCULATING EXCEEDENCE

The complexity of critical load models is such that it is by no means obvious what measure of deposition to subtract from which critical load to calculate exceedence. This section explains the approach used in this report.

Comparison with the Critical Load Function
Posch (1999) provides a set of functions for calculating exceedence. This divides the zone of exceedence into four regions depending on the values of $CL_{max}S$, $CL_{min}N$, and $CL_{max}N$. Separate algorithms for calculating exceedence are provided for each region, together with computer code for performing the calculations. This formulation would be very difficult to use within the context of our Monte Carlo analysis. Fortunately, the methods used for critical load calculation in the UK allow simplification of the Posch (1999) algorithms into a single formula:

$$Ex(S+N) = (*S_{dep} + NO_3^-{}_{dep} + NH_4^+{}_{dep}) - (CL_{max}S + (\min (CL_{min}N,\ NO_3^-{}_{dep} + NH_4^+{}_{dep})) \quad (1)$$

where the subscript *dep* represents wet and dry deposition; *S, non-marine S; and the last expression means "take the lower value of $CL_{min}N$, and $(NO_3^-{}_{dep} + NH_4^+{}_{dep})$". Alternatively, this could be expressed as "If $N_{dep}<CL_{min}N$, then $Ex=S_{dep}-CL_{max}S$, otherwise $Ex = S_{dep} + N_{dep} - CL_{max}S - CL_{min}N$".

This gives the same values as Posch (1999) without the need to define regions. However, it remains true that deposition reduction requirements will differ depending on the position of N and S deposition in relation to $CL_{max}S$ and $CL_{min}N$ e.g. if $N_{dep} < CL_{min}N$ then reduction of N deposition will have no effect on exceedence. Note also that there is no need to make alternative assumptions about the acidity produced by NH_4^+ transformations: these are already incorporated in the method. See the discussion below for the derivation of equation (1) and some alternative formulations.

Comparison with the Critical Load for Acidity
The UK also uses a critical load for acidity (Hall *et al.* 2001), defined as:

$$CL(A) = CL_{max}S + *BC_{dep} - * Cl_{dep} - BC_u \quad (2)$$

By substitution, the value for exceedence of *CL(A)* is:

$$Ex(S+N) = (*S_{dep} + NO_3^-{}_{dep} + NH_4^+{}_{dep}) - (CL(A) + *BC_{dep} - * Cl_{dep} - BC_u + (\min (CL_{min}N,\ NO_3^-{}_{dep} + NH_4^+{}_{dep})) \quad (3)$$

Although this equation has apparently got more parameters than equation (1) and thus might be expected to be subject to more uncertainty, the extra parameters are still required to calculate $CL_{max}S$, and the uncertainty is thus the same. (The value of *Ex(S+N)* given by equations (1) and (3) is of course also the same).

Comparisons with $CL_{nut}N$

Fortunately the calculation of the exceedence of the eutrophication critical load is absolutely straightforward i.e.

$$Ex\ (CL_{nut}N) = (NO_3^-{}_{dep} + NH_4^+{}_{dep}) - CL_{nut}N \qquad (4)$$

1.2 Discussion of Exceedence

Derivation

The value of exceedence in equations (1) and (3) can be derived directly from the underlying mass balance equation (see Sverdrup and De Vries, (1994); UBA, 1996; Eq 5.13)

$$S_{dep} + N_{dep} - BC_{dep} + Cl^-{}_{dep} = BC_w - BC_u + N_i + N_u + N_{de} - ANC_{le} \qquad (5)$$

The critical load is defined by specifying a critical ANC leaching $ANC_{le(crit)}$ which can be used to link chemical changes to harmful effects. Hence at critical load:

$$S_{dep} + N_{dep} = BC_w + BC_{dep} - Cl^-{}_{dep} - BC_u + N_i + N_u + N_{de} - ANC_{le(crit)} \qquad (6)$$

Because in most cases marine S ≈ marine Cl^- + marine BC, this can be expressed in non-marine form as:

$$*S_{dep} + N_{dep} = BC_w + {}^*BC_{dep} - *Cl^-{}_{dep} - BC_u + N_i + N_u + N_{de} - ANC_{le(crit)} \qquad (7)$$

This is equivalent to:

$$CL(S+N) = CL_{max}S + CL_{min}N \qquad (8)$$

from the definitions $CL_{max}S = BC_w + {}^*BC_{dep} - *Cl^-{}_{dep} - BC_u - ANC_{le(crit)}$ and in the UK, $CL_{min}N = N_i + N_u + N_{de}$.

Hence exceedence = deposition minus critical load, or

$$Ex(S+N) = (*S_{dep} + NO_3^-{}_{dep} + NH_4^+{}_{dep}) - (CL_{max}S + CL_{min}N) \qquad (9)$$

However, it must be recognised that the N sinks $N_i + N_u + N_{de}$ cannot operate unless the N is actually present, and thus the lower of the values N_{dep} and $CL_{min}N$ must be used. This gives:

$$Ex(S+N) = (*S_{dep} + NO_3^-{}_{dep} + NH_4^+{}_{dep}) - (CL_{max}S + (\min (CL_{min}N, NO_3^-{}_{dep} + NH_4^+{}_{dep})) \qquad (10)$$

which is equation (1).

Alternative Formulations

In certain European countries, the rate of denitrification N_{de} is made dependent on available N. The means that the slope of the Critical Load Function is no longer –1, but between –1 and 0, and exceedence has to be defined in a somewhat more arbitrary way. Though any point on the line still represents zero exceedence, the sum of the S and N reductions necessary to reach zero exceedence will vary depending on which point is chosen (unlike the UK method where they are the same for all points on the sloping line). Posch (1999) defined exceedence as the shortest path to the critical load function, and hence it is necessary to calculate the S and N reductions needed to reach this point. This is the reason for division of the exceeded area into 4 regions as discussed above. In the UK, the slope of –1 implies that a decrease in S deposition would be exactly countered by an equivalent increase in N deposition, provided $N_{dep} > CL_{min}N$. Where denitrification is made dependent on available N, this is no longer so and a reduction in S deposition will always be more effective in reducing exceedence than an equivalent reduction in N deposition.

High Sea-salt Areas

In high sea-salt deposition areas, the approximation represented by equation (6) may not be very good. It can be corrected by subtracting a factor of 0.008 multiplied by the *marine* chloride deposition:

$$Ex(S+N) = (*S_{dep} + NO_3^-{}_{dep} + NH_4^+{}_{dep}) - (CL_{max}S + (\min (CL_{min}N, NO_3^-{}_{dep} + NH_4^+{}_{dep}) - 0.008.(Cl^-_{dep} - *Cl^-_{dep})) \quad (11)$$

assuming units are eq ha^{-1} y^{-1}. This compensates for the ANC added by sea-salt, which is slightly alkaline.

Effect of N Transformations

A related issue is what assumptions to make about NH_4^+ transformations in the catchment. NEGTAP (2001; Section 5.5.1) calculated exceedences in two ways depending on whether NH_4^+ was assumed to contribute 1 or zero H^+ to the catchment. The differences were considerable. If exceedence is calculated by equations (1) or (3) there is no need to make assumptions about NH_4^+ transformations. Exceedence is independent of the details of N transformation in the catchment, *provided* all N inputs are either immobilised, denitrified, taken up into plants or leached as nitrate. Ammonium leaching is not allowable, normally a reasonable assumption. Ammonium deposition *must* be included when calculating exceedence of acidity critical loads. If it is not included, exceedence will be underestimated.

At first sight this seems paradoxical, because the chemical form of nitrogen affects acid production and consumption e.g. uptake of one NH_4^+ by a plant adds one H^+ to the soil; uptake of NO_3^- removes one H^+. The paradox disappears when the whole system is considered. Van Breemen, Mulder and Driscoll (1983) showed that the ANC generated by N transformations in a system was $NH_4^+{}_{out} - NH_4^+{}_{in} - NO_3^-{}_{out} + NO_3^-{}_{in}$. To calculate it, it is only necessary to know the fluxes crossing the system boundaries and not the details of internal transformations. As we assume $NH_4^+{}_{out} = 0$, the ANC generation becomes $NO_3^-{}_{in} - NH_4^+{}_{in} - NO_3^-{}_{out}$. Now suppose we set up two model ecosystems with differing chemical forms of N input, all expressed in eq $ha^{-1}y^{-1}$. In both systems, N input is 300, immobilisation is zero, uptake is 150 and denitrification is 60. The value of

$CL_{min}N$ is therefore 210 and nitrate leaching is 300-150-60 = 90. System A has NH_4^+ input of 100 and NO_3^- input of 200. It therefore generates 200-100-90 = 10 $eq.ha^{-1}yr^{-1}$ of ANC from nitrogen processes. System B has NH_4^+ input of 200 and NO_3^- input of 100. It therefore generates 100-200-90 = -190 $eq.ha^{-1}yr^{-1}$ of ANC from nitrogen processes. System A and System B generate different amounts of ANC from N transformations, hence it might be expected that the critical loads would be different. However, the ANC *inputs* to the systems are also different. The ANC input due to N deposition is (NH_4^+ - NO_3^-). System A has an input of 100-200 = -100. System B has an ANC input of 200-100 = +100. If we add the ANC input to the system to the ANC produced by the system, we get the same answer for both systems, namely –90. It can readily be seen that this would be true for any values of NH_4^+ and NO_3^- deposition. The contribution of N transformations to ANC leaching, and thus to the critical load, is the sum of ANC input and ANC production in the catchment. Hence the critical load is independent of assumptions about H^+ production during internal N transformations.

Another point to note is that $CL_{min}N$ is not the same as the *acidity* consumed by N transformations in the ecosystem; rather it is the *nitrogen* consumed. $CL_{min}N$ is the same for both System A and System B. If it were necessary to do calculations for a system in which N outputs exceeded N inputs (which at steady state would have to mean that there was some input of organic N) it would be perfectly possible, but $CL_{min}N$ would have to be allowed to go negative.

2 SENSITIVITY ANALYSIS

Table A5.1 summarises the sensitivity analyses from the Monte Carlo runs using the UK methodology. The terms have been grouped into deposition terms linked to output from atmospheric transport models, and catchment parameters. Abbreviations are explained above. The Table indicates the importance of each parameter to the overall uncertainty, expressed as a percentage fraction, given deposition in 1990 and 1997. *CL(A)* is evaluated using equation (2); $CL_{max}S$, using equation (8) of Appendix 4; $CL_{min}N$, using equation (31) of Appendix 4; $CL_{max}N$, using equation (33) of Appendix 4; and exceedence using equation (1). Zero values indicate that uncertainty in the parameter contributes <0.05% to the overall uncertainty.

Table A5.1 needs interpretation with caution because of the correlation structure of the input data. It must be remembered that correlation does not necessarily imply causation. The most outstanding example of this is $CL_{min}N$, which is the sum of the last three parameters in the table. The sensitivity analysis indicates, however, that base cation and calcium uptake (BC_u and Ca_u) have more influence on variation than immobilization and denitrification (N_i and N_{de}) which are two of these parameters. This is because BC_u and Ca_u are highly correlated (r=0.99) with N uptake, not that they themselves have any influence on $CL_{min}N$. This effect depresses the scores of N_i and N_{de} which are genuinely influential. The other correlated sets are base cation, calcium and chloride deposition ($BC_{dep,}$ $Ca_{dep,,}$ Cl_{dep}; r=0.99) and the weathering parameters (ANC_w and Ca_w; r=0.90). These must therefore be considered in groups, and other evidence also used to draw conclusions. The effects of correlated parameters are only artefacts in the sense that they do not represent causation. If the correlation structure of the Monte Carlo analysis reflects that of the real world, then the analysis will be accurate. However, there is also some uncertainty in the value of the correlation coefficients used to connect the various parameters, and this is not accounted for in the analysis.

Not all the correlation structure used in this analysis is reflected in the critical load function. The UK implementation of critical loads assumes effectively that N and base cation uptake are fixed values for any ecosystem and are unrelated to each other. If, in the real system, base cation uptake is limited by nitrogen uptake, then $CL_{max}S$ ought to increase as N deposition reduces below $CL_{min}N$, since BC_u will decrease. This reflects the fact that the BC and N uptake values used in the UK are essentially default values used for broad classes of ecosystem, and not site-specific. This source of error is to a large extent taken into account in our Monte Carlo analysis, however.

Table A5.1: Sensitivity Analysis of the Steady State Mass Balance Equation

Parameter		CL(A)		$CL_{max}S$		$CL_{min}N$		$CL_{max}N$		Exceedence	
		1990	1997	1990	1997	1990	1997	1990	1997	1990	1997
S dep	eq/ha/y	0.0	0.2	0.0	0.2	0.1	-0.1	0.0	0.2	45.2	18.1
NO_3 dep	eq/ha/y	0.0	-0.1	0.0	-0.1	0.0	0.1	0.1	0.0	6.8	5.2
NH_4 dep	eq/ha/y	-0.2	-0.1	-0.1	-0.1	0.0	0.0	-0.2	0.0	8.1	8.3
BC dep	eq/ha/y	5.1	5.3	4.9	5.4	-0.4	0.0	6.3	8.2	-4.9	-8.1
Ca dep	eq/ha/y	5.2	5.4	4.3	4.8	-0.4	-0.1	5.2	7.0	-4.2	-7.1
Cl dep	eq/ha/y	5.1	5.4	4.3	4.8	-0.4	-0.1	5.2	7.1	-4.6	-7.3
Cl*dep	eq/ha/y	0.0	-0.1	0.0	-0.1	0.0	0.0	0.0	0.0	0.0	0.1
Total Deposition		**15.6**	**16.6**	**13.6**	**15.5**	**1.3**	**0.4**	**16.9**	**22.5**	**73.8**	**54.2**
ANCw	eq/ha/y	25.5	26.2	14.2	15.0	0.0	0.0	28.9	27.3	-7.2	-14.0
Ca w	eq/ha/y	26.2	26.9	14.9	15.4	0.0	0.0	30.5	27.7	-7.8	-14.4
Bcu	eq/ha/y	-6.2	-6.4	-15.8	-15.9	28.9	29.8	0.0	0.0	1.1	1.7
Ca u	eq/ha.y	-7.1	-6.4	-16.3	-15.3	27.8	28.7	-0.1	0.0	1.3	1.6
Q	m3/ha/y	0.0	0.0	0.0	-0.1	0.0	0.1	0.0	0.0	0.0	0.0
[BCl]	ueq/l	0.0	0.1	0.0	0.1	0.0	0.0	0.0	0.0	0.0	0.0
Ca/Alcrit	mol/mol	-10.6	-10.5	-6.8	-6.8	0.1	0.0	-11.6	-11.3	5.0	9.4
Kgibb	m6/eq2	-0.5	-0.7	-0.3	-0.4	0.0	0.1	-0.6	-0.4	0.7	0.3
N immob	eq/ha/y	-0.1	0.0	0.0	0.0	8.7	8.0	8.6	8.4	-1.3	-2.4
N uptake	eq/ha/y	-8.2	-6.4	-18.1	-15.6	30.5	30.8	-0.1	0.0	1.6	1.4
N denit	eq/ha/y	0.0	0.0	0.0	0.0	2.5	2.2	2.4	2.3	-0.1	-0.6
Total Land		**84.4**	**83.6**	**86.4**	**84.6**	**98.6**	**99.7**	**82.8**	**77.4**	**26.1**	**45.8**

Table A5.1 shows that S and N deposition do not affect the uncertainty in critical load values, though of course they affect the uncertainty in exceedence. Base cation, calcium and chloride deposition have a moderate influence on critical load uncertainty, however. All three have an independent effect on $CL_{max}S$, and thus $CL_{max}N$, but only Ca deposition should affect *CL(A)*, the other two appearing because of correlation effects. This illustrates that uncertainty in deposition estimates increases critical load uncertainty to some extent.

Weathering rates, both of base cations and Ca, have a strong influence on uncertainty in the $CL_{max}S$, $CL_{max}N$, and CL(A) parameters. Weathering rates have long been recognized as a major source of uncertainty in critical load calculations. The next strongest influence is uptake of base cations, Ca and N. As already stated, the apparent influence of BC_u and Ca_u on $CL_{min}N$ is a correlation artefact, as is the influence of N_u on $CL_{max}S$ and *CL(A)*. Both BC_u and Ca_u should affect $CL_{max}S$, and it is noticeable that their contribution to variance in $CL_{max}S$ is greater than it is to CL(A), which should only be affected by Ca_u. It is interesting to note that although N_u, BC_u and Ca_u contribute to the variance of $CL_{max}S$ and $CL_{min}N$, they do not contribute to the variance of $CL_{max}N$, even though $CL_{max}N = CL_{max}S + CL_{min}N$. This appears to be a compensation mechanism whereby a negative effect on $CL_{max}S$ is compensated by a positive effect on $CL_{min}N$.

This may account for why the confidence limits round $CL_{max}N$ are narrower than those of the other parameters (Table A5.2).

The choice of critical ratio has a consistent and moderate effect on all the critical load variances, except $CL_{min}N$. The K_{Gibb} parameter has a smaller effect than in some published studies, due to the choice of a log-normal distribution over a relatively narrow range. Runoff (Q), limiting base cation concentration $[BC]_l$ and non-marine chloride deposition have no significant effect on the variance in any critical load parameter.

The influences on the variance of exceedence are rather different. In 1990, uncertainty in sulphate deposition dominated the variance in exceedence, but after the substantial reduction of S deposition between 1990 and 1997, influences were more evenly spread. Uncertainty in deposition of N species made a moderate contribution in both 1990 and 1997. In 1997, deposition and land parameters accounted for approximately the same proportion of variance in exceedence. Taking 1997 as an example, the order of influence on the variation in exceedence was sulphate deposition; weathering rates; choice of Ca/Al ratio; NH_4^+ deposition; base cation deposition; N immobilisation; BC uptake; N uptake; denitrification and K_{Gibb}.

Strictly, this analysis applies only to the Liphook site. The influence of each parameter depends on both its absolute value and the range within which it is known. These can vary both spatially and temporally. The example of exceedence in 1990 and 1997 shows that a reduction in deposition over time reduces uncertainties in deposition and makes the uncertainty in the land-based parameters relatively more important. These results can perhaps be taken as typical for sensitive areas exposed to average UK deposition levels, but further work is needed to quantify uncertainties in other situations.

3 UNCERTAINTY ANALYSIS

Table A5.2 shows the mean values of the various critical load parameters together with their standard deviations and coefficients of variation.

Table A5.2. Means, standard deviations and coefficients of variation of the predicted critical loads

	Mean, eq ha^{-1} y^{-1}		Standard deviation, eq ha^{-1} y^{-1}		Coefficient of variation, %	
Emission in year	1990	1997	1990	1997	1990	1997
CL(A)	555	557	205	205	37	37
$CL_{min}N$	783	779	171	170	22	22
$CL_{max}S$	835	861	249	251	30	29
$CL_{max}N$	1618	1640	212	225	13	14
EXCEEDENCE	830	- 44	431	331	-	-

Comparing the years 1990 and 1997 with their different depositions, changes in *CL(A)* and $CL_{min}N$ are within the range of random variation in the Monte Carlo analyses, whereas $CL_{max}N$ and $CL_{max}S$ alter slightly because of a small change in BC_{dep} between the two dates. Exceedence has however declined dramatically, and the confidence interval has narrowed (CV is not a meaningful statistic for exceedence). The confidence limits on $CL_{max}N$ are strikingly narrower because of the compensation of errors mechanism discussed above. The CVs for *CL(A)* are larger than those for $CL_{max}S$ – a somewhat counterintuitive result, because *CL(A)* is equal to $CL_{max}S$ with base cation uptake and deposition (and their uncertainties) removed from the mass balance. The standard deviations and coefficients of variation in Table A5.2 are similar to those reported by Barkman and colleagues in Swedish forest sites (see Appendix 4) even though these authors modelled variation in fewer parameters.

The uncertainty in both deposition and critical loads can be indicated approximately in pictorial form on the same graph as in Figures A5.1 and A5.2. These figures show the median values of the critical load function and the 5^{th} and 95^{th} percentile confidence limits generated by the Monte Carlo analysis. These have been generated by connecting the confidence intervals of the nodes of the CLF with straight lines. This will only be an approximation to the confidence intervals at intermediate points in the critical load function. Because the uncertainty in $CL_{max}N$ is less than that of the others, the lines are not parallel. Deposition is represented by rectangles bounded by 50^{th} and 95^{th} percentile confidence limits. These are generated from the means and standard deviations of the input data, assuming normality. For the nitrogen species, the standard deviation used to generate the confidence intervals was the square root of the sum of the variances of nitrate and ammonium deposition. This assumes S and N deposition are independent.

The diagrams illustrate graphically progress towards attaining zero exceedence and the uncertainties involved at this particular site. Deposition reduced considerably between 1990 and 1997, and it has been assumed that uncertainty reduced in proportion. In 1997, there was considerably more uncertainty on N deposition, elongating the rectangle. In 1990, it could be said with more than 95% confidence that deposition exceeded the median critical load. In 1997, the central estimate of deposition was close to the median critical load. If, however, 95% confidence is required that deposition does not exceed the critical load, the pale yellow rectangle must be brought under the red 5 percentile line. In this example, the critical loads have changed only slightly but if a greater change in base cation deposition had been included, the critical load lines would have changed position more markedly.

4 REFERENCES

Cronan, C.S. & Grigal, D.F. (1995) Use of calcium/aluminum ratios as indicators of stress in forest ecosystems. *Journal of Environmental Quality*, **24** , 209-226.

Draaijers, G. P. J., Vanleeuwen, E. P., DeJong, P. G. H. & Erisman, J. W. (1997) Base cation deposition in Europe.1. Model description, results and uncertainties. *Atmospheric Environment* , **31**, 4139-4157.

Hall, J. R., Ullyett, J., Hornung, M., Kennedy, F., Reynolds, B., Curtis, C., Langan, S., and Fowler, D. (2001) *Status of UK critical loads and exceedances Part I. Critical loads and critical load maps, update to January 1998 report*, CEH, Monks Wood, Cambs.

Hodson, M.E. & Langan, S.J. (1999) Considerations of uncertainty in setting critical loads of acidity of soils: the role of weathering rate determination. *Environmental Pollution*, **106**, 73-81.

NEGTAP (2001) *Transboundary air pollution: acidification, eutrophication and ground-level ozone in the UK*, CEH, Edinburgh.

Posch, M. (1999) Defining an exceedance function. In *Calculation and Mapping of Critical Thresholds in Europe* (Eds Posch, M., de Smet, P. A. M., Hettelingh, J.-P., and Downing, R. J.), pp. 29-32. RIVM, Bilthoven, The Netherlands.

Shaw, P. J. A. & Mcleod, A. R. (1995) The effects of SO_2 and O_3 on the foliar nutrition of Scots pine, Norway spruce and Sitka spruce in the Liphook Open-air Fumigation Experiment. *Plant Cell and Environment*, **18**, 237-245.

Skeffington, R.A. & Sutherland, P.M. (1995) The effects of SO2 and O3 fumigation on acid deposition and foliar leaching in the Liphook forest fumigation experiment. *Plant, Cell and Environment*, **18**, 247-261.

Sverdrup, H. & De Vries, W. (1994) Calculating critical loads with the simple mass balance method. *Water, Air and Soil Pollution*, **72**, 143-162.

UBA (1996) *Manual on Methodologies and Criteria for Mapping Critical Levels / Loads and Geographical Areas where they are Exceeded* **Texte 71:96**, Umweltbundesamt, Berlin.

Van Breemen, N., Mulder, J. & Driscoll, C.T. (1983) Acidification and alkalinization of soils. *Plant and Soil*, **75**, 283-308.

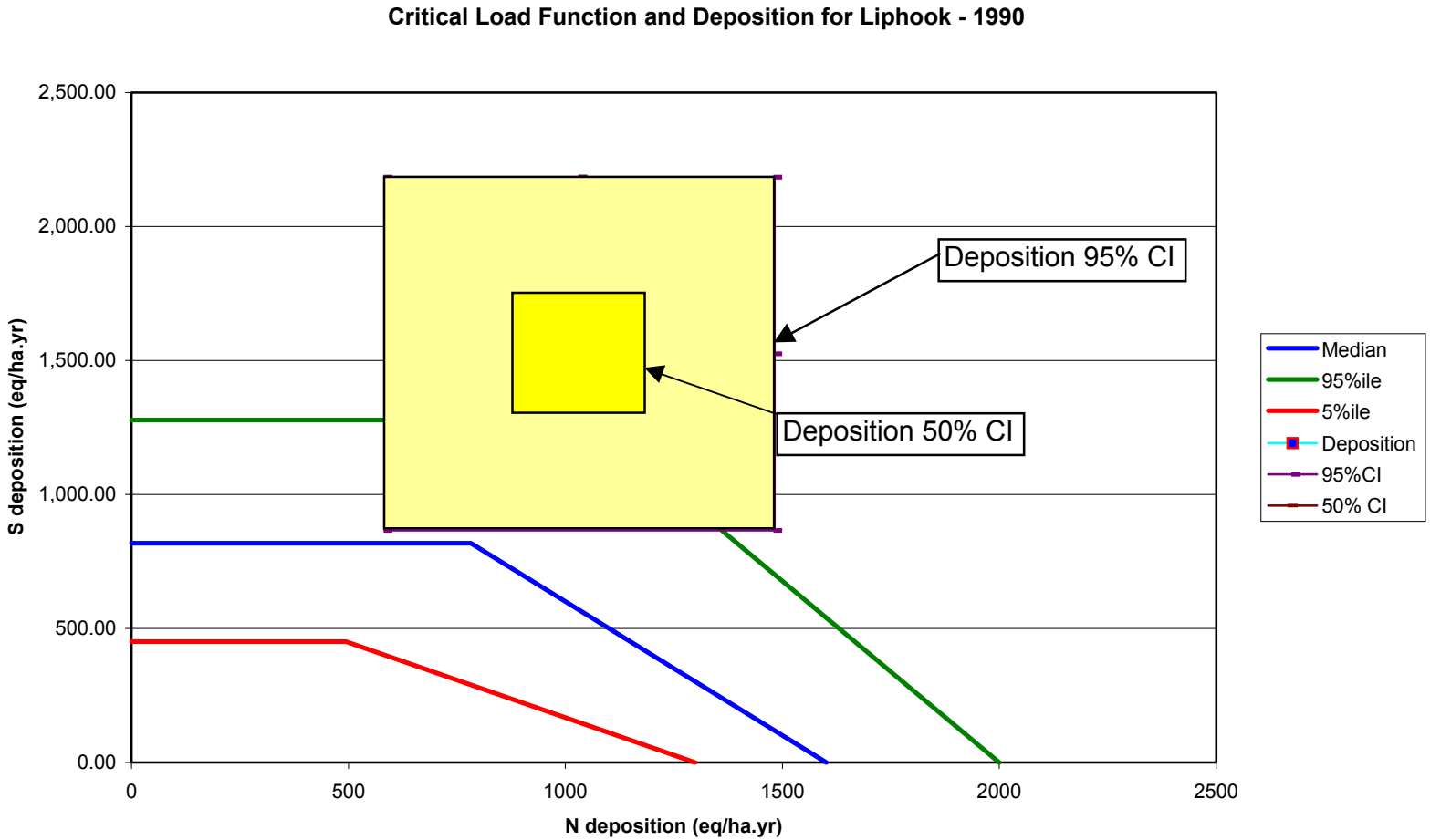

Figure A5.1 A pictorial representation of the uncertainty in both deposition and critical loads for the case of 1990.

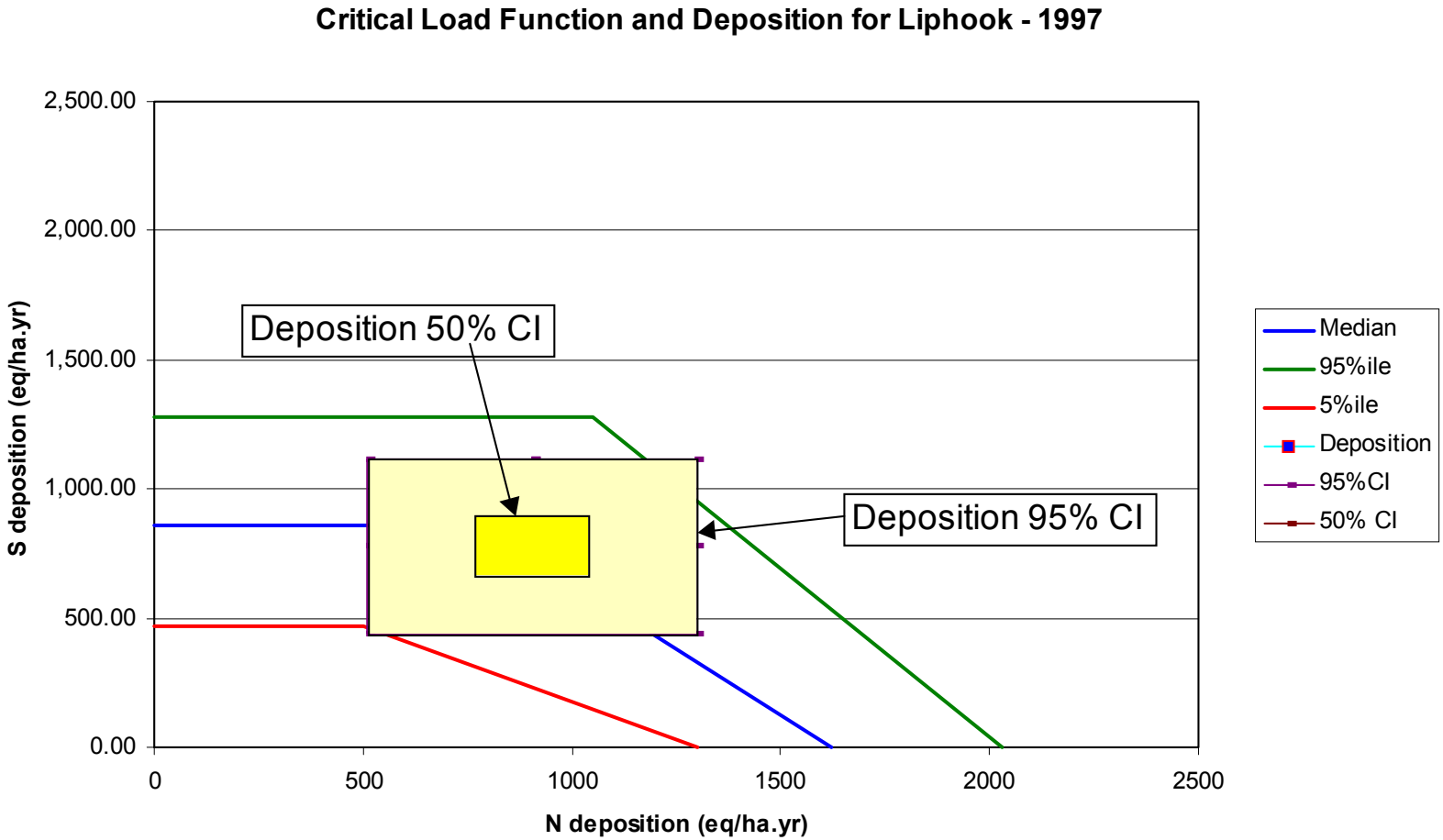

Figure A5.2 A pictorial representation of the uncertainty in both deposition and critical loads for the case of 1997

Appendix 6 Liphook critical loads case study outputs

CONTENTS

1 MONTE CARLO ANALYSIS OF EU AND UK CRITICAL LOADS AND EXCEEDENCES

In order to apply Monte Carlo (MC) analysis to the critical load equation for terrestrial ecosystems it is necessary to generate sequences of random numbers for each input in the equations. These sequences are then transformed into specified ranges with new distributions to reflect the real character of the data. For example, some variables may have a rectangular distribution, some may have a log normal distribution and some may have a triangular distribution. These data, drawn from their respective distributions, are then fed into the critical load equations to calculate the output critical loads. A large number of simulations have to be performed to generate a statistically significant output data set. This whole procedure has been undertaken using the Crystal Ball (2000) software package. This has been designed as an add-on to Microsoft Excel and utilizes an Excel spreadsheet to calculate the critical load values and the exceedences. The assumptions for all of the inputs are specified, outputs selected and the number of MC simulation trials specified. The program runs the full set of simulations to compute all of the output variables of interest. The software then undertakes a statistical analysis of the outputs as well as a sensitivity analysis to determine which parameters contribute significantly to the outputs. Before undertaking a run it is necessary to calculate the number of MC simulations required to produce a given level of accuracy. There are well known criteria based on statistical techniques for estimating the accuracy of the final output set, and the Kolomogorov statistic can be used to estimate the accuracy of the distribution. In order to achieve 95% confidence it is necessary to undertake over 750 simulations. We have chosen to conduct 1000 simulations in each Monte Carlo run.

In the first two sets of analyses, the MC technique has been applied to the critical load equation using the standard EU assumptions in which all of the base cations being deposited are considered. The main difference between the two runs are that in the first run the assumption is that most of the input distributions are uniform, as shown in Figure 6.1, whereas in the second run most distributions are assumed to be triangular, as shown in Figure 6.2. Thus the two runs give us information on the effects of differing input distribution assumptions. Figures 6.3 and 6.4 show the Monte Carlo simulation outputs in terms of the distributions of $CL_{max}S$, $CL_{min}N$ and $CL_{max}N$ for the two runs. In the case of the first run (Figure 6.3), the distributions are assumed to be rectangular with the exception of K_{gibb}, the Gibbsite equilibrium parameter. In the second run the distributions for the inputs are assumed to be triangular, reflecting the reality that atmospheric deposition and rainfall have a wide range of behaviour but are generally clustered around a mean annual value, and that therefore the value is likely to be in the centre of the distribution. The output distributions for these two runs show a wide spread of critical loads, but the spreads for the triangular distributions are smaller, indicating that the assumptions on the form of the inputs are important.

The Monte Carlo analyses for the UK version of the model all relate to the Liphook site in Hampshire. The primary difference with the EU application is that magnesium and potassium are deleted from the base cation deposition term because of the high levels of these in the UK and hence the bias that these give to any CL calculations for the UK. The results for Liphook simulation are summarised in Figures 6.5 to 6.8. These show the critical load results as well as the distribution of the exceedences for the 1990 and 1997 years. These 2 years were selected because there is a substantial data set for Liphook for

1990 and because by 1997 there was a large decline in S deposition and we can explore the effects of this reduction on exceedence. As might be expected the exceedence distributions for Liphook are relatively high in 1990 because of the high deposition of N and S for the area. However by 1997 these exceedence levels have fallen considerably.

Finally Crystal Ball can be used to investigate sensitivity analysis of each parameter in relation to the other parameters. For example Figures 6.9 to 6.11 show the relative sensitivity of the parameters specified in the critical load equation for the critical loads for sulphur and nitrogen. In each case the parameters are ranked according to their contribution to the variance and this ranking varies depending on the critical load function chosen. Thus $CL_{max}S$ has a different ranking of the parameters to the N critical loads.

Uniform Distribution: Nitrogen Immobilisation

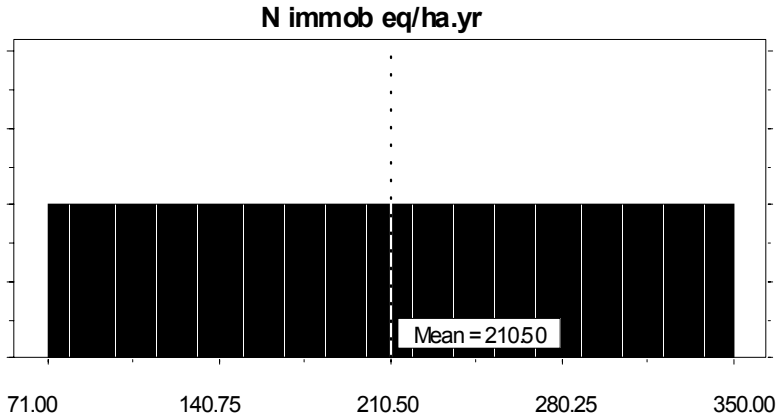

Minimum 71 eq $ha^{-1}yr^{-1}$
Maximum 350 eq ha^{-1} yr^{-1}
Mean 210.5 eq ha^{-1} yr^{-1}

Log Normal Distribution: K_{Gibb}

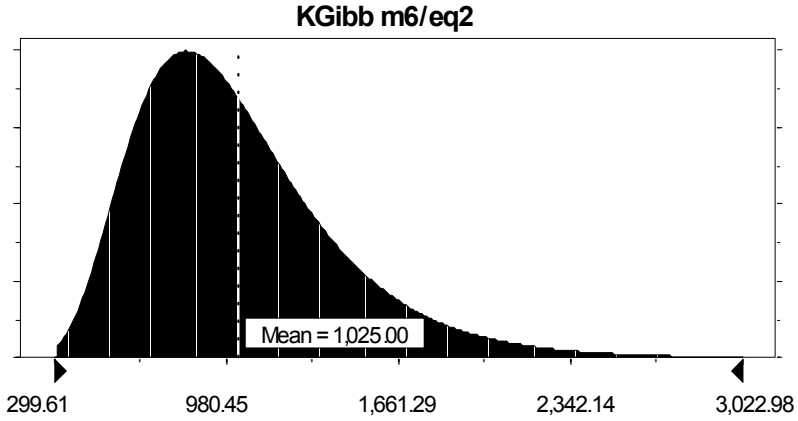

Mean 1025 m^6 eq^{-2}
Standard Deviation 410 m^6 eq^{-2}

Figure 6.1 Examples of 2 distribution types, namely uniform and log normal

Normal Distribution: S Deposition

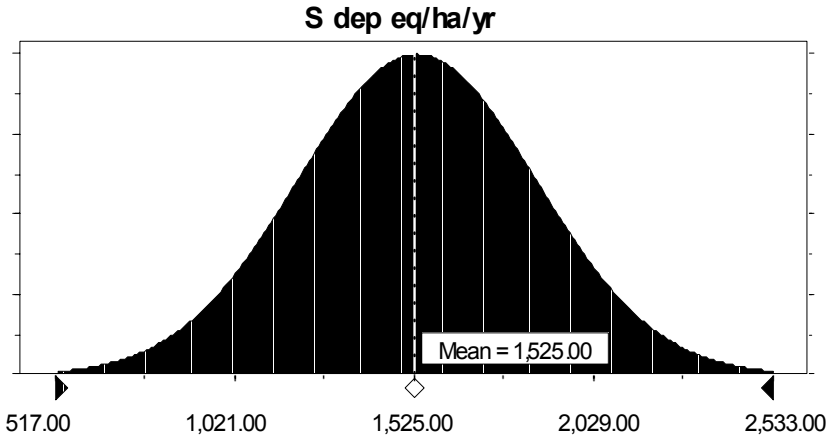

Mean 1525 eq ha^{-1} yr^{-1}
Standard deviation 336 eq ha^{-1} yr^{-1}

Triangular Distribution: Water Volume

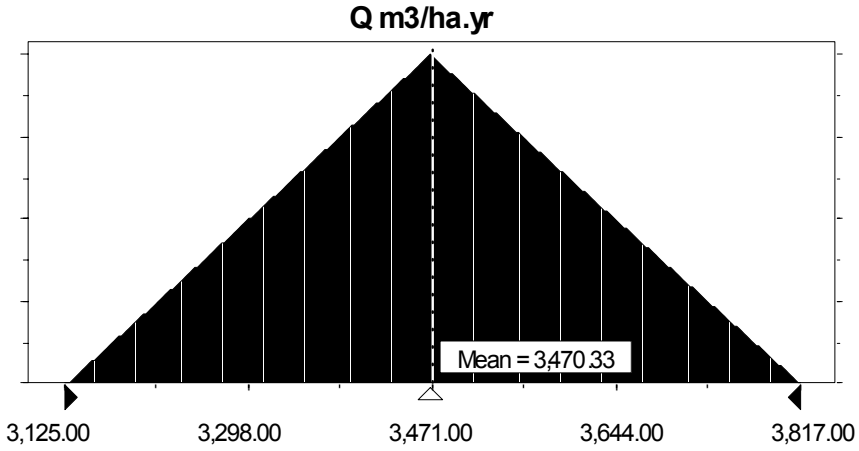

Minimum 3125 m^3 ha^{-1} yr^{-1}
Maximum 3817 m^3 ha^{-1} yr^{-1}
Most likely 3469 m^3 ha^{-1} yr^{-1}

Figure 6.2 Distribution types for run, namely triangular and normal

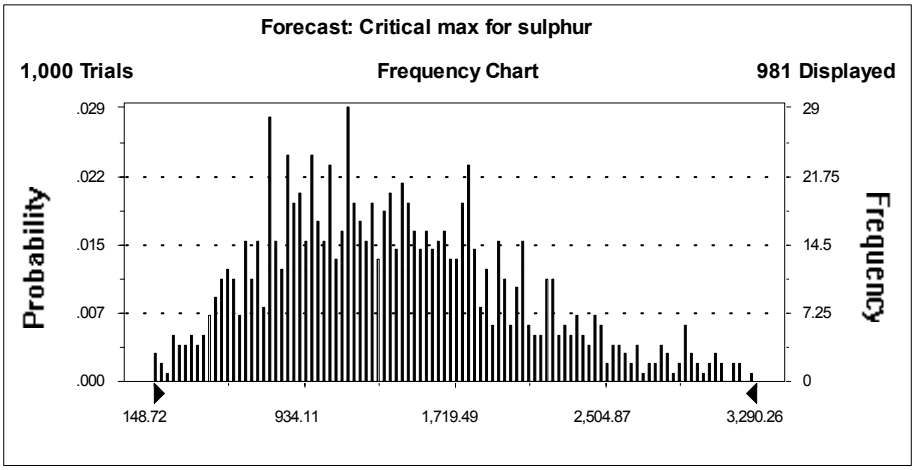

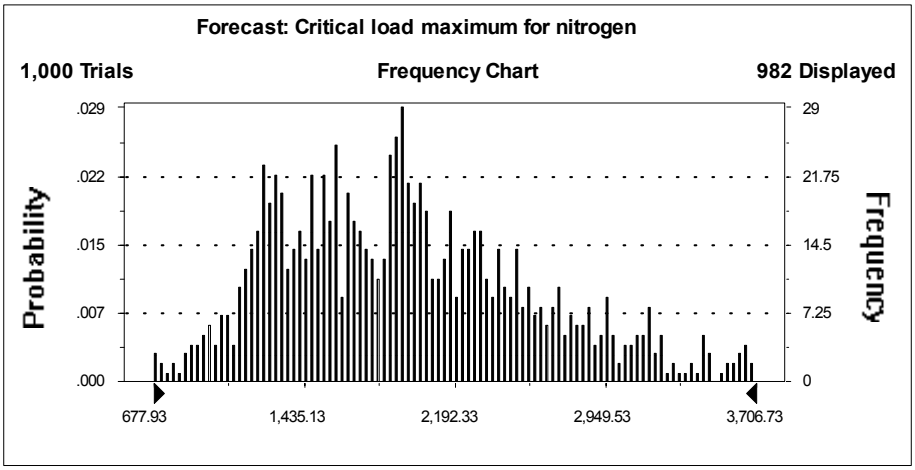

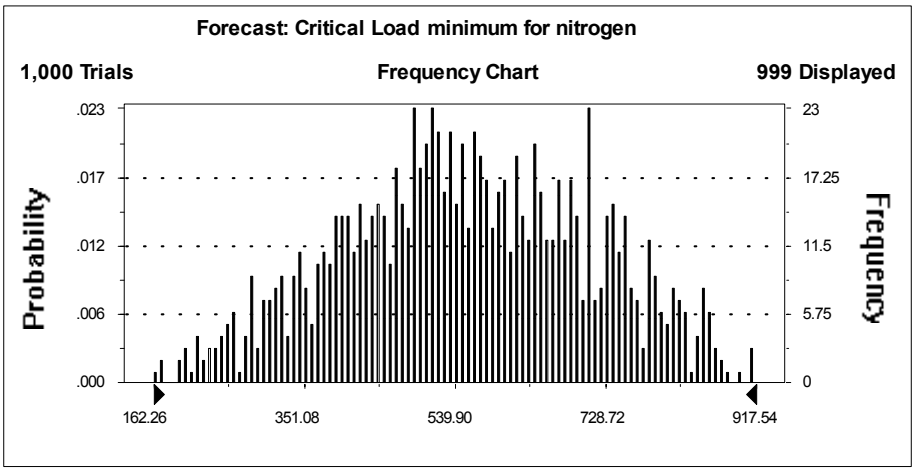

Figure 6.3 Critical Load Distributions for Sulphur and Nitrogen (EU model Monte Carlo simulation using rectangular distributions)

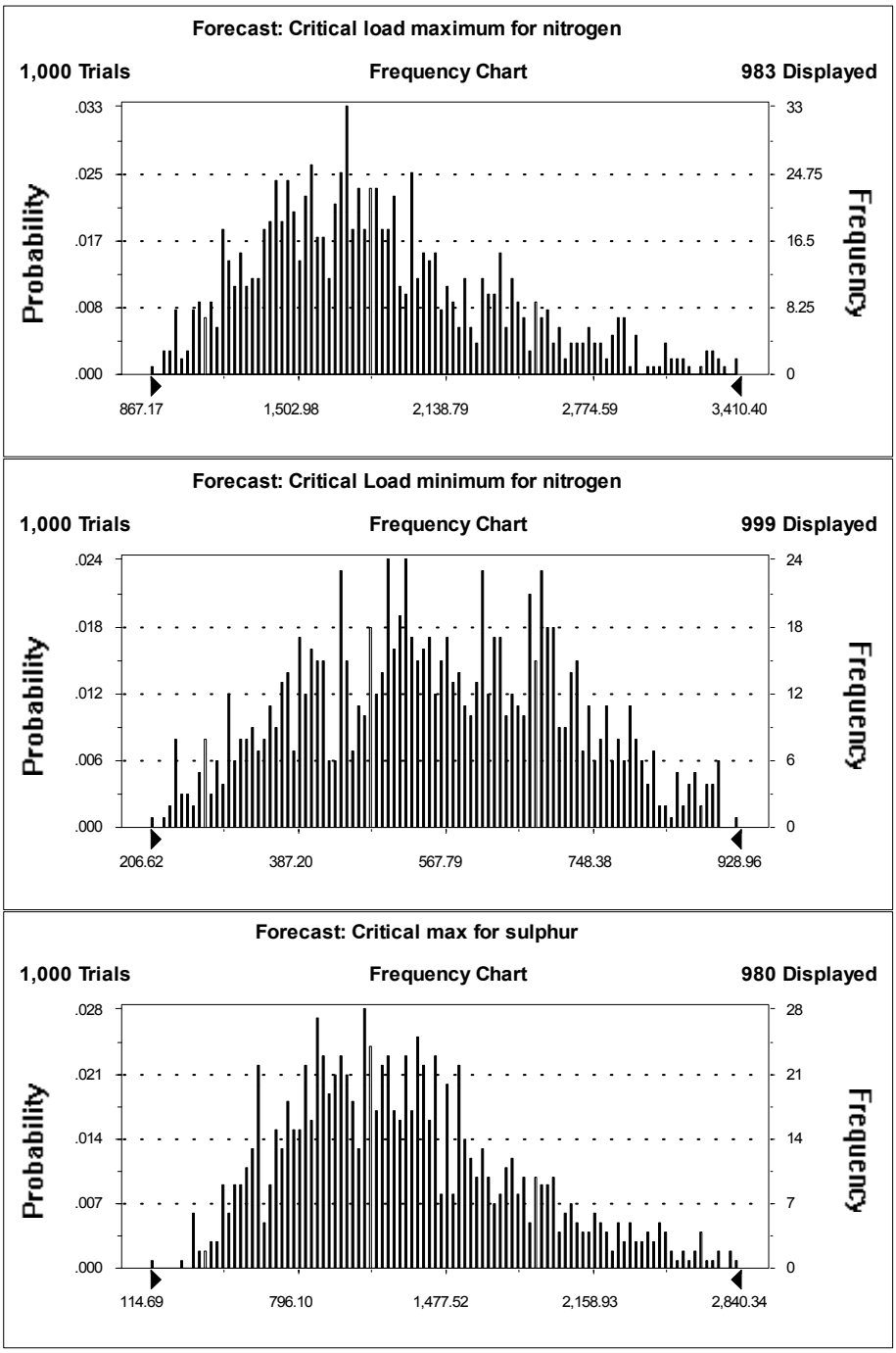

Figure 6.4 Critical Loads for Sulphur and Nitrogen for EU Monte Carlo Analysis with Triangular Distributions

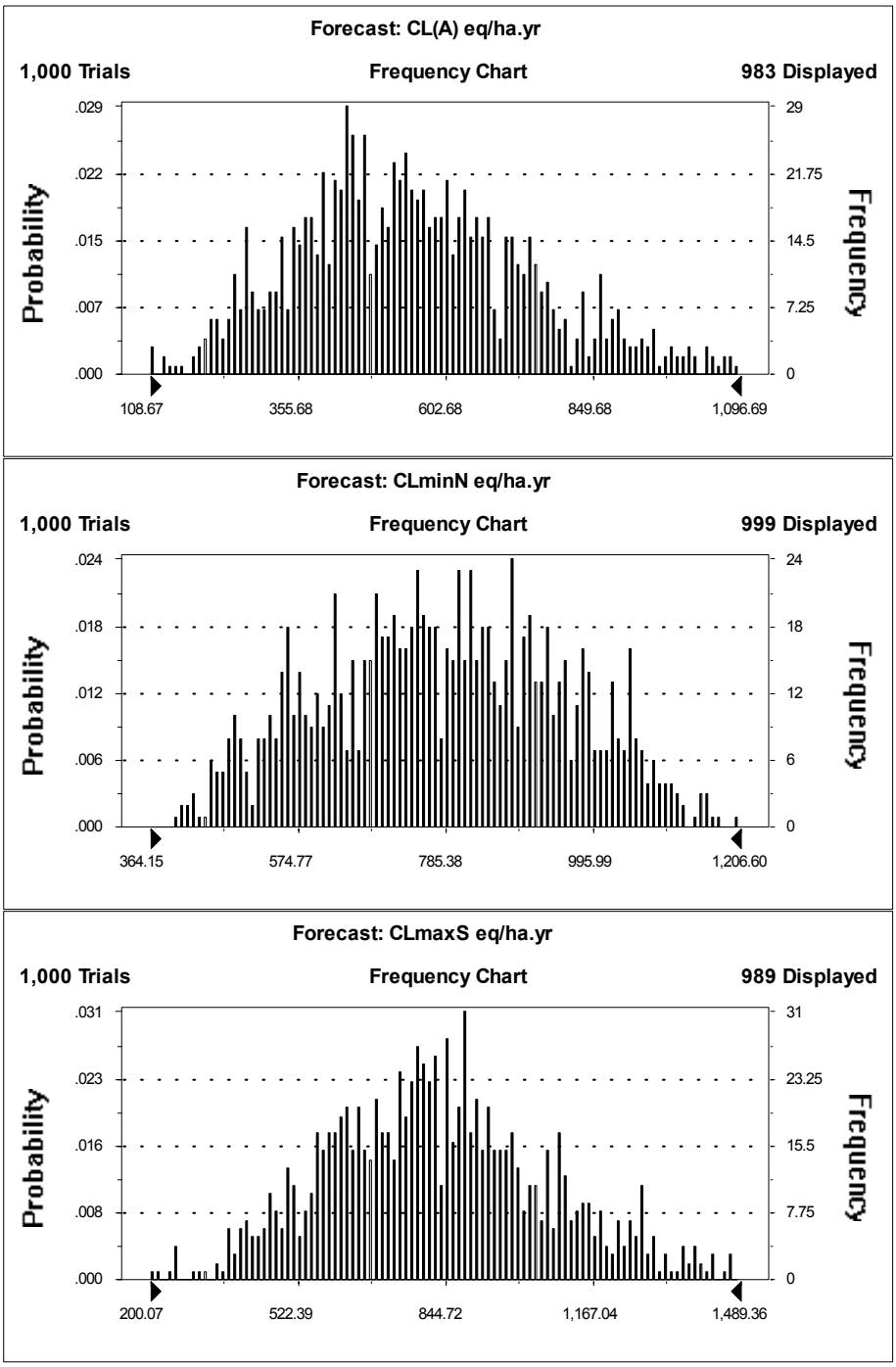

Figure 6.5 Critical Load Distributions for Liphook year 1990 (UK version of the model)

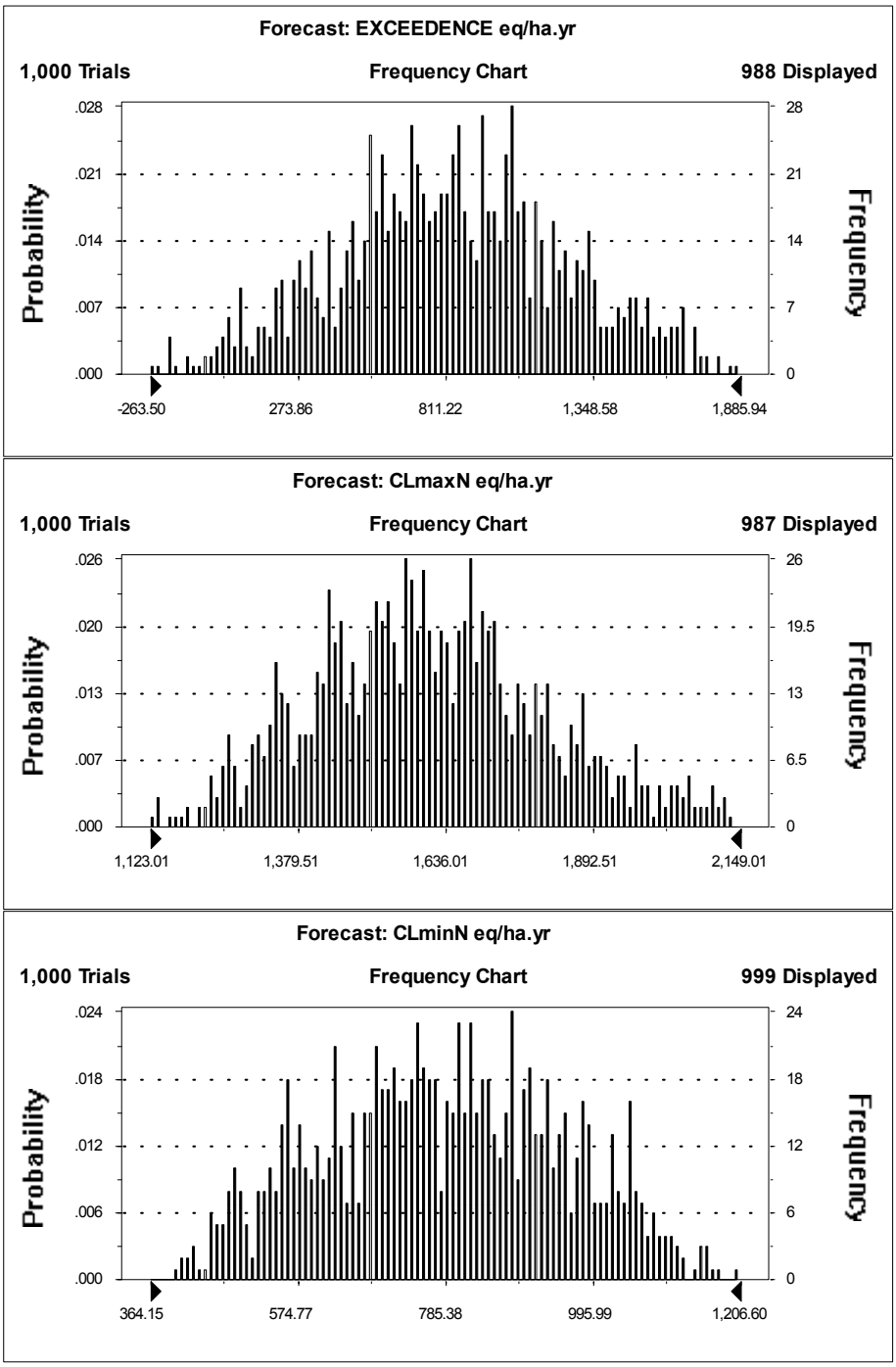

Figure 6.6 Critical Load and Exceedence Distributions for Liphook year 1990 (UK version of the model)

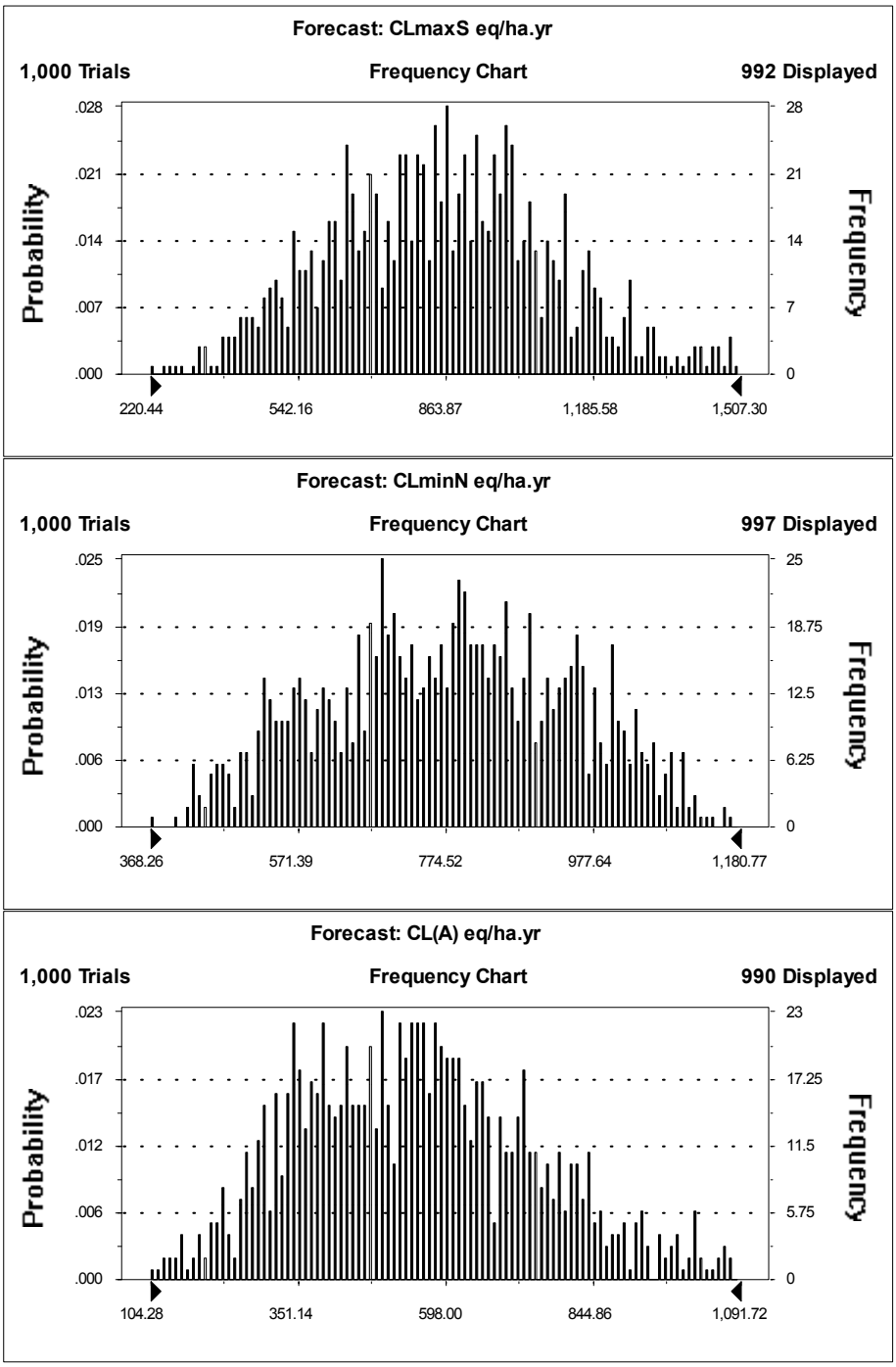

Figure 6.7 Critical Load Distributions for Liphook year 1997 (UK version of the model)

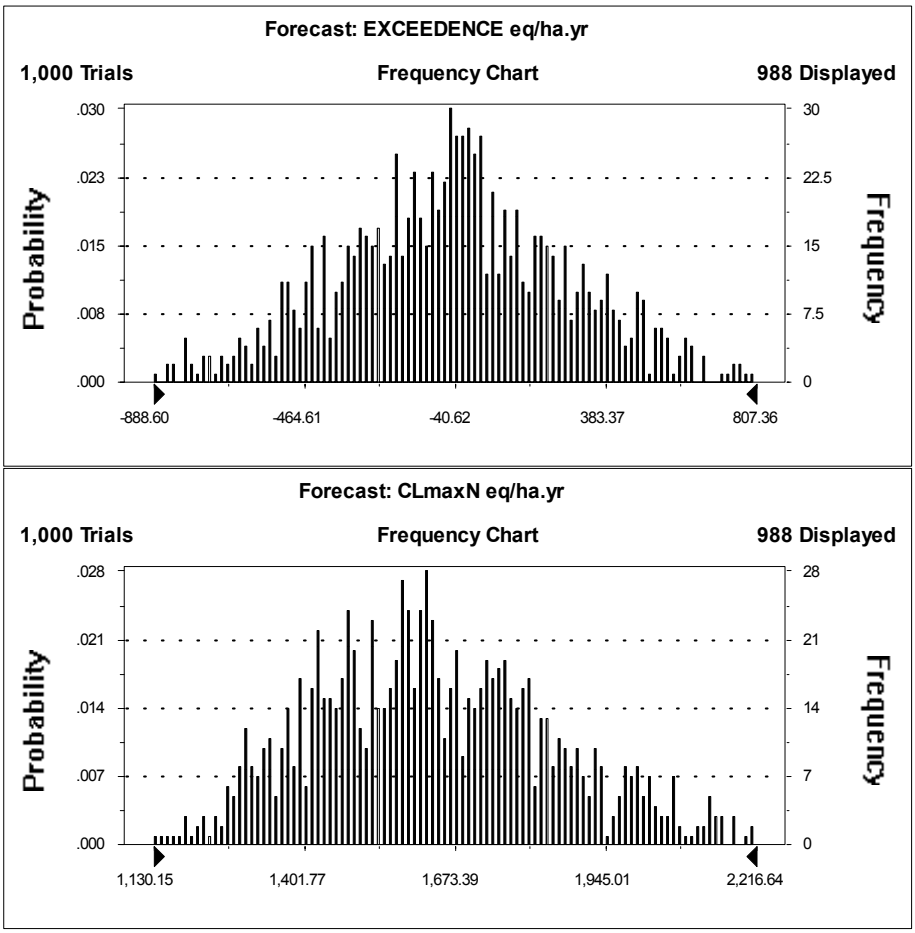

Figure 6.8 Critical Load and Exceedence Distributions for Liphook year 1997 (UK version of the model)

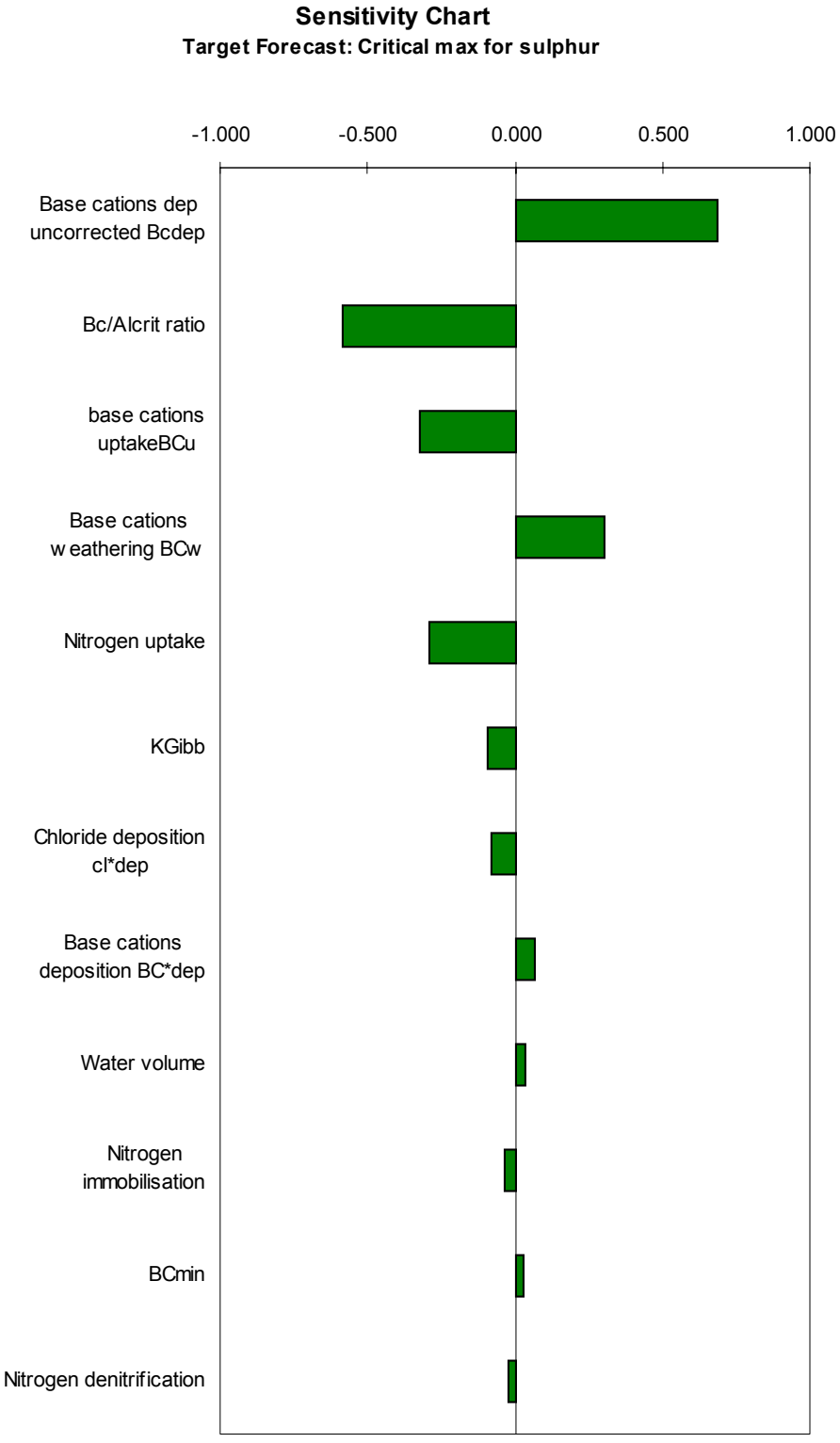

Figure 6.9 Sensitivity analysis for $CL_{max}S$

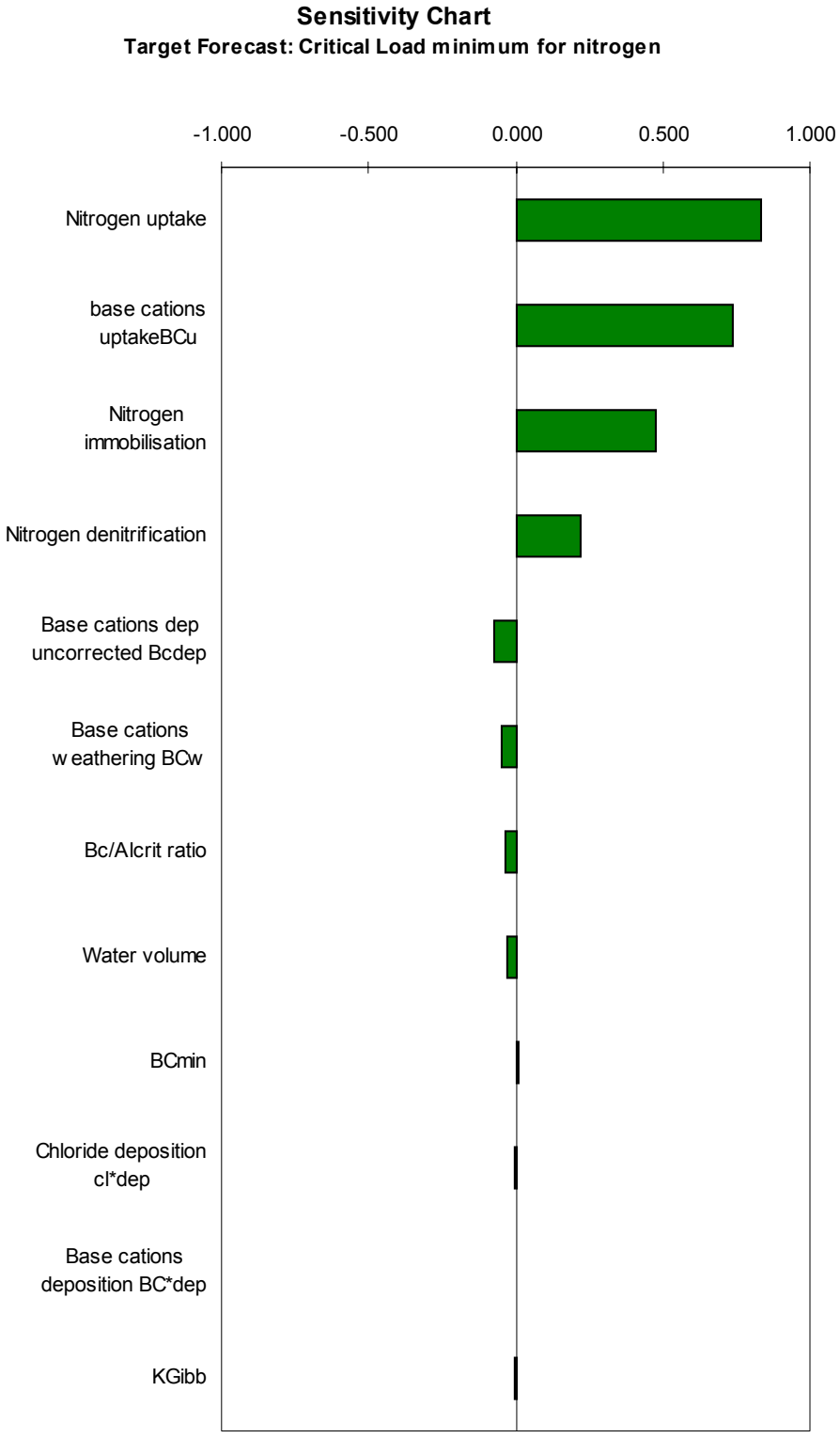

Figure 6.10 Sensitivity Analysis for $CL_{min}N$

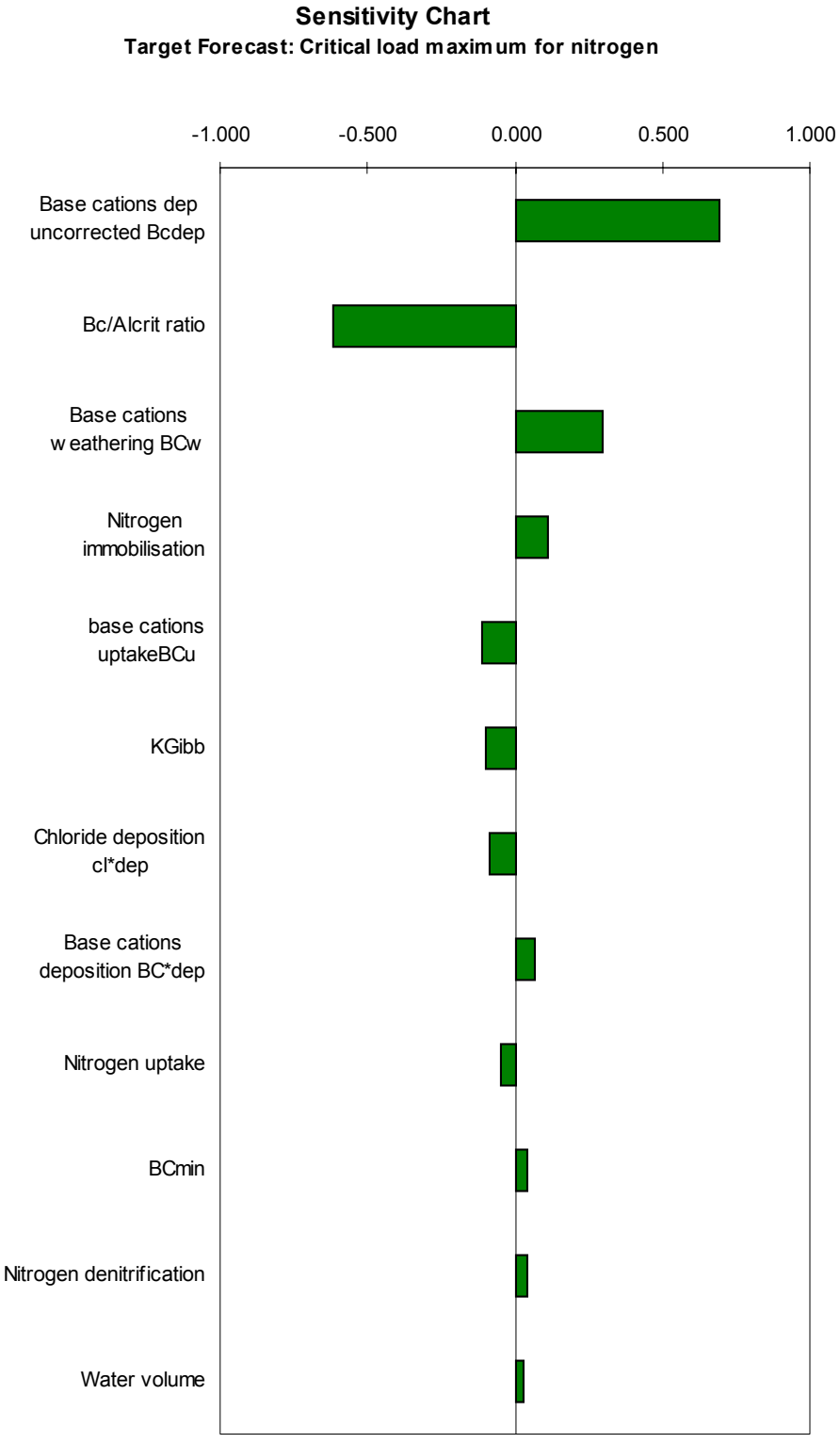

Figure 6.11 Sensitivity Analysis for $CL_{max}N$

Appendix 7 Implications of parameter variations for nitrogen deposition modelled using the HARM model

CONTENTS

FIGURES

1 Introduction

As set out in Chapter 4 of the main report, deposition model uncertainties have been assessed by (a) selecting the parameters believed to be most influential in affecting model output, (b) selecting a range of values for these input parameters and (c) running the models (TRACK, HARM and FRAME) using these values. The range of parameter values is set out in Table 4.4 in the main report. In the case of HARM and FRAME the upper parameter values were implemented one at a time (12 runs) against i) a base case of 1997 emissions, ii) 1997 emissions, plus an additional source of 75 kt NOx, and iii) 1997 emissions, plus an additional source of 150 kt NOx. A further batch of 12 model runs generated deposition with all parameters being varied and with the additional 75 kt NOx. The outcomes of both varying individual parameters and the full set of parameters display differential effects between dry and wet deposition, and hence different spatial impacts reflecting transport distance.

2 Effects of varying individual parameters

These have been explored by looking at changes in the national deposition budgets for wet and dry deposited S and N (oxidised and reduced) and by mapping some of the resulting patterns of deposition. The effects on the budget are summarised in Table 1, numbers of the model runs are shown in parentheses. Increasing the deposition velocity of NO_2 (1) has the expected effect of increasing overall dry deposition of oxidised N, although the magnitude of the effect is relatively small reflecting the greater importance of the deposition of nitric acid to the overall budget. The increase in dry deposition results in a small decrease in wet deposition. Changing the ratio of the rate of oxidation of NO to NO_2 to the reverse photolysis rate (2), affects both the oxidised and reduced N budgets to a limited extent. Larger changes are caused by varying the oxidation rates of NO_2 by OH (3) to HNO_3, and by O_3 (4) to NO_3. An increase in OH oxidation results in about a 20% increase in dry oxidised N deposition and a smaller increase in wet deposition. The resulting increase in ammonium aerosol production, via HNO_3 (3), is also reflected in more wet deposition of reduced N. The spatial implications of these changes to oxidised nitrogen deposition are illustrated in Figure 1. This shows that the increase in dry deposition under (3) occurs in a swathe from south east to north east England, close to the major source regions. The effects of increasing wet deposition, (3) and (4), occur in the upland areas of western and northern Britain. Modelled wet deposition also increases around the North and South Downs, where increasing NO_3 production feeds into more orographically enhanced wet deposition. The impact of increasing the ammonia reaction rate, with nitric acid (5), is largely confined to a reduction in dry reduced N deposition. Given the major contribution of HNO_3 to dry oxidised N deposition, the effect of increasing aerosol production (6) is unsurprising, with a decrease in dry oxidised N deposition and a smaller increase in wet deposition.

Scaling up the aerosol washout rate (7) has a substantial impact on wet deposition of all the pollutants considered (+ 20 – 26%). This effect would be amplified by the scaling of washout in HARM, as part of the representation of orographic enhancement, and would, therefore, be particularly significant in high rainfall areas of upland and western Britain.

Table 1 **Percentage difference from base case scenario for 12 parameter variations with 0, 75 and 150 kt NOx emitted from additional source**

Scenario	Added source	Dry S	Wet S	Dry NOy-N	Wet NOy-N	Dry NH-N	Wet NH-N
(1) vd NO2	0	0	0	+9	-0.3	0	-0.05
	75	0	0	+9	-0.3	+0.01	-0.05
	150	0	0	+9	-0.3	0	-0.03
(2) k1/J1	0	0	0	-4.6	-2.8	+0.02	-1.0
	75	0	0	-4.8	-2.8	+0.02	-1.0
	150	0	0	-4.9	-2.8	+0.02	-1.0
(3) k[NO2] [OH]	0	0	0	+19.6	+4	-0.2	+8.5
	75	0	0	+19.9	+4.2	-0.2	+8.5
	150	0	0	+20.1	+4.3	-0.2	+8.5
(4) k[O3] [NO2]	0	0	0	-8.7	+12.5	0	-3.8
	75	0	0	-8.5	+12.2	0	-3.8
	150	0	0	-8.4	+12.2	0	-3.8
(5) k[NH3] [HNO3]	0	0	0	-0.4	+0.2	-4.9	-0.5
	75	0	0	-0.4	+0.2	-4.9	-0.5
	150	0	0	-0.4	+0.2	-4.9	-0.5
(6) k[NH3]	0	0	0	-8.9	+2.7	+0.1	-1.7
	75	0	0	-8.92	+2.7	+0.1	-1.7
	150	0	0	-8.92	+2.7	+0.1	-1.7
(7) washout A	0	-1.9	+25.9	-9.7	+20.4	+1.7	+22.4
	75	-1.9	+25.9	-9.7	+20.6	+1.7	+22.5
	150	-1.9	+25.9	-9.7	+20.6	+1.7	+22.5
(8) vd HNO3	0	0	0	+17.3	-3	+0.09	-1.4
	75	0	0	+17.4	-3.1	+0.09	-1.4
	150	0	0	+17.4	-3.1	+0.09	-1.4
(9) ES02	0	+50	+49.9	+4.4	-1.6	-1.5	+14
	75	+50	+49.9	+4.3	-1.6	-1.5	+13.9
	150	+50	+49.9	+5.8	-1.6	-1.5	+13.9
(10) ENH3	0	0	0	-6.8	+2.3	+45.9	+16.2
	75	0	0	-6.8	+2.3	+45.9	+16.2
	150	0	0	-6.8	+2.3	+45.9	+16.3
(11) ENOx	0	0	0	+20.7	+16	-0.1	+5.4
	75	0	0	+20.5	+15.9	-0.1	+5.4
	150	0	0	+20	+15.8	-0.1	+5.3
(12) H	0	-9.5	+2.5	-8.6	+2.7	-9.5	+1.9
	75	-9.5	+2.5	-8.6	+2.7	-9.5	+1.9
	150	-9.5	+2.5	-8.6	+2.8	-9.5	+1.9

Given the significance of HNO_3 to the national oxidised N budget described above, it is unsurprising that scaling up the deposition velocity of HNO_3 (8) has quite a large impact. The spatial effect of this is illustrated in Figure 2. The pattern of increase in dry oxidised N deposition is very similar to that under (3) (see Figure 1), which is not surprising as these two parameter changes are doing very similar things. In the case of

(8), however, the actual deposition of more HNO_3 has the effect of reducing wet oxidised N deposition. There is a knock-on effect of this change on the reduced N budget through the reaction of NH_3 with HNO_3, leaving slightly more NH_3 to be dry deposited and reducing wet ammonium deposition.

As might be expected, varying the emission rates (up by 50% under (9), (10) and (11)) has a significant effect on deposition. The change in S deposition is linear with the change in emission, but it should be noted that the chemical coupling with ammonia results in an increase in wet deposition of reduced N. Hence the combined effect of increasing S emissions is greater in wet deposition dominated areas than in dry. The change in NH_3 emission results in a large increase in dry reduced nitrogen deposition, but a smaller increase in wet deposition. The spatial expression of this is illustrated in Figure 3. The change in dry reduced N deposition is roughly proportional to the change in emission close to source reflecting the short transport distance of this pollutant. The change in ammonia emission also has some impact on the oxidised N budget as more nitric acid is 'mopped up' by the ammonia as under (5). This reduces dry oxidised N deposition through eastern England. Changing NOx emissions results in an increase in dry deposition of 20 – 21%, and an increase in wet deposition of about 16%. The increase in dry deposition is linear with the change in emission, while the difference in wet deposition reflects some non-linearity in the oxidised N (see EA Technical Report P276).

Increasing the boundary layer height (12) in a model, which assumes instantaneous mixing, has the expected effect of reducing dry deposition and increasing wet deposition for all pollutants. This would be reflected by less deposition in source regions and more in remote areas.

3 Effects of varying multiple parameters

As described above, HARM has also been run varying all 12 parameter values simultaneously. In this case, parameter values were set both higher and lower than the default value. The effects of this have been explored by looking at changes in wet and dry deposition of oxidised and reduced nitrogen at the UK's 32 Secondary Network sites, plus the former network site of Liphook (see Chapter 6). The magnitude of change at some of these sites, compared with the base case (i.e. parameters set to their usual values) is shown in Figure 4. As suggested by Figures 4.27 and 4.28 in the main report, the magnitude of variability is greater at the more polluted sites (most of England, excluding the south west, and much of Wales). The cleaner sites, such as Strathvaich Dam and Alt a Mharcaidh, show less variability. Within this general pattern, however, there are some interesting spatial variations between wet and dry deposition and indeed in overall behaviour compared with the base case run. The four most north westerly sites (Achanarras, Strathvaich Dam, Alt A Mharcaidh and Polloch) stand out from the rest because the mean deposition from all 12 sets of parameter variations in less than the deposition under the base (control) case. Across the rest of the UK, the mean of the variants is higher than the base case. This may suggest that for these clean sites the models are more likely to overestimate deposition than underestimate, whereas for the rest of the country the reverse is true. We must, however, bear in mind that some key parameters for these upland sites (e.g. wind speed, precipitation amount) were not included in this analysis. Overall, the increases in deposition with different parameter sets were substantially larger than the decreases. Only two sites were the exception to

this: Strathvaich Dam and Polloch, where reductions in wet deposition of reduced and oxidised N were the largest changes recorded.

The dominant pollutant showing an increase in deposition under the various parameter sets is illustrated in Figure 5. This indicates some different regional behaviour, with changes in reduced N deposition dominating in most areas apart from eastern England. In eastern England, the largest increases were in wet oxidised and reduced N deposition. Outputs for all the sites in this area showed very similar behaviour and are illustrated by the charts for Thorganby and Barcombe Mills on Figure 4. There was then a group of sites across north west England, Wales and western Scotland, where the largest changes were in wet and dry reduced N deposition. The results from Llyn Brianne (Figure 4) are an example of this. In other areas, including south west England, Northern Ireland, north east England and much of Scotland, the largest changes were in dry reduced N deposition (e.g. Goonhilly, Hillsborough Forest and Achanarras on Figure 4). A pattern common across the whole of the UK was that increases in dry deposition of oxidised N were small.

With the exception of Polloch and Strathvaich Dam (see above), decreases in deposition under multiple parameter variations were of minor importance. This is clearly illustrated by Figure 4. The pollutants showing the most negative change are shown in Figure 6. Changes in oxidised N deposition (both wet and dry) are the largest element of any decrease across most of England and southern Wales. This area affected by changes in oxidised N is more extensive than the area which showed an increase in wet oxidised N deposition. Under these parameter sets the magnitude of the decrease in dry oxidised N deposition was greater than the magnitude of any increase. Only the results from Achanarras, in the far north east of Scotland, were the exception to this. The site at Strathvaich Dam also shows its largest change in wet oxidised N deposition (followed by wet reduced N), although the magnitude of any change here is small. The rest of the UK shows the largest decreases in deposition of wet and/or dry reduced N.

Based on the results of varying 12 model parameters simultaneously, it appears that for most of the UK HARM may be underestimating N deposition (oxidised and reduced) due to uncertainties in the values assigned to these parameters. This may also be true for the other models used in this exercise (TRACK and FRAME), but their results have not be explored in an equivalent manner. Only at the cleanest sites are uncertainties likely to mean that the standard model overestimates. Except in central and eastern England, where oxidised N deposition is most variable under the different parameter sets, most of the uncertainties in deposition are related to the representation of reduced N. This pattern needs to be considered in the light of whether reduced or oxidised N dominates the N budget in different areas. Changes in S deposition have not been considered.

If oxidised and reduced N deposition (total N) are taken together and considered at the national scale, then the full impact of the parameter variations can be seen. Figure 7 shows total N deposition for the base case, and then for the parameter sets producing minimum and maximum N deposition. The UK budgets are compared in Table 2.

Table 2 **Total N deposition (oxidised and reduced) (in kt N) under the base case and minimum and maximum values from 12 parameters varied simultaneously**

	Base	Minimum	Maximum
Total wet N	179.2	137.9	321.1
Total dry N	104.5	119.3	174.3
Total N	283.7	257.2	495.3

The lowest modelled deposition yields a total, which is 90.7% of the base case, while the maximum modelled total is 174.6% of the base case. As indicated above, the chosen parameter variations generally lead to more deposition than the base case (11/12 runs). Assuming that the uncertainties reflected in these parameter sets are reasonable, then there are major implications for the calculation of critical loads exceedence.

There are clearly two sets of issues which this exercise has not addressed: the significance of other parameters, not included in the overall analysis, and how far the HARM model (or the other models) is actually able to reproduce the patterns of deposition mapped, using data from the UK measurement networks. As a result of the latter, any inherent under or overestimation of deposition by the model cannot be taken into account in this analysis.

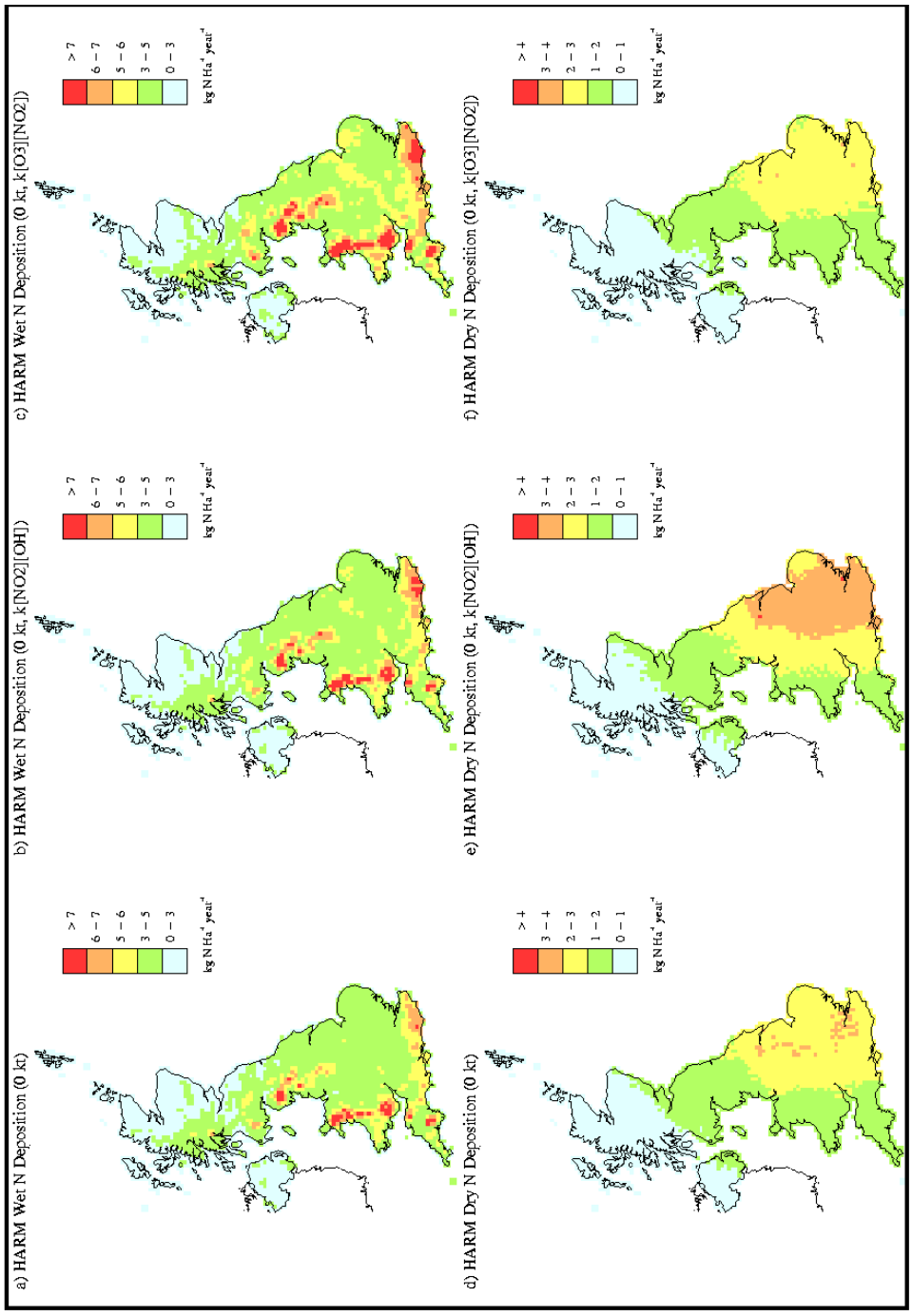

Figure 1 **Changes in the deposition of oxidised N caused by varying the oxidation rates of NO_2 by OH (b,e) and by O_3 (c,f)**

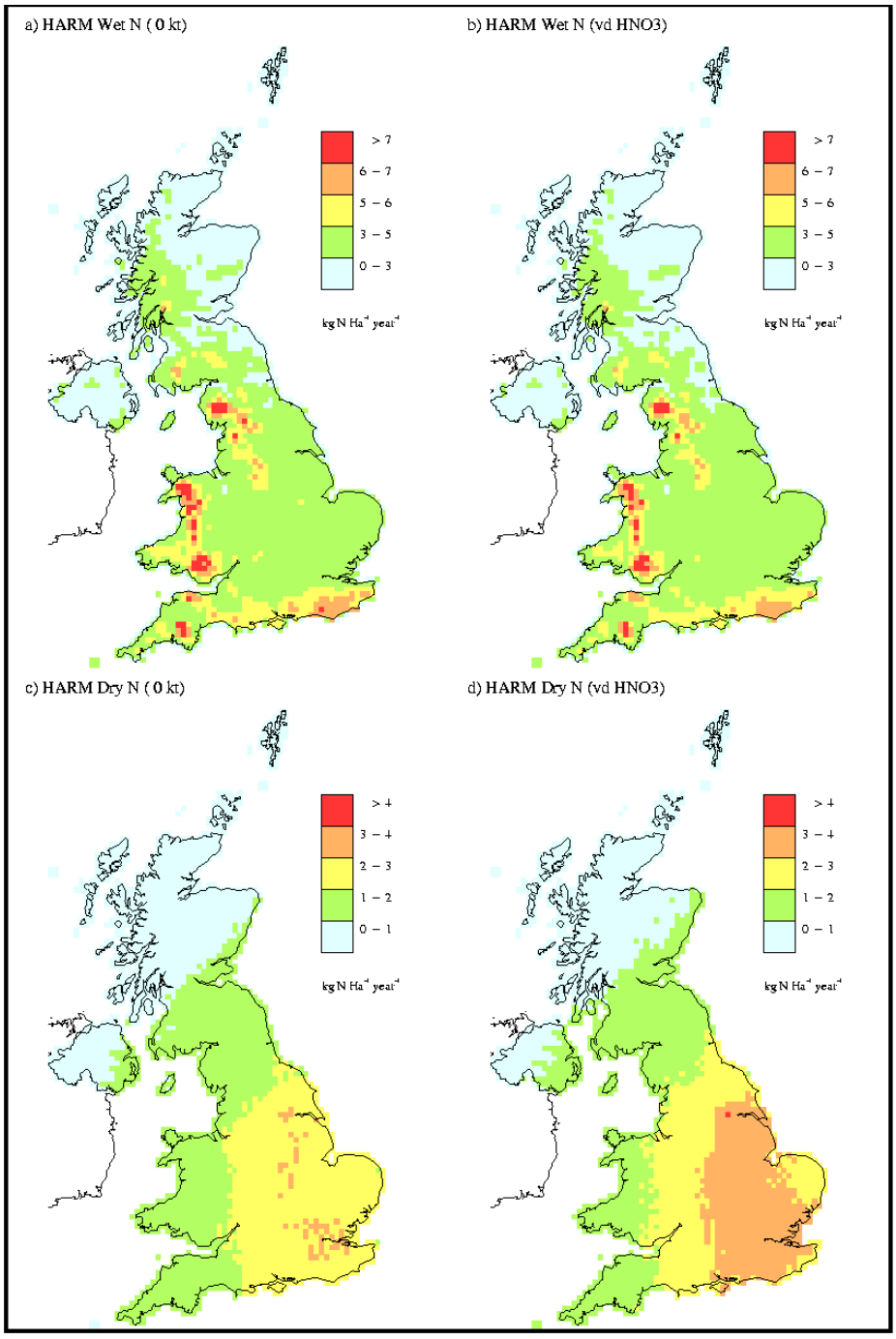

Figure 2 **Changes in oxidised N deposition with scaling the deposition velocity of HNO_3**

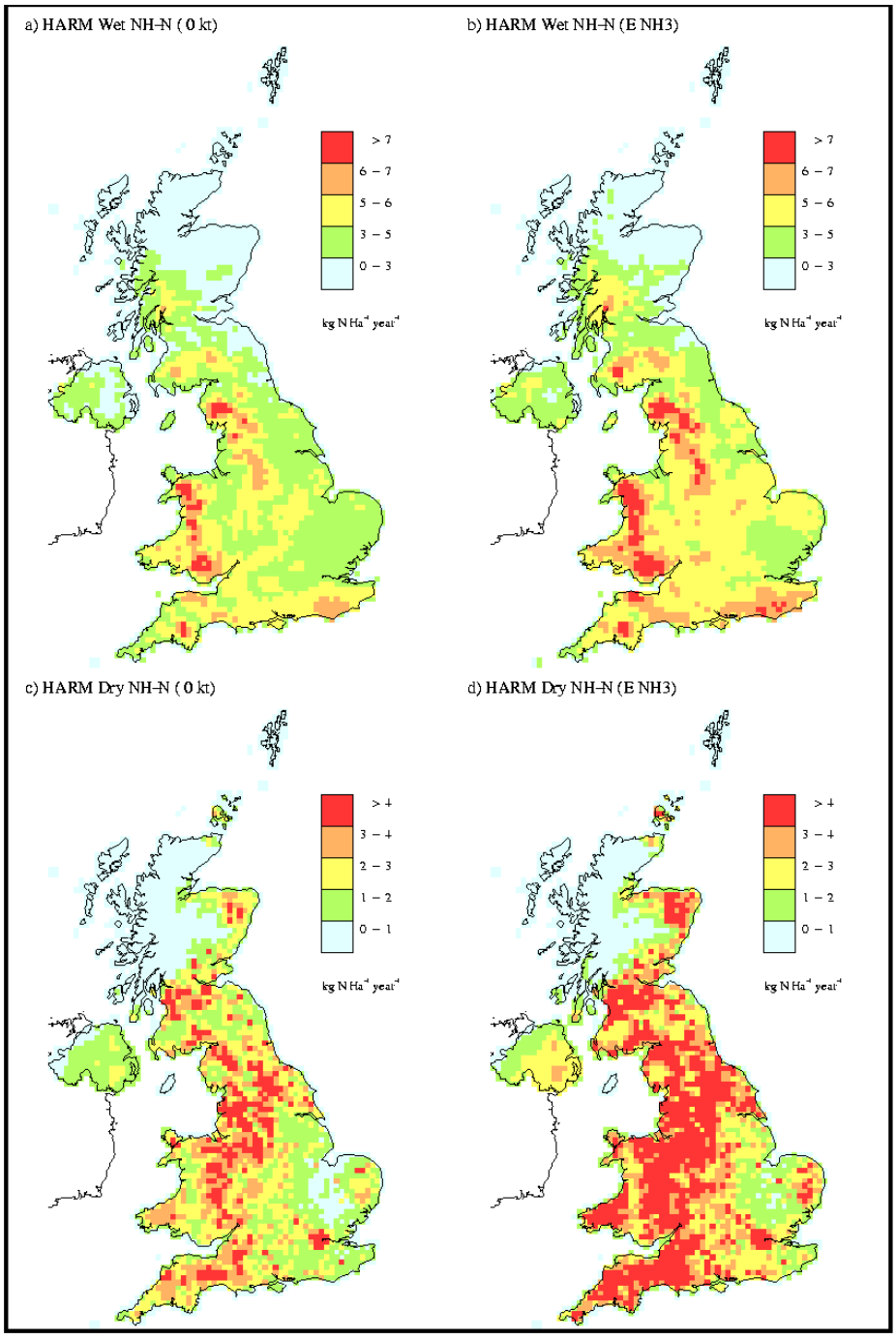

Figure 3 Changes in reduced N deposition with scaling of NH_3 emissions

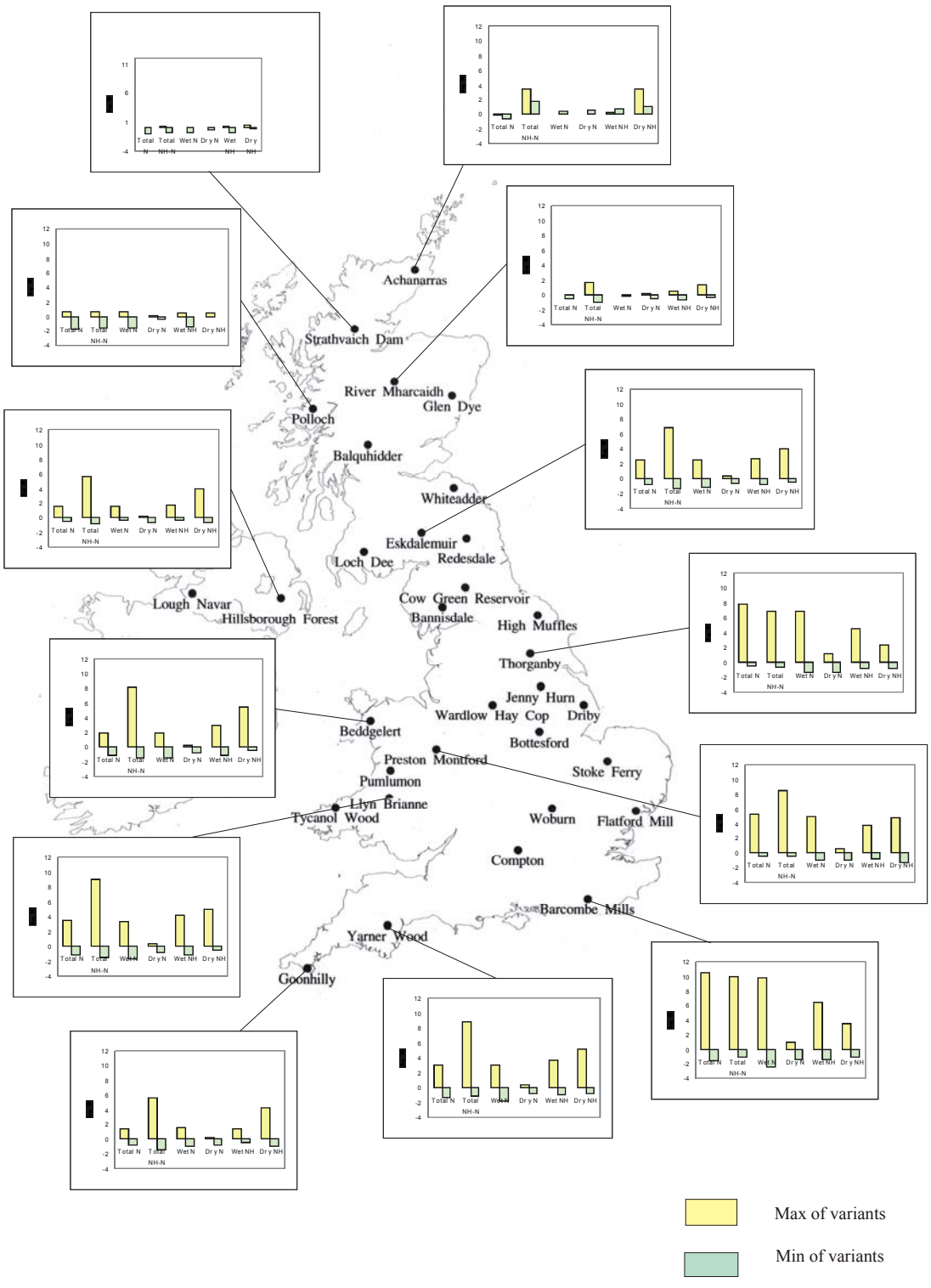

Figure 4 **Maximum and minimum values of N deposition at selected Secondary Network sites varying all 12 parameter values, compared with the value from the appropriate base case scenario**

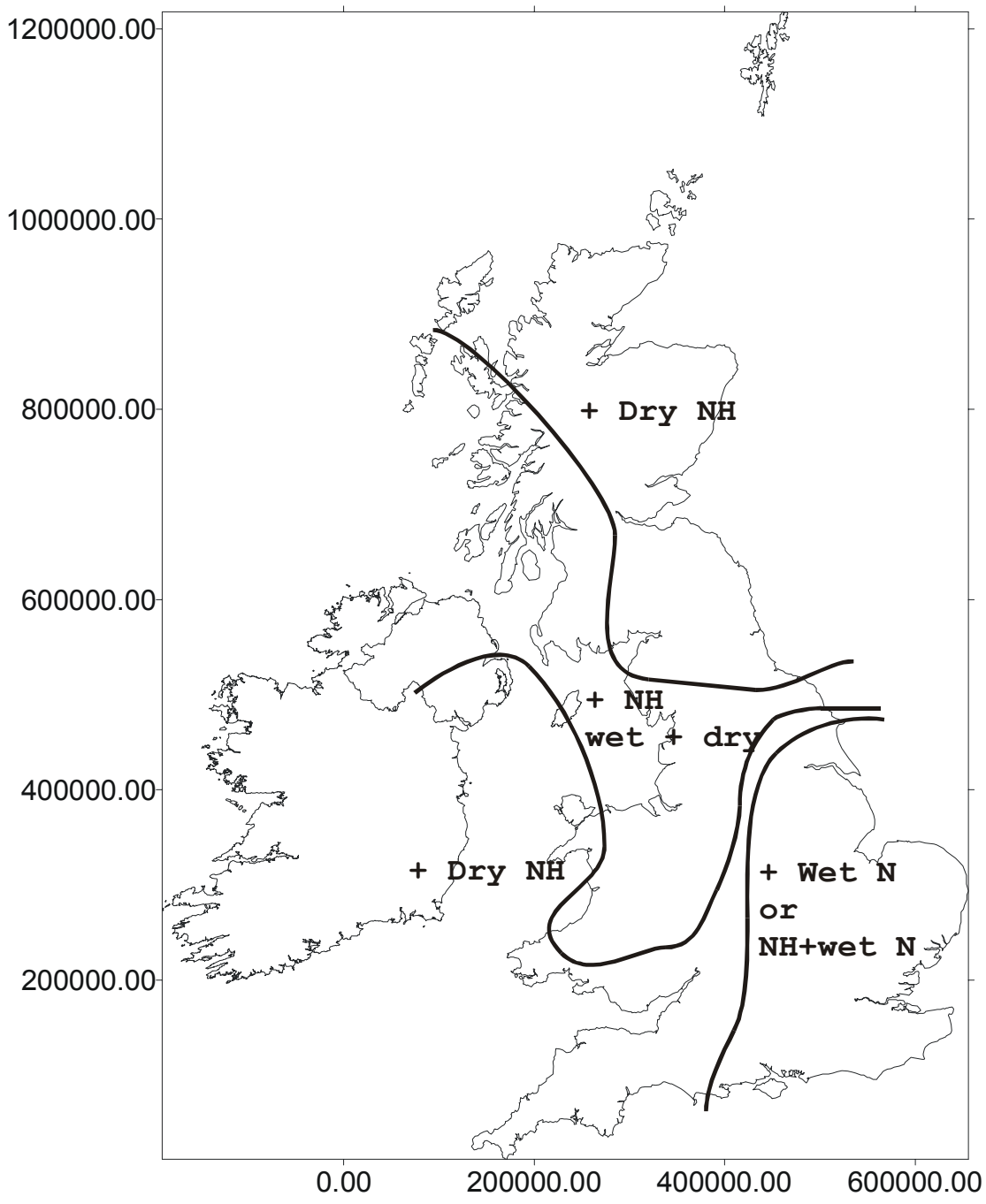

Figure 5 **Increased deposition under multiple parameter variations compared with base case**

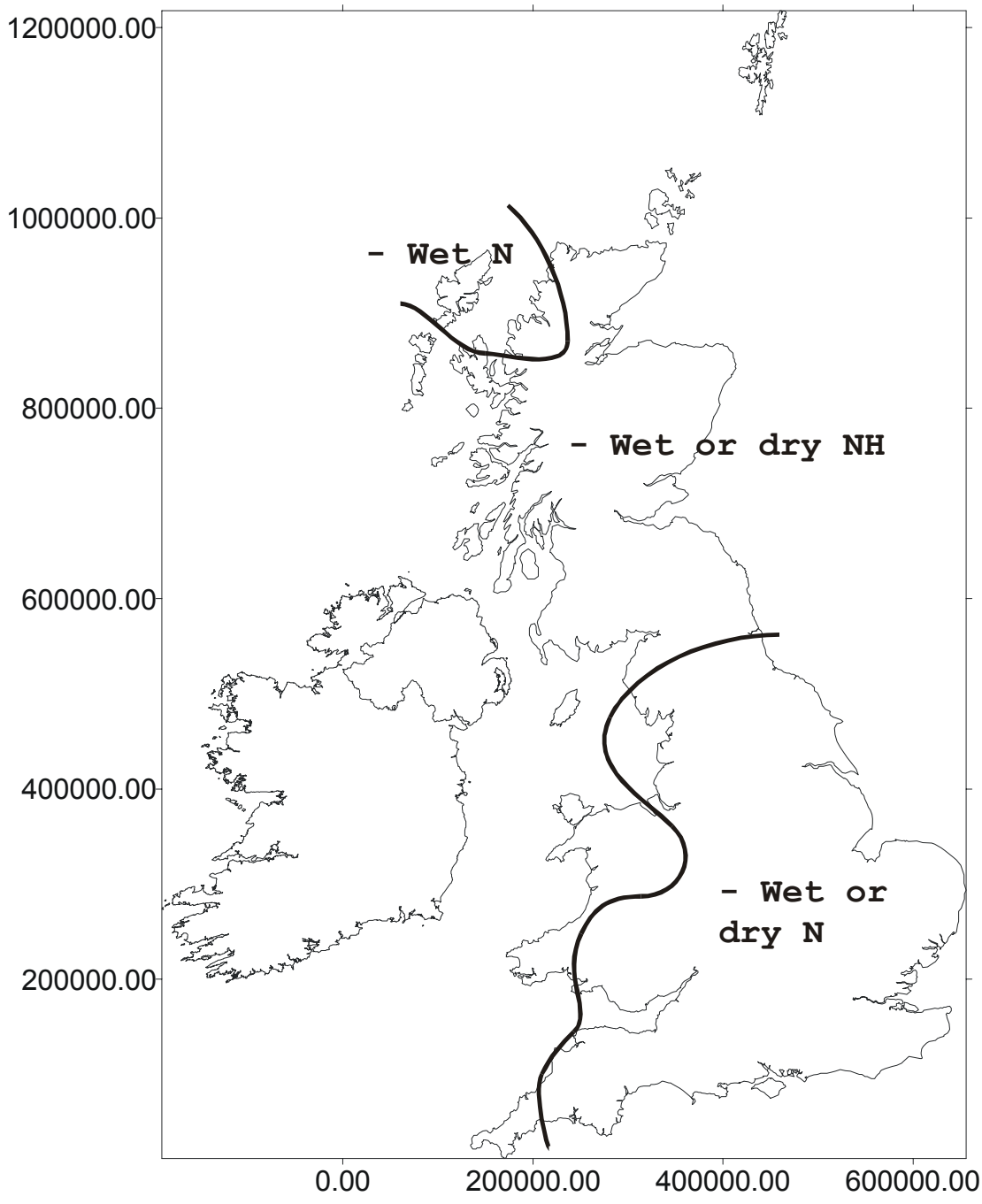

Figure 6 **Decreased deposition under multiple parameter variations compared with base case**

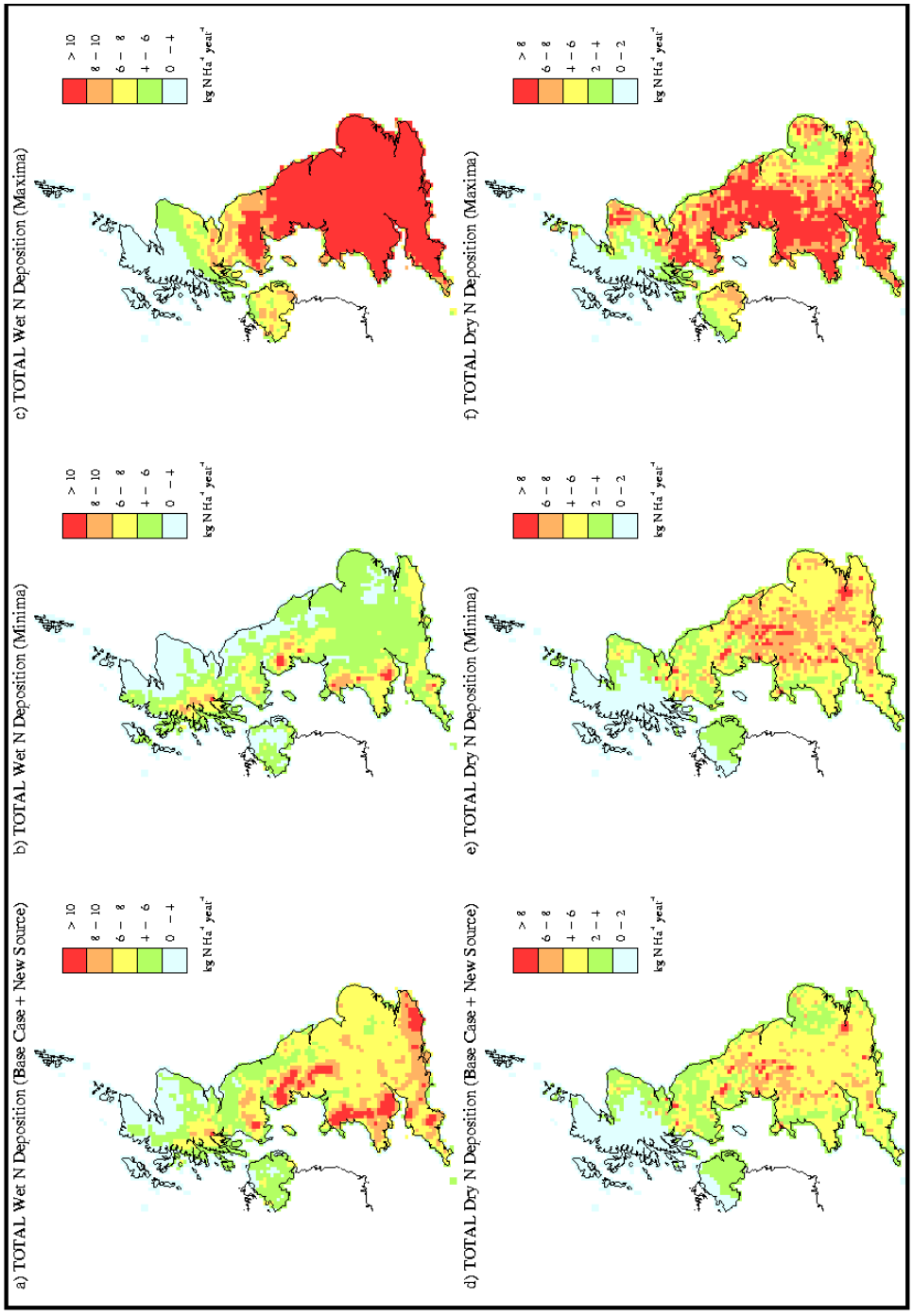

Figure 7 **Total N deposition (oxidised + reduced) for the base case compared with minimum (b,e) and maximum (c,f) values from model runs with all parameters varied**